CHARACTERISATION OF THE MOLECULAR INTERACTIONS BETWEEN INSULIN-LIKE GROWTH FACTORS AND THEIR BINDING PROTEINS

by

Melinda Robin Lucic, B.Sc.(Hons)

A thesis submitted to the
University of Adelaide, South Australia
for the degree of Doctor of Philosophy

October, 2000

Department of Biochemistry
University of Adelaide
Adelaide, South Australia

Table of Contents

Abstract

This thesis assesses the importance of amino acids 221 to 236 of bIGFBP-2 for IGF binding activity, by creating amino acid substitutions. Two different mutagenesis strategies were used to accomplish this.

The first involved a phage display approach. Numerous examples exist in the literature to show that phage display is a powerful approach for isolating optimal binding residues required for protein-protein interactions. To examine residues on bIGFBP-2 required for IGF binding activity, a phage display system was developed. The bIGFBP-2 gene was cloned into a variant of the pHEN1 phagemid in fusion to the filamentous bacteriophage protein gIIIp. In this vector bIGFBP-2 was expressed in *E. coli SupE* hosts, on the surface of filamentous phage particles. Furthermore, free bIGFBP-2 could be expressed in a non-suppressor bacterial host (eg. *E. coli* BL21 cells) to produce a functional IGF binding protein.

C-terminal deletion studies in our laboratory had previously shown that residues 222-236 of bIGFBP-2 were important for normal IGF binding activity. In the first part of this study, residues 221-230 were mutated using a limited amino acid substitution approach, and a large library of bIGFBP-2 mutants was screened for IGF-II binding using phage display. Western ligand blot analysis revealed a mutant in this region containing the amino acid substitutions Lys222Met, His223Gly, Leu228Gln and Lys229Glu which was compromised in its ability to bind both biotinylated IGF-I and mono-biotinylated IGF-II. Kinetic analyses, performed using BIAcore™ to assess both the IGF-I and IGF-II binding activities revealed that the net drop in the affinity was approximately 3-fold. This is in contrast to the 80-fold reduction in IGF binding activity, which was observed when residues 222-236 of bIGFBP-2 were deleted. This may suggest that other residues in this region strongly contribute to the IGF binding activity of bIGFBP-2.

The second strategy involved alanine substitution studies. To assess the region of the C-terminal deletion mutant not examined using phage display, five analogues were constructed by performing alanine substitutions across residues 232-236. Both Western ligand blot analysis and BIAcore™ studies did not give evidence to suggest a significant role for these residues in IGF binding activity.

In conclusion, this study reports on the novel use of phage display for studying IGF binding residues on bIGFBP-2. The results of this work further refine the C-terminal deletion studies and suggest that residues located between 221-230, and in particular 222, 223, 228 and 229, are important for normal IGF binding activity.

Statement of originality

This thesis contains no material which has been accepted for the award of any other degree or diploma in any University. To the best of my knowledge and belief, it contains no material that has previously been published by any other person except where due reference is made. The author consents to the thesis being made available for photocopying and loan.

Melinda R. Lucic

Acknowledgements

This is a long acknowledgement.....but there are so many people to thank!

It is with gratitude that I thank my supervisor, Dr John Wallace, for giving me the opportunity to do my PhD in his laboratory and for providing me both with support and ideas during my PhD project. I am also indebted to Dr Briony Forbes for support, guidance and the much valued advice throughout my studies. I thank Dr Goran Forsberg who got the bIGFBP-2 phage display project going, by designing the phagemid pGF14 and doing the preliminary ground work. Dr Briony Forbes and Ms Emma Hosszu also provided technical support for the analysis of protein expression of bIGFBP-2 in *E. coli* cells, and for this I am grateful. I am eternally grateful for the enthusiasm and efforts of my brother-in-law and consulting mathematician, Dr Nigel Bean in helping me to understand and analyse my BIAcore kinetic data, and for reading through my thesis. Also thanks to Dr Diana Lucic and Francine Carrick for proof-reading this thesis. I thank both Dr Terry Mulhern for assistance in generating a model of the bIGFBP-2 structure, and Dr Dusan Turk for the early release of the co-ordinates for the MHC class II fragment p41 Ii. Various members of the Cooperative Centre for Tissue Growth and Repair must be acknowledged for providing me with IGF tracer for analysis of my binding protein samples: Spencer Knowles, Kirsty Quinn, Zee Upton and Steve Milner. I also wish to thank the "behind-the-scenes" members of the Department: Jackie, Judy, Sheila, "Dad" Brian, Serge, Jan, Janet, Jenny, Joe, Amanda and Sharon.

Life in lab 212 would not have been the same without past and present fellow lab partners: "Yui" Sarawut Jitrapakdee, "Gap" Teerakul Arpornsuwan, Mark Nezic, Sam Lien, Vicky Avery, Kerrie McNeil, Jill Carr, Francine Carrick, Emma Hosszu, Stevey Polyak, Kathy Surinya, Anne Chapman-Smith, Graham "Guba" Hobba, Denise Miller and Sara Mortellaro. I want to thank all those named (and unnamed) for just being there, and for making life in the lab full of gossip and lots of fun.

I was supported during my PhD with an Australian Postgraduate Research Award and funds from the Cooperative Centre for Tissue Growth and Repair. I have also received generous financial support for conference attendance from the Department of Biochemistry, the Lorne Protein Conference, the Japanese Committee for the 4th International IGF Symposium

and a Young Investigators Travel Fellowship from the IUBMB and FEBS to attend the IUBMB meeting in Birmingham, UK.

Without the strength, love and support of my family, I could not have completed this mammoth task! I wish to thank my parents, Toni and Vesna Lucic, my Nena, Diana, Nigel, Simon and Joshi. I also wish to thank my new extended family "The Gunsons" for their love and support. A big "thank you" must also be given to the good old Mac, Biggus Diskus (which was kindly loaned to me by Diana and Nigel) for surviving long enough for me to write up the PhD (even if he did squeal a lot!).

I finally wish to thank my husband, Marcus Gunson, for listening, loving and encouraging me during my studies. He is the best husband anyone could ever have!

I dedicate this thesis in loving memory of my Baka, Ljuba Lucic.

Publications arising from this thesis

Refereed journals

Lucic, M.R., Forbes, B.E., Grosvenor, S.E., Carr, J.M., Wallace, J.C. and Forsberg, G. (1998). Secretion in *Escherichia coli* and phage display of recombinant insulin-like growth factor binding protein-2. *Journal of Biochemistry*, **61**:95-108

Conference abstracts

Lucic, M.R., Forsberg, G., Forbes, B.E. and Wallace, J.C. (September 1996). Characterisation of the Insulin-like Growth Factor Binding Protein-2 Phage Display System [Abstract]. Presented at 6th Biennial IGF Symposium, Sydney, Australia

Lucic, M.R., Forsberg, G., Forbes, B.E. and Wallace, J.C. (October 1996). Optimisation of the IGFBP-2 Phage Display System [Abstract]. Presented at the Australian Society for Biochemistry and Molecular Biology and Australian Society of Plant Physiologists Combined Conference, Canberra, Australia *

Lucic, M.R., Forbes, B.E., Forsberg, G. and Wallace, J.C. (October 1997). Phage Display Analysis of IGFBP-2 in the C-terminal Domain [Abstract]. Presented at the 4th International IGF Symposium, Tokyo, Japan

Lucic, M.R., Forbes, B.E., Forsberg, G. and Wallace, J.C. (February 1998). Investigation of the Importance of the C-terminus of IGFBP-2 for IGF Binding [Abstract]. Presented at 23rd Annual Lorne Conference on Protein Structure and Function, Lorne, Australia

Lucic, M.R., Forbes, B.E., Forsberg, G. and Wallace, J.C. (September 1998). Analysis of key residues for IGF Binding in the C-terminal Domain of IGFBP-2 [Abstract]. Presented at Australian Society for Biochemistry and Molecular Biology and Australian Society of Plant Physiologists Combined Conference, Adelaide, Australia *

Lucic, M.R., Forbes, B.E., Forsberg, G. and Wallace, J.C. (October 1998). Investigation of the Importance of Residues 221-230 in the C-terminal Domain of Bovine IGFBP-2 [Abstract]. Presented at the 7th Biennial IGF Symposium, Melbourne, Australia

Lucic, M.R., Forbes, B.E., Forsberg, G. and Wallace, J.C. (February 1999). Analysing C-terminal Mutants of Bovine IGFBP-2 Isolated from a Phage Display Library [Abstract]. Presented at the 24th Annual Lorne Conference on Protein Structure and Function, Lorne, Australia

Lucic, M.R., Forbes, B.E., Wallace, J.C. (July 2000). The Role of Residues 221-236 in bIGFBP-2 for IGF Binding [Abstract]. Presented at the Young Scientist Travel Fellows' Symposium, Birmingham, United Kingdom

* Poster prizes were awarded

Abbreviations

The following abbreviations were used in addition to those abbreviations which are commonly accepted.

Abbreviation	Full name
ALS	Acid labile subunit
Amp	Ampicillin
BCIP	5-bromo-4-chloro-3-indolyl-phosphate disodium salt
BSA	Bovine serum albumin
CBA	Charcoal binding assay buffer
CD	Circular dichroism
CFU	Colony forming units
CM5	Carboxymethylated dextran BIAcore™ sensor chip
CPM	Counts per minute
DMEM	Dulbecco's Modified Eagle's Medium
DMSO	Dimethyl sulphoxide
E. coli	*Escherichia coli*
ECM	Extracellular matrix
EDC	*N*-ethyl-*N'*-(diethylaminopropyl)carbodiimide
EDTA	Ethylenediaminetetraacetic acid
FTB	Fantastic terrific broth
gIIIp	Gene III protein from filamentous phage
gIXp	Gene IX protein from filamentous phage
gVIIIp	Gene VIII protein from filamentous phage
gVIIp	Gene VII protein from filamentous phage
gVIp	Gene VI protein from filamentous phage
HBS	HEPES buffered saline
HEPES	N-2-Hydroxyethylpiperazine-N-2-ethanesulphonic acid
HPLC	High performance liquid chromatography
^{125}I IGF	^{125}I radiolabelled IGF-I and IGF-II
IGF	Insulin-like growth factor
IGF-I and IGF-II	Insulin like growth factor-I and -II
IGFBP	Insulin-like growth factor binding protein
prefixes: h, b, r to IGFBP	Human, bovine, rat IGFBP
IGFBP-rP	Insulin-like growth factor binding protein-related protein
IPTG	Isopropyl-β-D-thiogalactopyranoside
IR	Insulin receptor
Kan	Kanamycin
L plates	Luria-Bertani plates for propagating bacterial cells
NBT	Nitroblue tetrazolium

NHS	*N*-hydroxysuccinimide
Ni-IDA	Nickel-iminodiacetate
Ni-NTA	Nickel-nitrilotriacetate
NMR	Nuclear magnetic resonance
NSB	Non-specific background
OPA+	One-phor-all plus reaction buffer from Amersham Pharmacia
PAGE	Polyacrylamide gel electrophoresis
PBS	Phosphate buffered saline
PBST	PBS Tween-20
PCR	Polymerase chain reaction
PEG	Polyethylene glycol
PFU	Plaque forming units
PMSF	Phenylmethylsulfonyl fluoride
PSB	Phage storage buffer
Rmax	Maximal binding capacity of the BIAcore™ sensor chip surface
RNAse A	Ribonuclease A
RU	Resonance unit
SDS	Sodium dodecyl sulphate
TAE	Tris acetate EDTA
TBE	Tris borate EDTA
TE	Tris EDTA
TEMED	N,N,N',N'-tetramethyl ethylene-diamine
TES	Tris EDTA sucrose
Tet	Tetracycline hydrochloride
TFA	Trifluoroacetic acid
Tris	Tris-(hydroxymethyl)aminomethane
Tween-20	Polyoxyethylene-sorbitan monolaurate
Type-I IGFR	Type-I insulin-like growth factor receptor
Type-II IGFR	Type-II insulin-like growth factor receptor
UV	Ultra-violet
WT	Wild type

Chapter One

INTRODUCTION

Overview

The function that a protein assumes in nature is often dependent on its interaction with other proteins in the biological system. Therefore, understanding how two proteins bind to each other can enable you to probe the physiological role of this interaction. In the case of growth factors either enhancing or reducing an interaction may give beneficial results and could potentially be used to therapeutic benefit.

Insulin-like growth factor activity is modulated by binding proteins. Therefore, the focus of this thesis is to understand the interaction between the two proteins. This review provides a general introduction to the insulin-like growth factor system. It outlines the importance of insulin-like growth factors in mammalian organisms and summarises the components which make up the system. Attention is then focussed on the interaction between insulin-like growth factors and their binding proteins, and what is known about the amino acid residues involved. Finally, the aims and strategies for this thesis are addressed.

1 Insulin-like growth factors: Introduction

At the molecular level the growth of organisms is difficult to define. The difficulty stems from the complexity of biological systems, in that molecules do not work as independent entities, but rather in cooperation with one another. A prime example of this is the insulin-like growth factor system, which comprises a complex interaction between the insulin-like growth factors (IGF), their receptors, insulin-like growth factor binding proteins (IGFBP) and the IGFBP proteases. Furthermore the actions of the IGF system are influenced by other factors, including nutritional status and growth hormone levels which modulate IGF expression (Thissen *et al.*, 1994).

1.1 IGF Protein Actions

Cultured cells require the presence of serum for long-term survival. Insulin-like growth factor-I (IGF-I) and insulin-like growth factor-II (IGF-II) are among the proteins present in serum that are able to stimulate both cell growth and differentiation. Both *in vitro* and *in vivo* data support the important role for IGFs in promoting cellular growth and differentiation.

Short-term observation of IGF administration to a cell culture shows the ability to stimulate acute anabolic effects on protein and carbohydrate metabolism and in longer term experiments, cell replication and differentiation (reviewed in Jones and Clemmons, 1995). This action of the IGF molecules is normally transmitted through the type-I insulin-like growth factor receptor (type-I IGFR; reviewed in Baserga *et al.*, 1997). However, above the normal physiological concentrations, IGF-I or IGF-II can act through the insulin receptor to cause hypoglycaemia (Froesch *et al.*, 1998). This occurs at one-twelfth the potency of insulin (Froesch *et al.*, 1998). In normal circumstances, free IGF-I concentrations are kept low by the IGFBPs (reviewed in Baxter, 1994), so it is unlikely that sufficient growth factor is available for binding to the insulin receptor to cause these effects.

In vivo studies, using IGF administration, IGF over-expression and gene knockout, have shown the important roles of IGFs in the growth and development of organisms. For example, offspring size is reduced in *igf1-/-* and IGF-II deficient mice, and there is an increased incidence of neonatal death for the *igf1* knockout mice (reviewed in Won and Powell-Braxton,

1998; Jones and Clemmons, 1995). The importance of IGF-I in humans has also been shown through a case study of an individual with partial IGF-I gene deletion associated with severe prenatal and postnatal growth failure (Camacho-Hubner *et al.*, 1999). Conversely, over-expression of IGF-I in mice is accompanied by a 30% increase in body weight, and most markedly a 50% increase in brain weight (Mathews *et al.*, 1988). Over-expression of IGF-II in mice is also associated with increased birth weight (Leighton *et al.*, 1995; Petrik *et al.*, 1999). In contrast to IGF-I however, it is interesting that disruption of the IGF-II gene does not alter the rate of survival in mice, but exerts its effect most notably in the reduction of body size (DeChiara *et al.*, 1990). It is possible that the loss of IGF-II expression in the mouse embryo may in part be compensated for by the presence of IGF-I. Why IGF-II does not compensate for the absence of IGF-I is still not understood.

The predominant source of circulating IGF is from the liver (Jones and Clemmons, 1995; Cohick and Clemmons, 1993) and exclusive deletion of the liver *igf1* gene in mice, shows that the liver is responsible for about 70% of circulating IGF-I (Yakar *et al.*, 1999). In addition to the liver-derived IGF, analysis of the literature suggests that these insulin-like growth factors are ubiquitous in all nucleated mammalian cell types. Therefore, as well as endocrine action, IGF-I and IGF-II can act in both autocrine and paracrine ways. Autocrine and paracrine modes of action were proposed to exist because it was found that IGFs were expressed by many different cell types other than the liver in rats (D'Ercole *et al.*, 1984) and in humans (Han *et al.*, 1987; Birnbacher *et al.*, 1998). Evidence for autocrine modes of action also come from the observation that cells over-expressing IGF in culture can grow and survive in serum-free conditions (Logie *et al.*, 1999).

The many roles that both IGF-I and IGF-II play in mammals is reflected in the recent reviews which focus on the role of the IGF system in myogenesis (Florini *et al.*, 1996) and kidney function (Feld and Hirschberg, 1996). IGF is also involved in bone generation which is summarised in a review by Schmid (1995). Furthermore, IGF-I has been used to treat growth deficiency (reviewed by Rosenfeld, 1998; Laron, 1999), osteoporosis (reviewed by Adams *et al.*, 1998) and type-I diabetes (Le Roith and Butler, 1999). There is also a potential use for IGF-I in the treatment of various neurodegenerative diseases, since IGF-I has been

shown to have a wide spectrum of actions on many central nervous system and peripheral nervous system tissues (Dore *et al.*, 1997).

In contrast to the normal role of both IGF-I and IGF-II in animal growth and development, high levels of growth factor expression have been linked to cancerous states (reviewed by Macaulay, 1992; Holly *et al.,* 1999). This has created concern for the use of IGF in therapy of disease (Bach, 1999). However, treatment of Laron syndrome (growth hormone resistant patients having growth hormone receptor defects, resulting in growth retardation and other defects) with IGF-I in humans, has not been linked to malignancy (Laron, 1999). It may be that controlled administration of IGF in diseased or altered states will not increase the risk of cancer formation. In situations when IGF levels are below the normal range, IGF administration may have beneficial, rather than detrimental effects.

Across species, there is a high degree of sequence and functional conservation for the IGF molecules (Upton *et al.*, 1998). This conservation of IGF sequences across a vast range of species during evolutionary history further suggests an important role for the IGF molecules in organism survival.

1.2 IGF Protein structure

The ability of IGF molecules to mimic the effects of insulin is probably due to the similarities in primary amino acid sequence and tertiary structure between the proteins. In 1978, Rinderknecht and Humbel determined the amino acid sequences for both IGF-I and IGF-II of humans (Figure 1.1) and later proposed a structure based on the 45% identity between the two IGF molecules and insulin (Rinderknecht and Humbel, 1978a; Rinderknecht and Humbel, 1978b; Blundell *et al.*, 1983). The pro-insulin primary amino acid sequence is divided into regions termed B, C and A (Figure 1.1). Superimposing this nomenclature onto the IGFs, the A and B domains of IGF-I and IGF-II resemble the A- and B-domains of insulin, whilst the C-domain of the two IGF molecules although not homologous to insulin, corresponds to the shorter C-domain of pro-insulin. The feature which distinguishes IGF from pro-insulin is the presence of an additional D-domain (Figure 1.1). Structural similarity between IGF and insulin was confirmed with the determination of the solution structures of human IGF-I (Cooke *et al.*, 1991; Sato *et al.*, 1993) and human IGF-II (Terawasa *et al.*,

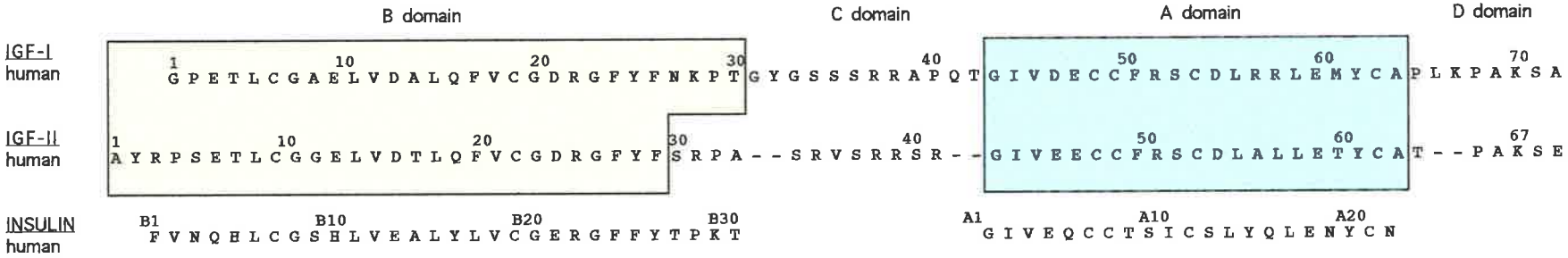

Figure 1.1 Alignment of human IGF-I, IGF-II and insulin. The boxed regions in the IGF molecules denote the B- and A-domains, which have homology to insulin. Pro-insulin (not shown here) also contains a C-domain, but this region is not homologous in sequence to the C-domains of the IGF molecules. The D-domain is unique to the IGFs.

1994; Torres *et al.*, 1995). These structures were in strong agreement with the predicted structure which had been generated from a model based on the crystal structure of insulin (Blundell *et al.*, 1983).

1.3 IGF Receptors

Cells recognise and respond to the presence of both IGF-I and IGF-II through cell surface receptors of which there are three characterised to date (Figure 1.2). Both IGF-I and IGF-II bind with differing affinities to the type-I IGFR, type-II receptor (type-II IGFR) and to the insulin receptor (IR). However, the mitogenic, transforming (anchorage independent growth) and anti-apoptotic effects exerted by these molecules have been shown to occur through the type-I IGFR (reviewed by Baserga *et al.*, 1997, and Sepp-Lorenzino, 1998).

The type-I IGFR is made up of two α and β chain disulphide-linked half-receptors, which dimerise to form the holoreceptor (Figure 1.2). The α-subunit of the type-I IGFR (706 amino acids) is the extracellular portion of the receptor and contains a cysteine-rich region (between residues 223-274) which is required for ligand binding (Gustafson and Rutter, 1990). The β-subunit (626 amino acids) is predominantly located intracellularly and is required for cell signalling (Hernandez-Sanchez *et al.*, 1995). The entire receptor has a high degree of homology to the insulin receptor, with the highest homology of 84% being located in the cytoplasmic tyrosine kinase region of the β-subunit (Ullrich *et al.*, 1986). As a result of the homology between the insulin and type-I IGFR, and the homology between the insulin and the IGFs, the ligands can bind to either receptor (Steele-Perkins *et al.*, 1988; Jones and Clemmons, 1995). The identification of hybrid IR and type-I IGFR highlights the similarity between the two receptors (Soos and Siddle, 1989). The hybrid receptors are formed from the combination of an αβ-subunit from each of the insulin and type-I IGFR (Soos and Siddle, 1989).

Genetic deletion of the type-I IGFR shows its important role for healthy cell survival (Baserga *et al.*, 1997). *In vivo*, homozygous mice with disrupted type-I IGFR genes died at birth (Liu *et al.*, 1993). Analysis of the mice showed ill-formed lungs and organs, thus emphasising a role for the receptor in normal embryonic development (Liu *et al.*, 1993). The type-I IGFR also appears to be important for the growth and maintenance of some cancerous cell lines. Evidence to support this statement comes from studies which show that an antibody

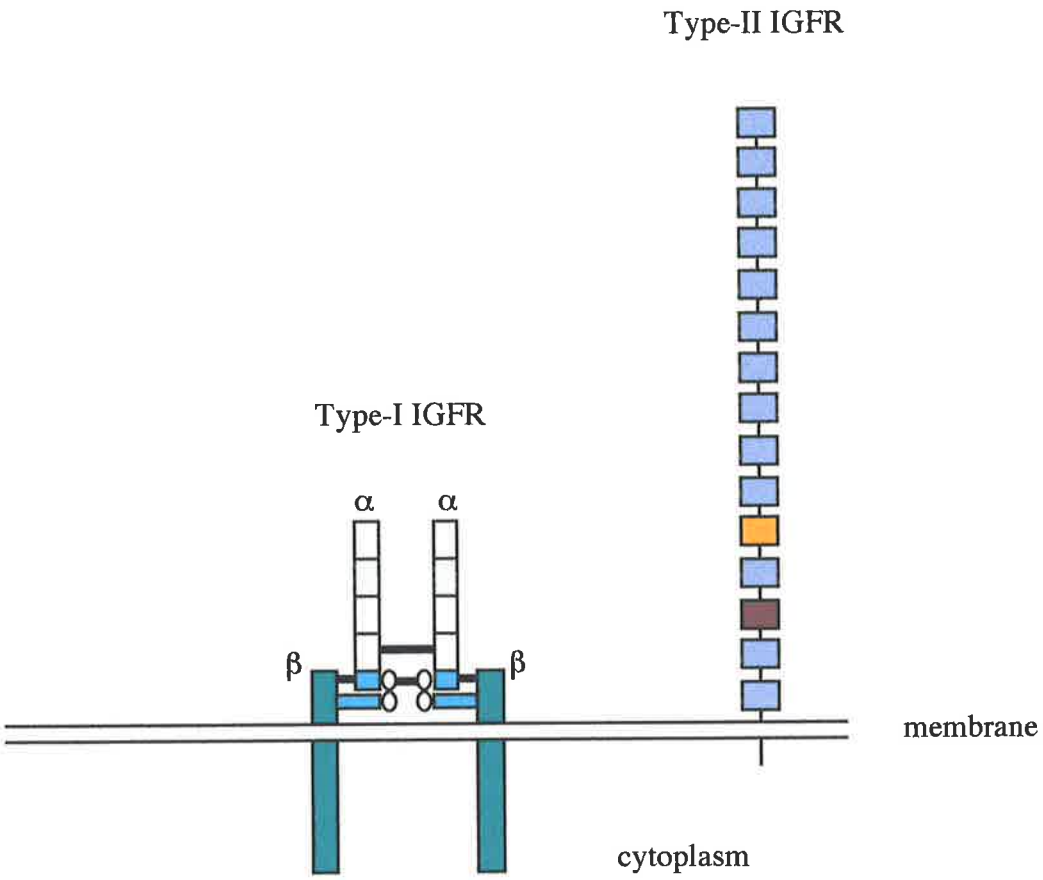

Figure 1.2 Schematic representation of the type-I IGFR and type-II IGFR. The structure of the type-I IGFR is similar to the highly related insulin receptor (Baserga *et al.*, 1997). The type-I IGFR structure shown is based on the structure described by Mulhern *et al.*, (1998). The IGF binding regions in the type-I IGFR involve the cysteine-rich regions (□) (Gustafson and Rutter, 1990). The extra-cytoplasmic domain of the type-II IGFR is made up of 15 conserved repeating sequences, each consisting of eight cysteine residues (the repeats are shown here as boxes; Morgan *et al.*, 1987). The IGF-II binding region for the type-II IGFR has been shown to involve repeat 11 (▩) (Schmidt *et al.*, 1995), and possibly a unique 43 amino acid stretch in repeat 13 (■) which acts to enhance IGF-II binding activity (Devi *et al.*, 1998).

which inhibits IGF interaction with the type-I IGFR, can suppress the growth of Wilms' tumour and rhabdomyosarcoma in mice (Gansler *et al.*, 1989; Kalebic *et al.*, 1994). Furthermore, type-I IGFR-negative cell lines are unable to be transformed by the simian virus 40 large tumour antigen, which normally confers anchorage independent cell growth (Sell *et al.*, 1993). Therefore, as well as having a role in normal development, the receptor appears to be involved in transformed cell growth and survival.

To date, the role of the type-II IGFR is less clearly understood. The affinity of IGF-II for the type-II IGFR is in the nanomolar range, and is approximately 100 times greater than the binding affinity seen for IGF-I with this receptor (reviewed in Braulke, 1999). In contrast to the type-I receptor, which is able to bind insulin, the type-II IGFR exhibits no detectable affinity for insulin (Braulke, 1999). A comparison of the primary amino acid sequence of the human type-II IGFR, to the independently cloned bovine cation-independent mannose-6-phosphate receptor, provided the first indication that, in mammals, these two receptors were the same (Morgan *et al.*, 1987). However, this similarity was not found to extend to the non-mammalian species, chicken and *Xenopus* , where the mannose-6-phosphate receptor was unable to bind to IGF-II (Clairmont and Czech, 1989). The human type-II IGFR has a 2264 amino acid extracellular domain divided into 15 repeating units, each with a highly conserved distribution of eight cysteine residues (Morgan *et al.*, 1987: see Figure 1.2). On the cytoplasmic face there is a 164 amino acid region, and its role in receptor signalling remains unclear (Braulke, 1999). A soluble form of the receptor is found in serum, amniotic fluid and urine (Causin *et al.*, 1988; Xu *et al.*, 1998). In transgenic mice which expressed the soluble receptor, there was a reduction in local organ size, especially the alimentary canal and uterus (Zaina *et al.*, 1998). However, the skin was not affected despite high levels of the secreted protein being found there (Zaina *et al.*, 1998). Soluble type-II IGFR expression can partially reverse organomegaly which is associated with the over-expression of IGF-II in mice (Zaina and Squire, 1998). Furthermore, expression of the soluble receptor in mice deficient for IGF-II does not further reduce local organ size (Zaina and Squire, 1998). These results suggest that soluble type-II IGFR reduces the bioavailability of IGF-II in these organs and therefore acts as a negative regulator of growth (Zaina and Squire, 1998). A role in controlling the bioavailability of IGF-II is also shown through deletion of the type-II IGFR. In mice

lacking the type-II IGFR, offspring were 35% larger than the normal progeny, although they showed a lower rate of survival due to ill formed organs, including the heart (Ludwig *et al.*, 1996). The defect caused by the type-II IGFR deletion could be rescued by the removal of IGF-II expression (Ludwig *et al.*, 1996), further supporting the role of the receptor in controlling IGF-II bioavailability.

While it can be seen that the type-II IGFR can control the bioavailability of IGF-II, the availability and activity of both IGF-I and IGF-II is also controlled by other means. As will be discussed below, the regulation of IGF activity can occur through the presence of serum and tissue-derived binding proteins. There is also transcriptional and translational control over IGF-I and IGF-II protein expression. One of the principal regulators of IGF-I expression is growth hormone (Thissen *et al.*, 1994), which controls the transcriptional levels of the IGF-I gene (Mathews *et al.*, 1986). For the purposes of this thesis, the genetic regulation of IGF expression will not be addressed, but reviews of the subject can be found in Phillips *et al.* (1998) and Engstrom *et al.* (1998).

1.4 IGF Binding Proteins

The IGFBP family is a group of proteins whose exact role *in vivo* has been difficult to decipher. This difficulty is due to the presence of 6 similar family members, named IGFBP-1 to IGFBP-6, which show some functional redundancy in the modulation of IGF activity (Jones and Clemmons, 1995). There are elements unique to each member as discussed below, which may confer a slightly different functional role for each IGFBP in the IGF system.

Recently the family of six has been extended by the discovery of proteins which have homology only to the conserved N-terminal part of the binding protein (reviewed in Oh *et al.*, 1998). The initial confusion at the nomenclature of these proteins was resolved at the 4th International Symposium on IGF in Japan in 1997, when it was decided that these proteins be called the insulin-like growth factor binding protein-related proteins (IGFBP-rP). A comprehensive summary of the IGFBP superfamily, comprising IGFBP-1 to IGFBP-6 and the IGFBP-rPs, can be found in a review written by Hwa, Oh and Rosenfeld (1999).

1.4.1 IGFBP actions, tissue delivery and distribution

In humans unbound IGF molecules exist for a short period of time, with an apparent half-life of between 10-12 minutes in the circulation (Guler *et al.*, 1989). In contrast, the half-life of these molecules when bound to an IGFBP increases to approximately 15 hours (Guler *et al.*, 1989), demonstrating one of the many effects that binding proteins exert on the IGF molecules. In addition to prolonging the half-life of the IGF molecules, the IGFBP family actions are summarised by Jones and Clemmons (1995) as:

i) the IGFBP family transport IGFs in plasma and maintain their concentrations in the vascular space;

ii) the IGFBP family enables tissue- and cell-type specific localisation;

iii) the IGFBP family modulate IGF and receptor interaction;

iv) the IGFBP family can have IGF-independent actions.

i. The IGFBP family transport IGFs in plasma and maintain their concentrations in the vascular space.

As discussed above, the IGFBP proteins increase the circulation half-life of both IGF-I and IGF-II, and provide a storage source of the growth factors for potential endocrine roles (Guler *et al.*, 1989). This is predominantly achieved by the 150-200 kDa IGFBP-3/acid labile subunit (ALS) ternary complex which is the major carrier for IGF in serum (reviewed in Rajaram *et al.*, 1997). The size of the IGFBP-3/ALS complex is proposed to inhibit the movement across the capillary endothelial barrier, since serum contains the ternary complex whilst lymph does not (Binoux and Hossenlop, 1988) (Figure 1.3). The remaining IGF is bound in smaller molecular weight complexes with the other five binding proteins (Weber *et al.*, 1999). As well as a role in plasma transport, these binding proteins can facilitate the movement of IGF out of the general circulation. Firstly, analysis of the migration of radiolabelled IGFBP perfused into a beating rat heart has shown that the binding protein can leave the vascular space and enter the surrounding tissue (Bar *et al.*, 1990a; Bar *et al.*, 1990b; Boes *et al.*, 1992). Furthermore, administration of labelled IGFBP-3 into the circulation of rats was found to rapidly cross the capillary endothelium to the extravascular compartments (Arany *et al.*, 1993) (Figure 1.3). The effect that IGFBPs exert on the migration of circulating IGF across vascular endothelial layers still remains to be investigated. A recent study comparing the

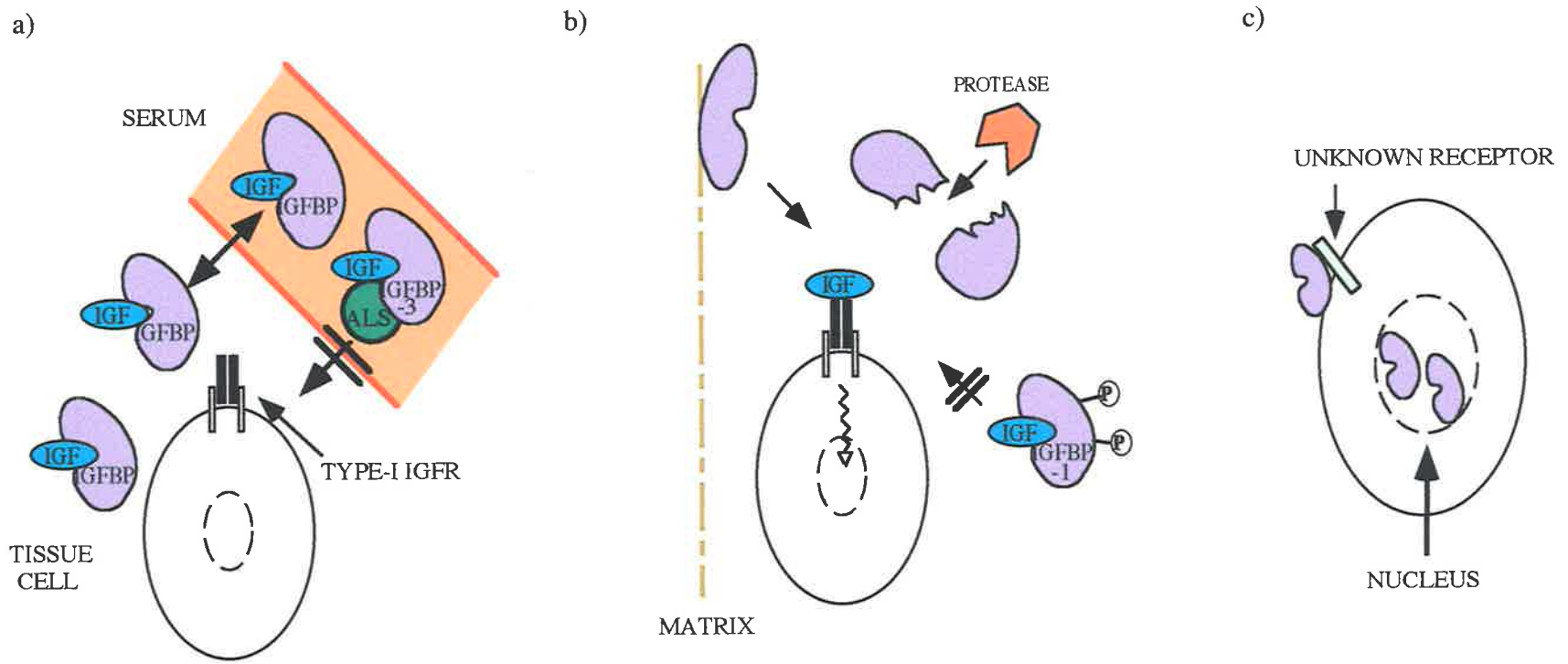

Figure 1.3 Schematic representation of the effects of IGFBP on the actions of IGF-I and IGF-II.
a) Binding proteins can maintain IGF in circulation, and can potentially modulate the movement of IGF into and out of the circulation. The ternary complex restricts movement of IGF out of circulation. IGFBP can inhibit IGF action by preventing interaction with the receptor.
b) Proteolysis of the binding protein, or the association of IGFBP with extracellular matrix, can release IGF from the complex thus enabling IGF to interact with its receptor. Phosphorylation of IGFBP-1 increases its binding affinity for IGF and may act to inhibit the release of IGF from the complex.
c) IGFBPs have functions independent of the IGFs. Both IGFBP-3 and IGFBP-5 can localise to the nucleus. IGFBP cell surface association through unknown molecules may play a role in the IGF independent actions.

transport of circulating radiolabelled IGF-I and LR^3IGF-I (an IGF analogue with low affinity for IGFBPs) to wound sites, showed that IGFBPs reduced the rate of IGF migration to extracellular fluid (Bastian *et al.*, 2000).

Although IGF-I and IGF-II share a high degree of sequence and structural similarity to insulin, the IGFBPs have previously been reported not to bind to insulin (Binkert *et al.*, 1989; Mohan *et al.*, 1989). However, more recent evidence using the sensitive BIAcore™ instrumentation showed that full-length IGFBP-3 could bind to insulin, but with affinities 1000 times less than those observed for IGF (Heding *et al.*, 1996). There is also some suggestion through affinity cross-linking studies and Western ligand blot analysis that the IGFBP-rP and proteolytic derivatives of IGFBP-3 do have some affinity for insulin (Vorwerk *et al.*, 1998; Oh *et al.*, 1998). However, the significance of this insulin binding ability has yet to be established.

ii. The IGFBP family enables tissue and cell-type specific localisation.

Differential expression patterns of the binding proteins during various developmental and physiological states, suggests that controlled expression and localisation of the binding protein is important for normal organism function. For example all the IGFBPs have different spatial locations at both the mRNA and protein level in embryonic mice (van Kleffens *et al.*, 1999). This is also true during human foetal life where the binding proteins exhibit tissue-specific expression (Funk *et al.*, 1992). In addition to transcriptional and translational control, localisation of binding protein is achieved post-translationally. The IGFBPs are able to interact with various cell surface proteins and the extracellular matrix (ECM) because of the presence of different amino acid motifs. The RGD motif in IGFBP-1 has been shown to enable interaction with cells through the $\alpha_5\beta_1$ integrins (Jones *et al.*, 1993a). IGFBP-2 has also been observed to bind to the surface of cells (Russo *et al.*,1997; Schedlich *et al.*, 1998) and to extracellular matrices (Arai *et al.*, 1996b; Khosla *et al.*, 1998). The involvement of the IGFBP-2 RGD motif in binding to integrin was suggested by Delhanty and Han (1993), and has only recently been confirmed (Rauschnabel *et al.*, 1999). It is also possible that cell and matrix binding occurs through association with the glucosaminoglycans such as heparin, which is able to bind to IGFBP-2 only when IGF-I or IGF-II are present (Arai *et al.*, 1996b). The ability of IGF/IGFBP complexes to bind to the ECMs may facilitate the localisation of IGF close to

receptors to enable cell signalling. For example, in human osteoblast cell cultures where the environment is rich in ECM, the IGF-II/IGFBP-2 complex stimulates cell proliferation (Khosla *et al.*, 1998). This is in contrast to a cell culture environment with little ECM where the addition of IGFBP-2/IGFII complex inhibits normal IGF-II activity (Khosla *et al.*, 1998). These observations suggest a potential mechanism for targeting IGFs to bone in hepatitis-C associated osteosclerosis, where adult patients exhibit increases in bone mass, associated with higher levels of IGFBP-2 (Khosla *et al.*, 1998).

Both IGFBP-3 and IGFBP-5 have been reported to bind to cell surfaces and to ECMs respectively. Amino acid substitution studies have shown that the C-terminal basic region, ^{228}KGRKR in human IGFBP-3, is important for cell association (Firth *et al.*, 1998). A role for binding to glycosaminoglycans has also been inferred from the observation that heparin can bind to IGFBP-3 fragments containing the basic amino acid stretches from the central and C-terminal regions of the protein (Fowlkes and Serra, 1996). In addition to this, heparin can prevent IGFBP-3 association with fibroblast monolayers (Martin *et al.*, 1992). Similarly, the ability of IGFBP-5 to interact with the fibroblast ECM (Jones *et al.*, 1993b) is also mediated by the corresponding C-terminal basic region in IGFBP-5 (Parker *et al.*, 1996). Studies by Arai and coworkers show this binding activity may be specific for heparin (Arai *et al.*, 1994; Arai *et al.*, 1996a), although IGFBP-5 is also able to bind types-III and -IV collagen, laminin and fibronectin (Jones *et al.*, 1993b). Binding of IGFBP-5 to the ECM coincides with a 7-fold reduced affinity for IGF-I (Jones *et al.*, 1993b) (Figure 1.3). The reduced affinity of IGF-I for IGFBP-5, when IGFBP-5 is associated with ECM, may provide a localisation and release mechanism for IGF to sites where IGF may be required (Jones *et al.*, 1993b). This was in part hypothesised from the observation that IGFBP-5 associated with a cell culture derived matrix was found to potentiate the biological action of IGF-I (Jones *et al.*, 1993b).

iii. The IGFBP family modulate IGF and receptor interaction.

Des(1-3) IGF-I is an IGF-I variant lacking the first three amino acids (Sara *et al.*, 1986; Francis *et al.*, 1986). It has a much reduced affinity for IGFBP (Szabo *et al.*, 1988), and as a consequence it is much more potent than intact IGF-I because it is more readily available for binding and stimulating the type-I IGFR (reviewed in Ballard *et al.*, 1996). Therefore, it can be hypothesised from this observation that IGFBP can reduce IGF activity by inhibiting

receptor interaction. In addition to this, intact binding proteins also exhibit approximately 10- to 40-fold higher binding affinities compared to the type-I IGFR for IGF-I (summarised in Zapf, 1995). Numerous examples exist in the literature showing that addition of binding protein to cell cultures can inhibit the actions of IGF. For example, a dose dependent reduction in DNA replication is observed with increasing amounts of IGFBP-4 *in vitro* (Mohan *et al.*, 1989). In addition to inhibiting IGF activity, binding proteins can assist IGF action. There is evidence to suggest that IGFBPs may bring the ligand in close proximity to its receptor where the binding protein is made to release the ligand, resulting in receptor signalling and potentiating IGF action. Possible potentiating factors are discussed above, but may include IGF/IGFBP complex association with, for example ECM, which may reduce the affinity of binding protein for IGF, enabling its release for receptor signalling (Jones *et al.*, 1993b) (Figure 1.3). Release of IGF from binding proteins may also be achieved through proteolysis. Proteolysis of binding proteins results in fragments with reduced affinity for IGF, which may free IGF for receptor interaction (see Section 1.4.3; Figure 1.3). Phosphorylation of IGFBP-1 is associated with an increase in affinity for IGF-I (Jones *et al.*, 1991). It is possible that the altered affinity of IGFBP-1 for IGF-I may influence the effect which IGFBP-1 exerts over IGF activity (Figure 1.3). Alternatively, IGF-independent mechanisms of IGFBP-1 (discussed below) may also play a role in enhancing IGF action. Potentiation of IGF action, which to date has been shown for IGFBP-1, IGFBP-2, IGFBP-3 and IGFBP-5 is reviewed in Rechler and Clemmons (1998).

iv. The IGFBP family can have IGF-independent actions.

As discussed above, it is generally accepted that the role of binding proteins is to modulate IGF action. However, there is growing evidence to challenge this view, and in fact IGF may modulate the function of the binding protein (Rechler, 1997). IGFBP-3 can associate with cell surfaces and has been shown to inhibit cell growth in an IGF-independent manner (reviewed by Oh *et al.*, 1998, and Rechler, 1997) (Figure 1.3). *In vitro* stimulation of cell migration, through the presence of high concentrations of IGFBP-1 is proposed to occur by an IGF-independent mechanism (Jones *et al.*, 1993a). The effect of basic fibroblast growth factor, which normally stimulates DNA synthesis in cells lacking the type-I IGFR, can be inhibited by N-terminal fragments of IGFBP-3 which have little IGF binding affinity (Zadeh

and Binoux, 1997). It is also interesting that both IGFBP-3 and IGFBP-5 localise to the nucleus of cells (they contain a putative nuclear localisation signal in the carboxy-terminal region; Schedlich *et al.*, 1998) suggesting that the binding proteins may have some transcriptional regulatory role (Figure 1.3). The identification of IGF-independent functions are so far recognised only for IGFBP-1, IGFBP-3 and IGFBP-5. The discovery of an IGF-independent role for the binding proteins will require a change of thought regarding the IGF system and how each of the components act to modulate cell behaviour. Indeed, some of the earlier studies which assumed that IGF itself modulated cell behaviour may need to be re-evaluated, since now it is apparent that the IGFBPs may have some role in controlling cell growth.

1.4.2 Genetic over-expression and knockouts to more clearly define the in vivo role of binding proteins

In many systems, ablation or over-expression of genes has been used to investigate the role of proteins *in vivo*. Gene knockouts of IGFBP-2 (Wood *et al.*, 1993), IGFBP-3 (Pintar *et al.*, 1999), IGFBP-4 (Pintar *et al.*, 1998), IGFBP-5 (Pintar *et al.*, 1999) and IGFBP-6 (Pintar *et al.*, 1998) have been created in mice. The loss of IGFBP-2 was shown to be associated with reduced spleen size (Pintar *et al.*, 1996), although there was a concomitant increase in the circulating levels of the other binding proteins which confounds this result (Pintar *et al.*, 1996). It was postulated that the other binding proteins may compensate for the IGFBP-2 loss (Pintar *et al.*, 1996). Gene knockout of IGFBP-3, -5 and -6 produced apparently normal, viable and fertile mice (Pintar *et al.*, 1999). However, homozygous mice which did not express IGFBP-4 were smaller than their heterozygous and wild type littermates (Pintar *et al.*, 1998). This observation is in contrast to the *in vitro* demonstration that IGFBP-4 inhibits IGF action (Mohan *et al.*, 1989), and thus the hypothesis that these mice would be larger in its absence. Cross-breeding of the mice, to produce combinatorial knockouts of up to three of the binding proteins has not appeared to have affected murine viability (Pintar *et al.*, 1999). If indeed the binding proteins are functionally redundant, then why are they so conserved? Is it possible that there are individuals in the population which lack one or more of the binding proteins, which can be compensated for by the over-expression of

the other members? These questions may be answered more readily when the human genome project has been completed and comprehensive gridded arrays of genes which include those for IGFBPs are available.

Over-expression of IGFBP-1 is proposed to make IGF unavailable for normal development in mice. Hepatic over-expression of IGFBP-1 in mice is associated with growth retardation, and reduced fertility and foetal survival (Gay *et al.*, 1997). Rajkumar *et al.* (1995) also showed that IGFBP-1 over-expression resulted in fasting hyperglycaemia. This supported the earlier findings of Lewitt *et al.* (1991), who found that the administration of IGFBP-1 in rat caused a rise in plasma glucose levels. Another phenotype observed in three independent IGFBP-1 over-expression studies in mice was a decrease in brain size (Gay *et al.*, 1997; Dai *et al.*, 1994; Rajkumar *et al.*, 1995), accounted for by the loss of IGF availability for normal brain development. IGFBP-2 and IGFBP-6 are predominant in cerebrospinal fluid (Roghani *et al.*, 1991), and it may be that sequestering the IGF from these binding proteins may disturb the normal balance of IGF/IGFBP complexes, and affect brain formation.

In conclusion, with growing information about the association of IGFBPs with various cellular conditions, it becomes more difficult to define the exact biological functions that these proteins assume. So far, very little information has been obtained by the generation of single null mutant mice for these proteins. Further combinations of the mutations and possibly the removal of at least the six IGFBP members may yield clearer effects to define their roles. The added complexity of their IGF-independent roles adds another dimension to how binding proteins can function *in vivo*.

1.4.3 Post-translational modification of binding proteins

Post-translational modification of an IGFBP modulates the binding protein's ability to control IGF activity, and possibly affects the IGF-independent functions. Three forms of post-translational modification that occur for different IGFBP members are proteolysis, phosphorylation and glycosylation.

i. Proteolysis

Analysis of the literature shows that proteolysis is a common regulatory mechanism used in many instances to control protein function. Proteolysis of the binding protein is proposed to

allow the release of IGF from the complex, freeing the IGF for receptor binding and signalling (Figure 1.3). The release of IGF occurs because the binding protein fragments have reduced binding affinity for the IGFs. For example, cleavage of IGFBP-3 with plasmin yields a 22 kDa fragment of IGFBP-3 with 50 and 20 times lower affinity for IGF-I and IGF-II respectively (Lalou, Lassarre and Binoux, 1995). Increased protease resistance of IGFBP-4 (Conover *et al.*, 1995) and IGFBP-5 (Imai *et al.*, 1997), through mutagenesis of the major cleavage site, results in inhibition of normal IGF-I action on cells and thus supports this hypothesis.

Proteolytic fragments of IGFBP-2 through to IGFBP-5 have been observed to occur *in vivo* in both normal and altered physiological states (reviewed in Conover, 1998). Furthermore, IGFBP proteolysis has been observed to increase in pregnancy and post-operatively (reviewed in Maile and Holly, 1999), when it may be expected that IGF may be required for foetal growth and wound repair, respectively.

Current evidence suggests that there are specific proteases for the different binding proteins. For example IGFBP-5 is cleaved by human dermal fibroblast conditioned medium, but IGFBP-1, -2, -3 and -4 are not proteolysed (Nam *et al.*, 1994). IGFBP-4 proteolysis is dramatically enhanced through binding to IGF (Fowlkes and Freemark, 1992; Conover *et al.*, 1993; Byun *et al.*, 2000), while IGF can reduce IGFBP-5 proteolysis in human osteoblast cell conditioned medium (Conover and Kiefer, 1993). Precise identification of the proteases responsible for the IGFBP proteolysis is still under investigation. Identification of the proteases involved in cleaving the IGFBPs has been predominantly confined to *in vitro* assays, and their significance *in vivo* is still to be determined (summarised by Maile and Holly, 1999). Some of the proteases implicated so far include plasmin for IGFBP-2 (Menouny *et al.*, 1997) and cathepsin D (Conover and De Leon, 1994), prostate specific antigen in seminal plasma (Cohen *et al.*, 1992) and matrix metalloproteinase-9 (Manes *et al.*, 1999) for IGFBP-3. Pregnancy-associated plasma protein-A, which was purified from human fibroblast conditioned medium, was shown to be an IGF-dependent protease for IGFBP-4 (Lawrence *et al.*, 1999). This was in part shown by the fact that protease activity specific for IGFBP-4 could be inhibited by antibodies directed against the pregnancy-associated plasma protein-A (Lawrence *et al.*, 1999). Recently it was also shown that complement secreted by fibroblasts and smooth muscle cells is involved in IGFBP-5 proteolysis (Clemmons *et al.*, 1999).

ii. Phosphorylation

Phosphorylation in the central region of IGFBP-1, at serine residues 101, 119 and 169, increases the affinity of recombinant human IGFBP-1 for IGF-I (Jones *et al.*, 1991; Jones *et al.*, 1993c). The mechanism of increased binding affinity of IGFBP-1 for IGF is not known, but is proposed to occur by either conformational change, or local ionic or steric interactions in the regions of the IGF binding site (Jones *et al.*, 1993c). Whether the increase in affinity involves a negative charge could be investigated by amino acid substitution of the serine residues with negatively charged amino acids. Interestingly, only the non-phosphorylated binding protein when administered with IGF-I, is reported to increase wound breaking strength in skin incisional wounds in rats (Jyung *et al.*, 1994). It may be the reduction in affinity of the non-phosphorylated IGFBP-1 for the IGF, or possibly another mechanism, which results in better wound healing.

Both IGFBP-3 and IGFBP-5 are reported to be phosphorylated (summarised in Coverley and Baxter, 1997). The increased production of phosphorylated IGFBP-3 in culture was found to be dependent on the interaction of IGF-I with type-I IGFR (Coverley and Baxter, 1995). As yet, the significance of the phosphorylation for both IGFBP-3 and IGFBP-5 is unknown. It is possible that like IGFBP-1, phosphorylation alters the IGF binding affinity. Alternatively, phosphorylation may have some other role, and this would need to be determined through further investigation.

iii. Glycosylation

Glycosylation of binding protein has been observed for IGFBP-3 (Zapf *et al.*, 1988), IGFBP-4 (Ceda *et al.*, 1991), IGFBP-5 (Conover and Kiefer, 1993), and for IGFBP-6 (Bach *et al.*, 1992). IGFBP-3 glycosylation does not appear to have a significant effect on IGF-I binding activity or on IGF-I/ALS ternary complex formation (Firth and Baxter, 1999). However, the study by Firth and Baxter (1999) showed that for IGFBP-3, glycosylation reduced the association of the binding protein with cell surfaces. It was therefore proposed that glycosylation of IGFBP-3 may regulate the cell surface binding activity of the protein (Firth and Baxter, 1999). Analysis of O-glycosylated IGFBP-6 also shows it is not altered in its IGF binding ability relative to non-glycosylated IGFBP-6 (Bach *et al.*, 1992). However, glycosylation of IGFBP-6 is observed to increase resistance to proteolytic cleavage by

chymotrypsin and trypsin (Neumann *et al.*, 1998). Therefore it may be possible that glycosylation of the binding proteins may increase their stability *in vivo*, although this would need to be investigated. The full significance of glycosylation for the binding proteins remains to be determined. Indeed the role of glycosylation may be different for each of the binding protein members.

1.4.4 IGFBP Structure

The primary amino acid sequence alignment for the six human binding proteins is shown in Figure 1.4. The human proteins range in size from 215 to 288 amino acids and are approximately 3 to 4 times larger than both IGF-I and IGF-II. Within the human IGFBP family, and across species, the most prominent feature of the alignment is the conservation of the pattern of cysteine residues clustered in the N- and C-terminal parts of the IGFBP. Other residues in these two regions are also homologous or similar across the family of proteins (Figure 1.4). IGFBP-2, which is the focus of this thesis, is very highly conserved across the species. The most variability for IGFBP-2 is in the central region of the protein (Figure 1.5). This would suggest that the N- and C-terminal ends of IGFBP-2 contain residues important for the structure and function of the protein *in vivo*. As will be discussed later, analysis of proteolytic fragments derived from IGFBPs demonstrates that both ends of the protein are required for full IGF binding activity.

Chemical reduction of IGFBP-3 shows that the disulphide bonds are important for the ability of the IGFBPs to bind strongly to IGFs (Sommer *et al.*, 1991). Recent determinations of the disulphide bond pairs in bovine IGFBP-2 (bIGFBP-2; Forbes *et al.*, 1998) and human IGFBP-6 (hIGFBP-6; Neumann *et al.*, 1998; Neumann and Bach, 1999) show they are clustered within the N- and C-terminal ends, and that disulphide bonds do not occur between the two regions. The disulphide bonding pattern has been determined for parts of human IGFBP-1 (hIGFBP-1; Neumann and Bach, 1999), the C-terminal end of bIGFBP-2 (Forbes *et al.*, 1998), for parts of rat IGFBP-3 (rIGFBP-3; Hashimoto *et al.*, 1997), the C-terminal end of IGFBP-4 (Standker *et al.*, 2000), for parts of human IGFBP-5 (hIGFBP-5; Kalus *et al.*, 1998), and for the entire hIGFBP-6 protein (Neumann *et al.*, 1998; Neumann and Bach, 1999). Although the full disulphide pairing pattern has been determined for human

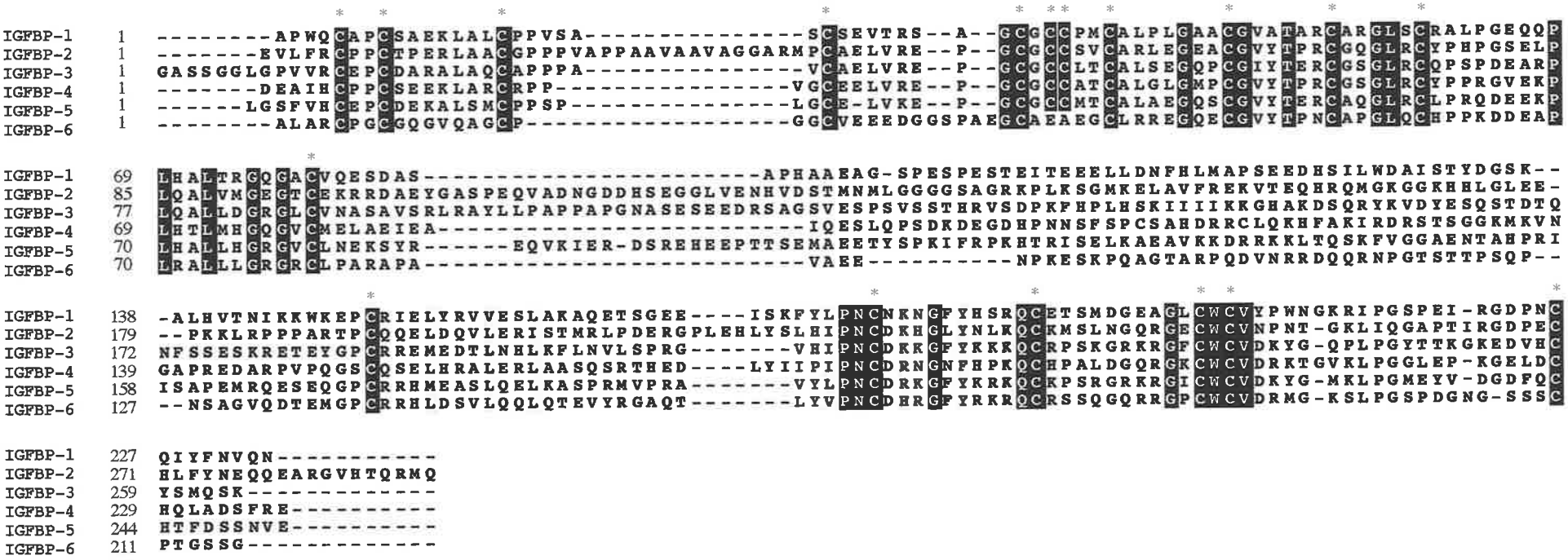

Figure 1.4 Sequence alignment of the six human IGFBPs. The alignment was created using ClustalW1.8 (Thompson *et al.*, 1994) and BOXSHADE3.21 (http://www.ch.embnet.org/software/BOX_form.html). Absolutely conserved residues are boxed in black. Conservative substitutions are boxed in grey. * Denotes conserved cysteine residues.

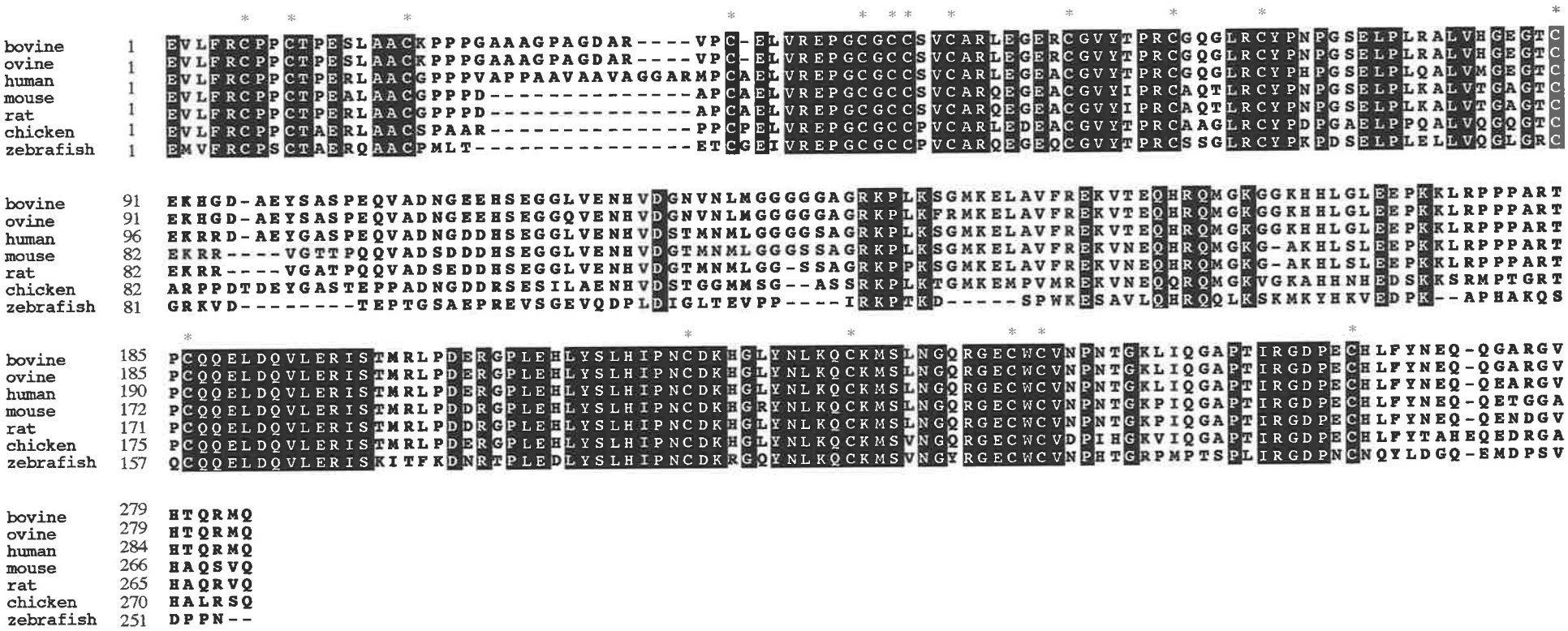

Figure 1.5 Alignment of IGFBP-2 protein sequences from bovine (Upton *et al.*, 1990; Bourner *et al.*, 1992), ovine (Delhanty and Han, 1992), human (Binkert *et al.*, 1989), mouse (Landwher *et al.*, 1993), rat (Brown *et al.*, 1990), chicken (Schoen *et al.*, 1995) and zebrafish (Duan *et al.*, 1999). Regions boxed in black represent absolute sequence conservation. Regions in grey contain conserved residue changes. * Denotes conserved cysteine residues. The alignment was created using ClustalW1.8 (Thompson *et al.*, 1994), and BOXSHADE3.21(http://www.ch.embnet.org/software/BOX_form.html).

IGFBP-6, partial characterisation of human IGFBP-1 shows it is different for the first four cysteines in the amino-terminal end (Neumann and Bach, 1999). The two additional and adjacent cysteine residues in the amino-terminal motif of IGFBP-1 to -5, GlyCysGlyCysCys most probably change the disulphide pairing relative to that seen for hIGFBP-6 (Neumann and Bach, 1999). Determination of the pairing pattern for IGFBP-1 to -5 is difficult using proteolytic cleavage methods due to the close proximity of the cysteine residues. However, it is unlikely that the adjacent CysCys residues form a disulphide pair, as this would require the formation of a rare *cis* peptide bond (Neumann and Bach, 1999). Figure 1.6 summarises the determined disulphide bonding pattern for IGFBP derived from the evidence discussed above.

Regions of proteins not involved in compact structural domains, are often detected through studies assessing protease susceptibility. A good example of this is seen in the study of the holo- and apo-forms of myoglobin where proteolytic data supports an unstructured stretch of protein in the apo-form being helical in the holo-form (Fontana *et al.*, 1997). Since proteolysis of binding proteins *in vitro* and *in vivo* is often confined to the central region of the protein (Figure 1.7), it suggests that this region of IGFBP is not intimately involved in secondary structures. These observations support the presence of at least two structured domains confined to the amino- and carboxy-terminal ends of the proteins. Interestingly, as discussed above, the disulphide bonds are confined to both the amino- and carboxy-terminal ends of the protein and probably act to stabilise their conformation. The disulphide bonds may also mask the effect of proteolytic cleavages in these regions, unless the bonds are all reduced prior to the analysis for peptide fragments.

The structural knowledge for insulin provided a good basis for the prediction of IGF structure based on amino acid sequence homology between the molecules (Blundell *et al.*, 1983). Unfortunately the binding proteins do not generally have sequence homology to any protein with known structure. Until recently structural information about the IGFBP family was confined to predictions based on computer modelling (IGFBP-3, Spencer and Chan, 1995; IGFBP-4, Landale *et al.*, 1995). As a consequence of the conserved cysteine patterning between the six different members of the IGFBP family, it has been assumed that the overall structure of all six proteins will be the same. A small fragment in the N-terminus of human IGFBP-5, Ala40 to Ile92, which retains IGF binding ability, albeit of reduced affinity, has

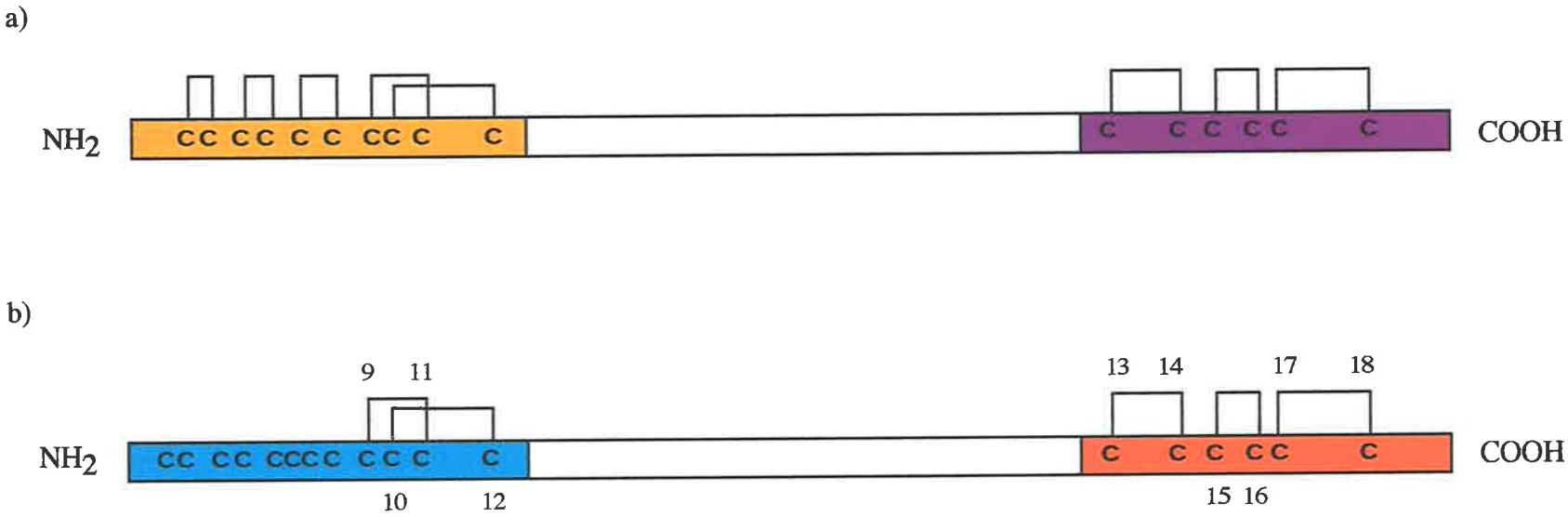

Figure 1.6 Schematic representation of the disulphide bonding pattern for cysteine residues in IGFBP.
a) Complete disulphide bonding pattern for hIGFBP-6 (Neumann *et al.*,1998; Neumann and Bach, 1999). Determination of amino terminal cysteine pairing for IGFBP-6 was shown to be different to that of hIGFBP-1 (1 does not pair 2 and 3 does not pair 4; Neumann and Bach, 1999).
b) Carboxy terminal disulphide bonds as determined for bIGFBP-2 (Forbes *et al*, 1998) and hIGFBP-4 (Standker *et al.*, 2000), and amino terminal bonds for hIGFBP-1 (Neumann *et al.*, 1998), bIGFBP-2 (Dr Briony Forbes, unpublished), IGFBP-3 (Hashimoto *et al.*, 1997) and hIGFBP-5 (Kalus *et al.*, 1998). Cysteines are numbered sequentially from 1 to 18, from the amino terminal end. Human IGFBP-1 to -5 have two additional cysteine residues in the amino terminal end relative to IGFBP-6, which may cause the different amino terminal disulphide pattern for hIGFBP-1.

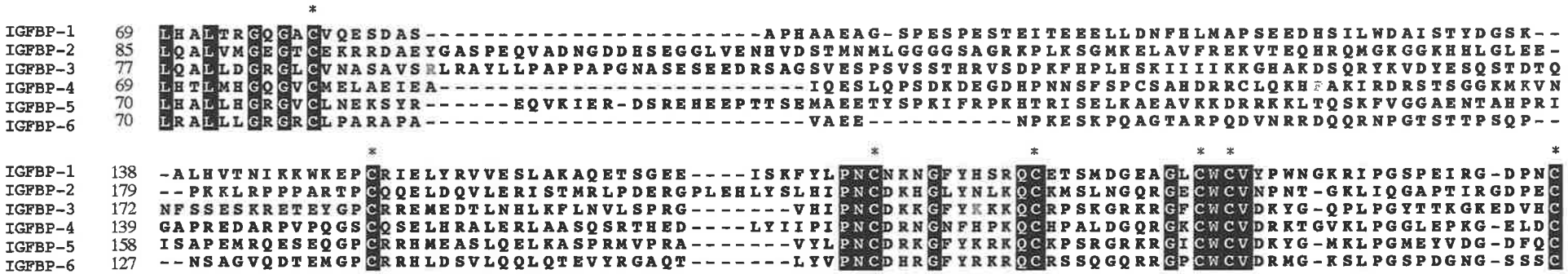

Figure 1.7 The proteolytically cleaved sites in IGFBP. The cleavage points across the binding proteins cluster to the central region, shown here on the alignment of the central and part of the C-terminal region of human IGFBP-1 to IGFBP-6. Cleavage points are marked in colour. Proteolytic sites are mapped in: IGFBP-2, **X** Wang *et al.*, (1988) (the residue was found on rat IGFBP-2, and was mapped onto human IGFBP-2), and **X** Ho and Baxter, (1997); IGFBP-3, **X** Binoux *et al.*, (1998) and **X** Okabe *et al.*, (1999); IGFBP-4, **X** Chernausek *et al.*, (1995) (the residue was found on rat IGFBP-4, and was mapped onto human IGFBP-4), **X** Standker *et al.*, (1999) and **X** Byun *et al.*, (2000); and in IGFBP-5, **X** Standker *et al.*, (1998). The conserved cysteine residues are marked by *.

been determined by nuclear magnetic resonance (NMR) studies to be a compact structure containing three short antiparallel β-strands (residues 46-47, 59-61, 78-82) (Kalus *et al.*, 1998) (Figure 1.8). A C-terminal fragment of human IGFBP-5, residues 135-246, which has no detectable IGF binding activity, was estimated to contain approximately 40% random coil conformation. The remaining part of the protein comprising the unconserved middle portion was unstructured (Kalus *et al.*, 1998). It remains to be seen whether the IGFBP-5 structure will be found to be similar to that of the other binding proteins. Full structural determination of IGFBP-5 and of the other binding proteins will be required to establish this.

1.5 Residues involved in the IGF/IGFBP interaction

The ability to alter the IGF/IGFBP interaction may enable us to further understand the roles that these complexes play *in vitro* and *in vivo*. As discussed earlier, IGF analogues with reduced IGFBP affinity but normal type-I IGFR affinity, demonstrate that binding proteins can act to suppress cell stimulation by IGF (Ballard *et al.*, 1996). Alternatively, the addition of a binding protein such as IGFBP-5 may enhance IGF-induced cell stimulation (Jones *et al.*, 1993b; see Section 1.4.1). With the discovery of IGF-independent roles for the IGFBPs, it would be interesting to alter the interaction of the binding protein for the IGF (both enhancing and reducing binding affinities) to further probe the binding protein's function.

Enhancing or reducing interaction of the binding proteins for the IGF may have therapeutic benefit. For example, a number of studies have shown that co-administration of IGFBP-1 with IGF to wounds has increased wound breaking strength (Jyung *et al.*, 1994; Tsuboi *et al.*, 1995; Galiano *et al.*, 1996). Also, IGF-I in complex with IGFBP-3 has been reported to improve wound tissue repair in both pig and rat wound models (Sommer *et al.*, 1991) Similar studies assessing a possible role for IGFBP-2 in enhancing IGF action at wound sites, showed that IGFBP-2 had no such action (Galiano *et al.*, 1996). However as previously discussed, an IGF-II/IGFBP-2 complex which is able to bind to ECM, can effectively stimulate human osteoblast proliferation (Khosla *et al.*, 1998). These results suggest that IGFBP-2 may be used to target IGF-II to skeletal tissue in cases of osteoporosis, to help increase bone mass (Khosla *et al.*, 1998). Therefore, modification of the binding protein affinity for IGF may have desirable effects on these activities.

(a

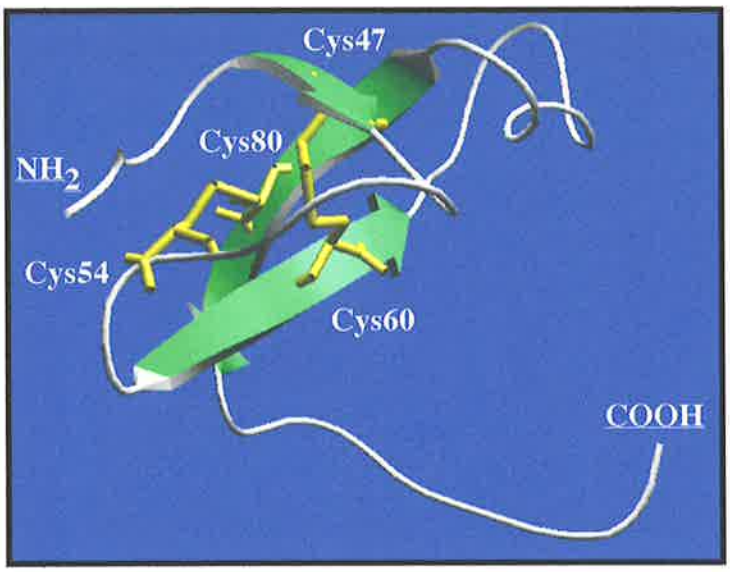

(b

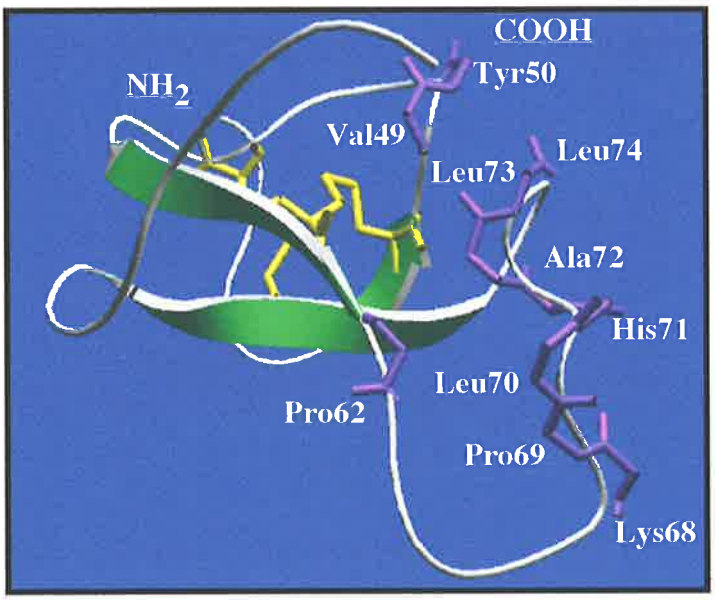

Figure 1.8 Structure of the N-terminal IGF binding fragment of human IGFBP-5 (Kalus *et al.*, 1998).
a) Residues Ala40 to Ile92 were shown to contain three anti-parallel β strands, disulphide bonded between Cys47 and Cys60, and Cys54 and Cys80 (Kalus *et al.*, 1998).
b) Residues involved in binding to IGF-II were shown to comprise Val49, Tyr50, Pro62 and Lys68 to Leu74 (Kalus *et al.*, 1998). The figures were constructed using Swiss-PdbViewer (Guex and Peitsch, 1997).

Knowledge of the residues involved in the interaction between IGF and binding protein may also have other benefits. As discussed in Section 1.1, there is growing concern about the development of IGF-based therapies because of the link between high plasma IGF concentrations and various forms of cancer (Holly *et al.*, 1999). Although there is a strong association between IGF and cancer, the ability to control IGF localisation and activity *in vivo* may avoid this potential problem. IGF activity could be controlled by the use of modified binding proteins. This could be achieved by better understanding the residues which enable the interaction between the binding proteins and IGFs, and furthermore, the interactions between binding proteins and tissues or extracellular matrices.

1.5.1 Residues on IGF required for IGFBP interaction

The residues on the insulin-like growth factors involved in both binding protein and receptor interaction have been investigated over the past two decades. Various techniques have been used. These include residue or domain swapping with the homologous insulin molecule, as well as amino acid deletions or mutations. Nuclear magnetic resonance structural studies have previously provided high resolution 3-dimensional structures of both IGF-I and IGF-II (Cooke *et al.*, 1991; Sato *et al.*, 1993; Terasawa *et al.*, 1994; Torres *et al.*, 1995) and of LR_3IGF-I (Laajoki *et al.*, 1998). More recently NMR has been used to study the structural binding epitopes required for IGF-I to interact with IGFBP-1 (Jansson *et al.*, 1998).

i. IGF Analogue Studies to Determine the Important IGF Residues

Analogue studies have shown the importance of the B- and A-domains of the IGFs in binding to the IGFBP. Homologue domain swapping of the B-domain of IGF-I to the corresponding insulin B-domain confers the ability for insulin to interact with IGFBP (De Vroede *et al.*, 1985) when normally insulin is unable to be bound. Conversely, replacement of the IGF-I B-domain with the insulin B-domain reduces serum IGFBP binding (Bayne *et al.*, 1988).

Des(1-3) IGF-I, a natural variant lacking the first three amino acids of the B-domain of IGF-I, has a reduced ability to interact with IGFBP (Szabo *et al.*, 1988). Sequential deletions from the amino-terminal end of IGF-I show the importance of Glu3 (Bagley *et al.*, 1989). This has been confirmed through single amino acid substitutions, with charge reversal to a

lysine or arginine at position 3 having the greatest impact on IGFBP interaction (Wallace *et al.*, 1989). The corresponding residue in IGF-II, Glu6, is also required for IGFBP binding (Francis *et al.*, 1993). Other B-domain amino acids involved in IGFBP binding include residues 15 and 16 of IGF-I. When mutated in combination with residues 3 and 4 binding to serum IGFBP is decreased up to 600-fold (Bayne *et al.*, 1988). The effect of structural change as a consequence of amino acid substitution has been investigated by Jansson and coworkers (1997). Using far ultra-violet (UV) circular dichroism (CD) spectroscopy they showed a reduction in the α-helical content of IGF-I when alanine substitutions were made at positions 15 and 16 (Jansson *et al.*, 1997). The importance of residues 15 and 16 of IGF-I in binding to IGFBPs has been confirmed by alternative substitutions which do not grossly affect structure, but still affect binding protein interactions (Magee *et al.*, 1999).

Sequential alanine mutagenesis across the entire IGF-I molecule implies that B-domain residues Gly7, Leu10 and Phe25 are involved in IGFBP interaction (Dubaquie and Lowman, 1999). The involvement of Gly7 is supported in an NMR study investigating complexes between IGF-I and IGFBP-1 (Jansson *et al.*, 1998). Charge reversal of Glu9 to Lys9, a residue located in the B-domain α-helix in IGF-I, decreased to varying degrees the affinity for each of the 6 binding proteins, and had some impact on type-I IGFR binding, without affecting the overall structure (Magee *et al.*, 1999).

Amino acid substitution of A-domain residues, Phe49, Arg50, and Ser51, in IGF-I (Clemmons *et al.*, 1992; Oh *et al.*, 1993), and the corresponding residues, Phe48, Arg49 and Ser50, in IGF-II (Bach *et al.*, 1993) implicated the involvement of this region in IGFBP interaction. Mutagenesis of residue Phe26 in IGF-II to either Ser or Leu also affects binding to IGFBP (Bach *et al.*, 1993) as well as the type-I IGFR and insulin receptor (Sakano *et al.*, 1991). The substitution of A-domain residues Ile43, Val44 or Leu54 for IGF-I by alanine reduces binding to IGFBP-1 up to 4-fold, but has a negligible effect on binding to IGFBP-3 binding (Dubaquie and Lowman, 1999). The difference is hypothesised to occur because these amino acid side-chains of IGF may be important for IGFBP-1 binding, whilst the amino acid backbone may be required for IGFBP-3 (Dubaquie and Lowman, 1999). Consistent with this proposal is the observation that the different IGF analogues affect binding to each IGFBP

family member to varying degrees (Clemmons *et al.*, 1992; Bach *et al.*, 1993; Magee *et al.*, 1999).

Both mutagenesis (Bach *et al.*, 1993; Jansson *et al.*, 1998) and antibody binding studies (Manes *et al.*, 1997) provide support for overlapping but distinct type-I IGFR and binding protein interaction sites on the IGF molecule. Furthermore, IGF-I interaction with either the type-I IGFR or IGFBP-1 is mutually exclusive (Jansson *et al.*, 1998). Using surface plasmon resonance, Jansson *et al.* (1998) showed that pre-complexed IGF-I-IGFBP-1 is unable to interact with type-I IGFR. Although other explanations are possible, this is consistent with there being overlapping binding sites for the receptor and binding protein on the IGF molecules.

ii. IGF Structural Studies

Nuclear magnetic resonance studies have been used to determine the structure of IGF-I (Cooke *et al.*, 1991; Sato *et al.*, 1993) and IGF-II (Terasawa *et al.*, 1994; Torres *et al.*, 1995). Knowledge of the structures has enabled assessment of the mutagenesis data (discussed above), to determine the possibility of proposed residues participating in binding protein and receptor binding interactions (Figure 1.9). For example, Glu3 and Glu6 in IGF-I and IGF-II respectively, are solvent exposed and are not directly involved in the maintenance of IGF protein structure (Cook *et al.*, 1991; Torres *et al.*, 1995). This accessibility enables their involvement in IGFBP interactions. Proposed IGF-I residues involved in IGFBP interaction are shown in Figure 1.9.

Recently, NMR has been used to investigate residues on IGF-I interacting with IGFBP-1, by analysing backbone chemical shifts in the presence of the binding protein (Jansson *et al.*, 1998). Included in the residues perturbed in the presence of IGFBP-1 were: P2, E3, C6, G7, G19, P28-G30, G32, R36, R37, Q40-G42, P63, K65, P66, K68-A70 (Figure 1.9; Jansson *et al.*, 1998). Interestingly, work by Bagley and coworkers (1989) studying des(1-2) IGF-I suggested that Pro2 was not important for binding to either bIGFBP-2 or the L6-myoblast-derived binding proteins. However, as discussed above this may reflect the differences between the IGFBPs and the residues they interact with on the IGFs.

a)

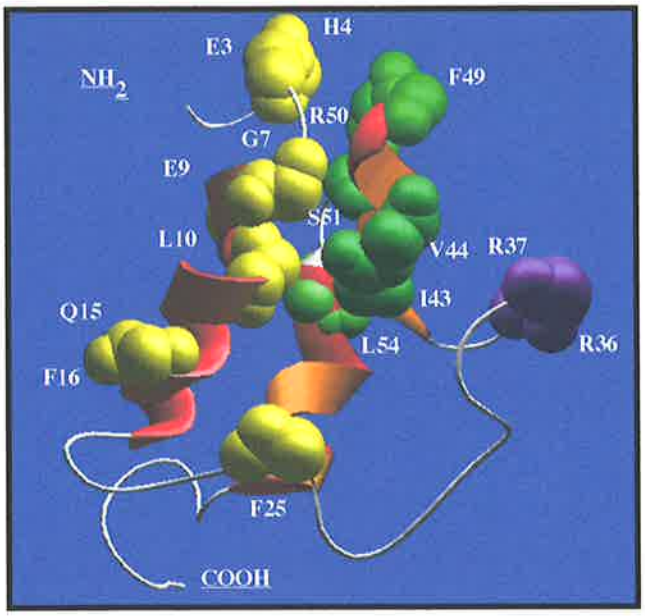

b)

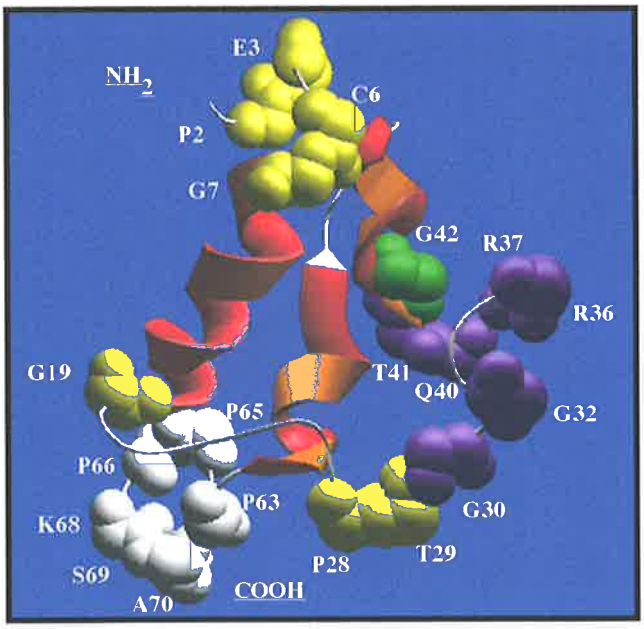

Figure 1.9 Residues on IGF-I proposed to be involved in the interaction with binding proteins.
a) Residues shown through mutagenesis to have a role in binding protein interaction. The role of each residue for the interaction varies with the different binding proteins (see text). b) Residues on IGF-I shown through NMR to experience backbone chemical shifts when IGFBP-1 is binding (Jansson *et al.*, 1998). Amino acids are shown from the B-domain (yellow), C-domain (purple), A-domain (green) and D-domain (white). The figures were constructed using Swiss-PdbViewer (Guex and Peitsch, 1997).

In the NMR study by Jansson *et al.* (1998), three arginine side-chains were found to participate in binding to IGFBP-1. Alanine substitution of each arginine residue in the protein showed that the analogues [R36A,R37A] IGF-I and [R50A] IGF-I were impaired in their ability to interact with IGFBP-1 (Jansson *et al.*, 1998). CD spectroscopy was used to confirm that the impaired affinity for IGFBP-1 was not due to gross structural changes in the proteins (Jansson *et al.*, 1998). Alanine substitution of R21, R36 and R37, and R56 IGF-I resulted in altered type-I IGFR interactions. A possible explanation for these results is that the binding sites for the receptor and binding protein overlap around residues 36 and 37 (Jansson *et al.*, 1998).

1.5.2 Residues on IGFBPs required for IGF interaction

At the onset of this project, little information was available describing the residues involved in the interaction of the IGFBPs with the IGF ligands. This was due in part to the more recent characterisation of the binding proteins relative to the IGFs. Binding proteins, unlike insulin and IGF, have no well characterised structural homologue (other than themselves) for which residue and domain swapping experiments can be performed with minimal structural impact. The current knowledge about the IGF binding residues in the binding protein is summarised below.

In the literature there are many instances of fragments of the binding proteins which either lose or retain the ability to interact with the IGF molecules. Although some fragments maintain IGF binding ability, their binding affinity is generally markedly reduced. This is thought to be due to partial loss of some of the IGF binding site residues involved in IGF interaction or loss of important structural features.

There are observations to suggest that both amino- and carboxy-terminal fragments of binding proteins maintain some IGF binding ability. Amino-terminal fragments include 21 kDa from IGFBP-1 (Huhtala *et al.*, 1986), 12.3 kDa from IGFBP-3 (Kubler *et al.*, 1999), and from IGFBP-4 both 13.2 kDa (Standker *et al.*, 1999) and 16 kDa fragments (Chernausek *et al.*, 1995). Carboxy-terminal portions include 13.4 and 13.8 kDa (Ho and Baxter, 1997) and 14 kDa fragments from IGFBP-2 (Wang *et al.*, 1988), and a 13 kDa fragment from human IGFBP-5 (residues 144-252), which has IGF-I binding activity that is visible by standard

Spencer and Chan (1995) characterised a C-terminal fragment of IGFBP-3 which bound to IGF-I (see page 26 and Figure 1.10c).

ligand blotting techniques (Standker *et al.*, 1998). A map of the cleavage sites can be seen in Figure 1.7. As can be seen in the figure, the cleavage of binding proteins is generally confined to the central portion of the protein. Mass spectrometry and sequence analysis shows that many of the amino- and carboxy-terminal fragments do not overlap, and this suggests that binding sites for IGF exist in both ends of the protein.

i. Residues in the N-terminal Domain

The studies discussed in this section are summarised in Figure 1.10a. Both proteolytic and recombinantly produced amino-terminal fragments of binding protein maintain some ability to bind IGF. For example, a 1-93 IGFBP-3 fragment (Hashimoto *et al.*, 1997) has been shown to bind IGF with approximately 4% of the affinity exhibited by full-length protein. This suggests, without doubt, a role for this region in growth factor binding. Early deletion work implied the importance of the first 60 amino acid residues of human IGFBP-1 (hIGFBP-1, Brinkman *et al.*, 1991a). However, the loss in binding resulting from the deletion of the first 60 amino acids of hIGFBP-1 could have been a consequence of a structural change, that would be consistent with its aberrant migration on polyacrylamide gel (Brinkman *et al.*, 1991a). With the recent knowledge of the disulphide bonding pattern for IGFBP-1, showing that Cys79 pairs with Cys53 (Neumann and Bach, 1999), it is clear that the unpaired Cys79 present in the Brinkman deletion mutant could have contributed to an alteration in the structure of the protein. This altered structural conformation would undoubtedly affect the binding affinity of IGFBP-1 for IGF, as observed by Brinkman *et al.* (1991a).

In our laboratory, a chemical footprint approach was used to study bIGFBP-2 residues involved in IGF binding. Recombinant bIGFBP-2 was iodinated in the presence and absence of either IGF-I or IGF-II, and Tyr60 was found to be protected in the binding protein-IGF complex, irrespective of which IGF was bound (Hobba *et al.*, 1996). Binding analyses of amino acid substituted bIGFBP-2 variants, Tyr60Ala and Tyr60Phe, indicated that the aromatic side-chain, and hydrogen bonding potential of the tyrosine residue were important structural determinants for the IGF binding site (Hobba *et al.*, 1998). Alanine substitution of the adjacent valine, Val59Ala, also altered the binding characteristics of bIGFBP-2, whilst alanine substitutions for Thr61, Pro62, and Arg63 did not reduce IGF binding affinities (Hobba *et al.*,

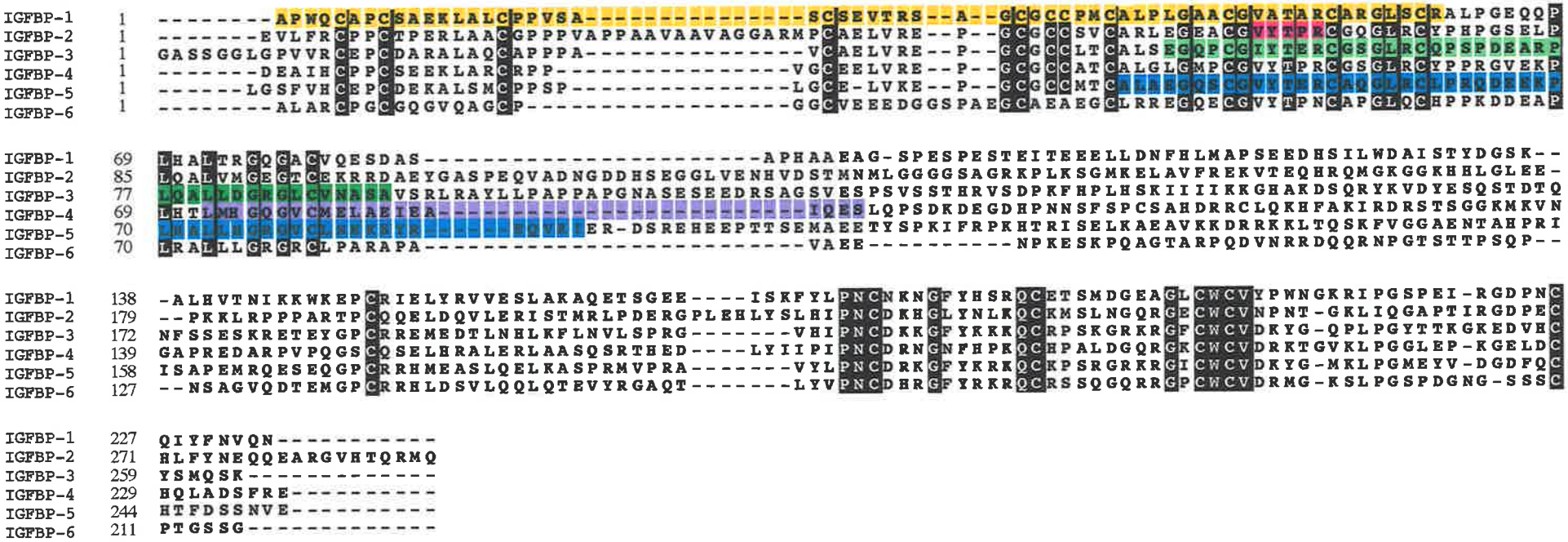

Figure 1.10a Sequence alignment of the 6 human IGFBPs, highlighting the N-terminal regions which were investigated for a role in IGF binding activity. Details of the studies can be found in Section 1.5.2. The regions which were studied on binding proteins isolated from different species are mapped onto the human protein. (PM)= point mutation, (F)= fragment, (Del)= a deletion.
IGFBP-1 (Del) Brinkman *et al.* (1991a); IGFBP-2 (PM) Hobba *et al.* (1998); IGFBP-3 (F) Hashimoto *et al.* (1997);
IGFBP-4 (Del) Qin *et al.* (1998); IGFBP-5 (F) Kalus *et al.* (1998)

1998). In agreement with the IGFBP-2 study, an NMR analysis of an amino-terminal IGFBP-5 fragment showed the involvement of the equivalent residues (Kalus *et al.*, 1998).

In 1998 Kalus and coworkers described an NMR structure for an amino-terminal fragment of IGFBP-5 (Kalus *et al.*, 1998). The fragment termed "mini IGFBP-5", comprised residues Ala40 to Ile92, and was found to be a rigid, three stranded anti-parallel β-sheet structure, containing two disulphide bridges (Figure 1.8). Relative to IGF binding by full-length IGFBP-5, BIAcore™ analysis of IGF-I and IGF-II binding to "mini IGFBP-5" showed 10- to 200-fold lower affinity due to a much greater rate of dissociation (Kalus *et al.*, 1998). Chemical shifts, detected through NMR analysis of "mini IGFBP-5" in complex with IGF-II, gave evidence for the involvement of residues Val49, Tyr50, Pro62 and Lys68 to Leu74 in the interaction. Interestingly, Hashimoto *et al.* (1997) generated a fragment for rIGFBP-3, Glu52 to Ala92 which had 0.008% of the binding affinity of the full-length protein for IGF-II, and encompassed the residues defined by Kalus *et al.*, (1998). The inclusion of amino acids 1 to 51, in Hashimoto's rIGFBP-3 amino-terminal fragment, further increased the affinity of the fragment to around 4% of the full-length protein (Hashimoto *et al.*, 1997). Furthermore, deletion studies suggest that residues between Leu72 to Ser91 of hIGFBP-4, which correspond to residues Leu73 to Glu110 of hIGFBP-5 when the sequences are aligned (Figure 1.4), are critical for IGF binding (Qin *et al.*, 1998).

ii. Residues in the Central Domain

The studies discussed in this section are summarised in Figure 1.10b. Although the IGFBP-5 fragment 95-134 had no detectable affinity for either IGF when analysed by BIAcore™ (Kalus *et al.*, 1998), deletion of the central non-conserved region of recombinant human IGFBP-3 comprising residues 89 to 184, reduced IGF-I and IGF-II binding 40-fold (Firth *et al.*, 1998). Other substitution and deletion studies have shown residues in the mid-region which are not directly involved in IGF binding activity. Despite deletion of residues 94 to 119, or 121 to 141, human IGFBP-4 retains IGF-I and IGF-II binding activity to apparently normal levels (Qin *et al.*, 1998). The central region of binding proteins therefore may not have specific affinity for IGF alone, but may help keep the two cysteine-rich domains of the molecule in the correct conformation for growth factor binding. This view is supported

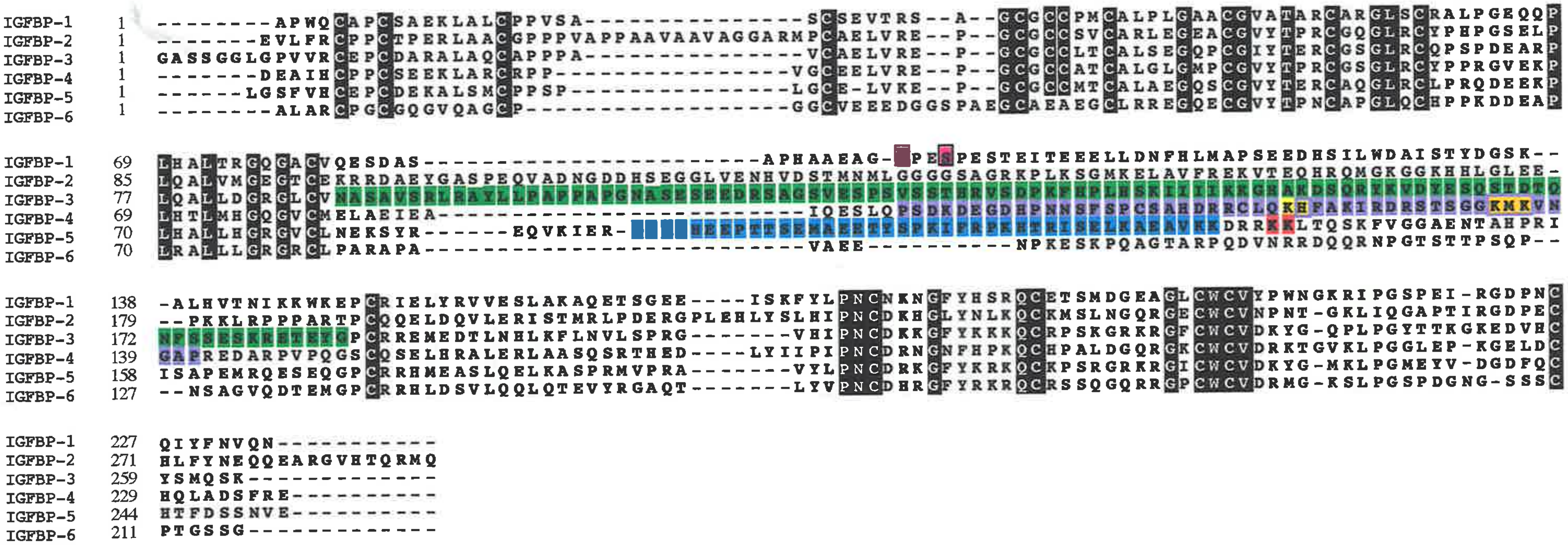

Figure 1.10b Sequence alignment of the 6 human IGFBPs, highlighting the central regions which were investigated for a role in IGF binding activity. Details of the studies can be found in Section 1.5.2. The regions which were studied on binding proteins isolated from different species are mapped onto the human protein. (PM)= point mutation, (F)= fragment, (Del)= a deletion.
IGFBP-1 (PM) Jones *et al.* (1993c); IGFBP-3 (Del) Firth *et al.* (1998); IGFBP-4 (Del) Qin *et al.* (1998);
IGFBP-4 (PM) Rees *et al.* (1997); IGFBP-4 (PM) Conover *et al.* (1995); IGFBP-5 (F) Kalus *et al.* (1998);
IGFBP-5 (PM) Imai *et al.* (1997)

through the work analysing the proteolysis of binding proteins where cleavage in this central region results in fragments with reduced IGF binding activity (see Sections 1.4.3 and 1.5.2).

Removal of cleavage sites through amino acid substitution of residues, predominantly located in the central region of the binding proteins, has not had a marked impact on the ability of the mutant molecules to interact with IGF. This has been confirmed by IGF-I solution binding assays with IGFBP-5 double mutant Lys138Asn, Lys139Asn (Imai *et al.*, 1997), and ligand blotting and solution binding assays with both IGF-I and IGF-II binding IGFBP-4 mutants Lys134Gln, Lys136Gln, Met135Leu and Met135Glu (Conover *et al.*, 1995). The double mutant IGFBP-4 molecule containing Lys120Asn and His121Asn maintains high affinity for IGF-I (Rees *et al.*, 1998). Substitution of residues, Ser98Ala and Ser101Ala, important for phosphorylation in IGFBP-1 did not affect the affinity of the molecule for IGF-I relative to non-phosphorylated IGFBP-1 (Jones *et al.*, 1993c). In summary, these results suggest that at least these residues in the central portion of the binding proteins are not major IGF binding determinants.

iii. Residues in the C-terminal Domain

The studies discussed in this section are summarised in Figure 1.10c. As discussed above in Section 1.5.2, it is clear that the amino-terminal domain of an IGFBP on its own is not sufficient for full binding function. The confusion for the role of the C-terminal end comes from conflicting reports on proteolytic fragments derived from the carboxy-terminal end of the binding protein, showing either an intrinsic binding ability (for example IGFBP-2, Ho and Baxter, 1997) or no binding function (for example IGFBP-5, Kalus *et al.*, 1998). Possible reasons for these differences are discussed below.

Solution binding assays of a recombinant C-terminal fragment of human IGFBP-3 (hIGFBP-3) comprising residues 151 to the carboxy-terminal end show the fragment binds to IGF-I (Spencer and Chan, 1995). Complementary to this, deletion of the C-terminal residues of hIGFBP-3, 185 to 264, markedly reduces affinity for IGF-I approximately 20-fold, and IGF-II 40-fold (Firth *et al.*, 1998). In contrast, C-terminal fragments from IGFBP-4 (Qin *et al.*, 1998) and IGFBP-5 (Kalus *et al.*, 1998) were observed to give different results. A glutathione S-transferase fusion carboxy-terminal fragment of human IGFBP-4, extending from either residue 121 or 142 to the final residue 237 was unable to interact with IGF (Qin

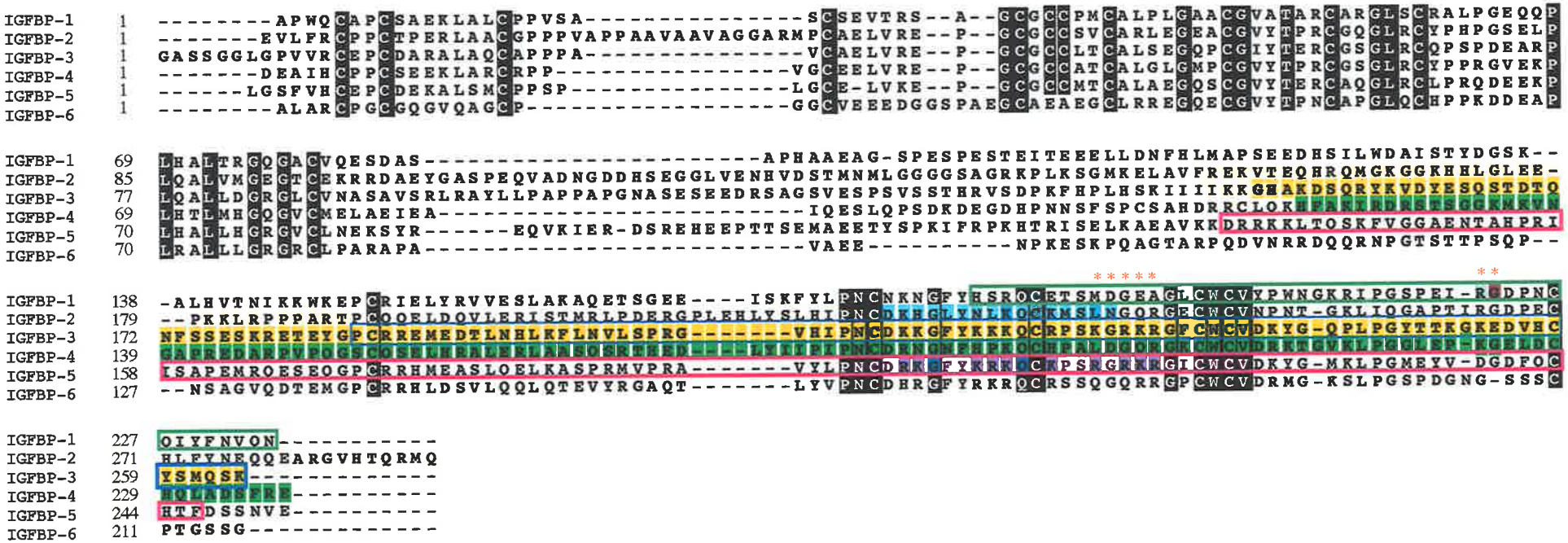

Figure 1.10c Sequence alignment of the 6 human IGFBPs, highlighting the C-terminal regions which were investigated for a role in IGF binding activity. Details of the studies can be found in Section 1.5.2. The regions which were studied on binding proteins isolated from different species are mapped onto the human protein. (PM)= point mutation, (F)= fragment, (Del)= a deletion, (Ab)= epitope where antibody binds and inhibits IGF binding.

IGFBP-1 (PM) Jones *et al.* (1993a); IGFBP-1 (PM) Brinkman *et al.* (1991b); IGFBP-1 (Ab) Schuller *et al.* (1993);
IGFBP-2 (Del) Forbes *et al.* (1998); IGFBP-3 (F) Spencer and Chan (1995); IGFBP-3 (Del) Firth *et al.* (1998);
IGFBP-3 (PM) Firth *et al.* (1998); IGFBP-4 (residues 121-237): Qin *et al.* (1998); IGFBP-5 : Kalus *et al.* (1998);
IGFBP-5 : Arai *et al.* (1996a); IGFBP-5 : Bramani *et al.* (1999) and Song *et al.* (2000)

et al., 1998). Similarly, a C-terminal fragment of IGFBP-5 was unable to bind to IGF (Kalus *et al.*, 1998). However, in both instances harsh reagents such as guanidine and urea were used in the isolation of these fragments for analysis (Qin *et al.*, 1998; Kalus *et al.*, 1998). Therefore, it may be possible that the fragments did not assume the correct structural conformation to enable IGF binding ability. Alternatively, in both of these instances, it may be that the important residues required for IGF binding were not present. Although the amino acid similarity and functional homology between the six different proteins suggest that the residues involved for IGF binding are similar, this may not be the case.

Knowledge of the disulphide bonding pattern for the C-terminal end of bIGFBP-2 was used in our laboratory to generate sequential truncations from the carboxy-terminal end to search for important IGF binding residues. Disulphide bond knowledge meant that deletions would not result in unpaired cysteine residues which could potentially disrupt protein structure, and impair binding (Forbes *et al.*, 1998). The removal of 14, 36 and 48 amino acid residues from the C-terminal end of bovine IGFBP-2 gave molecules which bound IGF essentially to the same extent as wild type protein (Forbes *et al.*, 1998). However, further removal of residues between 222 to 236 of bIGFBP-2 was accompanied by an 80-fold reduction in binding activity (Forbes *et al.*, 1998). In studies analysing hIGFBP-5, amino acid mutagenesis in its complementary region support the hypothesis that this amino acid stretch may be required for full IGF binding ability (Bramani *et al.*, 1999). Substitutions of conserved Gly203Lys and Gln209Ala, surrounding the heparin binding stretch, resulted in approximately 8- and 6-fold reduction in affinity for IGF-I respectively (Bramani *et al.*, 1999). In another study, removal of positively charged residues across the heparin binding stretch in hIGFBP-5, between Arg201 to Arg218, had minimal effects on the association constants for IGF-I (Arai *et al.*, 1996a). Mutagenesis of hIGFBP-3 residues, ^{228}KGRKR, to corresponding IGFBP-1 residues MDGEA (homologous to residues 235 to 239 of bIGFBP-2), did reduce normal IGF-II affinity 3-fold (Firth *et al.*, 1998). Generally mutations were found to have a greater impact on IGF-II than IGF-I binding (Firth *et al.*, 1998).

Mutagenesis performed further towards the C-terminal end of various IGFBPs has been shown to affect IGF binding activity. While mutation of Arg221Trp did not inhibit IGF-I binding activity (Jones *et al.*, 1993a), substitutions at Gly222 in the RGD integrin-binding

region of IGFBP-1 reduced IGF-I and IGF-II binding activity and resulted in dimer formation, suggesting structural change (Brinkman *et al.,* 1991b). Amino acid substitution performed in IGFBP-3 in the corresponding region, ^{253}KED, to homologous residues in IGFBP-1, RGD, reduced the affinity of IGFBP-3 for both IGFs between 4- and 6-fold (Firth *et al.*, 1998). Apart from substitutions to Cys226, other mutations in this region of IGFBP-1 were found to have little effect on IGF binding activity (Brinkman *et al.*, 1991b).

An alternative approach to determining residues involved in protein-protein interaction is to characterise the binding sites for antibodies which inhibit the two species binding to each other. Inhibition of IGF binding to IGFBP-1 was achieved by a monoclonal antibody binding to the C-terminal end of the binding protein (Schuller *et al.*, 1993). Mapping of the binding site showed that the epitope was located between C-terminal residues 188-234 (Schuller *et al.*, 1993). Although residue stretches 188 to 196 and 222 to 227 were implicated in the recognition regions for the antibody, the constructs used to define these regions were either known to cause conformational change in the protein (Brinkman *et al.*, 1991b) or could possibly exhibit change due to unpaired cysteine residues present in the deletion fragments.

1.6 This project

There is still a distinct lack of information regarding the IGF binding sites in the binding protein family. Much of the recent work has focussed on the amino-terminal end of the protein, suggesting a high affinity binding site in this region. The function of the C-terminal end however, is less well established.

As discussed in Section 1.5.2, there is evidence to suggest that the C-terminal end of IGFBP-2 contains sequences which enable IGF binding activity. Given that C-terminal deletion studies highlighted a region between residues 222-236 in bIGFBP-2 as being important for normal IGF binding activity (Forbes *et al.*, 1998), in this thesis the importance of this region has been investigated by performing amino acid mutagenesis studies.

During the course of this study, two approaches were used to analyse the importance of residues 221-236 of bIGFBP-2. Firstly, a monovalent phage display approach was selected to screen a bIGFBP-2 mutant library. This strategy can provide a powerful tool to screen large numbers of bIGFBP-2 variants, and is an approach which has been used successfully for

growth hormone (Lowman and Wells, 1993), and for many other proteins. After selecting a mutant library of bIGFBP-2 (mutated at amino acids 221-230) expressed on the surface of phage particles on IGF-II ligand, clones were randomly selected for DNA sequence analysis. Alignment of the DNA sequences showed that there were no clear sequence preferences to define which amino acids were important for IGF binding activity. Therefore, a number of bIGFBP-2 mutants were chosen for further characterisation.

Secondly, to circumvent problems associated with the phage display system, alanine-scanning mutagenesis was chosen to assess the role of residues 232-236 of bIGFBP-2 for IGF binding. The findings and implications of these studies are discussed.

Chapter Two

SECRETION AND PHAGE DISPLAY OF RECOMBINANT bIGFBP-2

2 Introduction

In Chapter 1, I described the deletion studies which were used in our laboratory to identify a C-terminal region involved in the IGF binding function of bIGFBP-2 (Section 1.5.2, Forbes *et al.*, 1998). Deletion studies such as these provide a preliminary approach to localising residues involved in protein-protein interactions. A loss in binding function prompts the following questions: Is the loss in binding because important residues directly involved in the interaction were removed? Alternatively, is the loss in binding due to a gross structural change, resulting from the removal of important structural components, which can then disrupt the entire protein conformation? Finally, is the reduction in binding due to a combination of both structural change and the removal of important binding residues? These possibilities can be further explored by creating amino acid substitutions, leaving the remaining protein intact, to look more closely at the role of particular amino acids in the binding interaction.

There are a number of approaches when looking at amino acid substitution studies, that can be used to answer the above questions. One strategy is to generate single amino acid substitutions, to look more closely at the involvement of each residue in a protein-protein interaction. Typically, amino acid substitutions involve changes to alanines, or to "safe" or conserved amino acid residues (Bordo and Argos, 1991). As discussed earlier, in Section 1.5.2, this has successfully been used in our laboratory to identify residues in the amino-terminal end of bIGFBP-2 involved in IGF binding (Hobba *et al.*, 1998), although many other examples of this approach have also been reported. For example the granulocyte colony stimulating factor receptor binding determinants have been determined (Young *et al.*, 1997) and the residues on the agouti protein that are involved in the melanocortin receptor binding have also been identified by these means (Kiefer *et al.*, 1997). A limitation when using amino acid substitution approach, is the need to make each individual plasmid construct, express and purify each mutant protein, and then characterise the mutated proteins by performing binding studies. Thus, although informative, this approach is labour intensive and can be difficult when investigating large numbers of amino acid residues. Furthermore, the amino acid substitutions which are created are confined to those which are predicted to be informative. The advances in molecular biology, both in polymerase chain reaction (PCR) and

other mutagenic strategies, has enabled large numbers of changes to be generated in protein sequences of interest. For example, cassette (Wells *et al.*, 1985) and random (Leung *et al.*, 1989) mutagenesis approaches are two well established techniques used to generate libraries of protein variants. More recently, the introduction of the rapid evolution of protein, using *in vitro* DNA shuffling (also called "sexual PCR", Stemmer, 1994), has enabled the generation of diverse libraries of protein sequences available for screening. The rapid development of mutagenesis procedures such as these, has met with the need to generate strategies that can be used to screen these libraries for desired properties.

In 1985, Smith's discovery that bacterial viruses could display foreign amino acid sequences on their coat proteins (Smith, 1985) opened the door to a new field of protein and peptide analysis. This important paper facilitated the development of a technique called "phage display" (described below) to aid in the selection of particular peptides or proteins from large pools of protein variants (Smith, 1985; Parmley and Smith, 1988). The discovery of phage display has led to its use for the study of antibodies (McCafferty *et al.*, 1990), enabling the *in vitro* maturation of binding to target antigens (reviewed in Dall'Acqua and Carter, 1998). Such a technique reduces the need for animal work and the long and expensive immunisations typically performed in the generation of antibodies. Phage generated antibodies are especially useful where the immunogen is toxic to the host or immunosuppressive. New binding functions have also been selected for in structured amino acid sequences other than antibodies (reviewed in Smith, 1998). Other important uses for phage display include the generation of peptide agonists/antagonists to proteins and receptors (reviewed in Kay *et al.*, 1998), the screening of protease specificities and for better protease catalytic function (reviewed in Lien *et al.*, 1999) and generally improving protein-ligand interactions (reviewed in Katz, 1997). Filamentous phage display has also been adapted to study protein stability and protein folding (reviewed in Forrer *et al.*, 1999). Finally, the ability of phage particles to promote a good immune response when injected into animals has meant that proteins which are normally difficult to generate antibodies against can be fused to the phage surface to promote antibody production (reviewed in Perham *et al.*, 1995). Following Smith's discovery that peptides could be displayed by filamentous phage particles (Smith, 1985), the generation of numerous other protein display systems which, like phage display, link protein to their coding DNA

sequences have been developed. Some of these systems involve protein display on other prokaryotic viral particles including lambda phage (Maruyama *et al.*, 1994; Mikawa *et al.*, 1996) and the T7 phage (Rosenberg *et al.*, 1996), and eukaryotic viral display systems, one of which uses the baculovirus *Autographa californica* (Boublik *et al.*, 1995). Other non-viral based systems include the expression of peptides and protein sequences on the *E. coli* outer membrane proteins OmpA (Francisco *et al.*, 1993) and LamB (Charbit *et al.*, 1987; Brown, 1992). Variable peptide sequences have also been linked to their plasmid-encoded DNA sequences by fusing peptides to the lac repressor protein and placing the lac repressor binding site into the plasmid (Cull *et al.*, 1992). Another important alternative approach is the polysome display of peptide (Mattheakis *et al.*, 1994) and protein (Hanes and Pluckthun, 1997) libraries. In polysome display, mRNA and nascent peptide complexes are generated by an *in vitro* transcription/translation system containing large libraries of random DNA sequences (Mattheakis *et al.*, 1994; Hanes and Pluckthun, 1997). This range of different approaches provides other systems when filamentous phage are not suitable for the display of particular proteins. For example, the filamentous phage system may be limiting when eukaryotic proteins require complex folding pathways and post-translational modifications, such as glycosylation, for their function. Another limitation for the display of proteins on the surface of filamentous phage is that the protein must be able to be secreted into the bacterial periplasm (reviewed in Marks *et al.*, 1992). Thus, the lambda and T7 phage display systems outlined above, complement the filamentous phage approach. The lambda and T7 viral proteins are not secreted through the bacterial periplasm and therefore may be better suited for the study of cytoplasmic proteins (Mikawa *et al.*, 1996; Rosenberg *et al.*, 1996).

For the analysis of IGF binding epitopes on bIGFBP-2, a filamentous phage display system was selected. This system was thought suitable because IGFBP contains disulphide bonds, and therefore would be required to be secreted into the periplasm for disulphide bond formation. Furthermore, IGFBP-2 is not glycosylated and is not reported to require other forms of post-translational modification for its function *in vivo* (Jones and Clemmons, 1995), thus making it suitable for expression in *E. coli*. Finally, bIGFBP-2 has been extensively studied regarding its affinities for the different IGFs (Forbes *et al.*, 1988; Szabo *et al.*, 1988; Bourner *et al.*, 1992) making it a suitable system to be further examined.

Phage display is introduced below, in the context of its use for analysing protein-ligand interactions. This theme is used to provide the reader with an understanding of how the system can function in the study of the IGFBP-IGF interaction.

2.1 Overview of filamentous phage and phage display

The technique of phage display involves the manipulation of bacterial viral particles (bacteriophage or phage) such that they express protein on their surface whilst packaging the DNA encoding for the protein within the body of phage particle. Therefore, by generating a library of phage particles expressing variant peptides or proteins on their surface, it is possible to select for interesting protein properties using a technique called panning (Parmley and Smith, 1988). Panning is achieved by coating a surface with, for example, a desired ligand and then exposing the phage to this surface to allow binding to occur (Parmley and Smith, 1988; Figure 2.1). After binding, the surface is washed to remove unbound phage (Figure 2.1). The bound phage can then be eluted with, for example, acid which disrupts the protein-protein interaction and allows recovery of phage (Figure 2.1). These particles can be used to reinfect bacterial cells, be reamplified, and can then be subjected once more to the same panning procedure. After each round of panning, a sample of phage particles can be analysed through DNA sequence analysis, in order to identify the protein sequence which facilitated binding to the chosen ligand. With progressive selection, the optimal binding sequences can be determined. These protein variants can then be analysed for their ligand binding properties in more detail.

A schematic diagram, showing the structure of a filamentous phage particle is summarised in Figure 2.2. The filamentous phage is made up of a closed, circular, single stranded DNA molecule coated in protein, which is encoded for by the phage DNA. The proteins on the surface of the particle include the major coat protein, gene VIII protein (gVIIIp), and the minor coat proteins, gene III protein (gIIIp), gene VI protein (gVIp), gene VII protein (gVIIp) and gene IX protein (gIXp) (reviewed in Rasched and Oberer, 1986). The other proteins encoded for by the phage DNA (products from genes *I*, *II*, *IV* and *V*) are used for the production of phage particles, but are not incorporated into the final product (reviewed in Rasched and Oberer, 1986). Phage particles are assembled as they are secreted from the bacterial cell (reviewed in Russel, 1991). The gVIIIp coats the majority of the phage DNA,

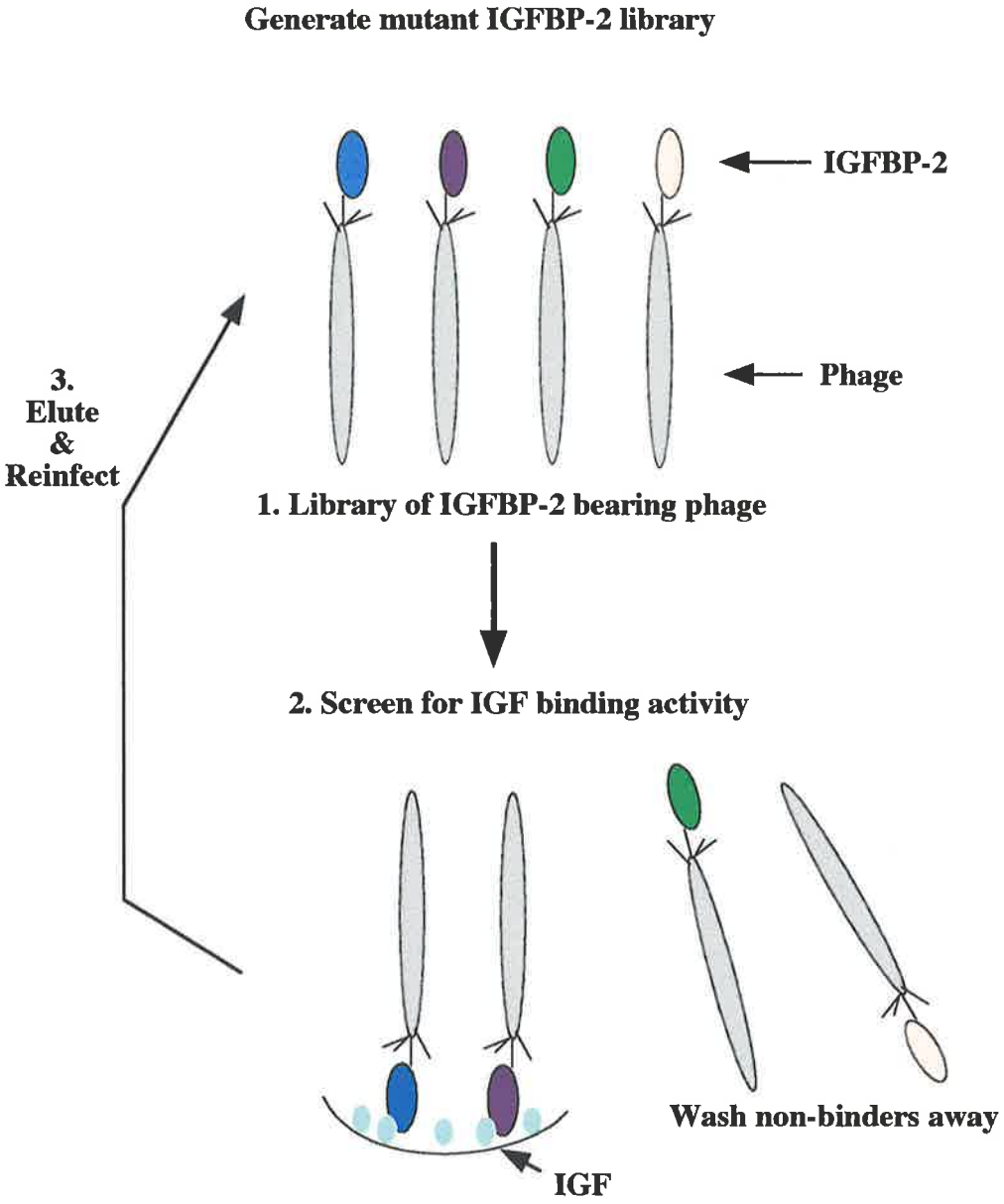

Figure 2.1 Schematic overview of the panning procedure used for selecting phage with desired ligand binding properties. The figure uses the example of bIGFBP-2 fused at low valency to the surface of gIIIp, which is the system that is used in this study. In this example, mutant binding proteins are selected by their ability to interact with insulin-like growth factor, which is bound to 96 well microtitre plates. In step 1, a library of mutations is created in bIGFBP-2, and the mutant proteins are expressed on the surface of the phage. The phage are prepared from the medium using PEG-precipitation. In step 2, the phage are screened on their ability to bind to IGF. After washing, the phage can be eluted using acid, and the eluted particles can be used to reinfect bacterial cells (step 3).

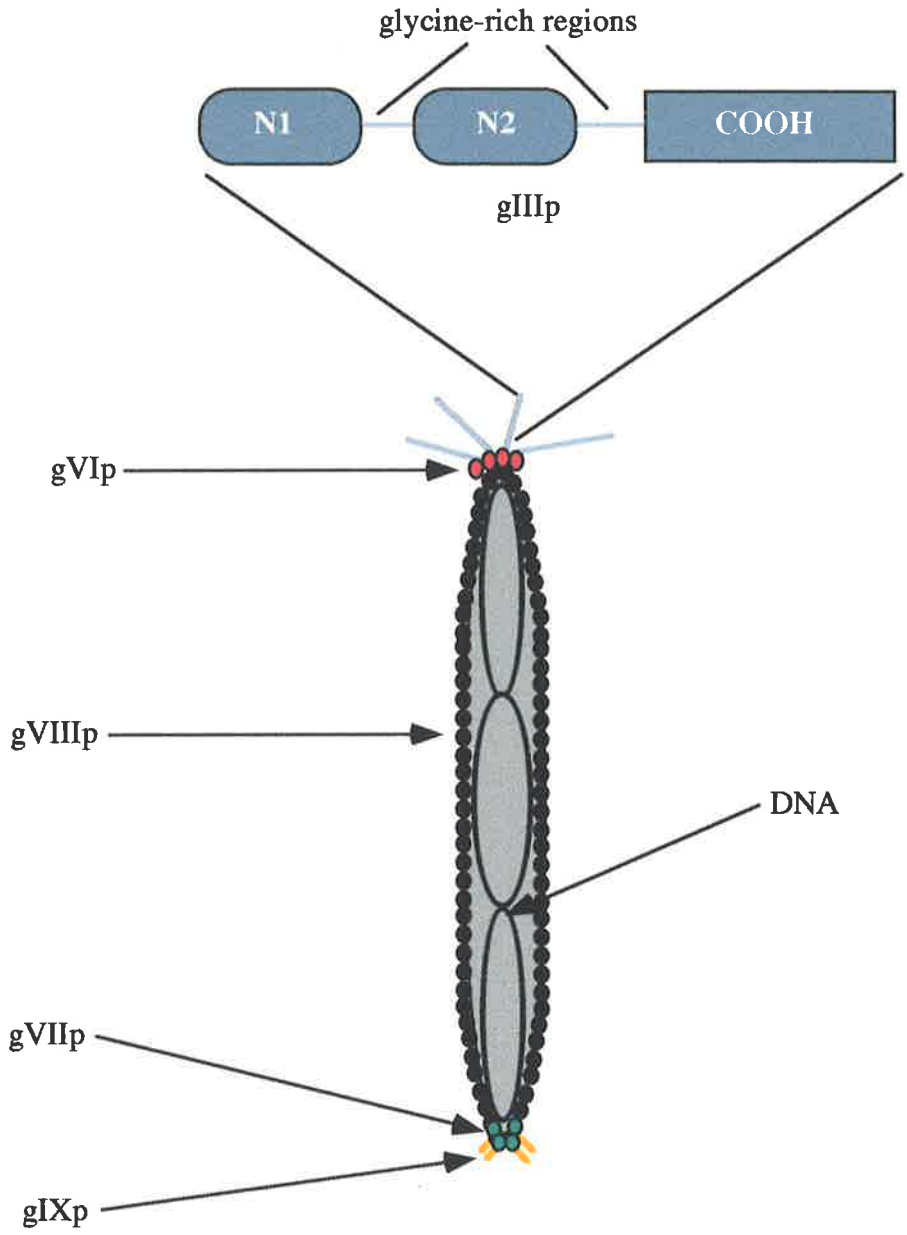

Figure 2.2 Schematic representation of a filamentous phage particle, showing the coat proteins and their distributions on the surface of the phage. The filamentous phage particle comprises a single stranded DNA molecule coated in protein. The major coat protein, which consists of approximately 2700 copies, is gVIIIp. The minor coat proteins located at the ends of the phage particle are gIIIp, gVIp, gVIIp and gIXp.

existing at approximately 2700 copies per viral particle (Newman *et al.*, 1977). Each minor coat protein occurs on average between three to five copies per phage particle (Woolford *et al.*, 1977; Goldsmith and Konigsberg, 1977; Simons *et al.*, 1981). These proteins are located at the polar ends of the particle, with gIIIp and gVIp being located at one end and gVIIp and gIXp at the other (Goldsmith and Konigsberg, 1977; Grant *et al.*, 1981; Simons *et al.*, 1981). Phage require gIIIp to infect bacterial cells. The amino-terminal region of gIIIp is required to produce infective phage particles (Armstrong *et al.*, 1981; Crissman and Smith, 1984) whilst the carboxy-terminal region is required to produce single unit length phage (Crissman and Smith, 1984). The infection process is a result of gIIIp attachment to the F-pilus (Jacobson, 1972) and the TolA surface protein (Click and Webster,1997; Riechman and Holliger,1997) present on *E. coli*.

Phage display can be achieved because the amino-terminal ends of the phage surface proteins, gIIIp and gVIIIp, are able to tolerate the insertion of foreign protein sequences (Smith, 1985; Ilichev *et al.*, 1989). gIIIp is a protein composed of three domains: N1, N2 and the carboxy-terminal region, joined together by two glycine rich linkers (Figure 2.2). The N1 region is involved in binding to TolA (Riechman and Holliger,1997; Lubkowski *et al.*, 1999), the N2 region to the F-pilus (Stengele *et al.*, 1990) and the carboxy-terminal end is responsible for anchoring gIIIp into the phage and for producing phage of normal unit length (Crissman and Smith, 1984). Proteins have been expressed both at the amino-terminal end of gIIIp (Hoogenboom *et al.*, 1991) and on variants lacking the amino-terminal region of the protein (where N1 and most of N2 are removed) (Bass *et al.*, 1990; Barbas *et al.*, 1991). In both instances, the presence of intact gIIIp (fusion protein-free) on the surface of the phage can compensate for the defective gIIIp fusion protein which may result from the insertion of large protein sequences, to produce infective phage particles (Bass *et al.*, 1990; Barbas *et al.*, 1991; Hoogenboom *et al.*, 1991). Furthermore, the insertion of large protein sequences into these regions has not been reported to affect the assembly of the gIIIp fusion protein onto the surface of the phage particle. Therefore, the limiting factor for gIIIp protein display is that the phage particle must retain intact copies of gIIIp to remain infective. gVIIIp is made up of two α-helices with the amino-terminal 5 residues being exposed free at the surface of the protein and of the phage particle (reviewed in Makowski, 1994). Insertion into the amino-terminal residues

has been possible, but is limited to approximately six amino acids when all copies of gVIIIp contain the fusion sequence (Greenwood *et al.*, 1991; Iannola *et al.*, 1995). However, by interspersing the gVIIIp fusion protein with gVIIIp that is not fused to protein, it has been possible to express large proteins such as antibody Fab fragments on the major coat protein (Kang *et al.*, 1991). Therefore, the limiting factor is not that gVIIIp cannot tolerate foreign gene insertions. Rather, it appears that the problem lies in the packaging of the phage containing large gVIIIp fusion proteins, as stable intact particles can only be produced if sufficient unfused gVIIIp is present (reviewed in both Makowski (1994), and in Perham *et al.*,(1995)).

Three approaches can be used to attach a protein or peptide onto either gIIIp or gVIIIp on the surface of filamentous phage (Figure 2.3; Smith, 1993). Phage display approaches involving the insertion of foreign DNA sequence immediately after *geneIII* or *geneVIII* in the phage DNA are called the type 3 and type 8 systems (Figure 2.3; Smith, 1993). Consequently, all copies of gIIIp or gVIIIp contain the fusion protein (polyvalent display). Two other systems can be used to reduce the amounts of fusion protein being displayed on the surface of the phage particle. The phage DNA can be engineered to contain both a normal copy of either *geneIII* or *geneVIII*, and an additional copy of either gene fused to DNA encoding the protein of interest (gIIIp display: type 33 and gVIIIp display: type 88) (Figure 2.3; Smith, 1993). Alternatively, the level of fusion protein display can be reduced by having the entire phage genome in the presence of a modified plasmid (phagemid) containing the protein fused to a copy of either gIIIp or gVIIIp (type 3+3 or type 8+8 systems) (Figure 2.3; Smith, 1993). To achieve this form of phage display, the phagemid is grown in the presence of intact phage DNA (provided by a helper phage) to supply all of the essential proteins required to produce viable phage. The development of the phagemid was facilitated by the discovery that a plasmid containing the intergenic region of filamentous phage DNA could be packaged in single stranded form in the presence of normal phage, encoding for the viral proteins (helper phage) (Dotto *et al.*, 1981).

The ability to control the amount of protein or peptide displayed on the surface of phage particles has important implications. Firstly, high levels of protein display may be useful to increase the chances of capturing molecules which exhibit a low affinity for a particular ligand (Cwirla *et al.*, 1990), as may be the case with short peptide sequences. It is also more likely

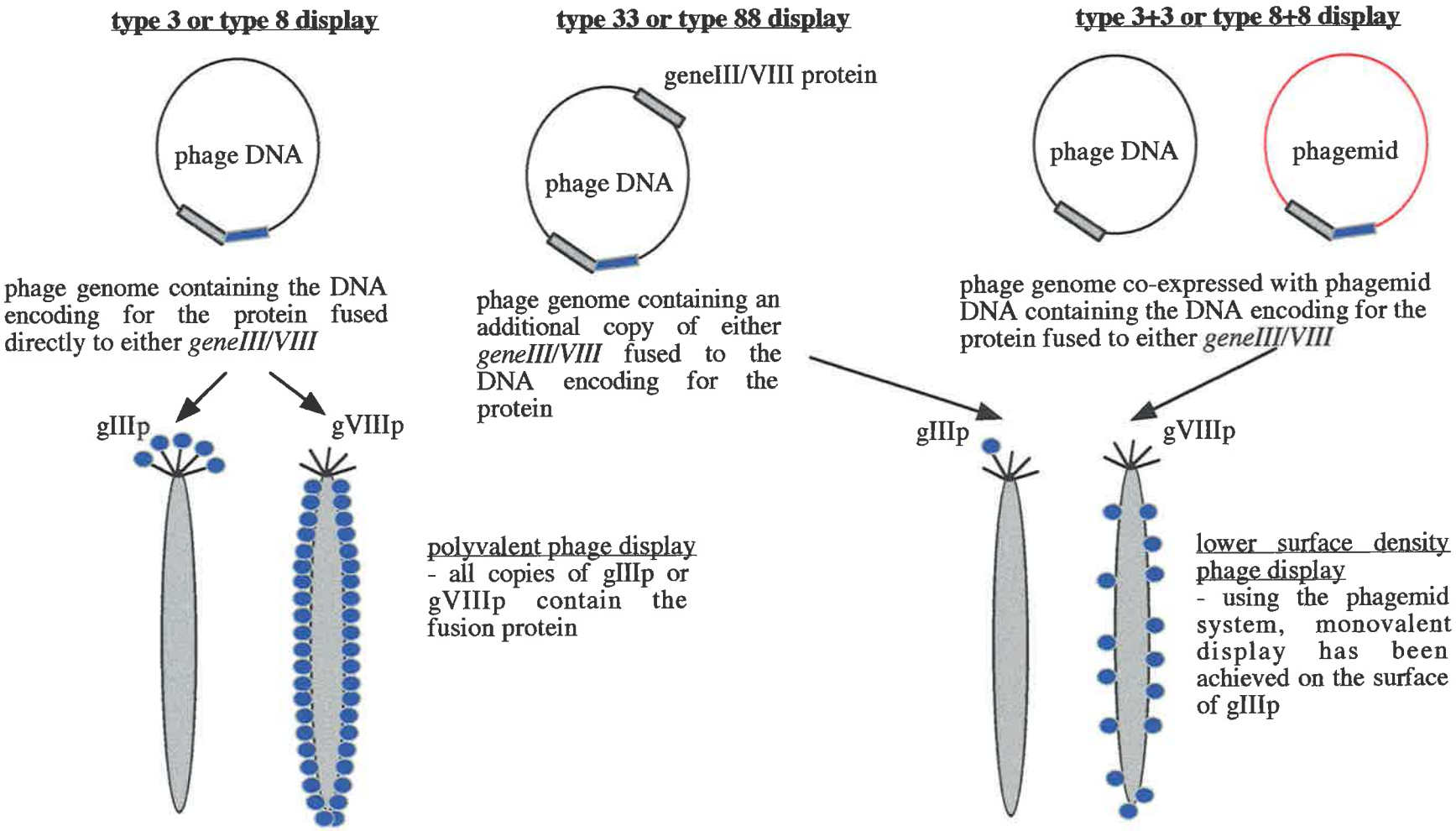

Figure 2.3 Overview of the systems available for phage display. The systems are described in Smith (1993). The type 3 approaches use gIIIp and the type 8 approaches use gVIIIp for protein display. In the type 3+3 or type 8+8 systems, phagemid DNA is preferentially packaged into the phage particles when the helper phage M13K07 is used. This occurs because the DNA for M13K07 contains mutations which reduce its packaging efficiency (Vieira and Messing, 1987).

that rare protein sequences present in a large library of different mutant proteins will be retained through the screening process. Although there are benefits to polyvalent display, there are also problems associated with using this approach. Multiple point attachment can enhance the binding of phage particles to target proteins (avidity) due to the display of peptides on all copies of gVIIIp (Cwirla *et al.*, 1990). This has hindered the separation of peptides exhibiting moderate affinities from those having higher affinities for a target protein (Cwirla *et al.*, 1990). Also as discussed above, the insertion of large amino acid sequences into either gIIIp or gVIIIp can result in phage which are not viable. By using the types 33, 88, 3+3 or 8+8, which result in the production of phage carrying both fused and unfused gIIIp or gVIIIp, the problems associated with polyvalent protein display on the surfaces of filamentous phage can be overcome (Figure 2.3).

For this project, a phagemid containing DNA encoding gIIIp was chosen for the display of bIGFBP-2 (Figure 2.4). The decision to use such a system was predominantly influenced by the work performed on human growth hormone (Bass *et al.*, 1990). Bass and colleagues, fused growth hormone onto gIIIp using the type 3+3 system to avoid the avidity effects, therefore enabling the selection of variants of human growth hormone that have strong receptor binding affinity (monovalent display; Figure 2.3) (Bass *et al.*, 1990). This monovalent system has resulted in the isolation of human growth hormone variants with higher binding affinities for the receptor than the native protein (Lowman *et al.*, 1991; Lowman and Wells, 1993). Similarly, monovalent phage display has been used to produce a variant of atrial natriuretic peptide that binds selectively to only one of its receptors (Cunningham *et al.*, 1994).

The choice to use the phagemid to achieve the display of proteins on filamentous phage, extends beyond the ability to display bIGFBP-2 at a lower valency. Firstly, plasmids can be transformed to high efficiencies in *E. coli* (Dower *et al.*, 1988) and therefore can be used to generate large libraries of protein mutants. Furthermore, it has been noted that DNA sequences inserted directly into phage DNA can be quite unstable and readily lost (Vieira and Messing, 1987). Therefore, phagemids may provide more stable alternatives to the use of normal phage DNA.

In this chapter, we show that bIGFBP-2, a 31 kDa protein with nine disulphide bonds, can be efficiently secreted and refolded in the *E. coli* periplasm. The bIGFBP-2 is displayed as

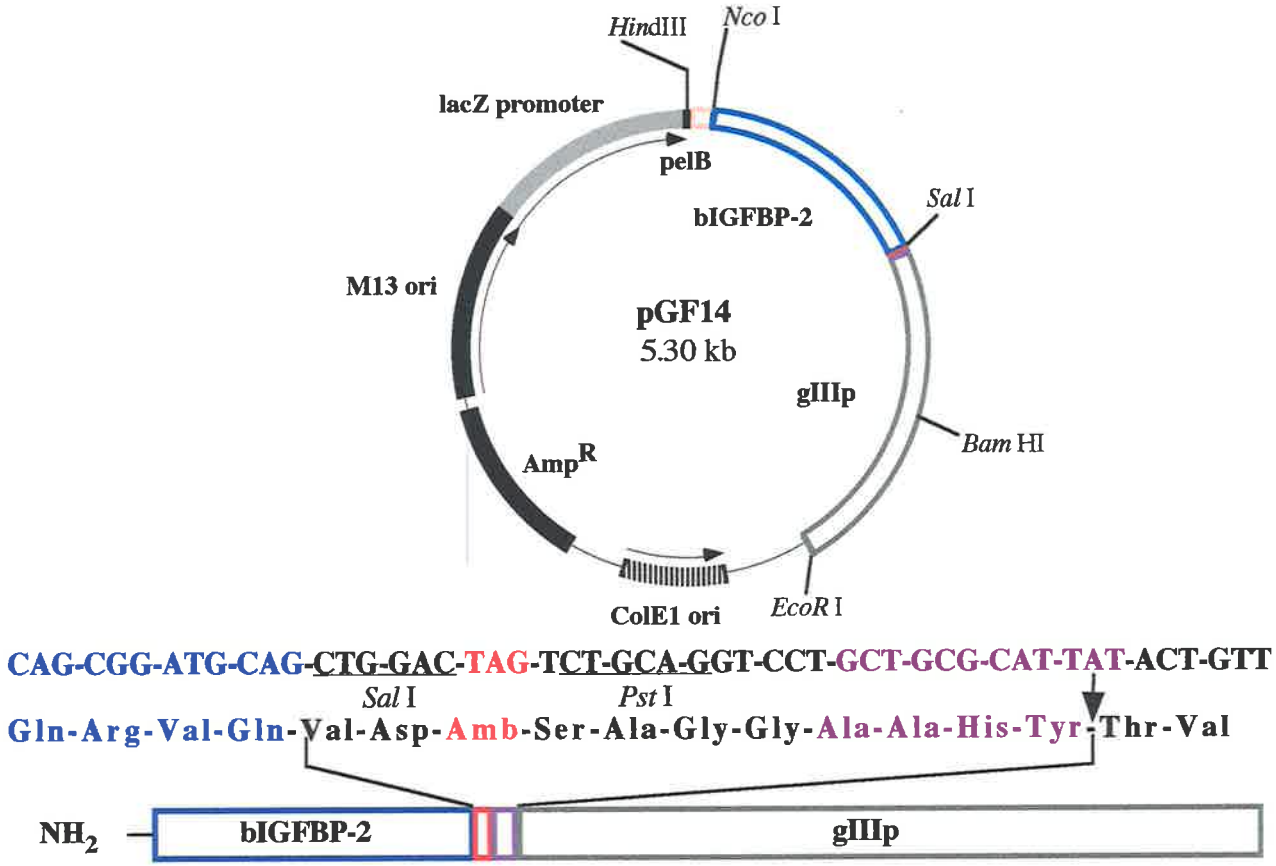

Figure 2.4 Phagemid pGF14, used to express bIGFBP-2 on the surface of filamentous phage. The vector contains an inducible *lacZ* promoter and DNA encoding for the pelB signal sequence for secretion of products to the periplasm. The translation originates at the pelB leader sequence, which is removed during secretion to generate bIGFBP-2. The phagemid is based on the vector pHEN1 (Hoogenboom *et al.*, 1991). However, in pGF14 the c-myc tag has been replaced by an H64A subtilisin cleavage site between bIGFBP-2 and gIIIp. The nucleotides coding for this cleavage site are placed 3' of an amber stop codon, resulting in production of bIGFBP-2 in a non-suppressor host, and the illustrated product after expression in a *supE* host strain. The H64A subtilisin site is indicated with an arrow.

an IGF binding molecule on filamentous phage using the pHEN1 (Hoogenboom *et al.*, 1991) derivative, pGF14 (Figure 2.4). Furthermore, the bIGFBP-2 bearing phage can be specifically enriched using immobilised IGF-II as a ligand.

2.2 Materials

The plasmid pHEN1 was obtained from Dr Peter Hudson (CSIRO, Division of Biomolecular Engineering, Parkville, Vic., Australia). Oligonucleotides were synthesised by Geneworks Pty Ltd (Adelaide, SA, Australia). Restriction enzymes were supplied by Pharmacia BioTech (Uppsala, Sweden) and H64A subtilisin was sourced from Genentech Inc. (South San Francisco, CA, USA). T4 DNA ligase was purchased from Roche Diagnostics (Castle Hill, NSW, Australia). PCRs were performed using Pyrostase (Molecular Genetic Resources, Tampa, FLA, USA), and the DNA sequencing enzyme, Sequenase® (Version 2.0), was sourced from United States Biochemicals (Cleveland, Ohio, USA). α-^{35}S or α-^{32}P dATP were purchased from Geneworks Pty Ltd (Adelaide, SA, Australia). Geneclean® was sourced from BIO 101 Inc. (CA, USA).

Membranes used for filtration of bacterial expression medium were Whatman® GD1UM filters (Whatman International Ltd, Maidstone, England). All other membrane filters were purchased from Millipore Corp. (Bedford, MA, USA). Nitrocellulose membrane used in Western blots was sourced from Schleicher & Schuell (Dassel, Germany). Western transfer was performed using a Multiphor II Novablot electrophoretic transfer unit (Pharmacia, Uppsala, Sweden). Pre-siliconised tubes (Sorenson BioScience Inc., Salt Lake City, USA) were used for collection of purified bIGFBP-2 protein, and for storage of lyophilised samples, to minimise protein loss. Acrylamide and bisacrylamide were obtained from Bio-Rad (Hercules, CA, USA) and Rainbow™ [^{14}C] methylated protein molecular weight markers were obtained from Amersham Pharmacia Biotech Pty Ltd (Castle Hill, NSW, Australia). All gels were cast and run using the Mini-Protean II Gel system from Bio-Rad.

Recombinant human IGF-I, long IGF-I and IGF-II were obtained from GroPep Pty Ltd (Adelaide, SA, Australia), mammalian derived bIGFBP-2 was prepared as described by Hobba *et al.*, 1996. Both ^{125}I IGF-I and ^{125}I IGF-II were kindly provided by Spencer Knowles and Kirsty Quinn from the Cooperative Research Centre for Tissue Growth and Repair (Adelaide,

SA, Australia). Affi-Gel® 10 gel was obtained from Bio-Rad. Both affinity and size exclusion chromatography were performed using the High Precision Pump P-500 system (Pharmacia Biotech, Uppsala, Sweden), with an online Pharmacia UV-1 monitor set at 280 nm. Reverse-phase high performance liquid chromatography (HPLC) was performed using two Waters 510 HPLC pumps (Waters, Sydney, NSW, Australia) with an online Waters 486 Programmable Multi-wavelength Detector set at 215nm. The 96-well plates used for the phage panning procedures were purchased from Costar (catalogue number 2595, Costar, Cambridge, MA, USA). Filamentous M13K07 helper phage were obtained from Stratagene. Bacto® tryptone and yeast extract products were obtained from DIFCO Laboratories (MI, USA).

All other reagents used were of analytical grade or higher. The following chemicals were obtained from Sigma Chemical Co. (St Louis, MO, USA): agarose (type I), ammonium persulphate, ampicillin (Amp), bovine serum albumin (BSA), Coomassie Brilliant Blue R-250, ethidium bromide, kanamycin (Kan), magnesium chloride, phenylmethylsulfonyl fluoride (PMSF), polyoxyethylene-sorbitan monolaurate (Tween-20), ribonuclease A (RNAse A), protamine sulphate, sodium dodecyl sulphate (SDS), N,N,N',N'-tetramethyl ethylene-diamine (TEMED) and Tris-(hydroxymethyl)aminomethane (Tris). Special grade phenol was purchased from Wako Pure Chemicals Industries Ltd (Osaka, Japan). Acetic acid, acetonitrile (far-UV grade), activated charcoal, chloroform, ethanol (RNAse-free), ethylenediaminetetraacetic acid (disodium salt) (EDTA), gelatin, glycine, potassium acetate, polyethylene glycol 6000 (PEG), sodium chloride (NaCl), disodium hydrogen orthophosphate, sodium dihydrogen orthophosphate and Triton X-100 were supplied by BDH chemicals Pty Ltd (Kilsyth, Vic., Australia). Isopropyl-β-D-thiogalactopyranoside (IPTG) was obtained from Diagnostic Chemicals Ltd, Charlottetown, Prince Edward Island. Sequencing grade trifluoroacetic acid (TFA) was obtained from Perkin Elmer (Applied Biosystems Division, Warrington, Great Britain).

2.2.1 Buffers, solutions and media

The growth media, phage solutions and gel running buffers were prepared by Mrs Jacquelyn Brinkman (Central Services Unit, Department of Biochemistry, University of Adelaide) using the methods described in Sambrook *et al.*, (1989). All solutions were made in

redistilled water filtered using the Milli-Q Ultra Pure Water System (Millipore Pty Ltd, North Ryde, NSW, Australia). Solutions marked (§) were sterilised by autoclaving.

Bacterial growth media and buffers

2YT (§)
1.6% (w/v) Bacto® tryptone, 1% (w/v) Bacto® yeast extract, 0.5% (w/v) NaCl
-adjusted to pH 7.0 with NaOH

Luria-Bertani plates (L plates) (§)
1% (w/v) Bacto® tryptone, 0.5% (w/v) Bacto® yeast extract, 1% (w/v) NaCl, 1.5% Bacto® agar
-adjusted to pH 7.0 prior to the addition of agar

Soft YT agar (§)
2YT medium, 0.7% (w/v) agar

Periplasmic Extraction Buffer (§)
10 mM Tris, pH 8.5, 1 mM EDTA

Solutions for DNA procedures

PCR reaction buffer (§)
50 mM Tris, pH 9.0, 20 mM $(NH4)2SO4$, 0.005% BSA, 0.25 mM dNTPs, 3 mM $MgCl_2$

Tris Borate EDTA (TBE) (§)
0.09 M Tris, 0.09 M boric acid, 2.5 mM EDTA

Tris Acetate EDTA (TAE) (§)
0.04 M Tris, 0.02 M sodium acetate, 1 mM EDTA

Ethidium bromide stain *(working stock)*
0.1 mg/ml ethidium bromide prepared in distilled water

10x DNA loading dye
50% (v/v) glycerol, 0.25% (w/v) bromophenol blue, 0.25% (w/v) xylene cyanol FF

Tris EDTA (TE) (§)
10 mM Tris, pH 7.5, 0.1 mM EDTA

Protein electrophoresis and protein transfer buffers

5x sample loading dye
312 mM Tris, pH 6.8, 12.5% (w/v) SDS, 50% (v/v) glycerol, 0.05% (w/v) bromophenol blue

Gel running buffer (§)
250 mM glycine, 25 mM Tris, pH 8.3, 0.1% (w/v) SDS

Blot buffer (§)
10 mM Tris, pH 7.5, 150 mM NaCl

Gel fixing solution
50% (v/v) ethanol, 10% (v/v) acetic acid

Gel destain
10% acetic acid

Protein transfer buffer
20 mM Tris, pH 7.5, 150 mM glycine, 20% (v/v) ethanol

Coomassie stain
0.3% (w/v) Coomassie Blue R-250, 10% (v/v) acetic acid

Gel drying solution
5% (v/v) glycerol, 30% (v/v) ethanol

Solutions for filamentous phage work

Phage precipitation stock solution (§)
20% (w/v) PEG, 2.5 M NaCl

Phage Storage Buffer (PSB) (§)
10 mM Tris, pH 7.4, 10 mM $MgCl_2$, 100 mM NaCl, 0.05% gelatin

H64A subtilisin cleavage buffer (§)
20 mM Tris, pH 8.5, 100 mM NaCl

Phosphate Buffered Saline (PBS) (§)
10 mM sodium phosphate, pH 7.4, 150 mM NaCl

PBS tween (PBST)
PBS, 0.1% (w/v) BSA, 0.05% (v/v) Tween-20

Chromatography solutions

Superose® 6 column buffer
10 mM sodium acetate pH 7.0, 150 mM NaCl, 0.05% (w/v) Tween-20
-filtered using 0.45 µm filter

Affinity column buffer
50 mM Tris pH 6.5, 150 mM NaCl, 0.05% (v/v) Tween-20
-filtered using 0.45 µm filter

HPLC buffer A
0.1% (v/v) TFA
-filtered using 0.2 µm filter

HPLC buffer B
80% acetonitrile, 0.088% TFA
-filtered using 0.2 µm filter

Charcoal binding assays

Charcoal binding assay buffer (CBA)
0.2 M sodium phosphate, pH 6.5, 150 mM NaCl, 0.25% (w/v) BSA
made fresh prior to use

Activated charcoal mix
CBA, 0.5% (w/v) activated charcoal, 0.02% (w/v) protamine sulphate
made fresh and stirred for at least 1 hour at 4°C prior to use

2.2.2 Bacterial strains

The genotypes of the *E. coli* strains used in this study are described below:

E. coli JM101: *supE thi-1 Δ(lac-proAB) [F' traD36 proAB lacI^{q}Z ΔM15]*

E. coli HB2151: *ara Δ(lac-proAB)thi [F' proAB lacI^{q}Z ΔM15]*

E. coli BL21: *E. coli* B F$^-$ *dcm ompT hsdS*($r_B^- m_B^-$) *gal*

2.3 Methods

2.3.1 DNA preparation techniques

Plasmid DNA was prepared using the alkaline lysis procedure described in Sambrook *et al.*, (1989). Digested DNA fragments were purified from agarose gel, by extraction using either Geneclean® (protocols and solutions supplied by the manufacturer) or the "freeze-squeeze" method (outlined below). Bands to be eluted were separated on agarose gel and were excised from the gel under short wave UV light. For the "freeze-squeeze" method, the gel fragment was frozen at -20°C. Immediately upon thawing, the gel fragment was squeezed through a 0.45 mm needle, using a 1 ml syringe, to facilitate the disruption of the agarose gel. The gel-DNA slurry was placed onto siliconised glass wool contained within a 0.5 ml Eppendorf tube, and the barrel of the syringe was rinsed with 3 x 100 µl of TAE to retrieve any residual sample. Incubation of the mix at room temperature for 15 minutes enabled the DNA to be eluted from the agarose gel. The agarose was then separated from the DNA by piercing the base of the Eppendorf tube and placing this tube into a 1.5 ml tube. This was spun at 9980 x g for 2 minutes and the 0.5 ml tube, containing the glass wool and agarose, was discarded. The DNA was precipitated by the addition of 1/10th of the volume of 3 M sodium acetate pH 5.2 and 2 x the volume of ice cold RNase-free absolute ethanol. The DNA was pelleted by centrifugation at 9980 x g for 40 minutes at 4°C. The pellet was washed in 80%

ethanol, and vacuum dried. The DNA was then resuspended in an appropriate volume of distilled water for further manipulation.

2.3.2 Plasmid constructions

The construction of the phage display vector pGF14 was performed by Dr Goran Forsberg and Mrs Sally Grosvenor in the Department of Biochemistry, University of Adelaide. To enable cloning of the DNA coding for bIGFBP-2 into the phage display vector, unique restriction sites were introduced into the bIGFBP-2 cDNA (cloned by Upton *et al.*, 1990) using site-directed mutagenesis on single stranded uracil containing DNA (Mutagene kit, Bio-Rad, Hercules, CA, USA). A 5' *Nco* I site and a 3' *Sal* I site were introduced into the DNA with oligonucleotides 4617 and 4618 (Table 2.1) respectively, and the 853 base pair *Nco* I/*Sal* I bIGFBP-2 coding fragment was cloned into the phagemid expression vector pHEN1 (Hoogenboom *et al.*, 1991), to produce the phagemid pHEN/bBP-2. To construct the phagemid pGF14 (Figure 2.4), the plasmid pHEN/bBP-2 was further modified by PCR. A modified fragment for subcloning into the vector was generated in a 20 µl final volume using 100 ng of each oligonucleotide 9138 and 9139 (Table 2.1), 10 ng pHEN/bBP-2, PCR reaction buffer and 1 unit Pyrostase. The reactions were performed using 40 cycles, comprising denaturation for 3 minutes at 94°C and annealing and extension for 3 minutes at 68°C. The resulting PCR product was digested with *Sal* I and *Bam* HI to yield a 620 base pair fragment which was gel purified and ligated into *Sal* I and *Bam* HI digested pHEN/bBP-2. This derivative of pHEN/bBP-2 lacks the *c-myc* reporter gene, enabling the expression of mature bIGFBP-2 without a C-terminal fusion which could interfere with bIGFBP-2 function. Instead, an amber stop codon (TAG) has been positioned directly after the *Sal* I cloning site followed by a sequence coding for a flexible linker with a H64A subtilisin (Carter *et al.*, 1989) cleavage site. The H64A subtilisin site allows for the enzymatic elution of phage during panning procedures.

primer	sequence (5'– 3')
4617	AACCAGCGGATGCAG**GTCGAC**TAGCCAGCCGGTGCCT
4618	GACTGCGGGG**CCATGG**CCGAGGTGCTGTTC
9138	GCAGGTCGACTAGTCTGCAGGTGGTGCTGCGCATTATACTGT
	TGAAAGTTGTTTAGCAAAACCTCATACAG
9139	AACGAATGGATCCTCATTAAAGCCAGAATGG

Table 2.1 The DNA primer sequences used in the construction of pGF14. The restriction sites which were introduced for cloning are marked in bold text. The amber stop codon which was introduced in the vector pGF14, is underlined.

2.3.3 Expression of bIGFBP-2 in supE and non-suppressor strains

The plasmid pGF14 was transformed into the *E. coli supE* strain JM101, and the non-suppressor hosts HB2151 and BL21 (using chemically competent cells, described in Sambrook *et al.*, 1989). The expression studies conducted in the *E. coli* JM101 strain were performed by Dr Goran Forsberg. Colonies were grown overnight in 2YT containing 2% (w/v) glucose and 100 µg/ml Amp, at 37°C. To optimise expression conditions, 100 µl of the overnight culture was added to 5 ml of 2YT containing 100 µg/ml Amp with varying concentrations of glycerol (0 to 8 g/l) grown at either 30°C or 37°C. At an OD_{600} of 0.8, some cultures were induced by the addition of up to 1 mM IPTG and grown overnight. Cells in growth medium were centrifuged in 1 ml aliquots at 10400 x g for 1 minute, and the cells and clarified medium were stored separately at -20°C. Periplasmic extractions were carried out by freeze-thawing of the cells. The frozen cell pellet was thawed at 4°C by adding 100 µl ice cold periplasmic extraction buffer while vortexing. After centrifugation, the supernatants were directly analysed or stored at -20°C.

For bIGFBP-2 characterisation, the protein expressed from pGF14 was recovered from the growth medium of BL21 cells. A 300 ml culture, consisting of 150 µg/ml Amp in 2YT, was inoculated with 100 µl of an overnight culture and induced at an OD_{600} of 0.6 using 0.8 mM IPTG, similar to the small scale studies described above.

2.3.4 Gel analysis and Western ligand blotting of bIGFBP-2 samples

Fractions from the periplasm and growth medium were subjected to SDS-polyacrylamide gel electrophoresis (PAGE) and ligand blotting. Samples were prepared by diluting the sample

loading dye with ratio 1:5, and heating at 100°C for at least 2 minutes. Non-reduced proteins were electrophoresed on a 10% or 12% (w/v) polyacrylamide separating gel and 4% (w/v) stacking gel at a constant current of 30 mA per gel. The protein was then transferred to a 0.45 μm nitrocellulose filter. Both Whatman 3 MM paper and the nitrocellulose filter were soaked in protein transfer buffer, and the transfer sandwich was assembled as described in the manual. The transfer was performed using a constant current of 0.8 mA per cm^2 for 1 hour at room temperature.

Ligand blots were performed by probing with ^{125}I IGF-II (Hossenlopp *et al.*, 1986). Filters containing the transferred protein samples (above) were dried and then incubated in a solution of blot buffer containing 1% (v/v) Triton X-100 for 30 minutes at room temperature. The filter was then blocked in blot buffer containing 1% (w/v) BSA for at least 2 hours at 4°C, after which the filter was rinsed with blot buffer containing 0.1% (v/v) Tween-20 for 20 minutes. ^{125}I IGF-II tracer was added to a fresh quantity of the latter buffer to give approximately 1 x 10^5 counts per minute (CPM) per ml. The filter was incubated with the tracer overnight at 4°C. The filter was washed 3 x 20 minutes with blot buffer containing 0.1% (v/v) Tween-20 at room temperature and was then dried. The filter was exposed to a storage Phosphor Screen (Molecular Dynamics, Sunnyvale, CA, USA) overnight, which was then processed on the Phosphor Imager (Molecular Dynamics) with ImageQuant software (Molecular Dynamics) to determine the relative amounts of bound tracer and hence the binding protein. By comparison with standardised amounts of bIGFBP-2, the IGF binding affinity of the unknown IGFBP samples could be quantified. Alternatively, samples were analysed directly by dotting onto nitrocellulose filters and probing the membranes with ^{125}I IGF-II as described above.

2.3.5 Purification and analysis of bIGFBP-2 from E. coli BL21 conditioned medium

After overnight growth at 37°C, the cells were removed by centrifugation at 7000 x g for 20 minutes at 4°C and the medium was adjusted to pH 7.0. In order to minimise protease activity, protease inhibitors PMSF and EDTA were added to final concentrations of 3 mM and 0.1 mM. The sample was applied to a long IGF-I (Francis *et al.*, 1992) affinity column (long

IGF-I was immobilised to Affi-Gel® 10 using the method described by the supplier) equilibrated with affinity column buffer and the column was then washed with 40 column volumes of the equilibration buffer, before elution with 0.5 M acetic acid. The eluted protein was then applied to a Brownlee Aquapore C4 (2.1 x 100 mm) BU-300 column with 7 µm particles (Applied Biosystems, USA), pre-equilibrated with 25% HPLC buffer B and 75% HPLC buffer A, at ambient temperature (approximately 20°C). Using both HPLC buffers A and B, elution of IGFBP-2 was achieved using a linear gradient from 20-50% acetonitrile over 30 minutes at a flow rate of 0.5 ml/minute. The purified samples of protein were quantified using HPLC (described above), by comparing the peak areas obtained at 215 nm, with that of known amounts of proteins standards loaded onto and eluted from the column. The purified material was lyophilised and stored at -20°C.

Correct processing of the signal sequence was determined by N-terminal sequencing of approximately 170 pmoles of purified bIGFBP-2. This was carried out by Mrs Denise Miller (Department of Biochemistry, University of Adelaide) on an Applied Biosystems 470A Gasphase Sequencer (Foster City, CA, USA) using the methods recommended by the supplier.

2.3.6 Solution charcoal binding assays

To characterise the bacterially produced protein, *E. coli* and COS-1 cell derived bIGFBP-2 were compared for binding to both IGF-I and IGF-II using charcoal binding assays (Szabo *et al.*, 1988). In brief, the first step was to titrate the binding protein with constant amounts ^{125}I IGF-I and ^{125}I IGF-II (abbreviated collectively as ^{125}I IGF) to standardise the two different binding protein samples. bIGFBP-2 was serially diluted, from 100 nM to 0.01 nM in CBA (Section 2.2.1). ^{125}I IGF was prepared by diluting the tracer in an appropriate volume of CBA so that 100 µl gave approximately 10000 CPM. Reaction mixes for each bIGFBP-2 dilution were prepared in triplicate or quadruplicate in a total volume of 300 µl (100 µl bIGFBP-2, 100 µl CBA, 100 µl ^{125}I IGF). The control for non-specific background (NSB) counts comprised ^{125}I IGF and CBA, in the absence of bIGFBP-2. Excess ^{125}I IGF mix was also retained to determine the total number of counts added per tube. The reaction mixes were allowed to equilibrate overnight at 4°C. Unbound tracer was then absorbed by the addition of 500 µl ice cold activated charcoal mix. After mixing, the

charcoal-containing tubes were then incubated on ice for 30 minutes. The charcoal: ^{125}I IGF complexes were removed from solution by centrifugation at 10400 x g for 3 minutes. A 400 µl aliquot of each supernatant was sampled and measured for radioactivity in a multi-channel gamma counter (Bromma, LKB). The amount of ^{125}I IGF specifically bound by bIGFBP-2, as a percent of the total tracer added was calculated using the following equation:

$$\% \ ^{125}\text{I IGF bound} = \frac{2x(\text{CPM-NSB})}{\text{total CPM}} \ x100$$

The experimental data was fitted to a semi-log dose response curve using both EXCEL (version 5, Microsoft) and Cricket Graph (version 1.3, Computer Associates Inc.) software.

The competition assays were conducted similarly to the titration experiments. A constant amount of binding protein which gave 50% binding in the titration experiments (4 ng per tube of bIGFBP-2) was used in the competition experiments, and the tracer was maintained at 10000 CPM per assay tube. Increasing concentrations of unlabelled IGF-I or IGF-II were added to each tube to compete with ^{125}I IGF for binding to the bIGFBP-2, and were incubated overnight at 4°C. The concentrations of both unlabelled IGF-I and IGF-II ligands used to compete for the ^{125}I IGF ranged from 0.004 nM to 35 nM, and the dilutions were prepared in CBA. The ^{125}I IGF bound at each concentration of unlabelled IGF was calculated as a percentage of the maximal ^{125}I IGF binding in the absence of competitor. The experimental data was fitted as described above.

2.3.7 Preparation and analysis of phage expressing bIGFBP-2

Phage were prepared from JM101 *E. coli* cells. A 2 ml overnight culture of cells containing pGF14 was grown in 2YT, 2% (w/v) glucose, 100 µg/ml Amp at 37°C with vigorous shaking. The subsequent day, the entire overnight culture was subcultured into 200 ml 2YT containing 100 µg/ml Amp and 50 µl M13KO7 stock solution (approximately 10^{12} plaque forming units (PFU) /ml, prepared as described by Sambrook *et al.*, 1989) giving a multiplicity of infection of approximately 10. The culture was grown at 37°C until an OD_{600} of 0.8 was reached. At this point, both IPTG and kanamycin were added to final concentrations of 0.02 mM and 5 µg/ml respectively, and the culture was incubated at 30°C overnight with

vigorous shaking. The bacteria were removed by centrifugation and phage particles were precipitated by the addition of the phage precipitation stock solution (Section 2.2.1, diluted 1:5 in the medium). In order to optimise the yield of phage precipitated from the bacterial culture, two procedures were compared to achieve the highest phage numbers. Firstly, after 30 minutes incubation of the PEG solution with the bacterial medium at room temperature, the sample was centrifuged at 8000 x g for 15 minutes (Procedure "A"). Secondly, a procedure was adapted from the pSKAN phagemid display system catalogue (MoBiTec, Gottingen, Germany) whereby phage were precipitated for a minimum of 2 hours at 4°C followed by centrifugation at 8000 x g for 40 minutes at 4°C (Procedure "B"). The pellets from either of these two procedures were dissolved in 2 ml PSB. The preparations were stored at 4°C.

Phage preparations were titred as PFUs as described by Sambrook *et al.* (1989) to determine the number of particles containing the helper phage DNA. Samples of phage were serially diluted (usually to between 10^8 to 10^{10}-fold) in PSB (Section 2.2.1) and 50 µl was added to 100 µl JM101 culture and briefly mixed. Molten soft YT agar was cooled to 45°C, and the bacterial-phage mix was added to 3 ml of the agar. The mix was rotated gently to ensure dispersion but to avoid bubble formation, and poured onto pre-warmed L plates. After allowing the agar to set at room temperature, the plate was incubated overnight at 37°C and the plaques were counted. Colony forming units, CFUs, were determined to establish the number of phage particles containing the phagemid, pGF14. For CFU determination, the phage preparations were diluted in PSB, and 50 µl was mixed with 50 µl of a fresh JM101 culture. The mixture was incubated at room temperature for 5 minutes and then at 37°C for 15 minutes before plating onto L plates containing Amp at 100 µg/ml. The plates were grown overnight, and the colonies were counted the next day.

The panning procedures were developed by Dr Goran Forsberg at the Department of Biochemistry, University of Adelaide. The panning was performed in 96 well microtitre plates. The wells were coated with 0.5 µg IGF-II in 100 µl of 56 mM $NaHCO_3$, pH 9.6 for 3 hours at 37°C and blocked with 150 µl of 0.1% (w/v) BSA in PBST (Section 2.2.1) overnight at 4°C. The wells were rinsed once with 150 µl of PBST before 100 µl of freshly produced phage preparation, diluted in PBST to approximately 10^{10}-10^{11} CFU/ml, was added and incubated at 37°C for 30 minutes. Unbound phage particles were removed and the wells were washed ten

times with 150 µl of PBST at room temperature. Elution was then carried out using either 0.5 M or 2 M acetic acid, 0.5 µg of either IGF-I, IGF-II or bIGFBP-2 in PBS or 0.01 mg/ml H64A subtilisin in H64A subtilisin cleavage buffer. The competitive elutions were carried out for 1 hour at 37°C while acid or enzymatic elution was performed for 12 hours at 4°C. To reinfect bacteria with these phage particles, the acid eluted material was neutralised with 1M Tris base solution pH 9.6, and allowed to reinfect 2 ml of a culture of JM101 cells for 15 minutes at 37°C. The sample was added to 200 ml of 2YT containing 100 µg/ml Amp together with 50 µl of the M13KO7 preparation (approximately 10^{12} particles per ml). After 2 hours at 37°C, kanamycin and IPTG were added as described above and the sample was incubated at 30°C overnight.

To separate phage particles from free bIGFBP-2, size exclusion chromatography was carried out on a Superose® 6 HR column (Pharmacia BioTech, Uppsala, Sweden). The column was equilibrated and the samples eluted with Superose® 6 column buffer. The flow rate was 0.5 ml/minute and 100 µl of different phage preparations, approximately 10^{12} CFU/ml, were applied. Absorbance was measured at 280 nm and fractions of 1 ml were collected. The fractions were subjected to ligand dot blot analysis and determination of the number of CFUs, as described above.

2.4 Results

2.4.1 Vector constructs

The vector used for secretion and phage display of bIGFBP-2, pGF14, is based on the vector pHEN1 (Hoogenboom *et al.*, 1991) and is shown in Figure 2.4. This vector contains a *lacZ* promoter and encodes a pelB leader sequence which is removed during secretion (Figure 2.6). To obtain the initial plasmid pHEN/bBP-2, the cDNA coding region for bIGFBP-2 (Upton *et al.*, 1990) was cloned directly into pHEN1 and the stop codon in the cDNA removed to allow expression of the IGFBP-2:gIIIp fusion protein. The vector pHEN/bBP-2 was then further mutated to yield pGF14. Using PCR, the *c-myc* reporter gene was removed and an amber stop codon, TAG, was placed directly after the *Sal* I cloning site. Thus, bIGFBP-2 is not fused to c-myc which could possibly affect its function. In addition, a site for enzymatic cleavage of the fusion protein with H64A subtilisin was introduced C-terminally to the amber

stop codon position, providing an alternative elution approach for the panning procedures. To ensure optimal H64A subtilisin accessibility and avoid inhibitory sequences, the region located N-terminally to the cleavage site contains a hydrophilic spacer (Matthews and Wells, 1993). In addition, the amino acid residues in P1' and P2' (according to the nomenclature of Schechter and Berger, 1967) are convenient for H64A subtilisin cleavage (Carter *et al.*, 1989; Forsberg *et al.*, 1992; Matthews and Wells, 1993) (Figure 2.4). The DNA for the H64A subtilisin recognition sequence was also designed to contain a unique *Pst* I site to facilitate further engineering and construction of libraries in the C-terminal region of IGFBP-2.

2.4.2 Expression and secretion of functional bIGFBP-2 and bIGFBP-2:gIIIp fusion product

Compared to several other products that have been successfully displayed on filamentous phage (Clackson and Wells, 1994), bIGFBP-2 is a complex protein consisting of 284 amino acids and 18 cysteine residues interconnected as disulphide bonds (the C-terminal cysteine are all disulphide bonded (Forbes *et al.*, 1998), and the N-terminal cysteine residues have all been shown to disulphide bond, Dr Briony Forbes, unpublished). Therefore, whether bIGFBP-2 could be efficiently expressed, secreted and correctly folded in the *E. coli* periplasm was investigated. To obtain large amounts of recombinant bIGFBP-2, an *E. coli* production system is preferable in many respects to a mammalian cell based method, particularly in the case of a non-glycosylated protein such as bIGFBP-2.

Initial secretion studies were carried out by using the plasmid pGF14 in two different *E. coli* non-suppressor strains: HB2151 and BL21. The periplasmic fractions were analysed for IGF-II binding activity by IGF-II ligand blotting. Both strains produced approximately the same amounts of correctly folded bIGFBP-2, but the product was much more stable in periplasmic extracts from the *ompT* host BL21 (data not shown). The bIGFBP-2 derived from the BL21 host could be further stabilised with the addition of 1 mM EDTA to the extracts (personal communication with G. Forsberg). On the ligand blots, the product from pGF14 expression has a molecular weight corresponding to mammalian derived bIGFBP-2 (Figure 2.5). The plasmid pGF14 was also transformed into a *supE* strain of *E. coli*, JM101. Optimal production of gIIIp-fused IGFBP-2 was obtained by growing the cells at 30°C after induction

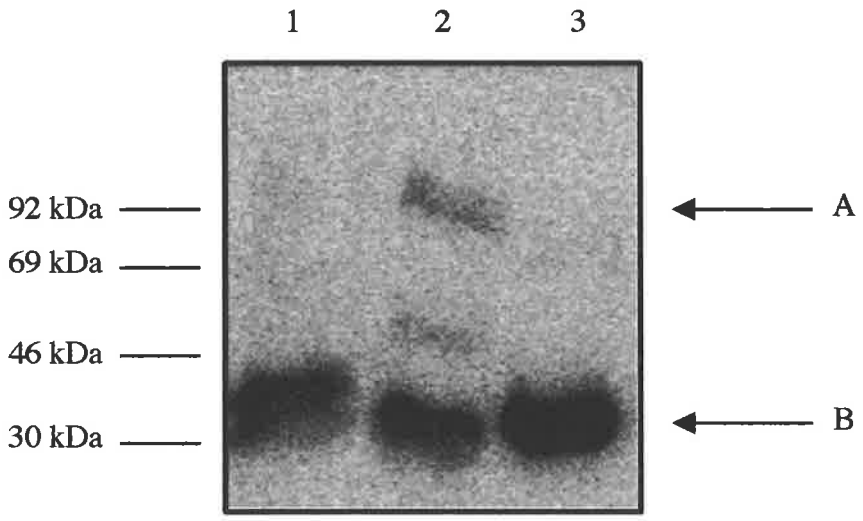

Figure 2.5 ^{125}I IGF-II ligand blot analysis of recombinant bIGFBP-2, derived from pGF14 expressed in *E. coli*.
Lane 1) expression of bIGFBP-2 in HB2151, a non suppressor host strain, 2) expression of bIGFBP-2 and bIGFBP-2:gIIIp fusion in JM101, a *supE* strain, and 3) 200 ng recombinant bIGFBP-2 obtained from COS-1 cells. The molecular weight standards are shown to the left of the blot. In lanes 1 and 2, 20 µl samples of periplasmic extract were analysed. The positions of the 31 kDa bIGFBP-2 (B) and the 74 kDa bIGFBP-2:gIIIp fusion protein (A) are indicated by the arrows. The bIGFBP-2:gIIIp fusion protein migrates at approximately 90 kDa. An IGF binding protein can be seen in lane 2 (approximately 46 kDa). This is likely to represent a breakdown product from the bIGFBP-2:gIIIp fusion protein.

with 0.02 to 0.1 mM IPTG (personal communication with G. Forsberg). Using these conditions, both gIIIp-fused bIGFBP-2 (M_r= 74 kDa) and non-fused bIGFBP-2 (M_r= 31 kDa) were obtained, as determined by the ligand blots (Figure 2.5). Assuming that the fusion partner does not affect the IGF binding properties in this assay, Phosphor Imager analysis of ^{125}I IGF binding indicates approximately 5-10% read-through of the TAG codon. A value of 5-10% read-through however may represent a slight over-estimation, because it is known that free bIGFBP-2 exists in culture medium (above) whilst the carboxy-terminal end of gIIIp retains the protein in the bacterial membrane (Boeke and Model, 1982).

To characterise the *E. coli* derived bIGFBP-2, the protein was prepared from the BL21 cells transformed with pGF14. Expression from this strain and purification from the growth medium was chosen to minimise the chances of proteolysis of bIGFBP-2, which was observed to occur in periplasmic extracts (personal communication with G. Forsberg). In addition, recovery from the growth medium obviated the need to perform large scale freeze-thawings. The bIGFBP-2 was purified with affinity chromatography using immobilised long IGF-I, an IGF-I variant with a 13 amino acid residue extension peptide at the N-terminal end (Francis *et al.*, 1992). The affinity purified material was then subjected to reverse phase HPLC. According to analytical reverse phase HPLC and SDS-PAGE (Figure 2.6), the purified product was homogeneous and had the same size and purification characteristics as the mammalian derived bIGFBP-2. In the bigger shaker flasks, 265 µg IGFBP-2 could be recovered from 300 ml of growth medium, resulting in a production level of approximately 0.9 mg per litre, which is well above the amount of recombinant IGFBP-4 reported to be purified from an alternative *E. coli* expression system (Honda *et al.*, 1996). The purified product was also analysed by N-terminal sequencing which showed the single sequence NH_2-Glu-Val-Leu-Phe, was identical to the native sequence (Figure 2.6). This material was compared to recombinant bIGFBP-2 from COS-1 cells for binding to both IGF-I and IGF-II using competitive charcoal binding assays (Szabo *et al.*, 1988). With either ^{125}I labelled IGF-I or ^{125}I labelled IGF-II (Figure 2.7), the abilities of the respective growth factor to compete with the tracer were indistinguishable. The concentrations of unlabelled IGF able to cause 50% displacement of ^{125}I IGF-II from the binding protein, were estimated to be 0.35 nM for IGF-II and 1.8 nM for IGF-I (Figure 2.7b).

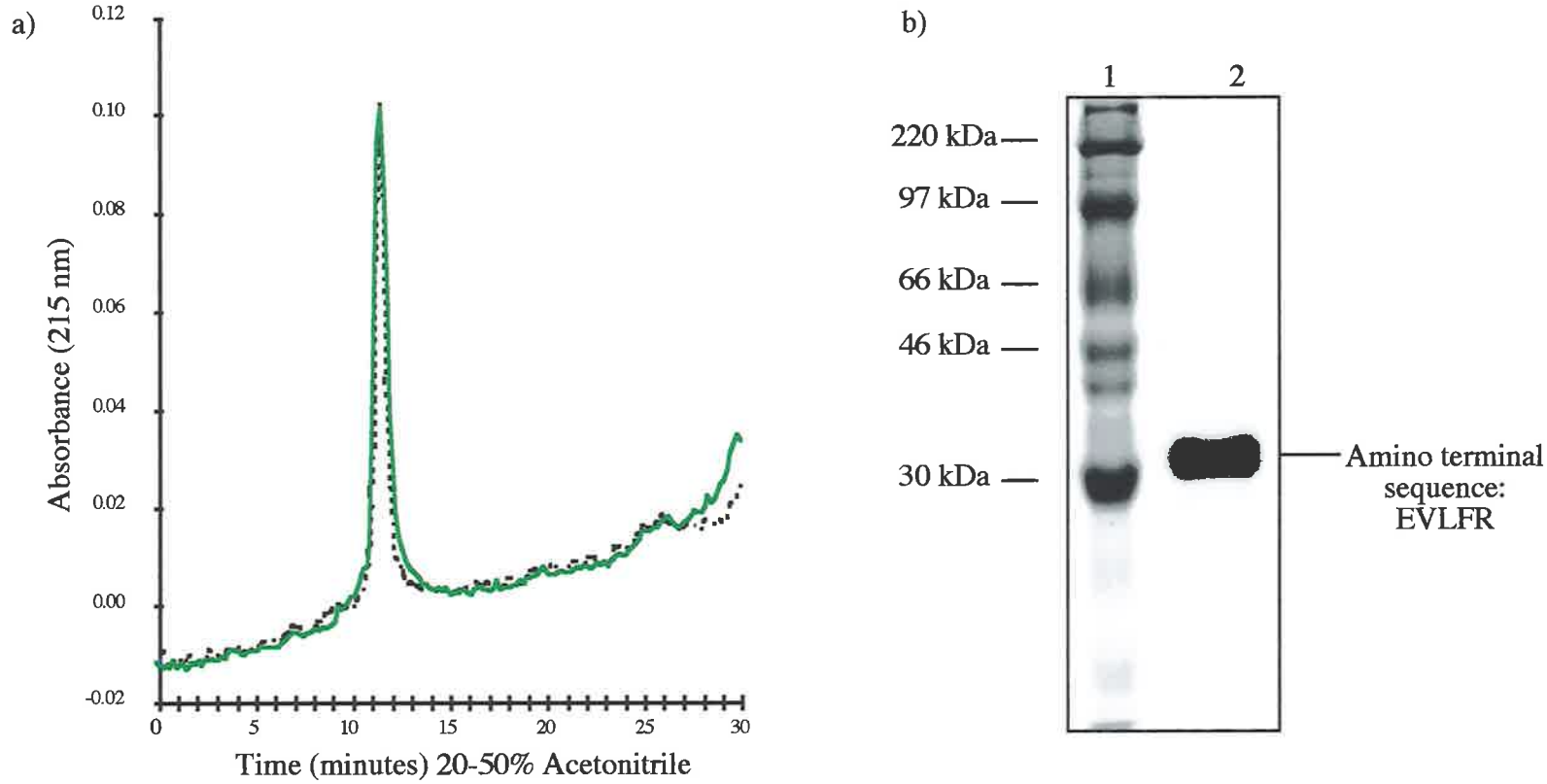

Figure 2.6 Comparison of COS-1 cell derived bIGFBP-2 to that derived from BL21 *E. coli* cells.
a) Analysis of purified bIGFBP-2 from COS-1cells (----) and from BL21 cells (___) using reverse phase HPLC on a C4 analytical column. The retention time was assessed on a 20-50% acetonitrile gradient over 30 minutes at room temperature.
b) 10 μg of purified BL21 expressed bIGFBP-2 (lane 2) was analysed on a Coomassie Brilliant Blue R-250 stained 12% polyacrylamide gel. Protein molecular weight markers (lane 1) show the correct molecular weight of the product. Sequence analysis of the five amino terminal residues of bacterially expressed bIGFBP-2 showed correct processing of the pelB signal sequence (the amino acid sequence was found to be EVLFR).

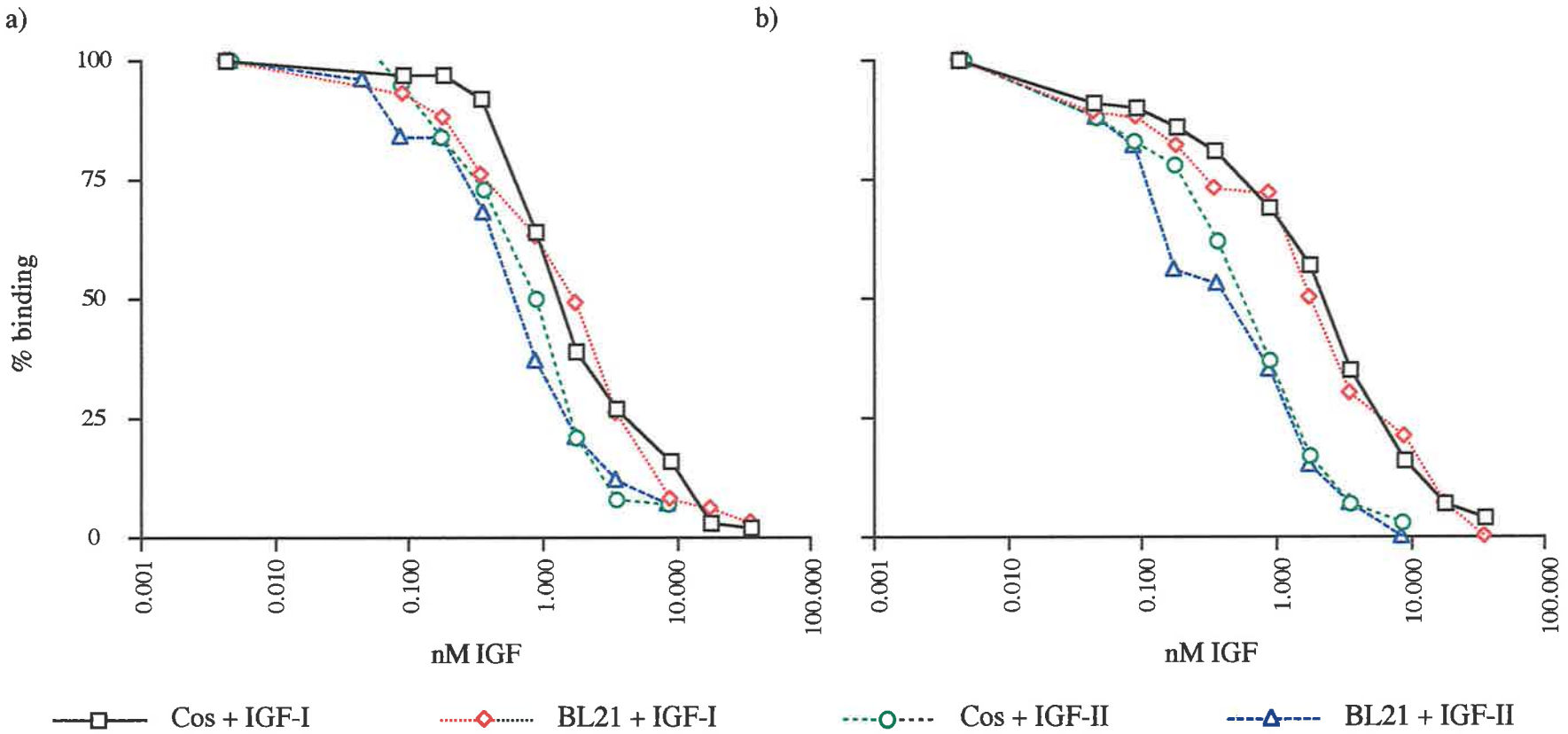

Figure 2.7 Competitive charcoal binding assays showing that the bacterially expressed (*E. coli* BL21) bIGFBP-2 binds both IGF-I and IGF-II with the same affinity as bIGFBP-2 expressed in mammalian COS-1 cells.

The assays contained 4 ng of binding protein. The amount of ^{125}I IGF bound at each concentration of unlabelled IGF was calculated as a percentage of the maximal ^{125}I IGF binding in the absence of competitor.

a) Competition experiments performed using ^{125}I IGF-I as the tracer.

b) Competition experiments performed using ^{125}I IGF-II as the tracer.

The fact that the *E. coli* protein exhibits affinities for IGF-I and IGF-II indistinguishable from the mammalian cell derived product, we can conclude that correctly folded IGFBP-2 is produced as a secreted product in *E. coli*. In addition, IGFBP-2 can also be produced as a fusion to gIIIp with retention of IGF-II binding activity.

2.4.3 Analysis of the expression conditions for pGF14 derived bIGFBP-2

One of the purposes of the *E. coli* production system is to obtain and characterise several bIGFBP-2 variants from the phage display system. To facilitate their characterisation, it is important to have a robust and simple production system. Since it was observed that large amounts of bIGFBP-2 leaked out from the periplasm, the aim was to optimise the shaker flask method where a greater amount of the secreted product is preferentially obtained in the growth medium.

The impact of medium composition and IPTG induction were investigated in the *E. coli* strains BL21 and HB2151. The accumulation of bIGFBP-2 in the growth medium was measured using IGF-II ligand blotting. Addition of glycerol as an extra carbon source to the growth medium, at a concentration of 2 g per litre, improved the bIGFBP-2 level 2-fold in BL21. However, at a glycerol concentration of 8 g per litre the yield was significantly reduced (Figure 2.8). The addition of IPTG to the culture medium during growth also increased the levels of bIGFBP-2 production. Addition of 1 mM IPTG increased the yield almost 2-fold (Figure 2.8). The combination of glycerol and IPTG only had a small synergistic effect on the levels of bIGFBP-2. The combination of 1 mM IPTG and 2 g per litre glycerol, tested in small scale cultures, gave a final yield of approximately 4 mg per litre of IGFBP-2 in the growth medium, as determined by ligand blotting. The amount of bIGFBP-2 found in the medium was estimated to represent more than 50% of the secreted product, since the assessment of the periplasmic levels suggested that lower amounts of bIGFBP-2 were found here. These results were similar to those obtained with the cell line HB2151, although this strain produced consistently lower yields (data not shown). The maximum level in HB2151 growth medium, estimated in small scale cultures was in the order of 1 mg per litre.

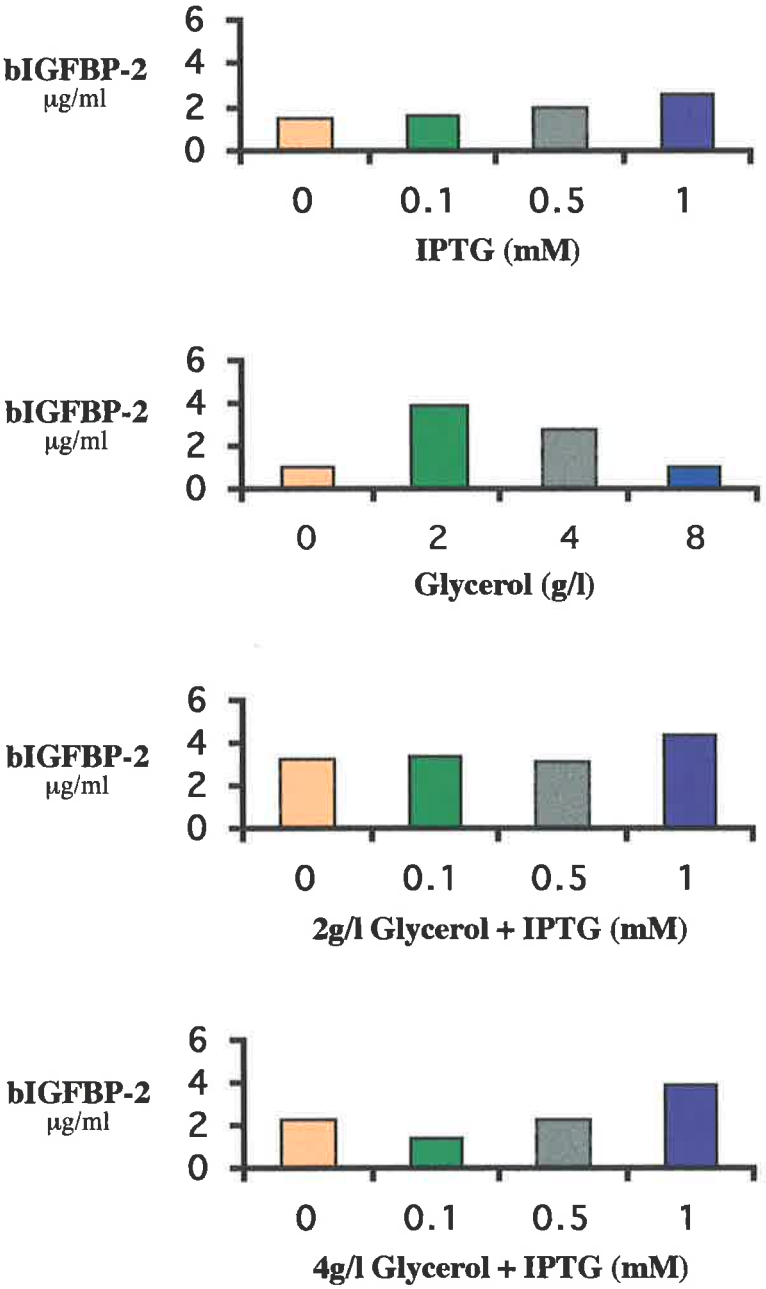

Figure 2.8 Production levels of bIGFBP-2 in the growth medium using different culture conditions. Growth medium from the shaker flask cultures of BL21 were analysed using ligand blotting. The levels were estimated against bIGFBP-2 standard derived from mammalian cells. The highest levels of bIGFBP-2 production were obtained using addition of 2 g/l of glycerol or induction with 1 mM IPTG.

2.4.4 Display of active bIGFBP-2 on phage and panning for bIGFBP-2 bearing phage

In order to display bIGFBP-2 on the phage, different expression conditions were investigated. The expression of fusion protein was suppressed by high levels of glucose in the growth medium prior to infection (Hoogenboom *et al.*, 1991). Protocols, identical to or adapted from different studies (Bass *et al.*, 1990; Hoogenboom *et al.*, 1991; Barbas *et al.*, 1991) were examined. For the display of bIGFBP-2, an amalgam of these methods, as described in Section 2.3.7, gave an optimal display of bIGFBP-2 with final titres of approximately 10^{10} CFU/ml and 10-fold higher PFU/ml. The phage particles were partially purified and concentrated using precipitation with PEG. A comparison of the phage yields with two different preparation procedures showed that longer precipitation and centrifugation times did not increase final phage numbers (Table 2.2). The IGF-II binding activity of the phage was demonstrated using size exclusion chromatography (Figure 2.9) and IGF-II ligand blotting of the fractions obtained. Here, approximately 90% of the IGF-II binding activity co-eluted with the phage particles in fractions 8-11 (Figure 2.9). Interestingly, approximately 10% of the IGF binding activity was found in fractions of lower molecular mass, which may correspond to co-precipitated IGFBP-2 not incorporated in the phage. Using the described procedure for production and PEG-precipitation, the ratio of free to phage-bound bIGFBP-2 was minimised.

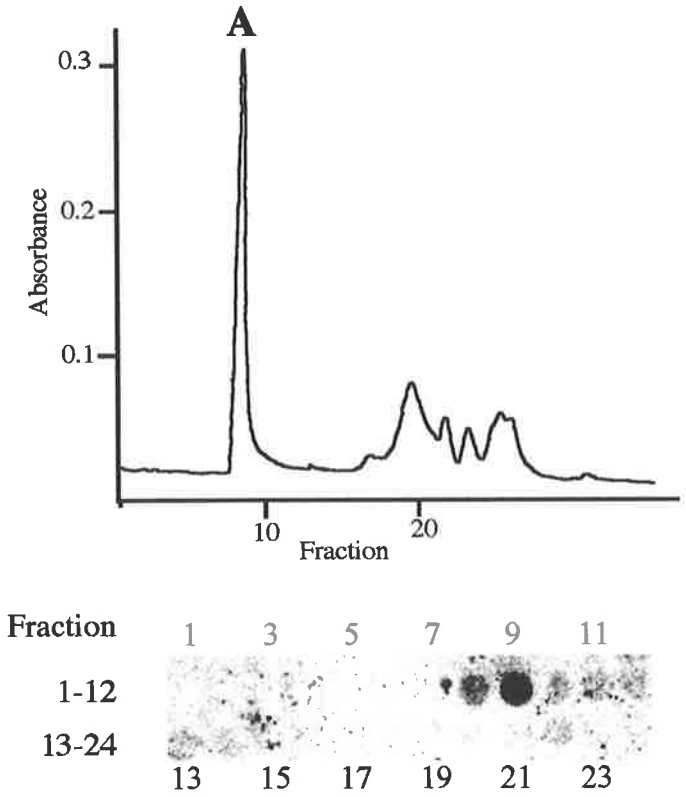

Figure 2.9 Incorporation of bIGFBP-2 into the phage particles, as analysed using size exclusion chromatography of a PEG-precipitated phage preparation (Section 2.3.7). The fractions were collected and analysed for IGF-II binding activity by ligand dot blot and for phage particles, measured as CFU/ml. Integration of the ligand dot blot signals showed that more than 90% of the IGF-II binding activity co-eluted with the phage particles (peak A) in fractions 8-11.

Preparation	"A" yield	"B" yield	"B" vs "A"
1	3.0×10^{12}	1.2×10^{12}	–
2	1.16×10^{11}	1.78×10^{11}	+
3	3.38×10^{12}	3.39×10^{12}	+
4	8.0×10^{12}	1.08×10^{13}	+
5	1.7×10^{12}	1.02×10^{12}	–
6	2.99×10^{12}	1.75×10^{12}	–

Table 2.2 A comparison of the yields of phage particles from bacterial culture supernatant, generated using two different preparation techniques. Phage particles were prepared by PEG-precipitation using either procedure "A" or "B" (Section 2.3.7). Briefly, procedure "A" involved a 30 minute precipitation time and a 10 minute centrifugation time to harvest the phage particles. Procedure "B" used a 2 hour precipitation and a 40 minute centrifugation time for phage isolation. The phage yields were determined as colony forming units as described in Section 2.3.7. The yields from "B" were scored relative to "A", by assigning a "+" when yields from "B">"A". When the yields from "B" < "A" a "–" was assigned. Using a Sign test, the hypothesis that procedure "A" and procedure "B" yielded the same numbers of phage particles could not be rejected.

The final step in the development of the phage display method of bIGFBP-2, was the establishment of a panning method where bIGFBP-2 bearing phage were enriched by binding to an immobilised ligand. Here, the panning was performed in an IGF-II coated microtitre plate. Both the blocking method and washing procedures were found to have a substantial influence on the final enrichment. The use of 1% BSA as blocking agent resulted in more unbound bIGFBP-2 bearing phage, as determined by ligand dot blots, compared to when lower amounts of BSA were used (personal communication with G. Forsberg). It is unclear whether these effects originated from IGFBP contaminations in the BSA preparations or if excess BSA caused steric hindrance of bIGFBP-2 binding. In addition, gelatin and Tween-20 were examined as blocking agents. The optimal blocking agent was found to be 0.1% BSA. this concentration resulted in a higher final enrichment of bIGFBP-2 expressing phage over non-specific binding phage particles isolated from the BSA blocked wells (personal communication with G. Forsberg). As indicated by others (Barbas *et al.*, 1991; Bass *et al.*, 1990), appropriate washing procedures are crucial for a good phage enrichment. Here, washing of the wells was performed ten times to obtain a high degree of enrichment and the

titres of non-specifically bound phage were less than 10^4 CFU/ml in the final washing fractions (Table 2.3).

Wash number	IGF-II well phage titre (CFU/ml)	Non-coated well
wash 2	$5.1x10^7$	$1.4x10^7$
wash 4	$1.7x10^5$	$2.1x10^5$
wash 6	$2.2x10^4$	$1.0x10^4$
wash 8	$2.2x10^4$	$8.8x10^3$
wash 10	$1.5x10^4$	$9.2x10^3$

Table 2.3 Analysis of the phage numbers during the washing procedures. Phage, approximately 10^{11} CFU/ml, were applied to the IGF-II coated wells or to control wells that were not coated. The wells were washed ten times, and the wash fractions were titred for CFU (Section 2.3.7).

Several options were investigated for elution of bIGFBP-2 displaying phage from the immobilised IGF-II: elution with acid, competitive elution using IGF-I, IGF-II or bIGFBP-2 and enzymatic elution using H64A subtilisin cleavage. An example of the results are shown in Table 2.4. Using the competitive elution with IGF, enrichment levels of 18 to 32 times over non-specifically bound phage were obtained, while levels up to 11300-fold was obtained with the acid and 6400-fold using H64A subtilisin (Table 2.4). The competitive elutions were carried out at 37°C, while acid and enzymatic elution were carried out at 4°C. Repetition of these experiments confirmed the ability to pan using each of these techniques, although there was difficulty in getting good reproducibility with the competitive elution approach.

Thus, significant amounts of correctly folded bIGFBP-2, that binds IGF-II in ligand blots, can be displayed on the bacteriophage surface. In addition, phage displaying IGFBP-2 can be specifically enriched on IGF-II coated microtitre plates.

Elution	IGF-II Well phage titre (CFU/ml)	Non-coated well	Enrichment
0.5 M HAc	$2.8x10^7$	$3.0x10^3$	9300
2 M HAc	$6.8x10^7$	$6.0x10^3$	11300
IGF-I	$4.8x10^6$	$2.6x10^5$	18
IGF-II	$3.8x10^6$	$1.2x10^5$	32
IGFBP-2	$2.3x10^6$	$9.6x10^4$	24
H64A subtilisin	$4.5x10^7$	$7.0x10^3$	6400

Table 2.4 Analysis of the elution procedures used to retrieve phage. Phage, approximately 10^{11} CFU/ml, were applied to the IGF-II coated wells or to control wells that were BSA blocked but not IGF-II coated. After ten washes, the phage were eluted as described in Section 2.3.7. The phage titres were measured as CFU/ml. Enrichment is defined as the ratio of the number of phage derived from an IGF-II coated well compared to phage numbers derived from a non-coated well.

2.4.5 Recovery of pGF14

To confirm that the eluted phage contained single stranded phagemid DNA representing intact IGFBP-2, phagemid DNA was prepared from individual clones obtained after panning and reinfection. Restriction mapping did not show any differences between wild type pGF14 and the prepared phagemids (personal communication with G. Forsberg). In addition, JM101 were infected with helper phage and phage eluted from IGF-II coated wells. The resulting phage preparation (approximately 10^{10} CFU/ml) contained equivalent levels of phagemid bearing phage and displayed similar levels of biologically active bIGFBP-2 as the original preparation before panning.

2.5 Discussion

In this study, recombinant bIGFBP-2, with full IGF-I and IGF-II binding activity, has been shown to be efficiently secreted and prepared from *E. coli*. Notably, in the shaker flask significant amounts of the bIGFBP-2 leaked from the periplasm of the cells to the medium. Such leakage has been described for a variety of heterologous proteins (Hockney, 1994). The mechanisms for this process are unknown but to some extent are dependent on the amino acid sequence of the product (Knappik and Pluckthun, 1995; Forsberg *et al.*, 1997). Using an *ompT* host cell, approximately 4 mg/l was obtained in small scale shaker flasks as determined

by ligand blotting. Using a two-step purification procedure, involving affinity chromatography and reverse phase HPLC, bIGFBP-2 was recovered at a purity of more than 95% from the *E. coli* growth medium. Long IGF-I, which was used for the capture, has approximately 6-fold lower affinity for IGFBPs than native IGF-I (Francis *et al.*, 1992), but bIGFBP-2 was efficiently captured on the column. This system can therefore be used for preparation of bIGFBP-2 variants to study how changes in structure alter biological properties. Importantly the yield described here was higher than that routinely obtained from mammalian cells. The *E. coli* system therefore provides a means for recombinant production of large amounts of different bIGFBP-2 variants derived from the phage display libraries for functional characterisation. The yield is also high enough to initiate studies to obtain information regarding the three-dimensional structure of bIGFBP-2. Previously such studies have not been possible because of the lack of purified material.

In addition, the same vector used for secretion can be used to display bIGFBP-2 as a fusion to gIIIp on filamentous phage and retain its IGF binding activity. These phage particles fused to bIGFBP-2 were selectively enriched using panning on an IGF-II coated microtitre plate. As a first step in the development of a phage display system, the production of phage displaying bIGFBP-2 was optimised. Despite the size of bIGFBP-2 and its high number of disulphide bonds, the CFU titres, percentage displayed material and the enrichment levels of bIGFBP-2 displaying phage over non-specifically bound phage were in accordance with the observations made for the phage display of other proteins (Bass *et al.*, 1990; Barbas *et al.*, 1992; Matthews and Wells, 1993). A critical step in the use of phage display is the panning procedure where products are sorted on the basis of various physical and biochemical properties. The sorting can be controlled by the method in which phage particles are eluted from the ligand. After extensive washing to reduce the background levels of non-specifically bound phage, the phage bearing bIGFBP-2 could be eluted using several different methods (Table 2.4). This has several interesting implications. For instance, binding of the phage to IGF-II, followed by competitive elution with IGF-I, would result in a selection towards relatively stronger binding to IGF-I compared to IGF-II. Alternatively, the reverse process or variants on this theme should be possible. The significance of such an approach is that that some of the binding proteins, including bIGFBP-2 (Szabo *et al.*, 1988; Bourner *et al.*, 1992),

exhibit a binding preference for IGF-II and the residues responsible for this could be identified in this manner. Here, immobilised IGF-II was used for panning, but it could be replaced by some of the other ligands for bIGFBP-2 like IGF-I or integrin (see Section 1.4.1). Therefore, the panning can be used to sort for variants with higher affinity for IGF-II, which may show residues in bIGFBP-2 that are critical for the interaction to occur. By replacing those residues by site-directed mutagenesis, variants with a lower affinity could also be investigated.

One potential problem in this system is the relatively high affinity between IGF-II and bIGFBP-2 ($K_a > 10^9$/M). Mutants of IGFBP-2 with a higher affinity for IGF-II than wild type might be difficult to elute with acid or by competition with IGF-II. In fact, to some extent this may have been observed with displayed wild type bIGFBP-2, where competitive elution or elution with 0.5 M acetic acid left a significant number of phage bound to IGF-II compared to elution with 2 M acetic acid (Table 2.4). To avoid this potential problem and to allow studies aimed at selecting mutants of IGFBP-2 regardless of the affinity for IGF-II, an enzymatic cleavage site was introduced between the IGFBP-moiety and the phage. In addition, to select for mutants with different properties, it would be possible to use combinations of different elution methods in a single experiment, such as washing with IGFBP-2 prior to enzymatic elution or include truncated variants of IGF-II with a reduced affinity for IGFBPs (Francis *et al.*, 1993) in the system.

As discussed in Section 1.5.2, some data are available regarding the IGF binding site on IGFBP. There are N- and C-terminal regions in the different IGFBPs with high sequence homologies (see Figure 1.4) which probably constitute the IGF binding site. Therefore, it is anticipated that using the described phage display system we can screen libraries of bIGFBP-2 mutants to assess for important and optimal binding residues present across the protein. The use of the phage display system for these purposes is the topic of Chapter 3. Also as mentioned earlier, using this expression system we may now be able to produce large quantities of bIGFBP-2 for a more detailed structural characterisation of the protein.

Chapter Three

MUTATIONAL ANALYSIS OF AMINO ACIDS 221-230 IN bIGFBP-2 TO DETERMINE A ROLE IN IGF BINDING

3.1 Introduction

The results discussed in Chapter 2 show that the phagemid, pGF14, can be successfully used to secrete bIGFBP-2 protein from *E. coli*, or to display bIGFBP-2 on the surface of phage in a functional IGF binding form. As outlined in Chapter 2, by developing a phage display system, it is then possible to use this approach to screen large libraries of mutant proteins for desired ligand binding properties. The physical link between the protein of interest and its encoding DNA facilitates the identification of interesting variants, which can then be expressed and analysed in more detail (Section 2.1).

In this chapter, a C-terminal region of bIGFBP-2 was selected for mutational analysis on the basis of deletion studies performed in our laboratory (Forbes *et al.*, 1998). The sequential deletion of amino acid sequences from the C-terminal end of bIGFBP-2, demonstrated that residues 222 to 236 were important for normal IGF binding activity (Forbes *et al.*, 1998; summarised in Figure 3.1 and in Section 1.5.2). This loss in binding activity was not a result of major changes in the structure of the protein, as shown by the analysis of the 1-221 amino acid bIGFBP-2 mutant on SDS-polyacrylamide gel and by tryptic digestion (Forbes *et al.*, 1998). There is also additional evidence to suggest that this C-terminal region of the IGFBP may be involved in IGF binding activity. Firstly, H64A subtilisin cleavage of bIGFBP-2, between residues Leu215 and His216, was inhibited when IGF ligand was bound to bIGFBP-2 (personal communication with Steven Polyak, unpublished, Figure 3.2). In this case, IGF may have inhibited cleavage by binding to a site overlapping the H64A subtilisin cleavage site. Alternatively, the binding of IGF could have induced a structural change, thus making the site inaccessible for H64A subtilisin cleavage. Secondly, Schuller *et al.* (1993) demonstrated that a monoclonal antibody that bound to residues located between amino acids 188-234 of human IGFBP-1, inhibited IGF interaction with the IGFBP. These amino acids correspond to amino acids 227 to 284 of bIGFBP-2 which are highlighted in Figure 3.2. The inability of the IGF to bind in the presence of antibody may be explained by overlapping binding sites, steric hindrance or due to a conformational change caused by the antibody binding. Unfortunately, these questions were not addressed in the study (Schuller *et al.*, 1993).

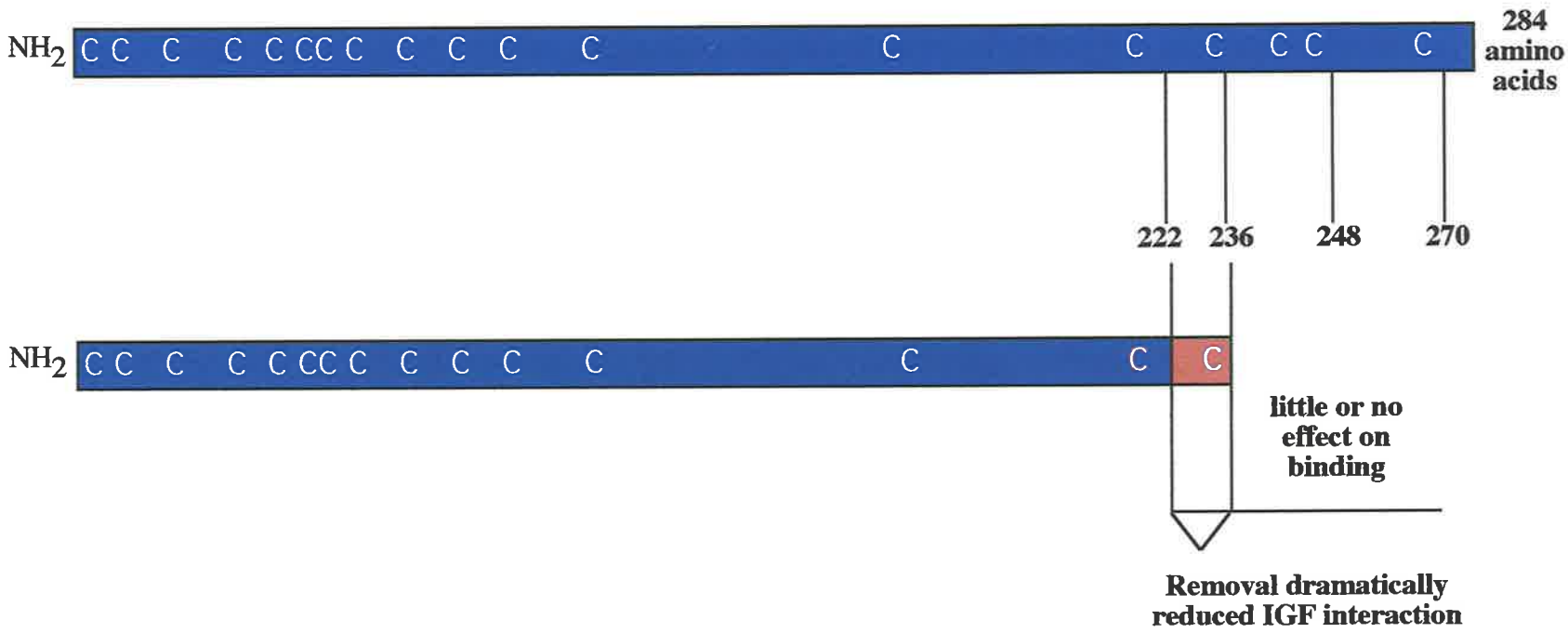

Figure 3.1 Summary of the deletion study used to determine the residues in the C-terminal end of bIGFBP-2 required for IGF binding (Forbes *et al.*, 1998). Removal of blocks of residues, up to amino acid 236, had little or no effect on the IGF binding ability of the resultant molecule. However, removal of residues, 222 to 236, reduced the ability of the bIGFBP-2 deletion mutant to bind to IGF up to 80-fold (Forbes *et al.*, 1998).

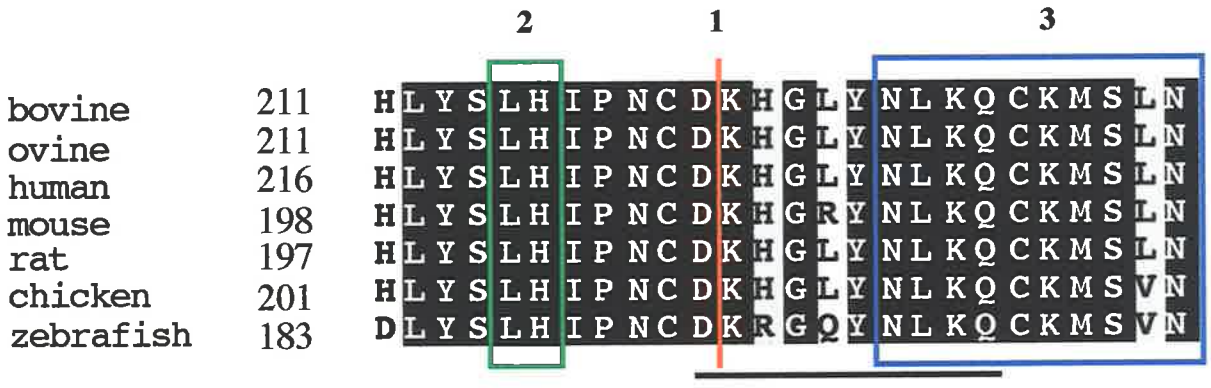

Figure 3.2 Alignment of the C-terminal residues of IGFBP-2, from the different species, highlighting the region of the protein being investigated in this study (underlined in black, residues 221-230 of bIGFBP-2).
1) C-terminal truncation to this region in bIGFBP-2, reduced the ability of the resultant molecule to bind to IGF (Forbes *et al.*, 1998).
2) Cleavage with H64A subtilisin, between Leu215 and His216 of bIGFBP-2 was inhibited when IGF was bound (Steven Polyak, personal communication).
3) A monoclonal antibody binding to IGFBP-1 inhibited IGF interaction (Schuller *et al.*, 1993). This antibody was found to recognise an epitope located somewhere between residue 227 to the C-terminal end, shown here on bIGFBP-2.

To further investigate the role of this region in IGF binding activity, the residues 221 to 230 of bIGFBP-2 were targeted both for mutagenesis (Figure 3.2), and for screening using the phage display system. A totally random mutagenesis approach was avoided since a random library across 10 amino acid residues generates $32^{10}=1.126 \times 10^{15}$ codon possibilities. Due to limitations in the transformation efficiencies of *E. coli* (approximately 10^9 transformants per μg plasmid, Clackson and Wells, 1994), a mutagenesis approach was chosen to minimise codon numbers, thus confining the library size to approximately 6.7×10^7 variants.

In this chapter, the *E. coli* strain XL1-Blue was selected as a host for the phage display of bIGFBP-2, as opposed to the *E. coli* JM101 cells that were used in Chapter 2. XL1-Blue were used here, as techniques for the generation of high plasmid transformation efficiencies using this strain have been well documented (Zabarovsky and Winberg, 1990; Chuang *et al.*, 1995). Furthermore, the F episome in XL1-Blue cells can be maintained by selection with tetracycline and, like JM101 cells, these cells contain the *supE* mutation to permit read-through of the amber stop codon.

In summary, this chapter focuses on the generation and screening of a mutant library of bIGFBP-2 proteins expressed on the surface of phage particles. The results following four rounds of panning of the C-terminal bIGFBP-2 mutant library against IGF-II and the findings from these experiments are discussed.

3.2 Materials

The vector pGF14 used in the mutagenesis is described in Figure 2.4. The DNA polymerase, Pwo, was purchased from Roche Diagnostics (Castle Hill, NSW, Australia) , and Taq thermostable polymerase, was from Promega Corp. (Madison, WI, USA). DNA restriction enzymes *Nco* I, *Pfl* M1, NEBuffer3 and BSA were purchased from New England Biolabs (Beverly, MA, USA). *Pst* I and *Hin*d III were sourced from Geneworks Ltd (Thebarton, SA, Australia), while *Bam* HI, *Sal* I and reaction buffer "One-phor-all Plus" (OPA+) were obtained from Amersham Pharmacia Biotech Pty Ltd (Castle Hill, NSW, Australia). All DNA primers were purchased from Geneworks Ltd. All PCRs were performed in a Corbett FTS-320 Thermal Sequencer (Corbett Research, Mortlake, NSW, Australia). DNA sequencing was performed using the ABI PRISM™ Dye Terminator Cycle Sequencing

Ready Reaction Kit (Perkin Elmer), and reactions were analysed at the DNA Sequencing Centre (Institute for Medical and Veterinary Science, Adelaide, SA, Australia). PCR products were purified from agarose gel using either Geneclean® (Chapter 2) or by electroelution using the S & S Biotrap from Schleicher and Schuell (Beverly, MA, USA) and the BT1 and BT2 Schleicher and Schuell membranes. Polyacrylamide gels were prepared and run using the Electrophoresis Apparatus GE-4II from Pharmacia (Uppsala, Sweden). All chemicals were of analytical grade or higher. Glycogen and Proteinase K were obtained from Roche Diagnostics. Chemicals purchased from Sigma Chemical Co. included the following: dimethyl sulphoxide (DMSO), lithium chloride, lysozyme and tetracycline hydrochloride (Tet). Sodium bicarbonate was from APS Finechem (Auburn, NSW, Australia). Isopropanol was obtained from BDH Laboratory Supplies (Pool, England). Electroporation cuvettes (0.2 cm gapped) and the Gene Pulser™ electroporation apparatus were from Bio-Rad (Hercules, CA, USA). Small scale plasmid preparations were performed using the BresaSpin™ Plasmid Miniprep kit obtained from Geneworks Ltd, using the manufacturer's instructions. All of the reagents used in the phage panning experiments are described in Section 2.2.

3.2.1 Buffers, solutions and media

The growth media (see below and Section 2.2.1), phage solutions (Section 2.2.1) and Tris EDTA sucrose (TES) buffer were prepared by Mrs Jacquelyn Brinkman (Central Services Unit, Department of Biochemistry, University of Adelaide), using the methods described in Sambrook *et al.*, (1989). All solutions were made in redistilled water filtered using the Milli-Q Ultra Pure Water System (Millipore Pty Ltd, North Ryde, NSW, Australia). Solutions marked (§) were sterilised by autoclaving.

Medium

SOC medium (§)
2% (w/v) Bacto®tryptone, 0.5% (w/v) Bacto®yeast extract, 10 mM NaCl, 2.5 mM KCl, 10 mM $MgCl_2$, 10 mM $MgSO_4$, 20 mM glucose

Solutions

Tris EDTA sucrose buffer (§)
25 mM Tris pH 8.0, 10 mM EDTA, 40 mM sucrose

Superose®6 DNA buffer
0.1 M sodium acetate, 20% RNAse-free ethanol
-adjusted to pH 7.0 and filtered through a 0.45µm filter. After filtration, SDS was added to a final concentration of 0.05% (w/v)

3.2.2 Bacterial strains

The genotypes of the *E. coli* strains used in this study are described below:

E. coli GM119: *dam3 dam6 metB1 galK2 galT22 lacY1 tsx7 supE44*

E. coli JM109: *e14⁻(McrA⁻) recA1 endA1 gyrA96 thi-1 hsdR17*(r_K-m_K+) *supE44 relA1* Δ(*lac-proAB*) [F' *traD36 proAB lacI^{q}ZΔM15*]

E. coli XL1-Blue: *recA1 endA1 gyrA96 thi-1 hsdR17 supE44 relA1 lac*[F' *proAB lacI^q ΔM15* Tn10 (Tet^r)]

3.3 Methods

3.3.1 Phage display using the E. coli strain XL1-Blue as a host

The suitability of XL1-Blue cells as hosts for the generation of phage displaying bIGFBP-2 was assessed prior to their use. XL1-Blue cells containing the vector pGF14 were superinfected with M13K07 helper phage, and phage particles expressing bIGFBP-2 on their surface were generated as described in Section 2.3.7.

3.3.2 Analysis of XL1-Blue cell-derived phage by SDS-PAGE and Western ligand blotting

To ensure that phage particles were expressing bIGFBP-2, PEG-precipitated phage particles (Section 2.3.7) were analysed by Western ligand blotting (described below). Sample loading dye (Section 2.2.1) was added to 20 µl of the PEG-precipitated phage preparation, and the sample was heated at 100°C for 5 minutes to facilitate phage disruption. After heating, the sample was immediately put on ice. Protein markers, purified COS-1 cell-derived bIGFBP-2 protein (as a standard) and M13K07 helper phage were similarly prepared for electrophoresis. The samples were electrophoretically separated on a 10% polyacrylamide gel (4% stacking gel), using the buffers described in Section 2.2.1. The gel was electrophoresed at 30 V overnight at room temperature, and then the following day the voltage was increased to 100 V

for 3 hours (25 hour total electrophoresis time). The protein transfer and the ligand blot procedures were performed as described in Section 2.3.4.

3.3.3 Establishment of panning using IGF-I coated wells

Expression of bIGFBP-2 on the surface of phage was also confirmed by ensuring that phage could be enriched on IGF-coated wells (Section 2.3.7 and below). IGF-I and IGF-II were each coated onto microtitre plates as described in Section 2.3.7. The panning procedures and phage titrations were performed as described in Section 2.3.7.

3.3.4 Construction of the mutant bIGFBP-2 library: primer design and PCR mutagenesis

A library of mutations in amino acid residues 221 to 230 of bIGFBP-2 was generated using overlap extension PCR (Horton *et al.*, 1989). The PCR product was subsequently cloned into the phagemid, pGF14 (Figure 3.3). Primer MP739 (Table 3.1 and Figure 3.4) was designed so that the 10 amino acids targeted for mutagenesis were not totally randomised. This approach was selected to increase the chances of generating a complete library containing all possible mutants. Amino acids Asp221, Gly223, Tyr225 and Gln230 were varied less in the mutant library when compared to the surrounding residues, because of the general conservation of these residues across all binding proteins (Figure 1.4). If the conserved residues have important structural roles, then the chances of affecting the structure of the mutant molecules would be reduced. The primer BP2-SalI was designed to remove the *Sal* I site located at the 3' end of the *bIGFBP-2* gene cloned in the vector pGF14 (Figures 2.4 and 3.3). Removal of this *Sal* I site in the mutant library would enable the library to be cured of contaminating wild type pGF14 vector by restriction digestion with *Sal* I.

Maximal product yield from each PCR step was achieved by determining the concentration of magnesium sulphate required in each reaction and the optimal conditions are described below. Control reactions excluded the pGF14 template to ensure that no contaminating template DNA was present.

PCR 1 (Figure 3.3) was performed, in a final reaction volume of 100 µl, using 2 units Pwo polymerase, 1 x Pwo reaction buffer (containing 2 mM $MgSO_4$), 0.2 mM dNTPs,

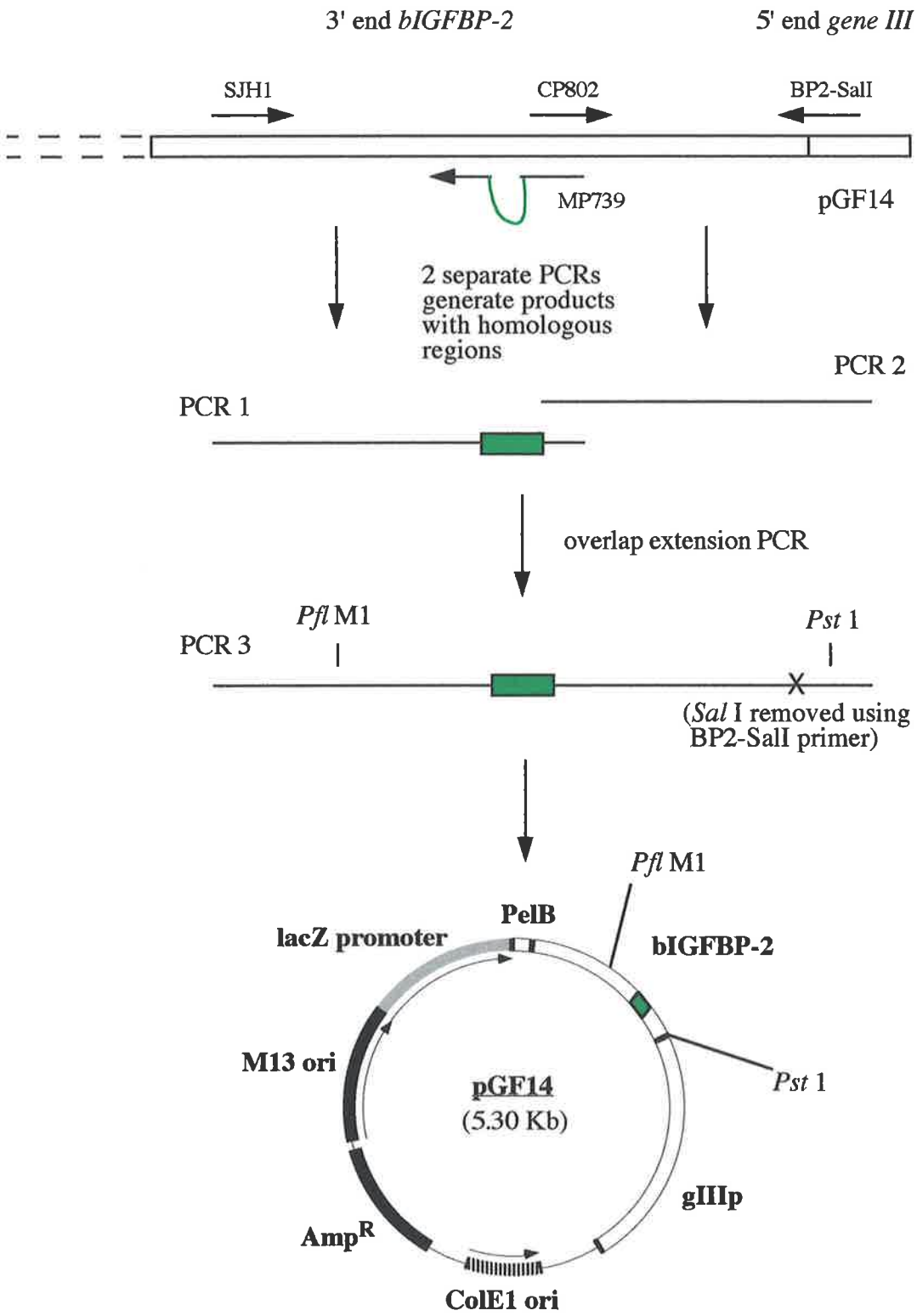

Figure 3.3 Overview of the strategy used to generate the C-terminal library of mutations in bIGFBP-2, between residues 221-230. The product of PCR 1 is generated from primers SJH1 and MP739. The product of PCR 2 is generated from primers CP802 and BP2-SalI. The product of PCR 3 is obtained by combining products from PCRs 1 and 2, and primers SJH1 and BP2-SalI. The region shown in green in primer MP739, contains the variable nucleotides encoding for the library of mutations between residues 221-230 in bIGFBP-2.

Figure 3.4 Primer MP739 used to create the C-terminal amino acid substitutions in bIGFBP-2, highlighting the range of amino acid residues that were possible at each codon. The primer (87 nucleotides long, see Table 3.1) was designed to limit the number of amino acid combinations to 6.71×10^7 possibilities, between residues 221-230. The symbol "n" either a, t, g or c. The stop codon generated at residue 227 (*) is an amber mutation, translated to glutamine in *supE* hosts. The complementary nucleotides present either side of the mutated region in primer MP739 are shown in small block text.

600 ng primer SJH1 (Table 3.1), 1.8 µg primer MP739 (Table 3.1, Figure 3.4) and 100 ng of pGF14 template. PCR 2 was performed similarly, but the primers CP802 (Table 3.1) and BP2-SalI (Table 3.1) were each used at 600 ng. The reactions were placed in a thermal cycler (preheated to 94°C), then denatured at 94°C for 3 minutes. The reaction was cycled 30 times using the following parameters: 94°C for 30 seconds, 65°C for 30 seconds and 72°C for 40 seconds. The final extension was performed at 72°C for 2 minutes. The products from PCR 1 (234 bp) and PCR 2 (120 bp) were gel purified using Geneclean® (Section 2.3.1). The yields obtained from the gel purification were estimated by gel analysis of ethidium bromide stained DNA and comparison to DNA standards of known quantities.

Primer	Sequence (5'- 3')
gIII*¶	ATATGTTAACTGTATGAGGTTTTGC
g3p4055¶	CGCGTTTTCATCGGCATTTTCGGT
PelB2297	AGCCGCTGGATTGTTATTACTCGC
MP739¶	ACAGTTGGGGATGTGTAGGGAGTAGAGGTG∞ACGCTGCCCGTTCA GAGACATCTTGCA
CP802	TGCAAGATGTCTCTGAACGGGCAGCGT
SJH1#	ATGGGCAAGGGTGGCAAACATCACCTC
BP2-SalI¶	AGCACCACCTGCAGACTACTGCATCCGCTGGTTGTGCACCCCTCG
p686BP2f	TCCTGGAGCGGATCTCCACCAT
p923BP2r¶	TGCTCGTTGTAGAAGAGATGAC

Table 3.1 The DNA primers used in the construction and sequencing of the bIGFBP-2 phage library. Sequences marked ¶ are antisense PCR or antisense sequencing primers. * Primer gIII was kindly provided by Dr Steven Polyak. # Primer SJH1 was kindly provided by Mr Sam Hodge. ∞ Represents a 30 nucleotide variable region in primer MP739, used to create the amino acid variability in residues 221 to 230 of bIGFBP-2, as shown in Figure 3.4.

The PCR products 1 and 2 were joined by overlap extension PCR (Horton *et al.*, 1989; Figure 3.3). In this 100 µl reaction, the enzyme and buffer conditions were the same as those described above, but the primers comprised 600 ng of both SJH1 and BP2-SalI, and 125 ng of each PCR product 1 and 2 were used as template. The reaction was placed in a 94°C preheated thermal cycler, for 25 cycles using the following parameters: 94°C for 30 seconds, 70°C for 30 seconds, 72°C for 25 seconds. The final extension was performed at 72°C for 2 minutes.

3.3.5 Purification of DNA from agarose gel

The product of PCR 3 (327 bp) was purified from agarose gel using either Geneclean® (Section 2.3.1) or electroelution. Electroelution was performed using the instructions supplied with the S & S Biotrap (Section 3.2). Briefly, electroelution was performed in 0.8 x TBE (Section 2.2.1), and the voltage was set at 150 V, with the current limited to 100 mA. The elution was performed at room temperature for 1 hour and 50 minutes and then the current was reversed for 20 seconds to elute residual DNA bound to the membrane. Following elution, the material was further purified by adding an equal volume of a 1:1 phenol:chloroform solution. This was mixed and then briefly centrifuged at room temperature to separate the layers. The upper phase was added to an equal volume of chloroform, mixed, and again centrifuged to separate the layers, and the chloroform was removed. The DNA was precipitated with 1/10th volume of 3 M sodium acetate pH 5.2, 50 ng/µl glycogen and 3 volumes of ice cold RNAse-free absolute ethanol at -20°C for 1 hour. The DNA was harvested by centrifugation at 9980 x g at 4°C for 15 minutes. The pellets were washed in ice cold 70% ethanol, and dried *in vacuo*. For cloning purposes, the DNA was resuspended in sterile, redistilled water and stored at -20°C.

3.3.6 Medium scale preparation of pGF14 DNA for library construction

The product of PCR 3 was cloned into the phagemid, pGF14, using restriction enzymes *Pfl* M1 and *Pst* I (Figure 3.3). These restriction enzymes were selected because their recognition sites were absent in the mutant bIGFBP-2 library, by virtue of the primer design. To enable cleavage of pGF14 DNA with the methylation sensitive enzyme *Pfl* M1, non-methylated pGF14 DNA was generated by transforming the phagemid into chemically competent *E. coli* GM119 cells (using the method of Sambrook *et al.*, 1989). To prepare the DNA, a colony from a freshly streaked plate of GM119 cells containing pGF14 was used to inoculate a 50 ml culture containing 2YT and 100 µg/ml Amp in a 1 litre shaker flask. The culture was shaken vigorously overnight at 37°C. The cells were pelleted at 3000 x g for 8 minutes at 4°C, the supernatant was discarded, and then the cells were resuspended in 3 ml TES buffer. Lysozyme (30 µl of an 100 mg/ml solution) was added to the cells, which were

mixed gently and then incubated on ice for 5 minutes. Freshly prepared 0.2 M NaOH, 1% SDS solution (6 ml) was added, gently mixed and put on ice for a further 5 minutes. Chromosomal DNA was precipitated by the addition of 4.5 ml 3 M sodium acetate pH 5.2 (mixed gently by inversion) and incubated on ice for 15 minutes (with occasional inversion during the incubation time). After centrifugation at 12000 x g for 8 minutes at 4°C, the supernatant (containing the plasmid) was removed. The plasmid DNA was precipitated by adding 8 ml isopropanol to the supernatant, incubating at room temperature for 5 minutes followed by centrifugation at 12000 x g (as described above). The pellet was drained and resuspended in 4 ml sterile redistilled water, 10 ml ice cold 4 M LiCl was added and then incubated on ice for 30 minutes to remove RNA. After centrifugation at 12000 x g (as described above), the pellet was drained and resuspended in 1.6 ml sterile redistilled water. Here, 8 µl 10 mg/ml RNAse A was added, and incubated at 60°C for 30 minutes to further remove contaminating RNA. Then, 32 µl of 10% SDS solution was added followed by Proteinase K (20 µl of 10 mg/ml stock), and the solution was gently mixed and incubated at 37°C for 15 minutes. This solution was diluted to 2 ml with sterile redistilled water and an equal volume of phenol was added. After gentle vortexing, the aqueous-phenol phases were separated by brief centrifugation and the aqueous phase was placed into a fresh tube. The phenol extraction was repeated on the aqueous phase. After the second phenol extraction, an equal volume of chloroform was added to the aqueous phase in a fresh tube. After vortexing, the layers were separated by centrifugation. The DNA from the aqueous phase was precipitated at -20°C for 30 minutes using 1/10th volume 3 M sodium acetate and 3 volumes of ice cold RNAse-free absolute ethanol. The DNA was harvested by centrifugation at 9700 x g for 10 minutes at 4°C, and washed twice in 4 ml 70% RNAse-free ethanol (centrifuged between each wash to reduce the loss of DNA). The DNA was air-dried and then resuspended in a total volume of 400 µl TE buffer (Section 2.2.1). Before purifying the DNA using size exclusion chromatography, the DNA was analysed spectrophotometrically at wave-lengths of 230, 260 and 280 nm to ensure that sufficient quantities were present for further purification.

The final stage of DNA purification involved size exclusion chromatography. The DNA was purified in two batches using a Superose®6 column (Section 2.3.7). The column was pre-equilibrated in Superose®6 DNA buffer, and 200 µl of the DNA was loaded onto the

column at 1 ml per minute. The elution was monitored at 280 nm, and the first peak, containing the plasmid DNA, was collected. The DNA was precipitated with 3 volumes of cold RNAse-free ethanol, at -20°C for at least one hour. The DNA was pelleted by centrifugation at 9700 x g for 10 minutes at 4°C, and washed twice in cold 70% RNAse-free ethanol as described above. The DNA was air dried and then dissolved in sterile redistilled water. The concentration and purity of the sample were assessed by agarose gel electrophoresis and spectrophotometry.

3.3.7 Cloning the PCR fragments to generate the mutagenic library

The PCR product 3 (Figure 3.3) and pGF14 (500 ng/reaction) DNA were individually digested with *Pfl* M1 and *Pst* I overnight at 37°C. The reactions contained: 1 x NEBuffer3, 0.1 mg/ml BSA, 8 units *Pfl* M1, 5 units *Pst* I, in a final volume of 50 µl. To obtain high quantities of product, multiple digests of PCR product 3 and phagemid DNA were performed rather than scaling up the reactions. The desired fragments were obtained by separating the DNA by agarose gel electrophoresis, and then purifying the DNA using electroelution (Section 3.3.5).

3.3.8 Ligation conditions to generate the mutant bIGFBP-2 library

The conditions for ligation were assessed in small scale reactions (20 µl volume) to determine the optimal vector:insert ratio required to maximise the product yields. For library production, the ligation reaction was performed in a final reaction volume of 100 µl, using vector:insert ratios of either 1:2 (0.35 pmol:0.7 pmol) or 1:5 (0.3 pmol:1.5 pmol). The ligation was performed by mixing the vector, insert and water, which was heated to 42°C for 2 minutes and then placed on ice, as described in Sambrook *et al.*, (1989). T4 DNA ligase buffer (supplied by the manufacturer, diluted 1/10) and 10 units of T4 DNA ligase were added to the reaction. The reaction was mixed, overlaid with paraffin oil and incubated overnight at 15°C. The amount of religated vector was estimated by performing control reactions containing no insert DNA. After ligation, the enzyme was heat denatured by incubation at 65°C for 10 minutes. To reduce the levels of contaminating religated pGF14 vector, the ligation mix was digested with the restriction enzyme, *Sal* I. This was performed by increasing the volume of the ligation reaction to 150 µl and adding 1 x OPA+ restriction enzyme buffer and 14 units of

Sal I restriction enzyme. After 1.5 hours of incubation at 37°C, the enzyme was heat denatured at 65°C for 20 minutes. The DNA from the reaction was then precipitated using 3 M sodium acetate, glycogen and ethanol as described in Section 3.3.5.

3.3.9 Preparation of electrocompetent E. coli XL1-Blue cells for transformation of the bIGFBP-2 mutant library

Ligations were transformed into XL1-Blue *E. coli* cells using electroporation. Electrocompetent cells were prepared by a method modified from that described by Chuang *et al.*, (1995). Care was taken to maintain the cells in a cold environment by performing the procedures in a 4°C room using pre-chilled pipette tips and Eppendorf tubes. Briefly, 300 µl of an overnight culture of cells (grown at 37°C in 2YT and 10 µg/ml Tet) was used to inoculate a 2 litre shaker flask containing 300 ml 2YT and 10 µg/ml Tet. The cultures were incubated at 18°C to 20°C with shaking at 250 rpm, until an OD_{600} of 0.5 to 0.8 was reached (approximately 44 hour growth time), and cells were then chilled on ice for 10 minutes. Cells were harvested by centrifugation at 3400 x g for 10 minutes at 4°C. The cells were then washed in decreasing quantities of ice cold sterile redistilled water four times (starting at 200 ml, reducing to 30 ml), harvesting the cells after each wash using the centrifugation conditions described above. Normally three cultures were used to generate one batch of competent cells and the final pellets were pooled and resuspended in a total volume of 1 ml cold, sterile 10% glycerol. The competent cells were aliquoted into 40-100 µl lots, were then snap frozen in a bath comprising dry-ice and ethanol and were stored at -80°C. To ensure that no contamination was present and to assess the numbers of cells surviving the freezing procedure, one tube was defrosted, diluted and plated onto L plates with (either 10 µg/ml Tet or 100 µg/ml Amp) or without antibiotic.

A similar procedure was used to generate electrocompetent *E. coli* JM109 cells.

3.3.10 Electroporation of the bIGFBP-2 mutant phagemid library into E. coli cells

The pGF14 mutant DNA library was transformed into XL1-Blue cells by a single electrical pulse of 2.5 kV (resistance: 200 ohms, capacitance: 25 µF). Both cuvette and cuvette

holder were pre-chilled at 4°C to maximise the numbers of transformants obtained. Control cuvettes contained cells with: i) religated vector to estimate the background levels, ii) uncut vector to estimate transformation efficiencies, or iii) no DNA to ensure that no contamination was present. After electroporation, cells were immediately resuspended in 1 ml SOC medium, and the cells containing the mutant library DNA were pooled in a shaker flask and grown with shaking for 1 hour at 37°C. At this point, samples of cells were diluted and plated on L plates containing 100 μg/ml Amp and 2% glucose, to estimate the numbers of transformants.

In the first attempt at transforming the mutant phagemid library, cells containing phagemid were immediately used to generate phage (see below). In the second attempt at library construction, cells were propagated overnight at 37°C (immediately after transformation) in the absence of helper phage. The next day, the library was stored at -80°C either as glycerol stocks of the cells containing the vector, or as DNA (prepared by small scale preparation procedures, Section 3.3.11). This second approach was used when the *E. coli* strain JM109 was used to propagate the mutant phagemid library.

3.3.11 Small scale preparation of DNA

Cells containing pGF14 and library variants were grown overnight at 37°C in 2YT containing 2% glucose and 100 μg/ml Amp. Initially, DNA was prepared using the alkaline lysis procedure described in Sambrook *et al.*, (1989). For sequencing reactions, DNA was further purified using the PEG-precipitation procedure described in Bulletin 18 (Applied Biosystems, 1991). DNA was also prepared from 2 ml of an overnight culture using the BresaSpin™ Plasmid Miniprep kit. The only alteration made to this procedure was in the final step, when the DNA was eluted from the purification spin column using 50 μl sterile redistilled water, and was stored at -20°C. The DNA prepared by these means was suitable for DNA sequencing reactions without any further purification.

3.3.12 DNA sequencing of mutant phagemid clones

Phagemid vector, pGF14, and mutant derivatives were sequenced using either the g3p4055 or gIIIp primer (Table 3.1), and the ABI PRISM™ Dye Terminator Cycle Sequencing

Ready Reaction Kit. The conditions used, were essentially as those described by the manufacturer. Optimal sequencing results were obtained using 1 µg template DNA and 100 ng of primer. After thermal cycling, the reactions were transferred to fresh tubes and were precipitated in 50 µl absolute RNAse-free ethanol, containing 2 µl 3 M sodium acetate pH 5.2. After mixing by vortex, the reaction was precipitated for 10 minutes on ice. The DNA was harvested by centrifugation for 30 minutes at 9980 x g and 4°C. The pellet was washed in 250 µl ice cold 70% ethanol (with 5 minute centrifugation at 9980 x g and 4°C), and was dried in vacuo.

3.3.13 Generation of phage expressing the bIGFBP-2 mutant library

The generation of the phage library resulted in the predominance of deleted clones. Therefore two different approaches for the propagation of phage particles were tested to reduce this problem.

In the first instance, to generate phage expressing the mutant library, cells electroporated with the mutant phagemid library were pooled and diluted 1/5 into 2YT medium containing 2% glucose and 100 µg/ml Amp. This culture was grown for 1 hour at 37°C, and then M13K07 helper phage were added at a multiplicity of infection of 10 (the cell number was estimated based on the assumption that an OD_{600} of 1 (represented approximately 1 x 10^9 bacterial cells per ml). After two hours of growth, the cells were induced to express the fusion protein by diluting the culture (1/10) into pre-warmed 2YT medium (30°C) containing 100 µg/ml Amp, 5 µg/ml Kan and 0.02 mM IPTG. This culture was grown overnight at 30°C. As a control, phage particles expressing wild type bIGFBP-2 were generated. Phage were precipitated from culture medium using the techniques described in Section 2.3.7. Phage were either used directly in panning experiments, or were stored in PBST containing 15% glycerol (snap-frozen in a bath containing dry ice and ethanol) at -80°C. Phage were reinfected into XL1-Blue *E. coli* using procedures described in Section 2.3.7.

In an attempt to reduce the numbers of clones containing shorter segments of bIGFBP-2 DNA, the phage were propagated using a method adapted from Harrison *et al.*, (1996). For this procedure, cells were transformed with the mutant library and were propagated overnight in the absence of helper phage (Section 3.3.10). Glycerol stocks of cells containing the library

of bIGFBP-2 mutants (500 µl of the mutant library) were used to inoculate a 50 ml culture containing 2YT, 2% glucose, 100 µg/ml Amp and 10 µg/ml Tet in a 500 ml shaker flask. Flasks were also prepared with cells containing the wild type pGF14 phagemid as a control. These flasks were grown with vigorous shaking at 37°C to an OD_{600} of 0.5. At this point, cells were infected with 5 x 10^9 M13K07 helper phage and were left for 30 minutes at 37°C with gentle agitation. The cells were harvested at 3300 x g for 10 minutes, then gently resuspended in 20 ml 2YT containing 100 µg/ml Amp, 5 µg/ml Kan and 0.02 mM IPTG. Cultures were grown for 3 to 4 hours at 30°C, and then phage were prepared as described in Section 2.3.7. To reinfect and amplify populations of phage particles, the conditions similar to those described in Section 2.3.7 were used. However, after infection with M13K07 the cells were harvested by centrifugation at 3300 x g for 10 minutes, and then resuspended in 20 ml 2YT containing 100 µg/ml Amp, 5 µg/ml Kan and 0.02 mM IPTG. Cultures were grown for approximately 3 to 4 hours at 30°C, before phage were prepared using the PEG-precipitation procedure (Section 2.3.7).

3.3.14 Panning of the mutant bIGFBP-2 phage library on IGF-coated wells

Panning experiments were performed using the procedures described in Section 2.3.7. Minor variations made to the technique included binding of phage particles to IGF-coated wells for either 1 hour or 3 hours at 37°C. The 3 hour incubation time was used to increase the chances of capturing clones that were less frequently represented due to shorter phage propagation times. Also, to reduce the chances of losing variant bIGFBP-2 phage particles, panning was performed with a reduced number of washes prior to phage elution (the numbers of washes performed was increased with consecutive rounds to 5 washes by round 4). This was done to ensure that conditions were not too stringent in the selection procedures, which may lead to the loss of minor library representatives. In every panning experiment, each condition was performed at least in duplicate. Phage particles eluted from each well were treated independently of one another, in subsequent reamplification and panning procedures.

3.3.15 Screening for pGF14 clone integrity using restriction enzyme analysis and colony PCR

After panning, phage were titred as CFU (Section 2.3.7), and the integrity of the DNA from these clones was assessed by restriction enzyme analysis, or by PCR. For restriction enzyme analysis, overnight cultures were prepared from the colonies of *E. coli* cells containing phagemid DNA. The DNA was prepared using the small scale procedure described in Section 3.3.11. Restriction digestion of purified DNA was performed with *Nco* I and *Bam* HI (liberating a 1.47 kb bIGFBP-2 containing fragment) or *Hin*d III and *Bam* HI (liberating a 1.57 kb bIGFBP-2 fragment). These enzymes were chosen for restriction digestion because they cut externally to the bIGFBP-2 gene. The conditions used for DNA restriction digestion were those described by the manufacturer.

Colony PCR was performed using a technique modified from Clackson *et al.*, (1996). Optimal PCR screening of colonies was achieved with reactions containing: 1 x Taq reaction buffer, 1.5 mM $MgCl_2$, 0.25 mM dNTP, 10% (v/v) DMSO, 100 ng primer g3p4055 and 100 ng primer PelB2297 in a final volume of 20 µl. Using a sterile toothpick, a single colony was added to each tube, and the tubes were heated at 94°C for 5 minutes to facilitate cell lysis. At this point, 1 unit of Taq DNA polymerase was added per tube, and the reactions were overlaid with paraffin oil. The reaction efficiency was assessed by including controls with template pGF14, or cells without the phagemid, or no cells. The reaction tubes were heated to 94°C for 2 minutes, then cycled 25 times using the following parameters: 94°C for 30 seconds, 51°C for 30 seconds and 72°C for 2 minutes. The final extension was performed for 4 minutes at 72°C. PCR products were analysed using agarose gel electrophoresis and stained with ethidium bromide.

3.4 Results

3.4.1 Establishment of phage display using E. coli XL1-Blue cells as a host for phage production and optimisation of panning conditions

To ensure that the *E. coli* XL1-Blue strain was a suitable host for the propagation of the mutant phagemid library, phage expressing wild type bIGFBP-2:gIIIp fusion protein were

prepared from cells containing phagemid pGF14. Analysis of the CFU:PFU ratio of phage prepared from these cultures showed phage particles containing the phagemid, pGF14, dominated approximately 10-fold over phage containing M13K07 DNA. Samples of phage isolated from the culture using PEG-precipitation (Section 2.3.7) were analysed by electrophoretic separation on polyacrylamide gel. Following Western transfer, this filter was probed with ^{125}I IGF-II. As can be seen in Figure 3.5, bIGFBP-2 protein was detected both as gIIIp-fused and unfused protein in the PEG-precipitated samples. When negative controls which contained the M13K07 helper phage were included on the blots, there was no detectable binding activity specific for the ^{125}I IGF-II ligand (data not shown).

Phage expressing bIGFBP-2 were panned on IGF-coated wells as described in Section 2.3.7, to ensure that sufficient levels of bIGFBP-2 were expressed to facilitate enrichment of phagemid containing particles. Initial panning experiments were performed using IGF-II, and the conditions that were used to coat plates and to pan using this ligand, were also found to be appropriate for panning using IGF-I. Table 3.2 shows the result of one experiment, where panning was performed using wells coated with either 0.5 µg IGF-I, IGF-II, or with BSA. Although free bIGFBP-2 protein was present in the PEG-precipitated preparations of phage (Figure 3.5), enrichment over non-specific binding was observed (Table 3.2). Similar results were obtained with subsequent experiments. These results confirmed that phage produced from XL1-Blue cells containing pGF14, expressed bIGFBP-2 to levels which could be used to enrich for IGF binding activity in panning experiments.

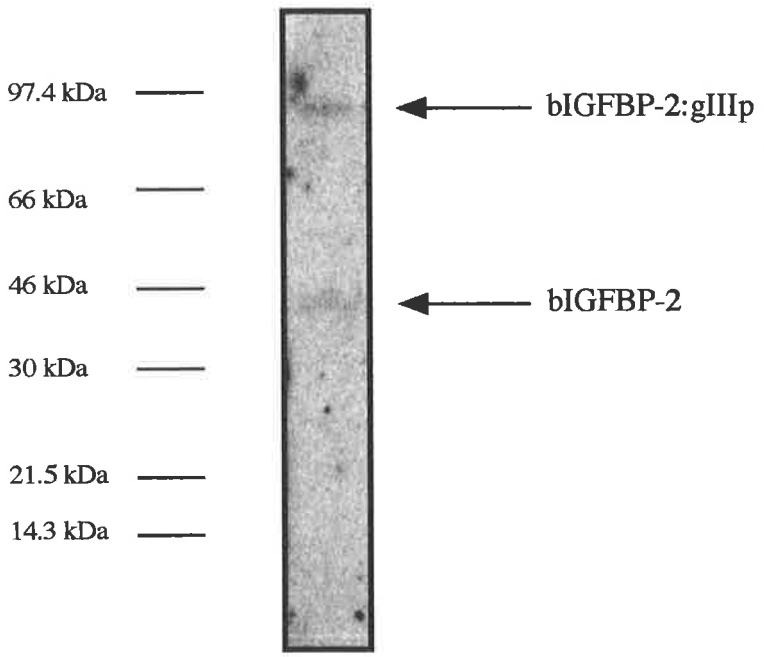

Figure 3.5 ^{125}I IGF-II ligand blot showing IGF-II binding activity in the phage preparations. The blot shows that phage prepared from XL1-Blue *E. coli* contain both bIGFBP-2:gIIIp fusion protein and free bIGFBP-2. The location of the molecular weight markers are shown to the left of the blot.

Well coating	Average numbers of eluted phage (CFU/ml)	Average enrichment (IGF/BSA)
IGF-I	1.158 (± 0.162) x 10^7	173
IGF-II	2.785 (± 0.668) x 10^6	42
BSA	6.705 (± 3.352) x 10^4	-

Table 3.2 Analysis of the panning procedure using IGF and BSA coated wells. Phage expressing bIGFBP-2 (3 x 10^{10} per well) were bound to IGF or BSA coated wells for 1 hour, and then the wells were washed 10 times and phage were eluted using 0.5 M acetic acid (Section 2.3.7). Eluted phage were titred as CFUs (Section 2.3.7), and the numbers were expressed as CFU/ml. The number of phage particles was estimated by determining the mean number obtained from 4 separate wells. The standard errors (at a significance level of 95%) for each of these values are shown in brackets.

3.4.2 Mutant library construction

A library of mutations in the C-terminal residues of bIGFBP-2 was generated by using a PCR-based approach (Figure 3.3, Section 3.3.4). The PCR reaction conditions used to generate the products for the overlap extension reaction were optimised by varying the concentrations of $MgSO_4$. Concentrations of $MgSO_4$, from 1.5 mM to up to 6 mM were assessed. Figure 3.6 shows the effects of different $MgSO_4$ concentration on the yield of PCR product 1 using primers the SJH1 and MP739. As can be seen, the maximal yield of PCR product was obtained using 2 mM $MgSO_4$, with reductions to the product yields as the concentrations increased. The reduction in the product yield as a function of increasing concentrations of $MgSO_4$ was also found for PCR product 2, using primers CP802 and BP2-SalI (data not shown). Therefore, based on these results all reactions (including the overlap extension PCR) were performed using 2 mM $MgSO_4$.

To generate large quantities of the purified overlap extension PCR product (PCR product 3, Figure 3.3) for the construction of the mutant library, it was important to optimise the agarose gel extraction procedures. Agarose gel extraction was used to purify the DNA fragments after each PCR step and following the restriction digestion of DNA for cloning. The PCR products were purified from agarose gel using either Geneclean® or electroelution (Section 3.3.5). Geneclean® yielded up to 50% of the product that was excised from the gel, while electroelution recovered between 65-80% of the DNA from the agarose gel (data not shown). Therefore, electroelution was used.

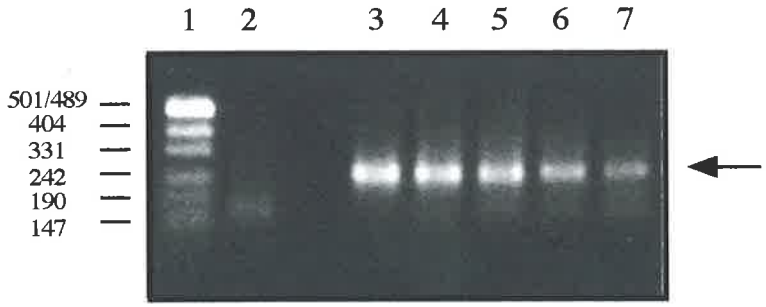

Figure 3.6 Analysis of the concentrations of $MgSO_4$ required to yield optimal amounts of PCR product during the construction of the mutagenic bIGFBP-2 library. Here, the reaction contained pGF14 template and the primers SJH1 and MP739 (Table 3.1 and Figure 3.3), with 2 mM (lane 3), 3 mM (lane 4), 4 mM (lane 5), 5 mM (lane 6) and 6 mM (lane 7) $MgSO_4$. The expected size of the product was 234 nucleotides (marked to the right of the gel). Lane 1 contains the pUC19 (*Hpa* II restricted) molecular weight markers, with the sizes of the bands shown on the left of the gel (in base pairs). Lane 2 contains a control reaction without template.

Small scale ligation reactions were performed to assess the optimal insert:vector ratio for the construction of the mutant library. As estimated by the numbers of transformants generated from small scale test ligations, a ratio of either 1:2 or 1:5 (vector to insert) produced similar yields of library product (Table 3.3). The efficiency of *Sal* I digestion in eliminating religated parent phagemid was assessed by comparing the numbers of Amp resistant colonies generated from control reactions that did not contain the insert DNA (Table 3.3). It was estimated that digestion of the ligation reaction reduced the contaminating wild type vector to $1/100^{th}$ of the starting amount (Table 3.3). Therefore, based on these results the purified digested PCR product 3 and phagemid vector, pGF14, were ligated using an vector to insert ratio of either 1:2 or 1:5. The mutant library was transformed (approximately 1.5 µg vector DNA) into XL1-Blue cells and generated an estimated library size of approximately 5.8×10^6 individual clones. The maximal number of different possibilities that could be generated from the library using the MP739 primer design was 6.7×10^7 (Figure 3.4). Following transformation of this mutant library it was noted that the colony sizes of the cells containing the mutant library varied considerably across the plate (data not shown).

DNA sample	Transformants per µg DNA
uncut pGF14	7.7×10^7
digested pGF14 (no insert)	1.1×10^6
digested pGF14, *Sal* I	1×10^4
digested pGF14 + insert (1:2)	1.12×10^7
digested pGF14 + insert (1:5)	9.04×10^6
digested pGF14 + insert (1:10)	4.25×10^6

Table 3.3 Small scale analysis to determine the optimal conditions for the ligation reactions used to create the mutant bIGFBP-2 C-terminal library. The phagemid, pGF14, and the PCR product 3 were digested using *Pfl* M1 and *Pst* I and gel purified as described in the Section 3.3.7. The digested phagemid was then ligated to increasing amounts of PCR product 3 insert DNA, ranging from a vector:insert ratio of 1:2, 1:5 or 1:10. A control reaction was performed where no insert DNA was added, to estimate the amounts of religated vector (digested pGF14, no insert). The efficiency of *Sal* I digestion in eliminating contaminating wild type pGF14 was determined by digesting the control ligation reaction (digested pGF14, no insert) with *Sal* I, and by determining the number of Amp resistant colonies obtained after transformation. Uncut phagemid was included as a positive control to ensure the cells were competent to DNA uptake. In each of the above conditions, 25 ng of DNA was transformed into approximately 2×10^9 XL1-Blue *E. coli* cells.

3.4.3 Production of phage expressing the mutant bIGFBP-2 and panning of this library

After transformation of the mutant library, the cells were used immediately to generate phage particles. The yield of phage particles following overnight growth was determined as 1.3 x 10^{10} CFUs/ml. Approximately 1 x 10^{9} CFUs from this preparation were added to each IGF-I and IGF-II coated well. After binding the phage particles to the IGF-coated wells, these wells were washed 10 times prior to elution with 0.5 M acetic acid and the samples were neutralised (Section 2.3.7). In these initial panning experiments, there was a reduction in the number of particles eluted after two rounds of panning to below 100. Therefore subsequent panning experiments were performed using less stringent wash conditions, where wells containing phage particles were washed only 5 times with PBST prior to elution with acid. This panning procedure yielded higher numbers of phage particles (greater than 1000 particles were eluted from each of the wells) after 3 rounds of selection. At this point, phagemid DNA was isolated from randomly selected clones for sequence analysis. Agarose gel analysis of the DNA preparations showed samples with aberrant gel mobility. The phagemid DNA obtained from the IGF-II coated wells was subjected to restriction analysis using both *Nco* I and *Bam* HI to assess DNA integrity. Restriction patterns of the DNA showed that of a total of 30 isolated clones, only one contained full-length *bIGFBP-2* DNA (Figure 3.7). Similar digests were also performed using only *Pst* I, which is located at the 3' end of the *bIGFBP-2* gene in pGF14 (Figure 3.3). However, *Pst* I did not cleave the DNA (data not shown). These results suggest that deletion of pGF14 phagemid DNA (containing the library of mutations) was occurring in the 3' end of the *bIGFBP-2* gene. Similar results were obtained when phagemid DNA was analysed from phage panned in duplicate IGF-II coated wells, and also from IGF-I coated wells (Figure 3.7, Table 3.4). To ensure that the original starting library was intact, clones obtained from the initial library transformation were also analysed by DNA restriction digestion. Of the 17 clones analysed, all contained full-length inserts (Figure 3.7, Table 3.4). This gave evidence that the high numbers of mutant library clones containing DNA deletions were a result of consecutive rounds of panning and phage amplification. This was substantiated when attempts to reamplify the stocks of phage containing the mutant pGF14

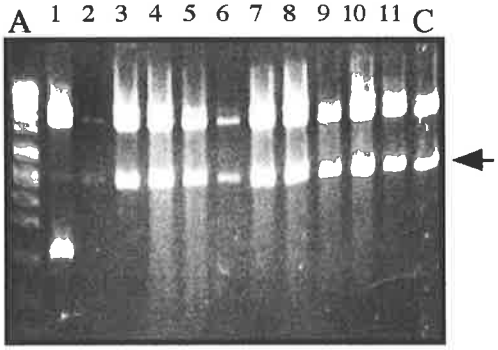

a) unpanned mutant library

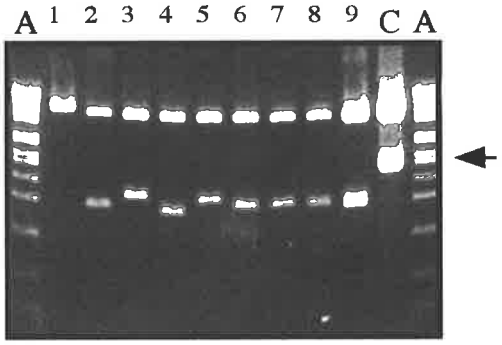

b) IGFII, well A

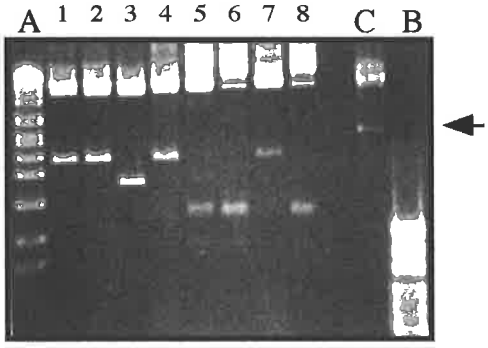

c) IGFII, well B

Figure 3.7 Restriction digest analysis of DNA from phagemids before panning, and after three rounds of panning on IGF-II coated plates. DNA was digested with either *Nco* I and *Bam* HI, or *Hind* III and *Bam* HI, and compared to parent pGF14 phagemid cut using the same enzymes. The expected fragment from the double digests is marked with an arrow. Lanes marked A contain *Eco* RI restricted SPP1 marker DNA (the sizes of each fragment are shown in Figure 4.4). Lanes marked B contain *Hpa* II restricted pUC19 marker DNA (the sizes of each marker are shown in Figure 3.6). Lanes marked C contain digested parent pGF14 phagemid DNA. The numbered lanes contain the randomly selected phagemid clones. The clone in Lane 1 on gel a) (unpanned mutant library) is a full-length clone which contains an internal *Bam* HI site within the mutated region of *bIGFBP-2*. In these experiments, phage were propagated by overnight growth in XL1-Blue *E. coli* cells.

library (by reinfecting XL1-Blue cells and by propagating the cultures overnight) also resulted in the accumulation of DNA deletions.

Sample	Intact clones	Truncated/deleted clones
transformed library	17	0
round 3, IGF-I well A	0	5
round 3, IGF-I well B	0	5
round 3, IGF-II well A	1	30
round 3, IGF-II well B	0	16

Table 3.4 Summary of restriction enzyme analysis performed on clones from the original unpanned library and clones obtained after 3 rounds of panning against IGF ligand. DNA was purified, and was digested with restriction enzymes *Hind* III and *Bam* HI, or with *Nco* I and *Bam* HI as described Section 3.3.15. The fragments obtained from the digests were compared to pGF14 phagemid DNA on an agarose gel visualised using ethidium bromide (Figure 3.7). Truncated clones were those that generated fragments of smaller than expected size upon digestion. Deleted clones did not generate any detectable fragment upon restriction digestion.

3.4.4 Analysis for the cause of the DNA deletions experienced during the amplification and panning of the mutant phage library

Experiments were performed to determine the cause of the *bIGFBP-2* gene deletions which accumulated as a result of phage propagation.

The accumulation of variable size deletions within the pGF14 mutant library was not apparently due to the host cell strain XL1-Blue. Transformation of the mutant pGF14 library into JM109 cells also resulted in the accumulation of deletions (data not shown). Interestingly, this is in contrast to the experience of phage display of IGFBP-3, which was performed in JM109 cells without the DNA deletion problems (Maria Galanis, personal communication; CSIRO, Parkville, Vic., Australia). Consequently, the use of JM109 cells for the propagation of phage expressing mutant bIGFBP-2 protein was not pursued.

Secondly, experiments were conducted to determine if the digestion or ligation conditions used to construct the phagemid library were the cause of the deletions which accumulated with phage propagation. For example, prolonged digestion with *Pst* I which is known to exhibit star activity (Malyguine *et al.*, 1980) could have resulted in cleavage at sites other than those preferred by the enzyme. Upon ligation, low numbers of clones which lack larger segments of

bIGFBP-2 encoding DNA may preferentially be amplified, and would dominate after several rounds of phage amplification. To test this possibility, wild type pGF14 was similarly cleaved with *Pfl* M1 and *Pst* I, religated and transformed into XL1-Blue cells. Phage particles were prepared from these cells and were reamplified three times in the absence of panning. After the third reamplification, colony PCR analysis of randomly selected clones showed no evidence for the accumulation of DNA deletions. The results of these experiments would suggest that the deletions observed in the mutant library were the consequence of inserting the mutated DNA sequence (PCR product 3) into the *bIGFBP-2* gene in pGF14.

In a second attempt at generating the mutant library, DNA from the initial ligation was once again electroporated into XL1-Blue *E. coli*. The transformation (approximately 1.5 µg vector DNA) was estimated to yield approximately 1.96 x 10^6 independent cells. In this instance, the phagemid library was transformed and propagated in the absence of helper phage (Section 3.3.10). Furthermore, as suggested by Harrison *et al.* (1996) the phage propagation time was minimised to reduce the chances of accumulating phagemid clones that contained shorter insert sequences. Therefore, phage were propagated for between 3 to 4 hours at 30°C, rather than overnight. As described in Section 3.4.3, restriction digest analysis of phagemid DNA prepared from the first phagemid library using *Pst* I suggested that the clones were losing DNA encoding the C-terminal end of bIGFBP-2. Therefore, panning was performed on IGF-II coated wells using the H64A subtilisin cleavage approach. The H64A subtilisin site, located directly after the C-terminal end of bIGFBP-2 (Figure 2.4) was chosen to select for release of only those clones containing DNA encoding the C-terminal end of bIGFBP-2.

Using this approach, there was a greater maintenance of full-length clones after rounds 2, 3 and 4 (Figure 3.8) of selection on IGF-II coated wells, in contrast to the initial attempts at library production. PCR analysis of phagemid DNA isolated from randomly selected clones after four rounds of selection on IGF-II, revealed that 71% clones were intact. These results suggested that the combination of reduced phage propagation times and more stringent panning procedures were beneficial in the maintenance of full-length pGF14 clones. Therefore, based on the results obtained from the 4th round selection procedures, individual clones were randomly selected and the DNA was sequenced to examine for the presence of favourable ligand binding sequences.

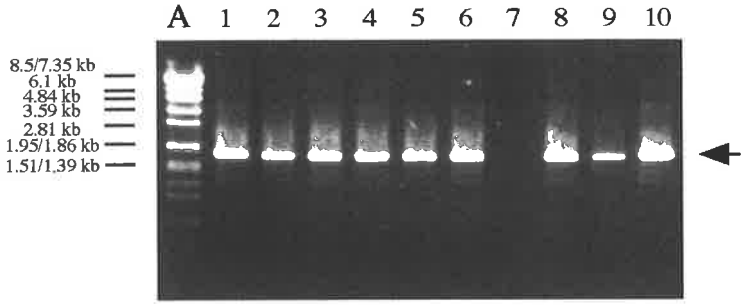

Round 2 phage samples

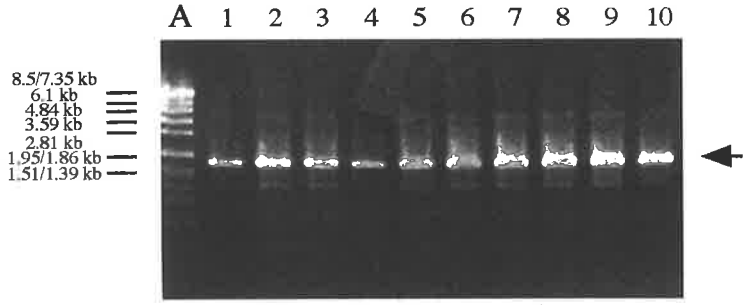

Round 3 phage samples

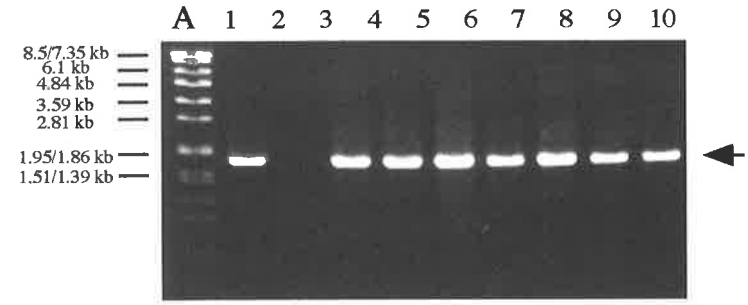

Round 4 phage samples

Figure 3.8 Colony PCR analysis used to assess the integrity of clones during the panning procedures. Panning was performed using H64A subtilisin elution, and phage were propagated for 3-4 hours at 37°C. Using these procedures, the problems associated with the accumulation of deleted clones over consecutive rounds of panning (shown above) were overcome. Lane A contains the *Eco*R I digested SPP1 marker DNA (the sizes of the markers are indicated to the left of the gels in kilobase pairs). Lanes 1-10 contain the products from the colony PCRs, performed on colonies containing the mutant phagemid library. The arrows indicate the 1.75 kilobase pair PCR product, which was used to confirm that the phagemid library contained the full-length *bIGFBP-2* DNA.

3.4.5 Sequence analysis of mutant bIGFBP-2 phagemid clones selected using IGF-II coated plates

Phagemid DNA isolated from four rounds of selection on IGF-II coated wells were sequenced and compared to the starting phagemid DNA library (Tables 3.5, 3.6a and 3.6b). The data is represented in histogram format by comparison of the prevalence of residues in the start library with the clones isolated after four rounds of panning against IGF-II ligand (Figure 3.9a and 3.9b). Interestingly, none of the sequences isolated before or after four rounds of panning contained the parent pGF14 clone (Tables 3.5, 3.6a and 3.6b). After four rounds of panning, only one sequence was found to occur twice in a total of 48 randomly selected clones (Tables 3.6a and 3.6b).

A comparison of the sequences before and after four rounds of panning performed on IGF-II ligand did not give evidence for the emergence of a strong consensus binding sequence (Tables 3.5, 3.6a and 3.6b). Most notable is the loss of the prevalence of the negatively charged Asp at positions 221 and 223 in duplicate panning experiments (Figures 3.9a and 3.9b). Asp is the residue present in all IGFBP-2 sequences isolated to date (Figure 1.5) and in all human IGFBPs, except for IGFBP-1 which contains an Asn (Figure 1.4). Glu which is also prevalent in the starting library at position 228 decreases in frequency in phage selected in duplicate wells after four rounds of panning on IGF-II coated plates (see Section 3.5).

During the sequence analysis of clones isolated from the fourth round of panning, three clones were found to contain bIGFBP-2 DNA encoding only the N-terminal part of the protein (Figure 3.10). All of these clones contained the H64A subtilisin cleavage site located at the end of the bIGFBP-2 fragment, and two of these clones, 4.72B and 4.77B, contained the cleavage site immediately fused to sequence encoding the N-terminal end of the gIIIp (Figure 3.10). These observations suggest that use of the H64A subtilisin cleavage site for the elution of phage from IGF-II coated wells was providing an effective selective process. The loss of the amber stop codon in all three clones probably resulted in a higher amount of the protein being expressed on the surface of phage particles, possibly increasing the chances of avidity effects. Fragments of this size obtained from other binding proteins (eg. hIGFBP-5 studied by

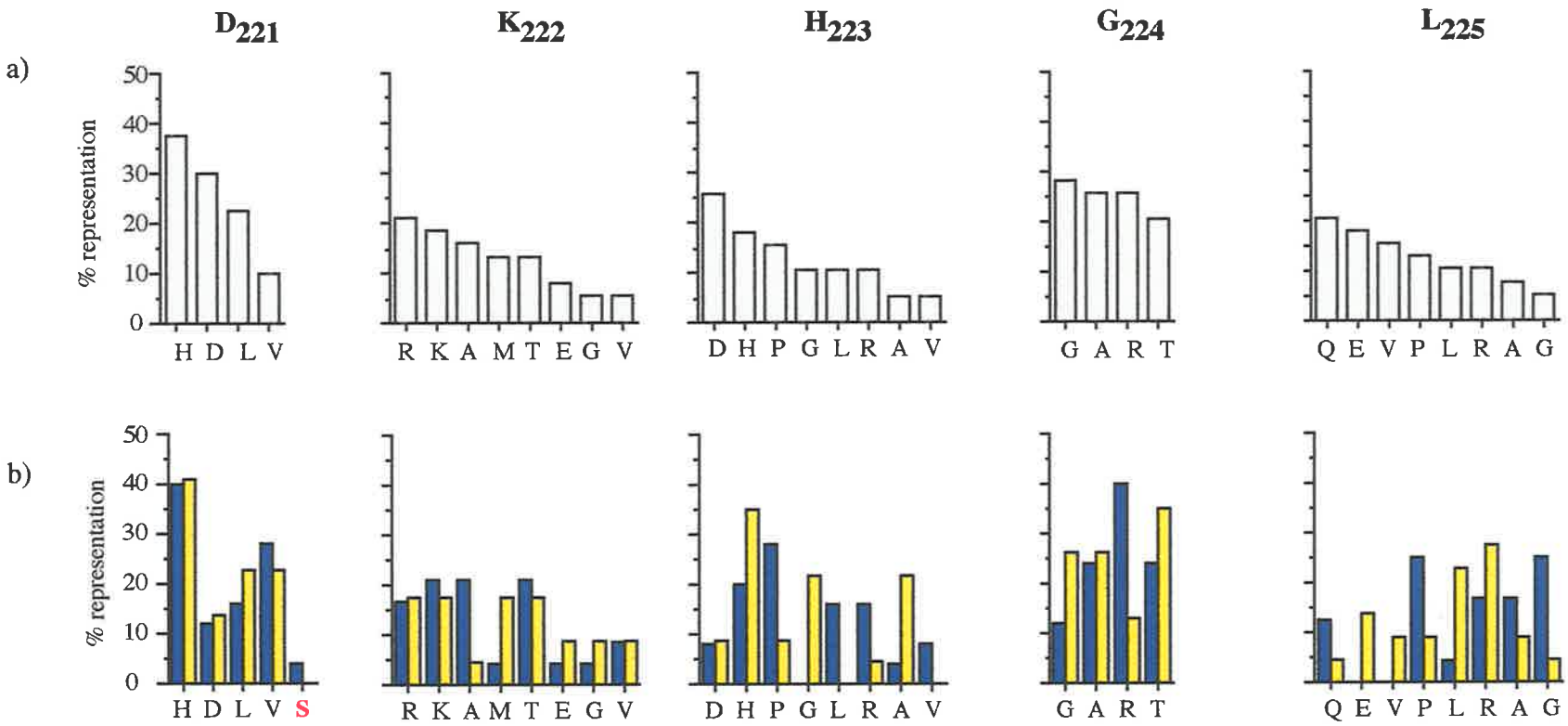

Figure 3.9a Comparison of the amino acid frequencies, at position 221-225 before and after four rounds of panning the mutant bIGFBP-2 library on IGF-II. Residues marked in red were not designed to occur in the original library. The native bIGFBP-2 sequence is shown above each graph in bold.
a) The frequencies of amino acids found in a total of 41 randomly selected clones from the unpanned library.
b) The frequencies of amino acids found in a total of 25 and 23 randomly selected fourth round clones, isolated from each duplicate well A (■) and well B (□) respectively.

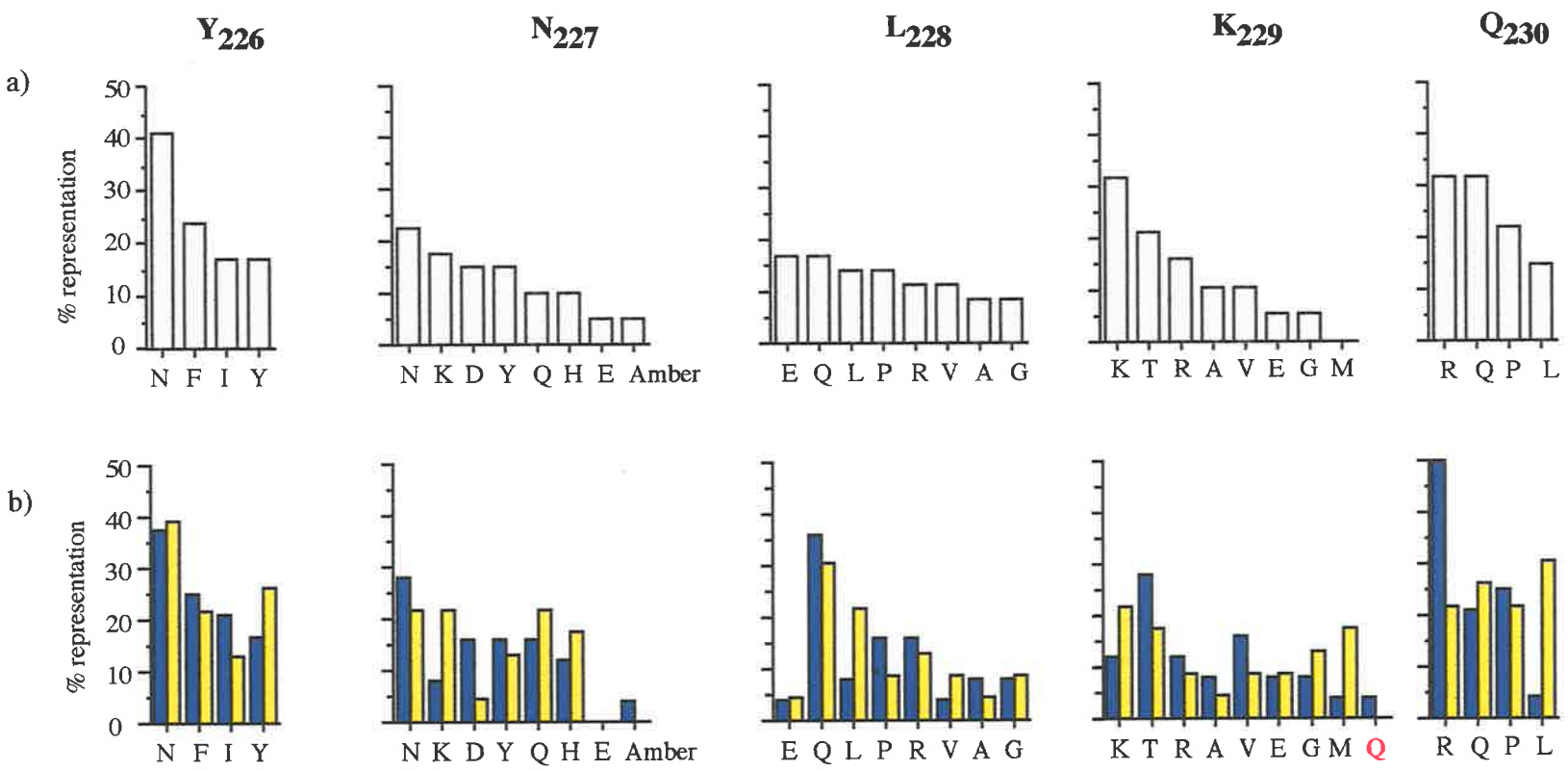

Figure 3.9b Comparison of the amino acid frequencies, at position 226-230 before and after four rounds of panning the mutant bIGFBP-2 library on IGF-II. Residues marked in red were not designed to occur in the original library. The native bIGFBP-2 sequence is shown above each graph in bold.
a) The frequencies of amino acids found in a total of 41 randomly selected clones from the unpanned library.
b) The frequencies of amino acids found in a total of 25 and 23 randomly selected fourth round clones, isolated from each duplicate well A (■) and well B (□) respectively.

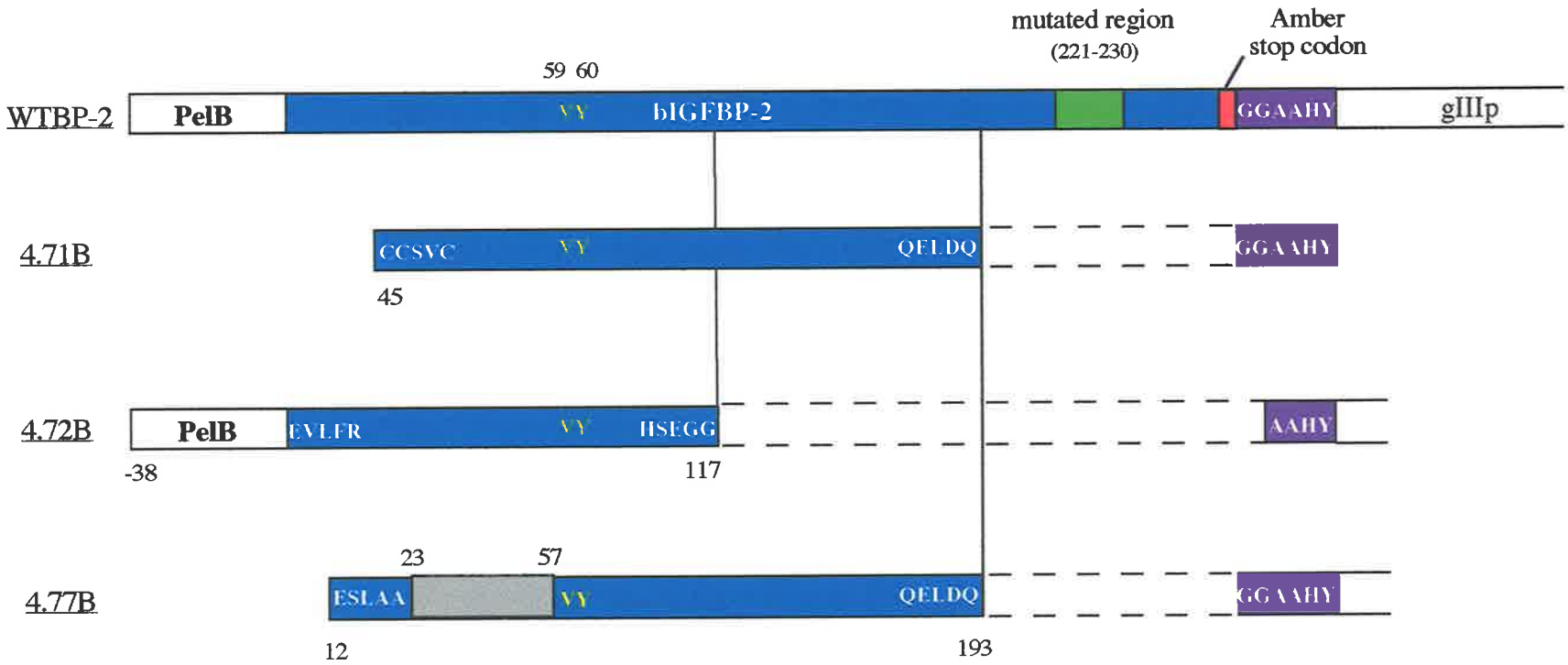

Figure 3.10 The proteins encoded by the clones isolated after four rounds of panning, which contained DNA deletions at the region encoding for the C-terminal end of bIGFBP-2. The DNA sequence data was obtained using the gIIIp primer (Table 3.1), which binds within the *gIIIp* gene. The amino acids of bIGFBP-2, encoded for by the deleted clones, are shown below each construct (confirmed by DNA sequence data). The region 221-230 that was mutated (green box) in the phage display screen, and the amber stop codon (red box), were absent in all 3 clones (denoted by the broken lines). Clones 4.71B and 4.77B both terminated at residue 193 of bIGFBP-2, and were then fused to an H64A subtilisin cleavage site. 4.71B and 4.77B were not clonal, since mutant 4.77B contained amino acid sequences between residues 23 to 57 (grey box) which were not native to bIGFBP-2. All three truncated clones clones contained the N-terminal residues, Val and Tyr, shown for both hIGFBP-5 (Kalus *et al.*, 1998) and bIGFBP-2 (Hobba *et al.*, 1998) to be important for IGF binding activity. The Val and Tyr residues in bIGFBP-2 (residues 59 and 60 of bIGFBP-2) are marked in yellow.

STARTING LIBRARY SEQUENCES

Clone WT	C	D	K	H	G	L	Y	N	L	K	Q	C
24	**C**	H	K	D	G	V	F	D	L	G	R	**C**
M10	**C**	H	R	D	T	P	Y	K	R	T	P	**C**
M1	**C**	H	R	A	A	Q	N	N	A	T	R	**C**
23	**C**	H	T	D	G	P	I	K	E	R	L	**C**
54	**C**	H	T	P	G	R	Y	E	E	K	Q	**C**
30	**C**	H	T	L	G	?	N	K	G	K	R	**C**
M7	**C**	H	A	L	A	Q	F	H	?	A	Q	**C**
11	**C**	H	M	D	R	P	F	K	V	T	Q	**C**
19	**C**	H	M	H	T	G	F	N	L	A	L	**C**
58	**C**	H	M	R	A	L	N	K	R	K	L	**C**
6	**C**	H	E	G	G	E	I	N	Q	R	R	**C**
7	**C**	H	V	H	A	L	F	Y	E	R	R	**C**
60	**C**	H	V	P	R	E	F	Y	Q	R	L	**C**
61	**C**	H	G	L	A	E	N	Z	P	V	R	**C**
63	**C**	H	?	D	R	A	Y	D	G	V	Q	**C**
34	**C**	D	K	D	A	R	N	H	V	A	R	**C**
62	**C**	D	K	D	G	P	Y	Y	Q	K	Q	**C**
13	**C**	D	K	H	A	Q	N	Q	L	T	P	**C**
1	**C**	D	R	D	T	E	F	E	Q	T	Q	**C**
59	**C**	D	R	H	T	E	I	Q	P	K	Q	**C**
16	**C**	D	R	G	R	R	Y	K	L	A	P	**C**
31	**C**	D	R	A	T	V	N	H	P	G	R	**C**
33	**C**	D	A	G	A	R	I	D	E	K	P	**C**
65	**C**	D	A	L	R	A	I	?	?	?	R	**C**
57	**C**	D	A	R	T	V	N	N	Q	R	P	**C**
9	**C**	D	A	V	R	L	Y	D	V	V	Q	**C**
8	**C**	D	G	H	T	E	Y	Q	Q	K	Q	**C**
55	**C**	L	K	G	R	Q	N	H	P	V	Q	**C**
20	**C**	L	R	H	G	G	N	Y	R	E	P	**C**
M3	**C**	L	R	P	G	Q	F	Y	?	?	R	**C**
3	**C**	L	T	P	A	E	N	Q	G	K	Q	**C**
15	**C**	L	T	R	A	V	N	Z	A	T	P	**C**
M9	**C**	L	M	R	G	L	I	K	L	T	L	**C**
22	**C**	L	M	?	?	?	F	N	P	?	Q	**C**
39	**C**	L	E	P	G	Q	N	Y	E	E	P	**C**
38	**C**	L	?	H	G	V	I	D	?	K	L	**C**
26	**C**	V	K	D	R	Q	N	N	V	R	R	**C**
41	**C**	V	K	P	R	Q	F	N	R	T	Q	**C**
10	**C**	V	A	V	R	V	N	N	E	K	P	**C**
40	**C**	V	E	D	T	A	N	N	A	K	R	**C**
M8	**C**	?	?	?	?	P	N	D	?	K	R	**C**
most frequent	***C***	***H***	***R***	***D***	***G***	***Q***	***N***	***N***	***E*** ***Q***	***K***	***R*** ***Q***	***C***

Table 3.5 Amino acid variability present in the mutant C-terminal bIGFBP-2 library prior to panning, compared to the wild type (WT) bIGFBP-2 sequence. The DNA sequences were used to determine the amino acids present at each position. The sequences are grouped according to the frequencies of the first 3 amino acids after the cysteine residues (Figures 3.9a and 3.9b). Invariant external cysteine residues are marked in bold. Z denotes an amber stop codon, which can be translated to glutamine in *supE* hosts. ? denotes residues which could not be assigned due to ambiguity present in the DNA sequence data. The most frequent residues, at each position, are highlighted at the bottom of the table in bold, italic text. The number of sequences shown here is 41.

(a)

FOURTH ROUND SEQUENCES
WELL "A"

Clone WT	C	D	K	H	G	L	Y	N	L	K	Q	C
67A	C	H	T	H	R	G	F	N	G	T	P	C
5A	C	H	K	H	A	G	N	D	Q	R	R	C
62A*	C	H	K	P	R	R	N	D	Q	A	R	C
66A*	C	H	K	P	R	R	N	D	Q	A	R	C
35A	C	H	R	L	A	L	N	Q	Q	T	R	C
30A	C	H	R	A	R	Q	N	K	Q	G	P	C
11A	C	H	V	P	G	P	N	N	G	V	Q	C
37A	C	H	V	L	R	R	I	Y	R	R	P	C
31A	C	H	G	P	A	R	Y	H	L	K	R	C
16A	C	H	?	H	A	A	?	H	Q	Q	?	C
3A	C	V	A	P	R	Q	N	N	Q	T	P	C
4A	C	V	A	R	T	P	F	H	R	T	P	C
36A	C	V	A	R	R	G	I	N	Q	V	Q	C
13A	C	V	A	V	G	G	F	N	P	R	L	C
69A	C	V	T	L	A	G	Y	Y	P	V	P	C
6A	C	V	T	R	T	P	I	Y	A	V	R	C
2A	C	V	M	P	R	A	F	K	E	E	Q	C
60A	C	L	K	P	T	P	I	Z	A	T	R	C
14A	C	L	K	L	T	Q	N	D	Q	E	R	C
34A	C	L	R	V	T	A	I	N	P	M	R	C
7A	C	L	E	H	G	?	F	Q	L	T	R	C
65A	C	D	T	H	R	A	N	Q	V	K	R	C
33A	C	D	T	R	A	P	Y	N	P	T	Q	C
68A	C	D	R	D	T	P	F	Q	R	G	Q	C
8A	C	S	A	D	R	G	Y	Y	R	K	R	C
most frequent	***C***	***H***	***K A T***	***P***	***R***	***P G***	***N***	***N***	***Q***	***T***	***R***	***C***

Tables 3.6a and 3.6b Amino acid variability present in the mutant C-terminal bIGFBP-2 library after four rounds of panning on IGF-II coated wells, compared to the WT bIGFBP-2 sequence. The library was panned in duplicate, and the results from well A are shown in (a), and the results from well B are shown in (b). The sequences are grouped according to the frequencies of the first 3 amino acids after the cysteine residues (top of the table is most frequent). Invariant external cysteine residues are marked in bold. Z denotes an amber stop codon, which can be translated to glutamine in *supE* hosts. ? denotes residues which could not be assigned due to ambiguity present in the DNA sequence data. * denotes duplicate sequences. The codons for the underlined residues, Q and S, were not designed to occur in the original library. The most frequent residues, at each position, are highlighted at the bottom of the table in bold, italic text. The number of sequences shown here in Table 3.6a is 25. The total number of sequences shown in Table 3.6b is 23.

(b)

FOURTH ROUND SEQUENCES
WELL "B"

Clone WT	C	D	K	H	G	L	Y	N	L	K	Q	C
75B	C	H	K	P	T	L	Y	H	Q	V	Q	C
48B	C	H	R	A	G	R	F	N	R	A	R	C
39B	C	H	R	P	A	R	N	D	G	K	P	C
74B	C	H	T	H	T	L	N	H	V	G	R	C
45B	C	H	T	G	G	L	F	Q	Q	T	P	C
24B	C	H	E	A	G	V	F	N	P	M	P	C
28B	C	H	G	D	R	R	I	Q	Q	E	L	C
23B	C	H	V	G	T	Q	I	Q	P	G	R	C
41B	C	H	A	G	G	E	F	H	R	K	R	C
46B	C	L	K	H	G	R	N	Q	L	T	L	C
44B	C	L	M	A	T	E	N	K	L	R	P	C
22B	C	L	T	H	T	L	Y	Q	Q	T	L	C
19B	C	L	E	A	R	A	I	K	E	T	R	C
20B	C	L	G	R	A	P	Y	N	L	K	L	C
27B	C	V	K	H	A	A	F	K	L	G	Q	C
43B	C	V	K	H	A	R	N	K	Q	V	L	C
70B	C	V	R	H	R	R	N	Y	A	M	Q	C
40B	C	V	T	G	T	G	N	Y	R	K	L	C
79B	C	V	V	D	T	E	N	H	L	M	Q	C
47B	C	D	M	H	A	?	Y	Y	Q	K	L	C
17B	C	D	M	G	G	L	Y	N	Q	E	Q	C
18B	C	D	R	A	A	P	Y	K	G	M	Q	C
42B	C	?	M	H	T	V	N	N	V	R	P	C
most frequent	*C*	*H*	*R K M T*	*H*	*T*	*R*	*N*	*N K Q*	*Q*	*K*	*L*	*C*

Table 3.6b Amino acid variability present in the mutant C-terminal bIGFBP-2 library after four rounds of panning on IGF-II coated wells, compared to the WT bIGFBP-2 sequence.

BIAcore™ analysis and NMR, Kalus *et al.*, 1998) are known to maintain IGF binding ability (see Section 1.5.2).

There was no defined consensus sequence obtained after four rounds of panning against IGF-II, therefore attempts were made to increase the numbers of rounds of binding selection in a subsequent experiment. However, DNA prepared after five rounds of binding selection showed a predominance of deleted phagemid clones. Therefore, attempts to conduct further rounds of panning were not pursued.

3.5 Discussion

The studies described in this chapter involved the generation of a phage library expressing mutations in amino acids 221 to 230 of bIGFBP-2 to assess the importance of these residues in IGF binding activity.

As discussed in Section 3.1, XL1-Blue *E. coli* were chosen as a host to propagate phage particles containing the bIGFBP-2 mutant library. In the first part of this study, XL1-Blue cells were shown to be a suitable host strain for the generation of phage particles expressing bIGFBP-2 on their surface. Western ligand blot analysis demonstrated that phage expressing bIGFBP-2 could bind iodinated IGF-II ligand. Interestingly, a bIGFBP-2 expressing population of phage particles generated from these cells contained a CFU:PFU ratio of approximately 10:1. This ratio was different relative to phage generated in *E. coli* JM101 cells, which contained 10-fold fewer CFU than PFU phage particles (Section 2.4.4). Although the reasons for this difference were not investigated, one explanation may be a greater copy number of the phagemid being present in the XL1-Blue strain. The presence of higher numbers of phagemid pGF14 would increase the chances of the DNA being packaged into the phage particles.

In addition to the panning procedures discussed in Chapter 2, experiments performed in this chapter showed that IGF-I could also be used for selection of bIGFBP-2 expressing phage particles. The ability to screen bIGFBP-2 mutant libraries against both IGF-I and IGF-II provides the opportunity to identify residues that are specifically involved in binding to either of these two ligands. As discussed in Section 2.5, this is potentially useful since it is known that bIGFBP-2 exhibits a preference for IGF-II binding in comparison to IGF-I (Szabo *et al.*, 1988; Bourner *et al.*, 1992). The use of phage display to examine the differential effects of residues important in ligand binding has previously been reported. The atrial natriuretic peptide has been altered to have a stronger preference for binding to one of its receptors, natriuretic peptide receptor A (Cunningham *et al.*, 1994). In this study, it was suggested that this selectivity may be useful for correlating the various activities of the peptide to the relevant receptor (Cunningham *et al.*, 1994). This may also be possible for IGFBP, which binds to both IGF-I and IGF-II. Therefore, the ability to engineer an IGFBP to have a stronger affinity for either IGF, may be used to selectively alter the action of either ligand. This may be beneficial for

furthering the knowledge of the actions of binding protein on IGF function. Furthermore as addressed throughout Chapter 1, the ability to specifically affect the action of one of the IGFs may have important therapeutic benefits.

A bIGFBP-2 mutant library was constructed by designing a primer to partially randomise residues 221-230 of bIGFBP-2. This approach was chosen to restrict the numbers of amino acid combinations to 6.71×10^7, thus increasing the chances of generating and screening a complete phage library. A similar mutagenesis strategy to that used in this study has been employed to investigate amino acid residues of transforming growth factor-α, which enable high binding affinity for the epidermal growth factor receptor (Tang *et al.*, 1997).

The sizes of the mutant bIGFBP-2 phage libraries that were created during the current study were smaller than the maximum number of combinations that were possible as a result of the primer design. This may be explained by the use of insufficient amounts of DNA in the ligation reactions and, as a consequence, a reduced amount of DNA transformed into *E. coli* XL1-Blue cells. In this study, each attempt at transforming the mutant bIGFBP-2 library used a total of 1.5 µg DNA to yield 5.8×10^6 and 1.96×10^6 transformants. In comparison, Barbas *et al.* (1992) transformed a ligation reaction containing 10 µg of vector DNA to generate a library size of 5×10^7 transformants. Similarly Cwirla and coworkers (1990) used a total of 20 µg DNA to generate a library size of 3×10^8.

During this study, problems were encountered involving the accumulation of clones with deleted segments of the bIGFBP-2 cDNA. Further analysis revealed that the accumulation of these deletions appeared to result from the construction of the C-terminal bIGFBP-2 mutant library. One hypothesis for the deletion of the bIGFBP-2 cDNA segments observed with this library, following progressive reamplification of phage, is that the mutant proteins which were produced may have been toxic to the cells. The toxicity of these clones may be attributable to the fact that the expressed protein is unstable and/or may not be folding in the correct conformation. In this study, transformation of the mutant bIGFBP-2 library into the XL1-Blue cells resulted in a variety of differently sized bacterial colonies found on growth plates. O'Neil and coworkers (1995) also reported the appearance of variable plaque morphologies when phage expressed functional but thermodynamically destabilised protein. Alternatively, the expressed bIGFBP-2 protein may interfere with an important process in the cells, for example

the secretion pathway, and therefore cells containing deletions in this protein grow more favourably. This was true in a study performed by Beekwilder *et al.* (1999), who showed that cells containing deleted protease inhibitor:gIIIp fusions grew more rapidly than cells containing the intact full-length clone.

Current evidence in the literature suggests that the ability to tightly regulate the expression of the protein:gIIIp fusion can alleviate the DNA deletion problem. For example, Beekwilder *et al.* (1999) reported overcoming the accumulation of phagemid deletion clones by replacing the *lac* promoter with the *psp* promoter, which more strongly suppressed the expression of the protein. In addition, Beekwilder and coworkers (1999) also demonstrated that by reducing the phagemid copy number (by replacing the plasmid origin of replication), they could increase the stability of the insert DNA. The decrease in the copy number of the phagemid was rationalised to create better promoter control, since sufficient amounts of lac I repressor protein would be available for suppression of the promoter (Beekwilder *et al.*, 1999). Another strategy reported to impose a tighter control over the expression of the gIIIp fusion protein has been to clone a transcription termination signal immediately upstream of the *lac* promoter (Krebber *et al.*, 1996). These researchers reasoned that the observed background expression levels often associated with the use of the *lac* promoter were due to independent transcriptional start sites (cryptic promoters) located upstream of this promoter (Krebber *et al.*, 1996). The insertion of the transcription termination signals resulted in tighter control of protein expression and therefore more stable clone maintenance (Krebber *et al.*, 1996). Furthermore, microscopy was used to show that cells exhibited a healthier cell morphology and experienced less cell lysis when compared to cells which expressed high levels of the gIIIp fusion protein (Krebber *et al.*, 1996). Similar to the systems used in both of the reports cited, this study employed a phagemid which used the *lac* promoter to control the expression of the bIGFBP-2:gIIIp fusion protein. Further studies using the phage display of bIGFBP-2 for mutant library screening may focus on modifying this vector by using the approaches discussed above. Therefore, by suppressing the expression of the fusion protein, it may be possible to alleviate the deletion problems which were encountered during the course of this study.

The precise mechanisms involved in the formation of plasmid deletions are still not well understood. However, one emerging theme observed from the phage display studies suggests

that expression and secretion of the protein is an important determinant in the loss of plasmid-encoded genes. In studies performed in the Gram positive bacterium, *Bacillus subtilis*, Cordes and coworkers showed that structural instability of the plasmid was strongly associated with the entry of the plasmid-encoded protein into the protein export pathway (Cordes *et al.*, 1996). They proposed that this occurred during the cotranscriptional and cotranslational entry of the protein into the secretion pathway, where the plasmid DNA is anchored to the bacterial membrane (Cordes *et al.*, 1996). Local regions of plasmid DNA associated with the membrane experience hypersupercoiling (Cordes *et al.*, 1996). Hypersupercoiled DNA in the cells can lead to the induction of topoisomerase-dependent nicking activity, creating free 3' -OH groups which could then be processed by an exonuclease (Cordes *et al.*, 1996). These processes could ultimately result in the loss of DNA fragments (Cordes *et al.*, 1996). In support of this idea, Cordes *et al.* (1996) found that high levels of DNA topoisomerase I in cells was associated with higher levels of plasmid deletions. Therefore, a greater understanding of the processes involved in the loss of plasmid encoded genes may help provide solutions, other than those described above, to the deletion problems associated with the study of proteins using phage display systems.

In this study, the use of shorter propagation times suggested by Harrison *et al.*, (1996) did help reduce the accumulation of smaller phagemid clones. In addition, panning was performed using H64A subtilisin to elute the phage particles improved the selection for phage which maintained the C-terminal end of the bIGFBP-2 clones. The use of these modifications to the phage propagation and elution procedures, permitted four rounds of panning to be conducted against IGF-II ligand. Comparison of the fourth round sequences to the original unpanned library, showed that the presence of negatively charged residues located at positions 221, 223 and 228 were most affected. A reduction in the frequency of the negatively charged residues at each of these sites may indicate that these negative charges cause an interference in the interaction between bIGFBP-2 and IGF-II. These residues may reduce the affinity of bIGFBP-2 for IGF-II because in the complex, other negatively charged residues are located in close proximity, and may result in repulsive forces being exerted between these two proteins. Alternatively, the negatively charged residues may affect internal protein structure which is important for the IGF-II-bIGFBP-2 interaction. The other mutated positions of bIGFBP-2,

namely 222, 224, 225-227, 229 and 230, had a variety of sequences that were still present after four rounds of panning. This may mean that this region of the protein is extremely tolerant to the insertion of a variety of amino acids.

Interestingly, studies performed on rat IGFBP-5 demonstrated that the conserved Gly203 and Gln209 residues were important for full IGF-I and IGF-II binding activity (Bramani *et al.*, 1999; Song *et al.*, 2000). In contrast, neither Gly203Lys nor Gln209Ala IGFBP-5 mutants had impaired heparin binding activity (Song *et al.*, 2000). This observation was interesting since residues adjacent to the Gly and Gln were known to be important for the heparin binding activity (Song *et al.*, 2000). At the corresponding positions, Gly224 and Gln230 in bIGFBP-2, there did not appear to be a strong selection for the native residues during the screening process. This was despite strong conservation of these residues across the IGFBP family (Figure 1.4) and to the findings of Song *et al.* (2000). However, accompanying these mutations in the sequences investigated were other changes which could have compensated for the alterations made to the Gly and Gln residues. Therefore, with the results obtained in this phage display study, it is difficult to establish the importance of these two residues in IGF binding activity of bIGFBP-2.

The involvement of a number of residues in the protein-protein interactions may explain why some phage display approaches require several rounds of binding selection, when only a few of these residues are targeted. For example, studies which screened for increased binding affinity of human growth hormone for its receptor (Lowman *et al.*, 1991) and for modifying the specificity of atrial natriuretic factor for one of its receptors (Cunningham *et al.*, 1994) used up to six or seven rounds of binding selection. The studies described in this chapter analysed clones after only four rounds of panning. Although attempts were made to increase the number of rounds of IGF-II binding selection, the accumulation of DNA deletions did occur, and as a result was not pursued further. However, it is possible that more rounds of selection may have been required for the emergence of a favourable binding consensus sequence. As discussed earlier, by modifying the promoter in the phagemid pGF14 to enable tighter control over the expression of the mutant bIGFBP-2 library, it may be possible in the future to extend the panning selection procedure to further rounds.

Interestingly, along with a majority of full-length *bIGFBP-2* clones obtained after four rounds of panning, clones missing fragments encoding the C-terminal end of the protein were identified. All three clones were devoid of amber stop codons, and contained an H64A subtilisin protease cleavage site. The absence of the stop codon may have increased the amounts of the truncated protein being expressed on the surface of the phage particles. Higher amounts of the protein on the phage surface may have facilitated multiple point attachment, which enabled the maintenance of these clones, even though they were likely to have a lower affinity for binding protein than the full-length protein. Certainly, multiple point attachment of peptides was shown to maintain peptide sequences exhibiting variable affinities (Cwirla *et al.*, 1990). As discussed in Section 1.5.2, studies on IGFBP show that the N-terminal end of the protein contains determinants which are important for binding to the IGFs (bIGFBP-2: Hobba *et al.*, 1998; hIGFBP-5: Kalus *et al.*, 1998). Furthermore, N-terminal fragments of IGFBP have been shown to maintain some IGF binding affinity (Section 1.5.2). Based on this observation, it would appear that the phage display system would be suitable for expressing only the N-terminal domain of IGFBP, to further study its binding epitopes. Future work focussed on analysing the C-terminal epitopes of bIGFBP involved in IGF binding, could be performed by removing the N-terminal IGF binding residues. This could be done by mutating the residues in the N-terminal region, around Tyr60, shown to be important for IGF binding activity (Hobba *et al.*, 1998). Alternatively, C-terminal fragments of the binding protein could be fused onto gIIIp. Studies have shown that it is possible to express C-terminal fragments of bIGFBP-2 in *E. coli* which maintain IGF binding activity (Francine Carrick, personal communication. Department of Biochemistry, University of Adelaide). By removing the N-terminal residues, it may be possible to generate a stronger selection procedure for isolating residues in the C-terminal end which are important for the binding process.

The aim of this chapter was to assess the role of residues 221 to 230 in the C-terminal end of bIGFBP-2 for IGF binding activity. The results of the panning procedure after four rounds of selection on IGF-II coated wells did not generate a clear consensus sequence to suggest the importance of particular residues for IGF binding. Consequently, it was pertinent to select a number of these clones to express and analyse the proteins in more detail. The

analysis of proteins isolated by the phage display approach described here, forms the topic of Chapter 4.

Chapter Four

EXPRESSION AND CHARACTERISATION OF SELECTED 221-230 bIGFBP-2 MUTANTS FROM THE PHAGE DISPLAY LIBRARY

4.1 Introduction

In Chapter 3, amino acids 221-230 of the 284 amino acid bIGFBP-2 protein were mutated by PCR to assess the importance of these residues in IGF binding activity. Four rounds of panning on IGF-II were performed using phage display. However, analysis of the clones remaining after panning failed to reveal which residues were optimal for IGF binding function. Because the C-terminal deletion studies performed by Forbes *et al.* (1998) suggested that this region was critical for bIGFBP-2 to bind to IGF, a sample of mutants isolated from the panning procedures was selected for further characterisation.

In this chapter, attempts were made to express a select number of bIGFBP-2 variants isolated after the panning procedures as described in Chapter 3. Only one mutant, 4.17B, which closely resembled the wild type bIGFBP-2 protein sequence, was expressed sufficiently to facilitate further IGF binding characterisation. The IGF binding ability of this mutant was assessed by standard ligand blotting techniques and by the use of a biosensor (BIAcore™ 2000 instrumentation). Based on the results obtained using Western ligand blot and BIAcore™ 2000 for the analysis of the bIGFBP-2 mutant 4.17B, the effects of the amino acid substitutions in the region 221-230 of the bIGFBP-2 are discussed.

The biosensor approach was chosen to study the bIGFBP-2 mutant because it offers a technique for analysing protein-protein interactions which is quick, simple to use, and is not dependent on vast amounts of protein samples or on radiolabelled proteins (reviewed in Canziani *et al.*, 1999 and Nice and Catimel, 1999). Biosensors use surface plasmon resonance technology to look at the interaction between two molecules in real-time (Nice and Catimel, 1999). As the molecule in solution (the "analyte") binds to the molecule covalently attached to the sensor surface (the "ligand"), a response is recorded in resonance units (RU) (Figure 4.1). The rate of analyte dissociation is then determined by passing analyte-free solution over the ligand while the loss in RU is monitored (Figure 4.1). Recently, this sensitive approach has been used to study the interaction between IGF (and IGF mutants), and the IGFBPs (Dubaquie and Lowman, 1999; Heding *et al.*, 1996; Hobba *et al.*, 1998; Jansson *et al.*, 1998; Marinaro *et al.*, 1999; Wong *et al.*, 1999) or fragments of the IGFBPs (Kalus *et al.*, 1998; Standker

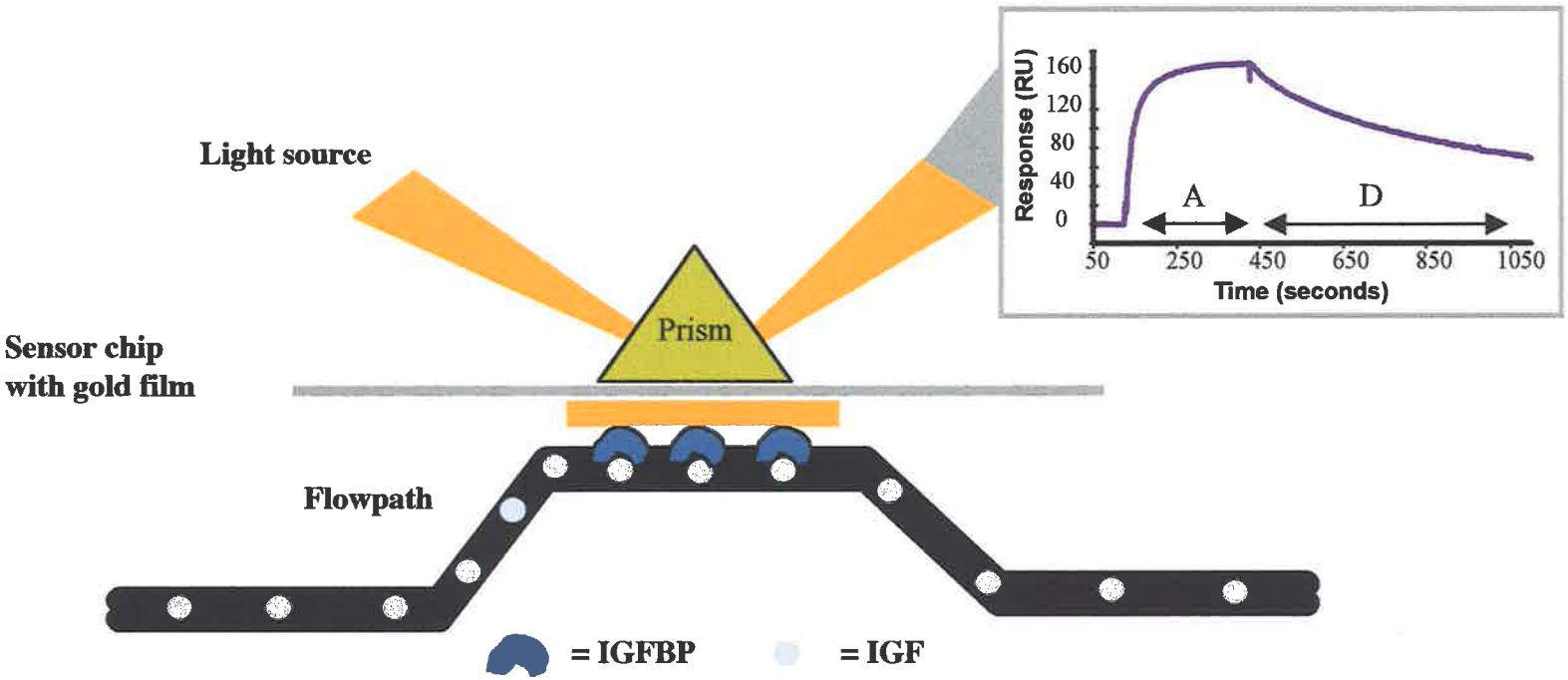

Figure 4.1 A diagrammatical representation of the BIAcore™ system, used to study the interaction between IGF and bIGFBP-2. When the analyte, IGF, binds to bIGFBP-2 (coupled to the gold surface through the carboxymethylated dextran matrix), the interaction causes a change in the angle of light diffraction. The change in the angle of light diffraction is recorded in resonance units (RU) over time. As IGF associates with the binding protein, there is an increase in RU shown here in the graph (marked "A"). As buffer is passed over the surface, dissociation of the IGF from the binding protein can be monitored (marked "D" on the graph).

et al., 2000; Francine Carrick, personal communication, Department of Biochemistry, University of Adelaide).

4.2 Materials

The restriction enzyme *Bsp*E I was purchased from New England Biolabs (Beverly, MA, USA), while *Eco*R I was purchased from Amersham Pharmacia Biotech Pty Ltd (Castle Hill, NSW, Australia). The enzymes and buffers used for the PCR are described in Chapter 3. The BresaSpin™ Gel Extraction Kit was obtained from Geneworks Ltd (Thebarton, SA, Australia). The purified mammalian expression vector, pGF8, was kindly provided by Dr Briony Forbes, and the phagemid pFdBDK61L from Dr Steven Polyak, both from the Department of Biochemistry, University of Adelaide (Adelaide, SA, Australia). Amicon Bioseparations Centricon® 10 centrifugal filter devices were purchased from Adelab Scientific (Norwood, SA, Australia). Recombinant human [Gly^1] IGF-II (media grade), biotinylated human IGF-I, mono-biotinylated human IGF-II (receptor grade) and receptor grade recombinant bIGFBP-2 were obtained from Gropep Pty Ltd (Thebarton, SA, Australia). The secondary antibody used in immunoblots was a goat anti-rabbit IgG (whole molecule) alkaline phosphatase conjugate, obtained from Sigma Chemical Co. (St Louis, MO, USA). Nitroblue tetrazolium (NBT) and 5-bromo-4-chloro-3-indolyl-phosphate disodium salt (BCIP) were obtained from Diagnostic Chemicals Ltd (Charlottetown, Prince Edward Island). Silenus horse radish peroxidase conjugated streptavidin was obtained from Silenus Laboratories Pty Ltd (Boronia, Vic., Australia). The reagents used for chemiluminescent detection of IGF ligand blots were the SuperSignal® West Pico Chemiluminescent solutions Luminol Enhancer and Stable Peroxide from Pierce (Rockford, IL, USA). X-ray film used for detection of the ligand blots was from AGFA Gevaert Ltd (Regency Park, SA, Australia). The computing densitometer (model 300A) was from Molecular Dynamics (Sunnyvale, CA, USA). Other materials used for Western ligand blotting procedures are described in Chapter 2. The BIAcore™ 2000 instrument, CM5 sensor chips, surfactant P20, and the amine coupling kit containing *N*-hydroxysuccinimide (NHS), *N*-ethyl-*N'*-(diethylaminopropyl)carbodiimide (EDC), and ethanolamine hydrochloride were obtained from BIAcore AB (Uppsala, Sweden). N-2-Hydroxyethylpiperazine-N-2-ethanesulphonic acid (HEPES) was obtained from BDH

Laboratory Supplies (Poole, England). Epicurian Coli® XL10-Gold™ ultracompetent cells were obtained from Stratagene (Willoughby, NSW, Australia). All materials and reagents for mammalian cell tissue culture are described in Sections 5.2 and 5.2.1.

4.2.1 Buffers, solutions and media

The growth media, chromatography buffers, protein electrophoresis and protein transfer buffers and solutions for DNA procedures were prepared as described in Section 2.2.1. All solutions were made in redistilled water filtered using the Milli-Q Ultra Pure Water System (Millipore Pty Ltd, North Ryde, NSW, Australia). Solutions marked (§) were sterilised by autoclave.

Solution for antibody blot

Developing buffer (§)
100 mM Tris, pH 9.5, 100 mM NaCl, 5 mM $MgCl_2$

Solution for BIAcore™

HEPES buffered saline (HBS)
10 mM HEPES, 150 mM NaCl, 3.4 mM EDTA, 0.05% (v/v) surfactant P20
-prepared fresh for each experiment from a 10 x concentration stock solution, and filtered using 0.2 µm filter

4.2.2 Bacterial strains

The genotype of the *E. coli* strains used in this study are described below:

E. coli XL10-Gold™: Δ(*mcrA*) 183D (*mcrCB-hsdSMR-mrr*)173, *endA1 supE44 thi-1 recA1 gyrA96 relA1 lac* Hte [F' *proAB lacI*^{q}*ZΔM15* Tn10(Tet^r) Amy Cam^r]

All other cell lines not described here, are outlined in Sections 2.2.2 and 3.2.2.

4.3 Methods

4.3.1 Expression of the mutant bIGFBP-2 proteins in bacterial cells and protein purification

Mutants selected for further analysis from the fourth round screening procedures in Chapter 3 are shown in Table 4.2. The phagemid DNA encoding for these bIGFBP-2

mutations was isolated from the XL1-Blue *E. coli* cells using the BresaSpin™ DNA plasmid preparation kit (Section 3.3.11). The pGF14 variants were transformed into *E. coli* BL21 using either chemically competent (Sambrook *et al.*, 1989) or electrocompetent (Section 3.3.9) cells. Control vectors used for transformation and expression studies included the wild type pGF14 phagemid and the phagemid pFdBDK61L. pFdBDK61L is a variant of pGF14 that encodes the non-biotinylated form of the biotin carboxyl carrier protein (Polyak, 2000). The transformations were plated onto L plates containing 2% glucose and 100 μg/ml Amp, and were grown overnight at either 30°C or 37°C. After transformation, the identities of the clones were confirmed by performing DNA sequence analysis as described in Section 3.3.12. Proteins were expressed from the cells using the conditions described in Section 2.3.3. Upon induction of protein expression with IPTG, cultures were grown overnight at either 30°C or 37°C. The same conditions were used for protein expression experiments performed in the *E. coli* strain HB2151.

The conditions used for the purification of the mutant proteins were those described in Section 2.3.5. However, for affinity purification, the sample was applied to a [Gly^1] IGF-II affinity column ([Gly^1] IGF-II was immobilised to Affi-Gel® 10 using the method described by the supplier). The amounts of purified mutant 4.17B protein were determined by performing HPLC using the conditions described in Section 2.3.5.

4.3.2 Subcloning and expression of the bIGFBP-2 variants in mammalian COS-1 cells

Generally, the bIGFBP-2 mutants exhibited low or undetectable levels of protein expression in growth medium isolated from *E. coli* cells. To determine if mammalian cell expression would yield better results, the mutants were subcloned into the vector pGF8His (Figure 4.2, described in Figure 5.2). pGF8His encodes bIGFBP-2 containing a C-terminal hexahistidine tag. This vector could be used to express the bIGFBP-2 mutants in the green monkey kidney cells, COS-1, which were routinely used in our laboratory for bIGFBP-2 expression.

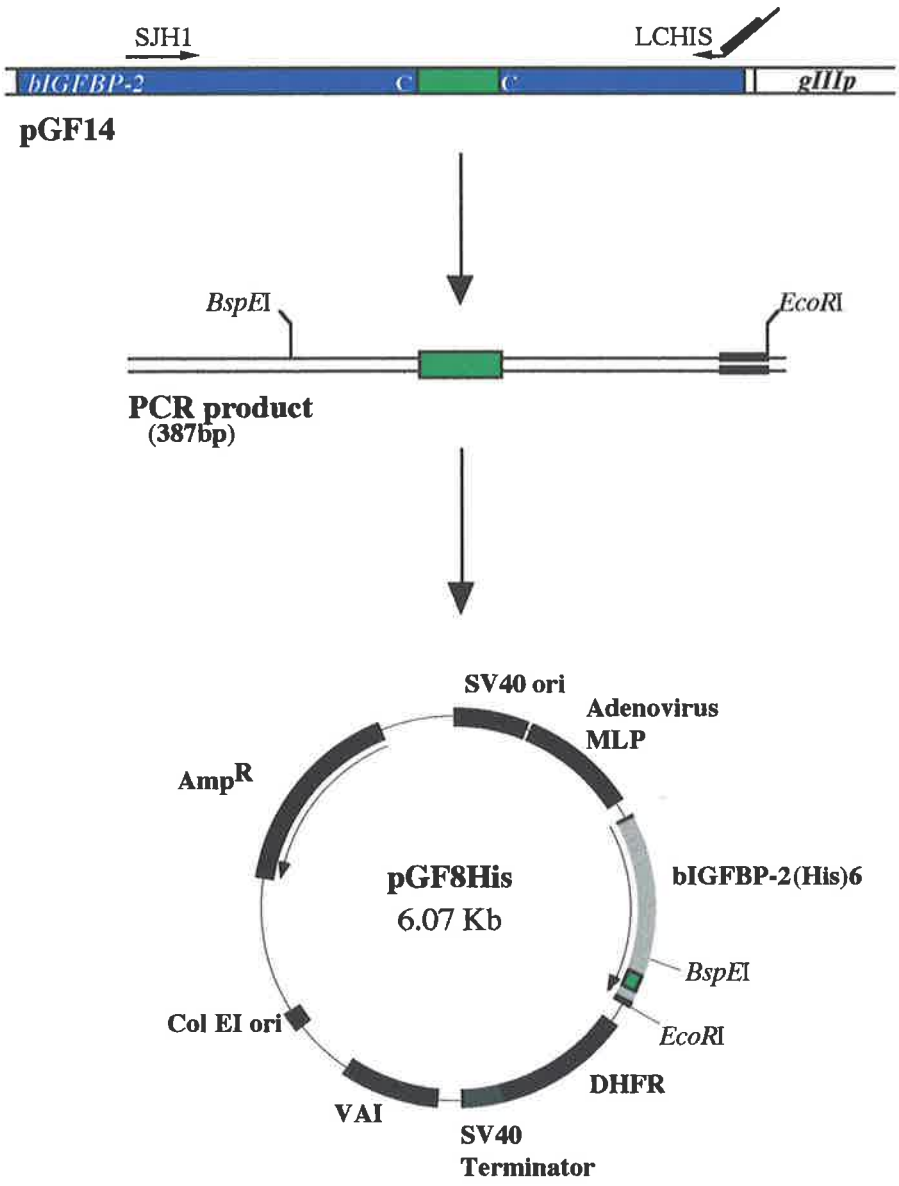

Figure 4.2 The strategy used to subclone the mutations from the mutant pGF14 constructs (Table 4.2), into the mammalian expression vector pGF8His. The pGF8His vector is described in Figure 5.2.

To subclone the mutations from the phagemid vector, a segment of the *bIGFBP-2* DNA containing the mutations was amplified by PCR using primers SJH1 (Table 3.1) and LCHis (Table 4.1). The PCR was performed in a final reaction volume of 30 µl using the following conditions: 1 x Pwo reaction buffer (containing 2 mM magnesium), 0.25 mM dNTP, 150 ng SJH1, 300 ng LCHis, 20 ng mutant pGF14 and 1 unit of Pwo polymerase. The reaction was placed in a thermal cycler (preheated at 95°C) and denatured at 95°C for 1 minute. The reaction was cycled 25 times using the following parameters: 95°C for 30 seconds, 60°C for 1 minute and 72°C for 3 minutes. The final extension was performed at 72°C for 3 minutes. The product was purified from the reaction mixture using the BresaSpin™ Gel Extraction Kit (protocols and solutions supplied by the manufacturer).

primer	sequence (5'-3')
LCHis	TTTAAGCTTGAATTCTTAGTGGTGGTGGTGGTGGTGC ACCCCTCGAGCCCCCTGCTGCTCGTTGTA

Table 4.1 LCHis is an antisense DNA primer used to create a hexahistidine tag at the C-terminal end of bIGFBP-2. The hexahistidine tag was created by substituting the final 5 amino acids of bIGFBP-2 for histidines (the 6th to last residue in bIGFBP-2 is a histidine, see Figure 5.2). LCHis was kindly provided by Ms Francine Carrick.

To clone the mutant DNA fragment into pGF8His, the PCR product and pGF8His vector were cleaved in separate reactions by performing double digests using the restriction enzymes *Bsp*E I and *Eco*R I. In a total volume of 50 µl, the reactions contained 3-5 µg of DNA (plasmid and pGF8His vector), 10 units of each restriction enzyme and 1 x concentration OPA+ reaction buffer. The restriction digests were incubated overnight at 37°C.

The digested PCR (235 base pair) and pGF8His vector (5824 base pair) were resolved on an agarose gel and the fragments were purified using the BresaSpin™ Gel Extraction Kit. The only alteration to the purification procedure was in the final step, when the DNA was eluted from the purification spin column using 50 µl sterile redistilled water. Restriction digested pGF8His vector and insert DNA were ligated in a final reaction volume of 20 µl using the conditions described in Section 3.3.8. For maintenance of the constructs, ligations were transformed into *E. coli* XL1-Blue using chemically competent cells (prepared by the method

described in Sambrook *et al.*, 1989) or into the ultracompetent XL10-Gold™ cells using the procedures described by the supplier.

The mutant pGF8His constructs were transfected into COS-1 cells for expression of the mutant bIGFBP-2 proteins as discussed in Section 5.3.5.

4.3.3 Western ligand and antibody blot analysis of the bIGFBP-2 mutants

Conditioned growth medium and purified protein samples were analysed on denaturing 12.5% polyacrylamide gels using the conditions and apparatus outlined in Section 2.3.4. For analysis of protein expression, 2 ml of conditioned growth medium was concentrated using Centricon™ 10 concentration units (using the methods supplied by the manufacturer), and a quarter of the remaining sample was separated by polyacrylamide gel electrophoresis.

The Western transfer conditions and ligand blotting procedures used were also described in Section 2.3.4. Instead of probing for IGF binding activity using ^{125}I IGF, blots were probed overnight at 4°C using biotinylated IGF-I or mono-biotinylated IGF-II (1 µg per 10 ml of blot buffer, Section 2.2.1). After incubation, the solution containing unbound biotinylated IGF was removed and 3 washes were performed in blot buffer containing 0.1% (v/v) Tween-20 (Section 2.3.4). The blots were then incubated in horse radish peroxidase conjugated streptavidin (diluted 1:10000 in blot buffer) at room temperature for 30 minutes. The conjugate was removed and 3 washes were performed in blot buffer containing 0.1% (v/v) Tween-20 as described above. The blots were developed using the SuperSignal® West Pico Chemiluminescent solutions using the method provided by the supplier. The blots were scanned using a densitometer and the signal intensity due to IGF interaction was assessed using the ImageQuant software. The IGF binding activity of the mutant 4.17B was compared to wild type bIGFBP-2 in two separate ligand blots.

Antibody blots were performed using an in-house rabbit polyclonal bIGFBP-2 antiserum (R92T) kindly provided by Dr Jill Carr (Institute of Medical and Veterinary Science, Adelaide, SA, Australia). As for the ligand blotting procedures (Section 2.3.4), after blocking of the filter in BSA solution, the filter was probed overnight at 4°C in 1 x blot buffer containing R92T antiserum (diluted 3:10000). The filter was washed 3 times in blot buffer containing 0.1% Tween-20 and each wash was performed at room temperature for 20 minutes. The

secondary antibody was diluted in blot buffer (1:20000) and incubated with the filter for 3 hours at room temperature with agitation. The secondary antibody was removed by washing the filter in blot buffer containing 0.1% Tween-20 for 20 minutes. Two subsequent washes were performed at room temperature for 20 minutes in developing buffer (Section 4.2.1). To detect the bound antibody, the filter was incubated at room temperature (in the dark) in developing buffer containing 0.25 mg/ml NBT and 0.25 mg/ml BCIP. The reaction was stopped by rinsing the filter in distilled water, and then soaking the filter in 1 mM EDTA pH 7.0.

4.3.4 IGF binding analysis of wild type and mutant bIGFBP-2 proteins using BIAcore™ 2000

The association and dissociation rates of the mutant and wild type bIGFBP-2 proteins for both IGF-I and IGF-II were compared using surface plasmon resonance on the BIAcore™ 2000 instrumentation. The binding protein sample was covalently attached to a carboxymethylated dextran sensor chip (CM5) using the amine coupling kit (Section 4.2) with the conditions described by the supplier. Automated coupling of the binding protein was performed using the immobilisation Wizard program available on the BIAcore™ 2000 software. For the coupling procedure, samples of wild type bIGFBP-2 and mutant 4.17B were prepared at a final concentration of 7 µg/ml in 10 mM sodium acetate pH 4.5. Both wild type bIGFBP-2 and 4.17B proteins were coupled onto separate channels of a CM5 sensor chip to final resonance values of either 100 RU or 500 RU (above the resonance value of the activated but non-derivatised chip). In each experiment to assess the differences in the refractive index due to changes in the buffers, and to monitor non-specific interaction with the carboxymethylated dextran matrix, a reference surface was prepared to which no bIGFBP-2 was bound.

To reduce possible mass transport limitation effects, experiments were conducted to assess the optimal flow rate of IGF over a wild type bIGFBP-2 coated surface. IGF-I and IGF-II stock solutions were each diluted to final concentrations of 16 nM in the HBS (16 nM was known to give less than 50% binding response on the surface containing 500 RU of binding protein). The 16 nM IGF solution was injected for 2 minutes over the bIGFBP-2

surface at a flow rate ranging from 5 µl/minute to 75 µl/minute. After injection of the IGF, the surface was regenerated by a 1 minute pulse of 100 mM HCl at 30 µl/minute. The results obtained for the different IGF flow rates were plotted and overlaid using BIAevaluation software (version 3.0). The effects of the different flow rates obtained for both IGF-I and IGF-II were assessed visually. The experiments were repeated 3 times.

To perform kinetic studies IGF-I and IGF-II were injected over the wild type bIGFBP-2 and mutant 4.17B surfaces in random order at 50 µl/minute. For each experiment, 6 serial dilutions of each IGF (from 250 nM to 3 nM, diluted in HBS) were injected in duplicate and the experiments were repeated three times. The IGF solutions were injected for 5 minutes, and then HBS buffer (in the absence if IGF) was injected over the surface for 15 minutes to monitor the IGF dissociation rate. The binding protein surface was regenerated by injecting 100 mM HCl solution for 90 seconds at 50 µl/minute. Experiments were replicated on both 500 RU and 100 RU binding protein surfaces.

The kinetic data was analysed using the BIAevaluation software (version 3.0) and also Matlab programs on a Unix workstation (with the help of Dr Nigel Bean, Department of Applied Mathematics, University of Adelaide). All binding curves were corrected for background by the subtraction of the signal obtained from the control channel. Apparent kinetic rates were generated by fitting both the experimental association and dissociation curves simultaneously. Using the BIAevaluation software, selected time points (the association phase: 170-426 seconds and dissociation phase: 508-1200 seconds) were used to fit the models across different data sets to compare both the wild type bIGFBP-2 and mutant 4.17B proteins. Fits were performed both globally (simultaneously across the entire concentration series for each IGF) and at individual concentrations of IGF. The method selected for the comparison of the mutant 4.17B to wild type bIGFBP-2 binding data was similar to that described by Heding *et al.* (1996), although a different model was selected for comparison of the binding curves. In this procedure, data obtained from the 50 nM concentration injections of both IGF-I and IGF-II over the mutant 4.17B and the wild type bIGFBP-2 were compared using the two-state reaction (with conformational change) model (see Appendix 1 for model descriptions). Using this approach, the value for Rmax (ie. the maximal binding capacity of the sensor chip surface) was manually optimised (assessed visually and by reduced χ^2 values when the fitted models

were compared to the experimental data) and fixed during the fitting procedures. All other parameters were fitted locally, and the refractive index value was fixed to zero (all binding curves were corrected for background by subtracting the response obtained from a blank surface).

To ensure that the coupling reaction was not responsible for the different IGF binding activity of the mutant 4.17B, binding activity was also assessed over CM5 surfaces covalently coupled to either IGF-I or IGF-II. The conditions used for coupling IGF to the CM5 surfaces were similar to those described by Hobba *et al.* (1998).

4.4 Results

4.4.1 Expression of mutant bIGFBP-2 molecules generated from the phage display screen

The aim of this work was to characterise the effects of mutations to residues 221-230 of bIGFBP-2 on its IGF binding activity. To do this was, a number of mutants isolated after 4 rounds of panning on IGF-II ligand using phage display (Chapter 3) were selected for further characterisation. The mutants selected for further study are shown in Table 4.2. Mutants were selected on the basis of their similarities to the wild type bIGFBP-2 sequence (for example, mutants 4.17B and 4.20B). The prevalence of histidine residues at amino acid 221 in the library (Tables 3.5, 3.6a and 3.6b) made mutants 4.30A and 4.48B interesting for comparison to one another and to the wild type bIGFBP-2 protein. For similar reasons, mutants 4.27B and 4.43B were selected to compare and contrast to one another and to the wild type bIGFBP-2 protein.

WT	*C*	*D*	*K*	*H*	*G*	*L*	*Y*	*N*	*L*	*K*	*Q*	*C*
4.17B	*C*	*D*	M	G	*G*	*L*	*Y*	*N*	Q	E	*Q*	*C*
4.20B	*C*	*L	*G	R	A	P	*Y*	*N*	*L*	*K*	L	*C*
4.30A	*C*	H	*R	A	*R	Q	N	K	Q	*G	P	*C*
4.48B	*C*	H	*R	A	*G*	*R	F	*N*	*R	A	*R	*C*
4.27B	*C*	V	*K*	*H*	A	A	F	K	*L*	*G	*Q*	*C*
4.43B	*C*	V	*K*	*H*	A	*R	N	K	Q	V	L	*C*

Table 4.2 The mutant phagemid clones (described in Chapter 3) that were selected for further analysis, to investigate the effects of the amino acid substitutions on the IGF binding activity of bIGFBP-2. Conserved residues are marked in bold italic font. Conservative amino acid substitutions are underlined. Non-conserved substitutions are in plain font. The residues encoded for by rare amino acid codons are marked * (see Section 4.5.1).

The phagemids encoding for the mutant proteins were purified from the *E. coli* XL1-Blue cells (the *E. coli* strain used for phage display, see Chapter 3), and were transformed into *E. coli* BL21 strain for protein expression. Transformation of the constructs into *E. coli* BL21 cells was attempted using both chemical and electrocompetent procedures. After transformation and overnight growth on plates, the *E. coli* BL21 colony sizes were dramatically reduced and often difficult to detect. The effects on the rate of BL21 growth were more pronounced when plates and cultures containing the transformants were propagated overnight at 37°C (data not shown). Propagation of cells at 30°C, resulted in larger colony sizes on plates and higher cell densities in liquid medium (2YT). However, attempts to express protein from the cells grown at 30°C were generally unsuccessful. The most successful results were obtained from the transformation of mutant 4.17B into BL21 cells, which had colony morphologies resembling BL21 cells containing wild type pGF14 (data not shown). Figure 4.3 shows an example of an expression experiment with mutant 4.17B and the other mutants. Interestingly, cells containing pGF14 (encoding wild type bIGFBP-2 and mutant variants) often had greater amounts of protein present in the culture medium after overnight growth (detected by Coomassie Blue stained polyacrylamide gels), than cells containing the negative control pFdBDK61L (Figure 4.3) or no vector.

An alternative cell line, *E. coli* HB2151, was used to test if poor protein expression was a result of using the *E. coli* BL21 cell strain. Although transformation of the HB2151 *E. coli* strain yielded greater numbers of transformants (with similar colony morphologies to untransformed cells), attempts to express protein from these cells were also unsuccessful.

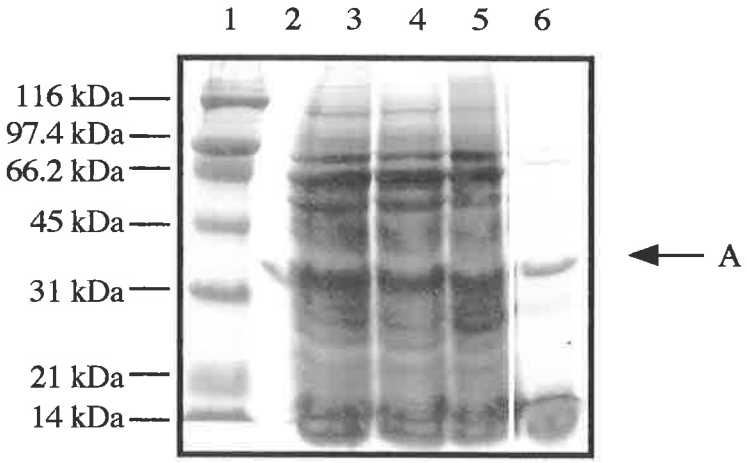

a) A Coomassie Blue stained non-reduced 12.5% polyacrylamide gel containing concentrated samples of bacterial cell growth medium. Lane 1 contains Bio-Rad molecular weight markers (the sizes indicated to the left of the gel) and lane 2 contains bIGFBP-2 standard. Lanes 3, 4, 5 and 6 contain concentrated medium from cells expressing phagemids 4.17B, 4.30A, 4.48B and negative control pFdBDK61L respectively. β-lactamase which is expressed from the pGF14 and pFdBDK61L phagemids is approximately 30 kDa in size (having a similar molecular weight to bIGFBP-2). Therefore, the band (marked A) seen in the negative control and lanes 3, 4 and 5 is most likely to represent β-lactamase.

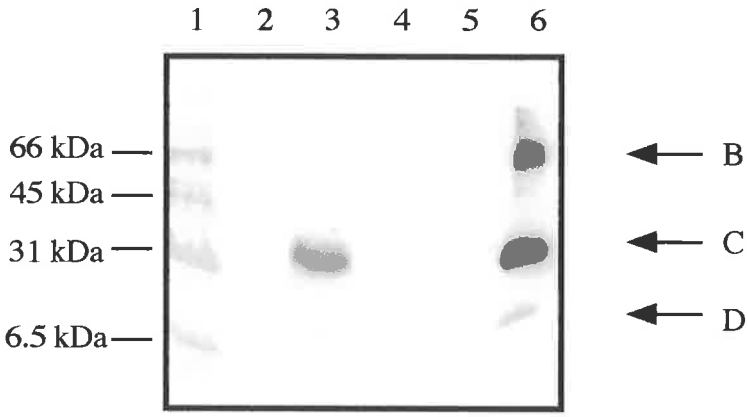

b) A second gel, of the medium analysed above, was Western transferred onto nitrocellulose membrane. The blot was probed with ^{125}I IGF-II ligand. Lane 1 contains Rainbow ^{14}[C] radiolabelled molecular weight markers (Amersham Pharmacia), with the sizes indicated to the left of the gel. Lanes 2, 3, 4, and 5 contain growth medium from cells expressing phagemids pFdBDK61L, 4.17B, 4.30A, and 4.48B respectively. In this experiment, only mutant 4.17B could be detected in the medium. Lane 6 contains bIGFBP-2 standard. The band marked B is bIGFBP-2 dimer and band C is full length bIGFBP-2. The band marked D is degraded bIGFBP-2. Unfortunately, the bIGFBP-2 polyclonal antiserum used throughout this study cross-reacted with bacterial proteins. Therefore, the antiserum was unsuitable for detecting binding protein in bacterial expression medium.

Figure 4.3 An expression experiment used to generate the bIGFBP2 mutants 4.17B, 4.30A and 4.48B from *E. coli* BL21 cells.

Restriction analysis performed on phagemid DNA isolated from HB2151 glycerol stocks of mutants 4.30A and 4.48B gave evidence that poor protein expression was not a result of major changes to the DNA encoding *bIGFBP-2* (Figure 4.4).

In a final attempt to express the proteins which did not express in *E. coli*, the mutations in phagemids 4.27B, 4.30A, 4.43B and 4.48B were PCR amplified (Figure 4.5) and subcloned into the mammalian expression vector pGF8His (Section 4.3.2 and Figure 4.2). Upon transfection of the wild type pGF8His and mutant constructs into COS-1 cells, analysis of the media over 5 days (using both antibody and IGF ligand) showed low to undetectable levels of mutant protein being expressed, despite expression of the wild type protein (data not shown). Therefore, the mammalian expression system was not pursued.

4.4.2 Characterisation of the 4.17B mutant protein

Of all of the mutants tested, phagemid 4.17B was the only construct capable of being expressed to levels that permitted further protein characterisation. Compared to wild type bIGFBP-2, expression levels were reduced. It was estimated, from several attempts at expressing and purifying the protein from bacterial growth medium, that the yields were between 20-45 μg per litre (with variable expression levels between different cultures).

As for the wild type protein (Chapter 2), mutant 4.17B was purified using IGF affinity chromatography and reverse phase HPLC. Purification using reverse phase HPLC showed that the protein exhibited a similar retention time to the wild type bIGFBP-2 protein (Figure 4.6). The purified protein was analysed on a 12.5% non-reduced polyacrylamide gel. Comparison to the wild type bIGFBP-2 confirmed that mutant 4.17B had the correct molecular weight (Figure 4.6). Interestingly, almost all attempts at purifying the 4.17B protein resulted in smaller molecular weight contaminants (Figure 4.6) which were detected with antibodies to bIGFBP-2. N-terminal sequence analysis of the mutant 4.17B confirmed that like the wild type bIGFBP-2 protein, it had been correctly processed during secretion from the bacterial cells (sequence NH_2 - EVLFR, see Figure 4.6).

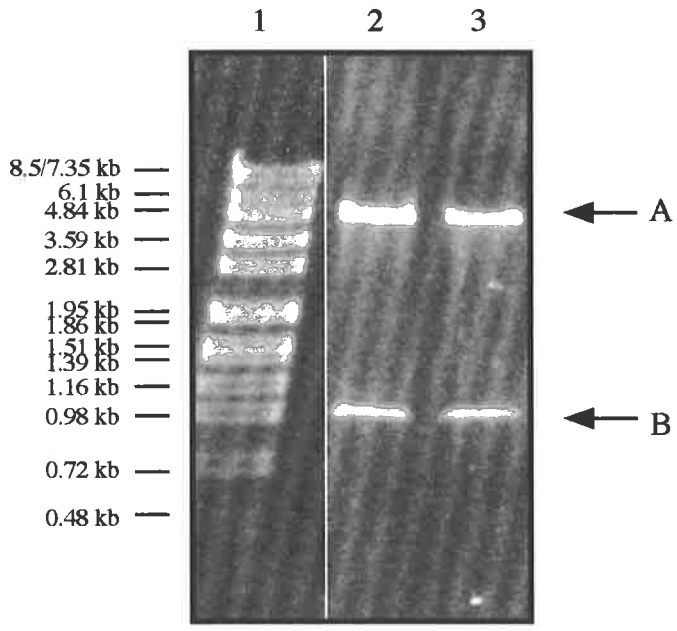

Figure 4.4 Restriction analysis of phagemid DNA isolated from HB2151 *E. coli* glycerol stocks containing mutants 4.30A and 4.48B. Digestion using *Pst* I and *Nco* I gave the expected fragment size of 870 base pairs (marked B). The fragment marked A (4.4 kb) represents the phagemid remaining after the *Pst* I/*Nco* I restriction digest. Lane 1 contains SPP1 marker DNA, with the sizes of the markers shown to the left of the gel. Lanes 2 and 3 contain digested 4.30A and 4.48B phagemid DNA isolated from HB2151 *E. coli* cells.

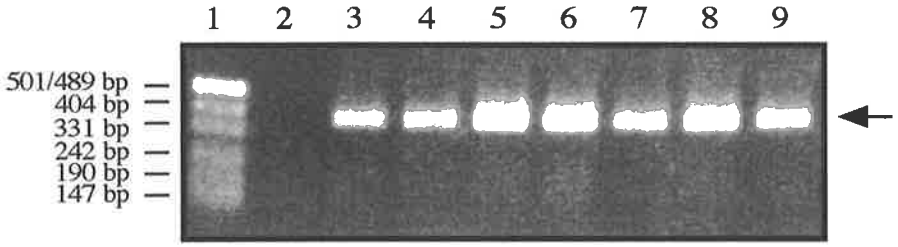

Figure 4.5 PCR amplification of the C-terminal bIGFBP-2 mutations, for cloning into the mammalian expression vector pGF8His. The PCR, using primers SJH1 and LCHis (Figure 4.2), gave the expected fragment size of 387 base pairs (marked by the arrow). Lane 1 contains pUC19 molecular weight markers, with the sizes of the markers shown to the left of the gel. Lane 2 contains the control reaction without DNA template. Lanes 3 to 9 contain PCR products from reactions containing phagemid templates pGF14, 4.17B, 4.20B, 4.27B, 4.30A, 4.43B and 4.48B respectively.

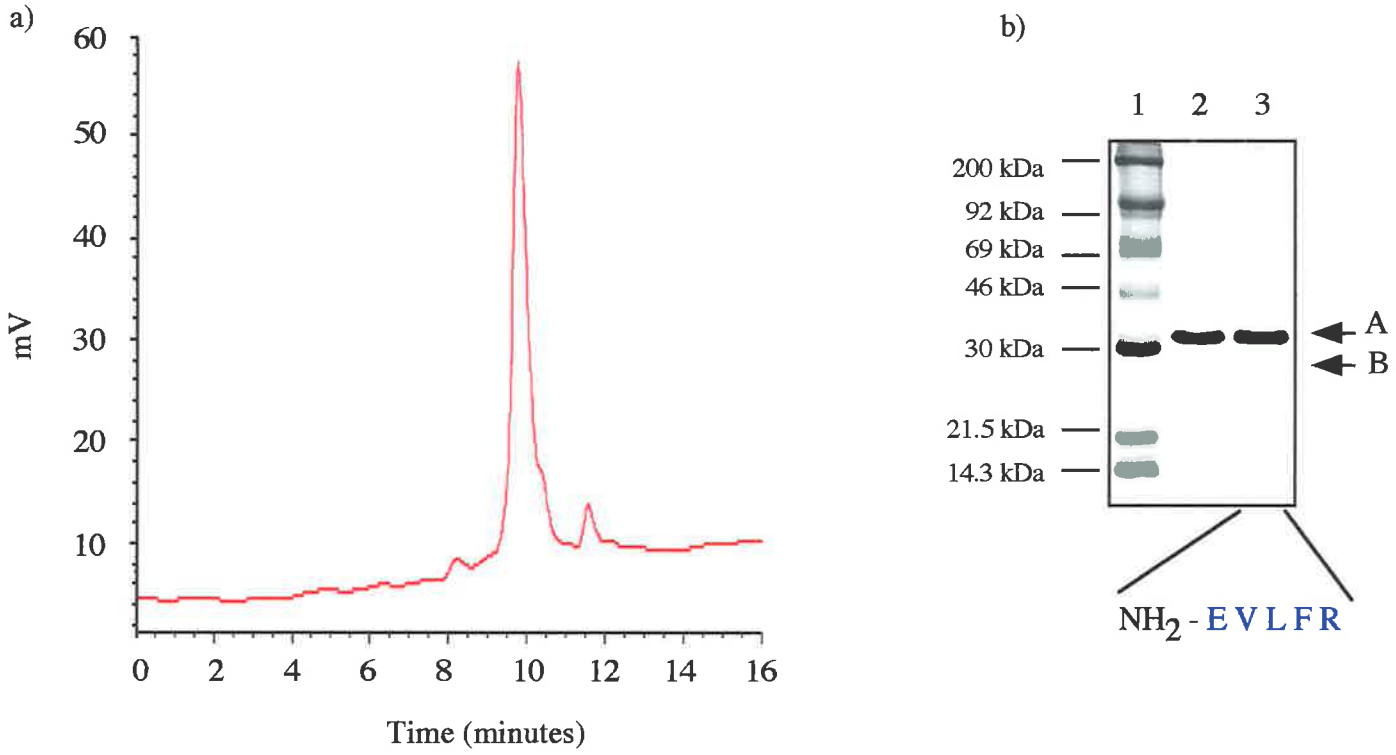

Figure 4.6 Analysis of the purified bIGFBP-2 mutant, 4.17B.
a) The purified protein was assessed by using a 15 minute 20-50% acetonitrile gradient on the HPLC (Section 4.3.1). The retention time on the column was similar to that seen for wild type bIGFBP-2.
b) 2 μg of HPLC purified wild type bIGFBP-2 (lane 2) and mutant 4.17B (lane 3) were analysed on a Coomassie Blue stained 12.5% polyacrylamide gel. Lane 1 contains Rainbow molecular weight markers (Amersham Pharmacia), with the sizes of the markers shown to the left of the gel. The band marked A is full-length binding protein. The band marked B represents a smaller fragment of the mutant 4.17B protein (confirmed by immunoblot, not shown here). Band B (in lane 3) is approximately 4% of the total sample (determined by densitometry). Amino acid sequence analysis of 4.17B confirmed that the mutant protein had been correctly processed for secretion from bacterial cells (the 5 N-terminal residues are shown in blue text).

4.4.3 Western ligand blot analysis to examine the IGF binding activity of mutant 4.17B

The IGF binding ability of mutant 4.17B was analysed by performing Western ligand blot analysis (Figure 4.7). Aliquots (200ng) of both wild type bIGFBP-2 and mutant 4.17B were compared for binding to biotinylated IGF-I or mono-biotinylated IGF-II. As can be seen in Figure 4.7, mutant 4.17B retained both biotinylated IGF-I and mono-biotinylated IGF-II less well than the wild type bIGFBP-2 (Figure 4.7). The bands, which were quantified using ImageQuant, which showed mutant 4.17B retained approximately 30% of the biotinylated IGF-I and approximately 55% of the mono-biotinylated IGF-II relative to the wild type bIGFBP-2 sample (Figure 4.7).

4.4.4 BIAcore™ analysis to examine the IGF binding activity of mutant 4.17B

To further investigate the effects of the mutations on the ability of 4.17B to bind to both IGF-I and IGF-II, studies were conducted using the BIAcore™ 2000 instrumentation. Due to limiting amounts of the mutant 4.17B protein, the experiments were performed by immobilising the binding protein to the surface of the CM5 chip (Section 4.3.4). The immobilisation Wizard program (provided with the BIAcore™ 2000 instrumentation) was instructed to immobilise 500 RU of wild type bIGFBP-2 and mutant 4.17B on separate channels of the same CM5 chip (1000 RU is equivalent to a sensor chip surface concentration of 1 ng/mm^2, Nice and Catimel (1999)). The actual amounts coupled to the sensor chip surface were 566 RU of wild type bIGFBP-2 and 509 RU of mutant 4.17B. Similarly, when immobilisation of 100 RU was targeted for wild type bIGFBP-2 and mutant 4.17B on separate surfaces, responses above background were obtained of 122 and 86 respectively.

The amount of active binding protein coupled to the CM5 surfaces was estimated by comparing the experimentally defined maximal binding capacity of the surface (Rmax) to the theoretically determined Rmax. Theoretical determination of the Rmax could be achieved because the stoichiometry of IGF binding to bIGFBP-2 was known to be 1:1 (Bourner *et al.*, 1992). Furthermore the arbitrary resonance unit, RU, which is measured by the BIAcore™ 2000 system is proportional to the molecular weight of the protein bound to the sensor chip surface (reviewed in Nice and Catimel, 1999). Therefore, the theoretical Rmax can be

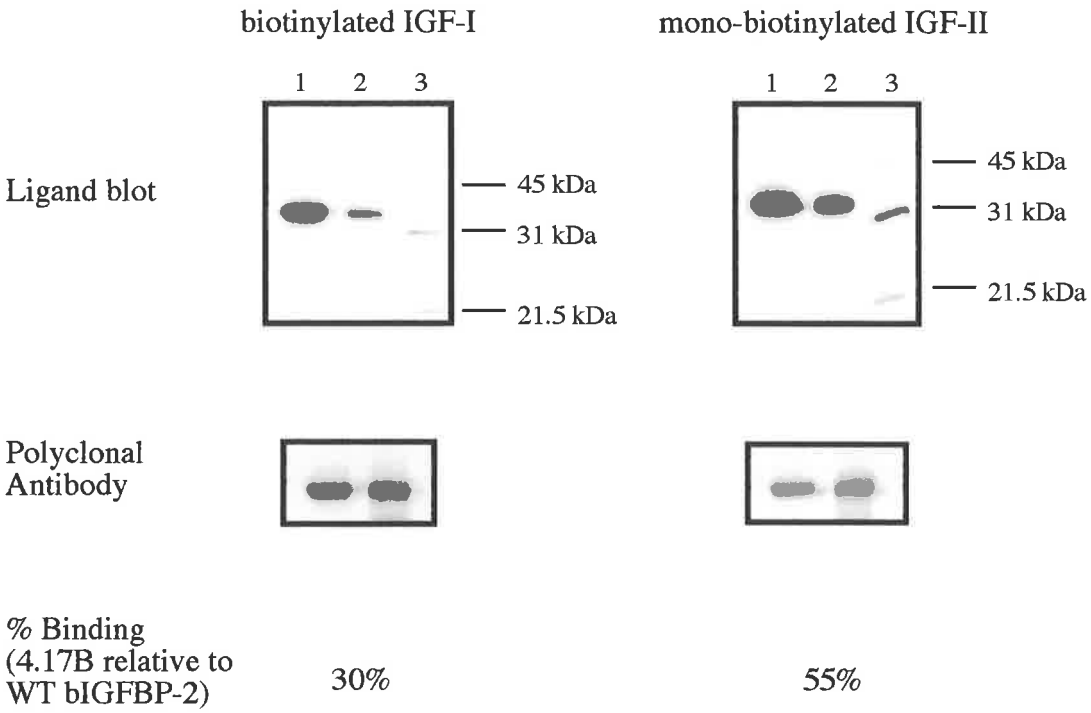

Figure 4.7 IGF-I and IGF-II binding ability of mutant 4.17B examined using Western ligand blot. 200ng of wild type mammalian cell derived bIGFBP-2 (lane 1), *E. coli* derived 4.17B (lane 2) were separated on 12.5% polyacrylamide gel and were transferred onto nitrocellulose membrane. The membranes were probed with either biotinylated IGF-I or IGF-II, and were developed as described in the Section 4.3.3. Lane 3 contains Bio-Rad broad range biotinylated molecular, with the sizes of the markers shown to the right of the blots. Relative to the wild type bIGFBP-2 signal, 4.17B retained approximately 30% of IGF-I and 55% of IGF-II on the blot (determined using densitometry). Antibody blots confirmed that similar amounts of wild type bIGFBP-2 and 4.17B were compared on the filter.

determined by the equation: $\frac{M_r analyte}{M_r ligand}$ * (the amount of ligand coupled to sensor chip surface, RU) * (stoichiometry of the interaction). On the 566 RU surface of the wild type bIGFBP-2 the ratio of observed:expected (approximately 115:137 RU) showed that about 80% of the surface was active. Similar comparisons made with the mutant 4.17B (approximately 93:124) surface showed that the surface binding capacity was approximately 75% of the expected value.

In preparation for kinetic studies, experiments were conducted on the wild type bIGFBP-2 coated biosensor surface to determine the optimal flow rate required for the delivery of IGF to the binding protein. If transport of the analyte to and from the ligand is slow compared to both the association and dissociation rates, the experimentally determined binding rates will be inaccurate (known as mass transport limited data, reviewed in Canziani *et al.*, 1999). A mass transport experiment is seen in Figure 4.8 which shows that increasing flow rates did affect the rates at which both IGF-I and IGF-II associated with the wild type bIGFBP-2 (on a surface containing 500 RU of bIGFBP-2). At flow rates above 50 µl/minute, the association rate was not significantly different (Figure 4.8). From these experiments, a flow rate of 50 µl/minute was selected for future kinetic studies to minimise mass transport limitation effects on the determined rates.

Kinetic experiments were performed by injecting a range of concentrations of both IGF-I and IGF-II onto the wild type bIGFBP-2 and mutant 4.17B protein coated sensor surfaces. To determine the rate constants, different binding models were assessed on the data obtained using the wild type bIGFBP-2 surface. In the first instance, a global approach (Roden and Myszka, 1996) was tested. Global analysis is performed by simultaneously fitting the association and dissociation phase data generated for a range of injected analyte concentrations (Roden and Myszka, 1996). The binding curves obtained using concentrations of IGF from 12 to 100 nM were initially analysed assuming a simple one to one interaction (Langmuir 1:1 model, see Appendix 1 and Figure 4.9). The results from fitting the binding data to the different interaction models are indicated by the black lines in Figure 4.9. As can be seen, it was difficult to fit the binding curves to the Langmuir 1:1 binding model (Figure 4.9). Figure 4.9 also shows the results obtained by fitting the data assuming a 1:1 interaction influenced by mass transfer, a heterogeneous ligand model, and a two-state reaction model (Appendix 1). Using the global fitting procedure, the best results were those obtained using two-state reaction model

a)

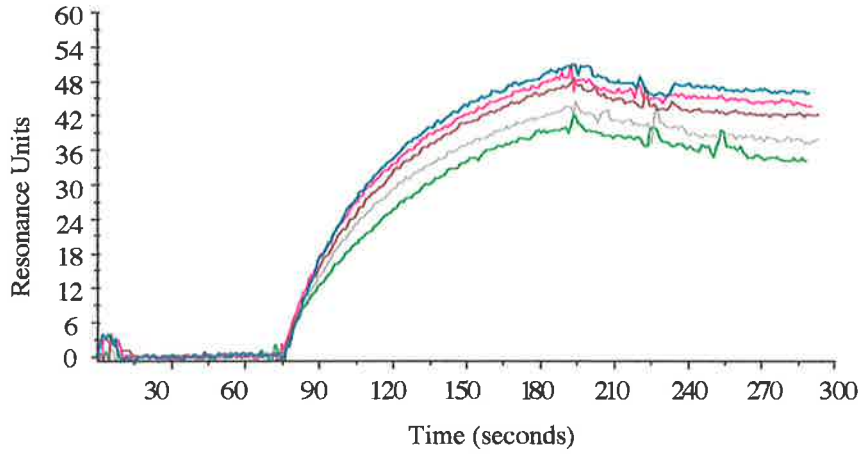

b)

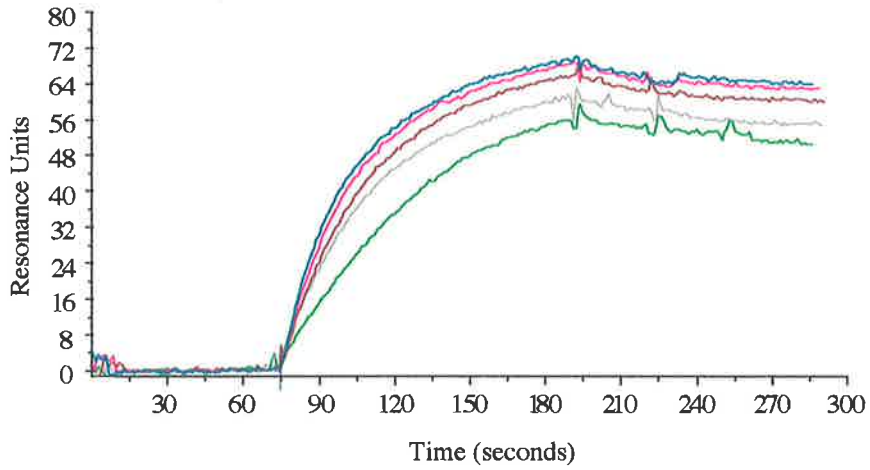

Figure 4.8 Analysis of the optimal flow rate required to reduce the effects of mass transport limitations experienced using BIAcore™ 2000. bIGFBP-2 (500 RU) was amine coupled to a CM5 chip, and a) 16 nM IGF-I or b) 16 nM IGF-II were flowed over the surface at 5 µl/minute (__), 15 µl/minute (__), 30 µl/minute (__), 50 µl/minute (__) and 75 µl/minute (__).

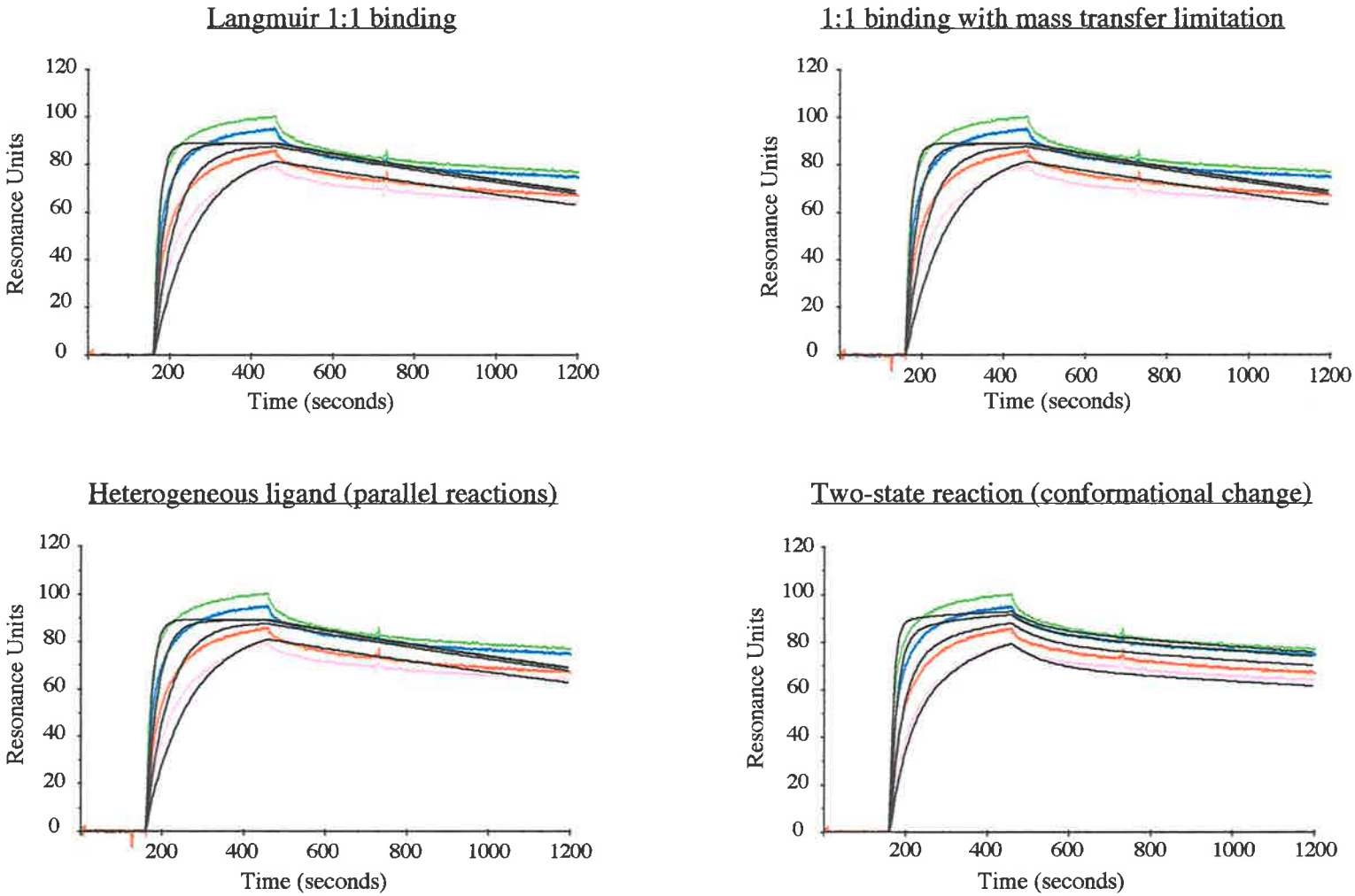

Figure 4.9 Analysis to determine the models which best describe the interaction between the sensor chip bound wild type bIGFBP-2 and IGF-I, using a global approach. In this example, the models were fitted to concentration curves obtained using 12 nM (___), 25 nM (___), 50 nM (___) and 100 nM (___) IGF-I. The black lines represent the results from fitting the binding data to the different kinetic models.

(Figure 4.9). However, as can be seen in Figure 4.9, even using the two-state model there were problems using the global approach, especially at the higher concentration ranges of IGF (see Section 4.5.2). The results were the same when the models were fitted to the IGF-II binding curves (Figure 4.10).

The binding models were also fitted to data obtained from individual concentrations of IGF analyte. Figure 4.11 shows the results of fitting the models to binding curves obtained using 50 nM IGF-I over the wild type bIGFBP-2 surface. The goodness of fit was assessed both visually and by low χ^2 values. The χ^2 values (provided by the BIAevaluation software) provided a standard statistical measure of the goodness of fit, by comparing the experimentally determined binding curves to the curves generated by fitting the data to the different binding models. Again, the best fits were obtained using the two-state reaction model (Figure 4.11). Attempts to fit the kinetic models to IGF-II binding curves generated similar results (Figure 4.12). Consequently for the purposes of this thesis, the mutant and wild type bIGFBP-2 protein were compared for IGF binding ability using the two-state reaction model. In this study, 50 nM concentration curves were used to generate both association and dissociation rates for comparison of the mutant wild type bIGFBP-2. This approach is similar to the study performed by Heding *et al.* (1996) who also used 50 nM IGF concentration curves to determine the rate constants (see Section 4.5). Figure 4.13 shows a representative subset of the sensorgram data (for qualitative comparison) that were used to generate the kinetic constants summarised in Table 4.3.

The amino acid substitutions in mutant 4.17B affected IGF-I and IGF-II binding activity in both the association and dissociation phases (Table 4.3). A comparison of the apparent affinity constant, $K_{A(app)}$ (Table 4.3), showed that the wild type bIGFBP-2 protein bound both IGF-I and IGF-II approximately 3-fold better than the mutant 4.17B. Similarly a comparison of the $K_{A(app)}$ determined using the 100 RU density surfaces differed between the wild type bIGFBP-2 and mutant 4.17B approximately 3-fold for both IGF-I and IGF-II (data not shown). The rates determined using the 100 RU density surface were within the standard errors observed in the rates determined using the 500 RU surface.

Preliminary experiments were performed to confirm that the binding activity of mutant 4.17B was not impaired due to the coupling of the protein to the biosensor surface. Single

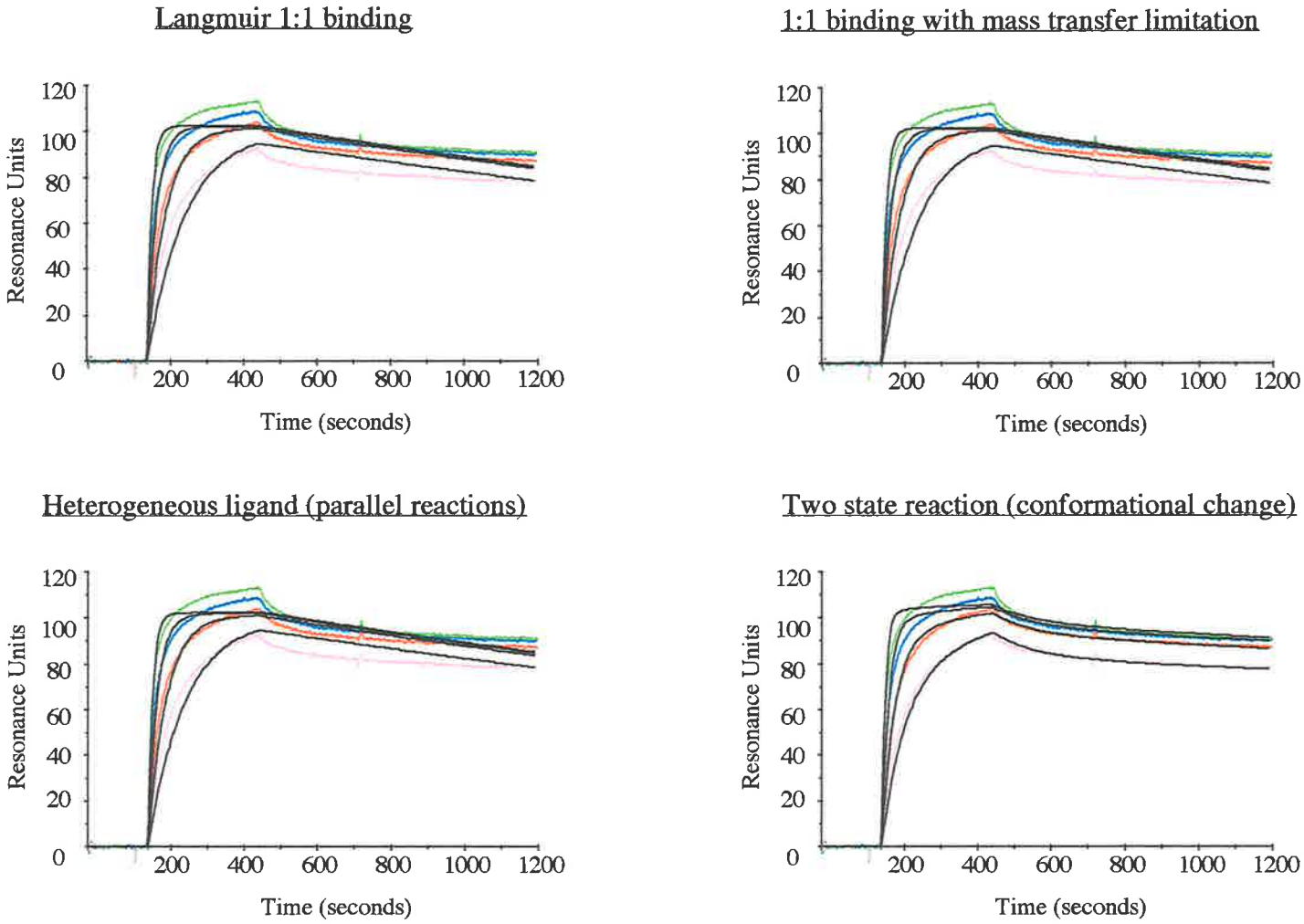

Figure 4.10 Analysis to determine the models which best describe the interaction between the sensor chip bound wild type bIGFBP-2 and IGF-II, using a global approach. In this example, the models were fitted to concentration curves obtained using 12 nM (___), 25 nM (___), 50 nM (___) and 100 nM (___) IGF-II. The black lines represent the results from fitting the binding data to the different kinetic models.

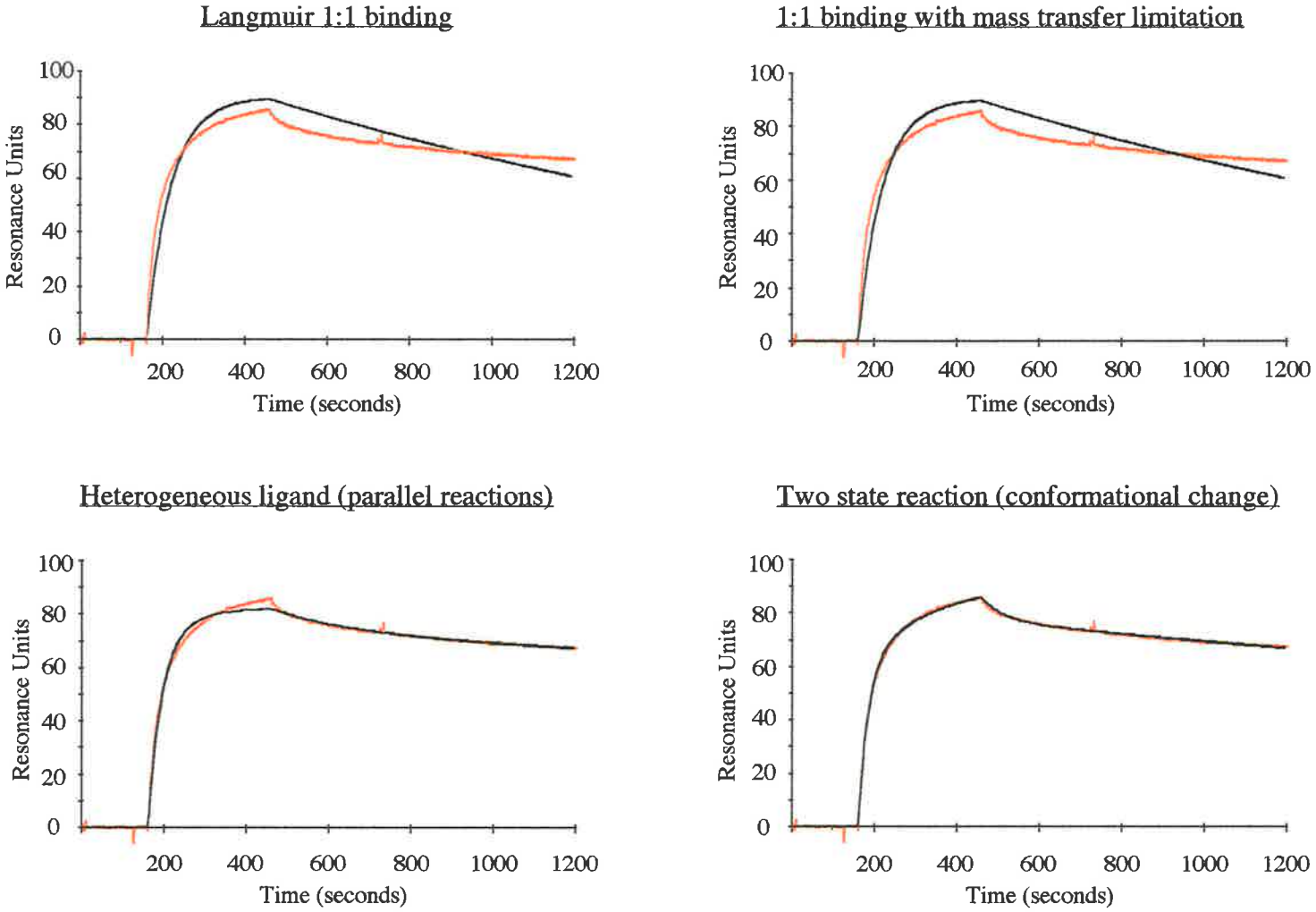

Figure 4.11 Analysis to determine the models which best describe the interaction between the sensor chip bound wild type bIGFBP-2 and IGF-I, using single concentrations of IGF-I. In this example, the models were fitted to concentration curves obtained using 50 nM (___) IGF-I. The black lines represent the results from fitting the binding data to the different kinetic models.

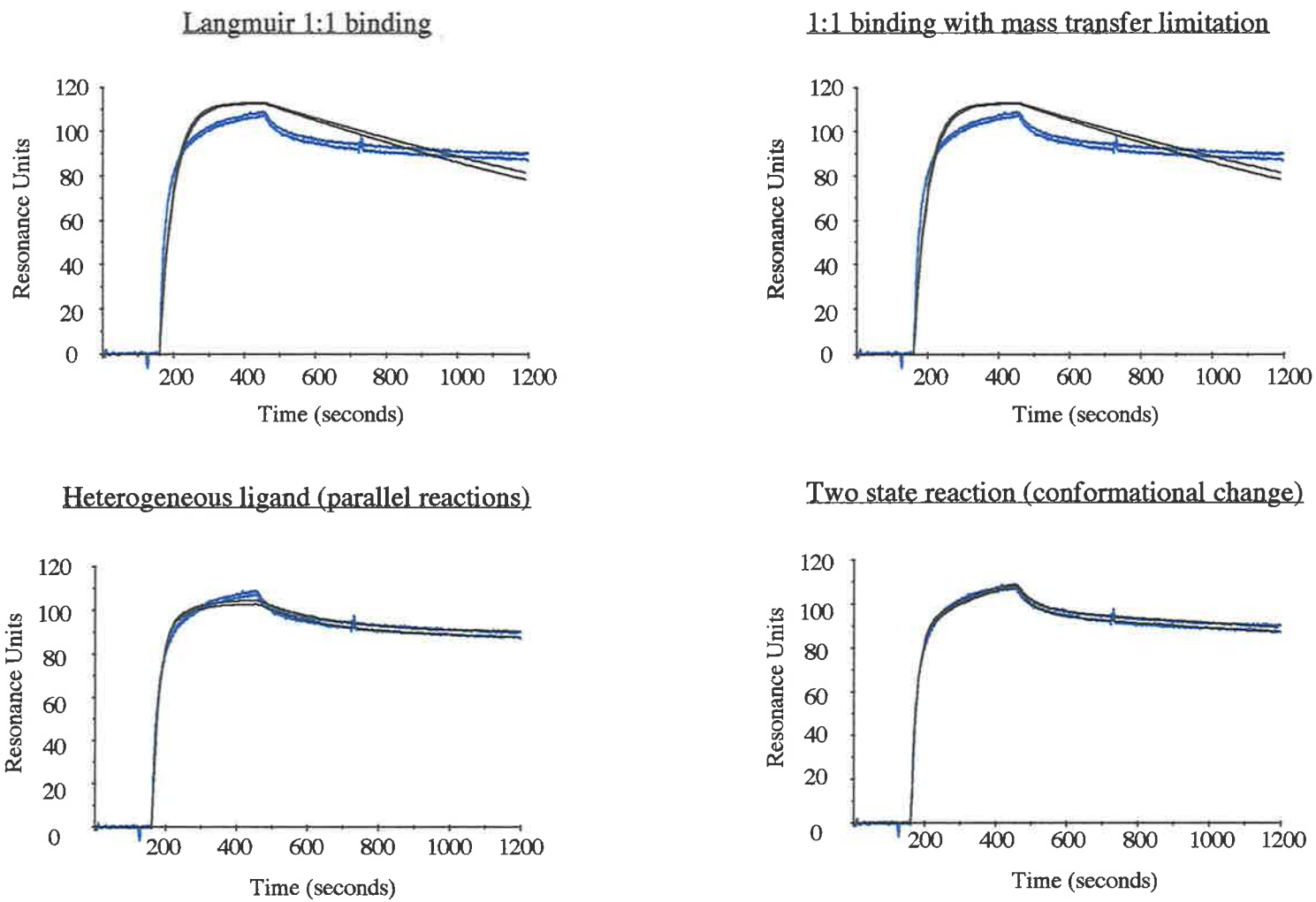

Figure 4.12 Analysis to determine the models which best describe the interaction between the sensor chip bound wild type bIGFBP-2 and IGF-II, using single concentrations of IGF-II. In this example, the models were fitted to concentration curves obtained using 50 nM (___) IGF-II. The black lines represent the results from fitting the binding data to the different kinetic models.

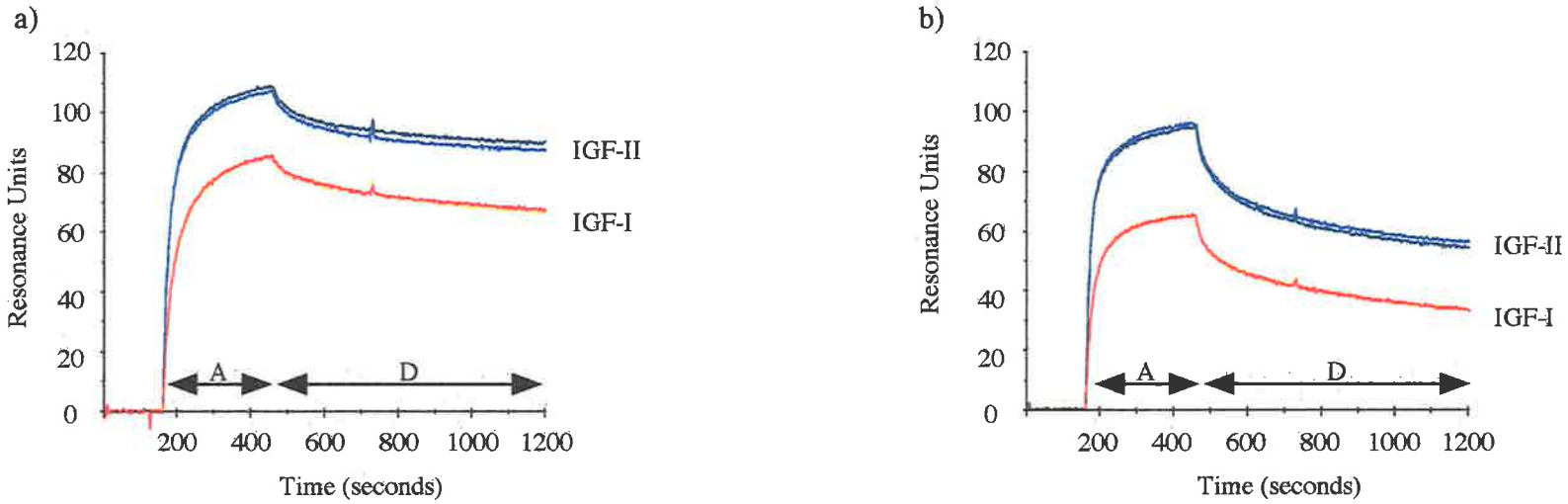

Figure 4.13 Comparison of the binding of 50 nM IGF-I and 50 nM IGF-II to (a) wild type bIGFBP-2 and (b) mutant 4.17B. The sensor chip surfaces in these experiments contained approximately 500 RU of binding protein. The arrow marked "A" represents the association phase of the curve, where 50 nM IGF was injected over the binding protein surface for 5 minutes at 50 µl/minute. The arrow marked "D" represents the dissociation phase of the curve where only buffer was injected for 12 minutes at the same flow rate.

injections of both wild type and mutant 4.17B were performed over biosensor surfaces coupled to either IGF-I and IGF-II. In this orientation, mutant 4.17B continued to exhibit reduced IGF binding activity relative to the wild type protein.

IGF-I	ka1 x10^{5} (1/Ms)	ka2 x10^{-3} (1/s)	kd1 x10^{-2} (1/s)	kd2 x10^{-4} (1/s)	$K_{A(app)}$ x10^{9} [a] (1/M)	relative $K_{A(app)}$ [b]
bIGFBP-2	5.6 ±10%	7.5 ±3%	1.1 ±30%	3.1 ±11%	1.3	1
4.17B	7.5 ±4%	3.9 ±2%	1.3 ±14%	5.7 ±7%	0.4	3.3

IGF-II	ka1 x10^{5} (1/Ms)	ka2 x10^{-3} (1/s)	kd1 x10^{-2} (1/s)	kd2 x10^{-4} (1/s)	$K_{A(app)}$ x10^{9} [a] (1/M)	relative $K_{A(app)}$ [b]
bIGFBP-2	8.9 ±12%	7.1 ±2%	1.3 ±27%	1.9 ±10%	2.5	1
4.17B	11 ±7%	4.1 ±6%	1.3 ±11%	4.6 ±7%	0.78	3.1

Table 4.3 Summary of the kinetic rates derived from the interaction of IGF-I and IGF-II with 500 RU of immobilised bIGFBP-2 and mutant 4.17B. The kinetic rates were obtained using the two-state reaction (conformational change) model, and data analysis was performed on the 50 nM concentration curves of IGF-I and IGF-II. The numbers are the means of the rates determined for 6 replicate concentration curves, with the standard errors (at a 95% level of significance) for the association and dissociation rate values shown as a percentage of the mean.
a. The apparent affinity constant, $K_{A(app)}$, was obtained by calculating the following equation: $\frac{ka1}{kd1} x \frac{ka2}{kd2}$, where ka1 and ka2 represent the association rates, and kd1 and kd2 represent the dissociation rates (Appendix 1).
b. The relative $K_{A(app)}$ is the ratio of $K_{A(app)}$(bIGFBP-2): $K_{A(app)}$(4.17B).

4.5 Discussion

The focus of this work was to compare the IGF binding activity of bIGFBP-2 mutants isolated from the phage display screening experiments described in Chapter 3. However, what became apparent during the course of these studies was the lack of knowledge regarding the IGF-IGFBP binding mechanism. Without a knowledge of the binding mechanism, interpretation of kinetic binding studies performed using BIAcore™ became difficult. Therefore, the following discussion is split into two components to address these issues. In the first part, the results of the expression and characterisation of the different mutant bIGFBP-2 proteins is addressed. The second part of the discussion addresses the implications arising from the BIAcore™ experiments, and suggests future work to determine the binding mechanism between IGF and IGFBPs.

4.5.1 The effects of amino acid substitutions at residues 221-230 of bIGFBP-2

The results described in this chapter show that the C-terminal region of bIGFBP-2 (residues 221-230) contains determinants which are important for normal IGF binding function. The bIGFBP-2 mutant 4.17B, containing the amino acid substitutions: Lys222Met, His223Gly, Leu228Gln and Lys229Glu was analysed using two different ligand binding approaches. Both Western ligand blot and BIAcore™ analyses showed that 4.17B had a reduced binding affinity for both IGF-I and IGF-II. These results confirm earlier deletion studies which demonstrated that residues in the region 221-236 of bIGFBP-2 were important for full IGF binding function (Forbes *et al.*, 1998). The current findings are also supported by a more recent publication studying human IGFBP-5 (Song *et al.*, 2000). In that study, amino acid substitutions of adjacent residues, in the corresponding region of rat IGFBP-5, were also found to affect IGF binding function.

Full-length mutant 4.17B could be purified from bacterial growth medium using the procedures developed for the wild type bIGFBP-2 (Chapter 2). Analysis of the IGF binding ability of mutant 4.17B, using Western ligand blot and BIAcore™, showed similar reductions in IGF binding activity. However using Western ligand blot, the reduction in binding relative to the wild type protein was greater using biotinylated IGF-I (30% of the binding activity of wild type protein) than mono-biotinylated IGF-II (55% of the binding activity of wild type protein). The relative differences in the $K_{A(app)}$ values generated using BIAcore™ (Table 4.3) shows a marginally greater effect of the mutations on IGF-I binding activity than for IGF-II binding. Although these differences on their own are not sufficient to explain the extent of the effect observed using Western ligand blot (personal communication with Dr Nigel Bean), the standard errors in the rate estimates (Table 4.3) means that it is not possible to reject a greater effect on IGF-I binding activity. The differences in the effects on IGF-I and IGF-II binding may result from subtle structural differences between the IGFs (compared in Torres *et al.*, 1995). As a result, IGF-I may be more sensitive to changes in amino acid side-chains altered in mutant 4.17B. Interestingly, N-terminal mutations and tyrosine iodination in bIGFBP-2 were also found have a greater effect on IGF-I binding activity versus IGF-II binding activity (Hobba *et al.*, 1996; Hobba *et al.*, 1998).

How are the amino acid substitutions in mutant 4.17B affecting its ability to bind to IGF? There are a number of possibilities which may explain this observation. In Chapter 3, the results of iterative panning experiments suggested that negatively charged residues were not optimal for IGF-II binding activity (Figures 3.9a and 3.9b). Interestingly, the mutations in 4.17B, at Lys222Met and Lys229Glu, removed the positively charged amino acids and substituted a negatively charged glutamate. In conjunction with a reduced IGF binding affinity, these results may explain the trends observed in the panning experiments. bIGFBP-2 variants containing negatively charged residues in this region would have a greater probability of being lost during panning if they had reduced IGF-II affinity. As discussed in Chapter 3, negatively charged residues may cause electrostatic repulsion between the IGF and binding protein. If the charge reversal in this region of bIGFBP-2 was responsible for the reduced IGF binding activity, it is possible that by mutating the residues on IGF which interact with the binding protein, that the binding affinity between the two proteins may be restored.

Alternatively, the loss in IGF binding activity may have resulted from changes to the structure of mutant 4.17B. In support of structural change, smaller molecular weight fragments (possibly proteolytic fragments) were often found in purified samples of full-length 4.17B protein (Figure 4.6). Structural changes to the protein may have resulted from the His223Gly substitution. To date, a lack of structural knowledge of the binding protein makes it difficult to predict the effects of amino acid substitutions (see Chapter 6). Unfortunately, insufficient amounts of mutant 4.17B were purified to enable biophysical analyses to be performed on the protein.

One approach which could be used to study the structure of mutant 4.17B would be CD. In the absence of structural information, far-UV CD could be used to detect changes to the protein secondary structure (reviewed in Kelly and Price, 1997), by comparing spectra from the wild type protein to the mutant protein. Circular dichroism has been previously used by our laboratory to assess the structural integrity of mutant bIGFBP-2 molecules (Hobba *et al.*, 1998). Also, current work in our laboratory is investigating the use of tryptophan fluorescence to assess the structural changes in the binding proteins (Forbes *et al.*, 2000). In bIGFBP-2, a single tryptophan residue is located at position 243 (Figure 1.5). Its proximity to the mutated region 221-230 in bIGFBP-2, may make it a useful probe to analyse changes in the structure of

mutant 4.17B. A third approach to assess structural changes in the bIGFBP-2 mutant may be to analyse its integrin binding activity. The integrin binding site in IGFBP-2 (^{260}RGD in bIGFBP-2) is located in the C-terminal end of the binding protein (Section 1.4.1), and changes in integrin binding affinity could be used to indicate structural change. Altered protein structure and/or reduced protein stability, may also explain the poor expression of the other mutants (Table 4.2) which contained many residue substitutions in region 221-230 of bIGFBP-2. Poor protein expression of these variants was observed in both bacterial and mammalian expression systems.

Recombinant expression of proteins can be a problem, if the genes encoding the protein contain codons which are rarely used in the host organism (Kane, 1995; Zhou *et al.*, 1999). The presence of a single rare codon (or even worse, multiple rare codons), can decrease protein expression levels and result in smaller protein fragments, presumably due to frameshifting and premature termination of translation (Kane, 1995). Furthermore, transformation and attempts to express genes containing rare amino acid codons in bacterial cell hosts, can result in host cell death (Zahn, 1996). Analysis of the codons within the bIGFBP-2 gene, and their frequencies in bacterial cells, shows that many codons (approximately 18%) are used at 10% or less in *E. coli* (determined using the *E. coli* Codon Usage Analysis 2.0 by Morris Maduro, http:\\www.biology.ualberta.ca\pilgrim.hp\usage2.oc.html). Furthermore, in designing the library of mutations using primer MP739 (Figure 3.4), the codon usage was not optimised for *E. coli*. Analysis of the codons used to generate the mutant bIGFBP-2 library, shows that 14 of a total of 64 possibilities are represented at less than 1% in *E. coli* (determined using the codon usage table in Kane, 1995). Furthermore, of the bIGFBP-2 mutant clones selected for expression, all but mutant 4.17B contained rare amino acid codons used at a frequency of less than 1% in *E. coli* (determined using the table in Kane, 1995; see Table 4.2). There are tools to test if poor protein expression is due to rare codons within gene sequences. Recently, modified strains of BL21 have become available commercially (for example, BL21-CodonPlus™ from Stratagene), which contain higher concentrations of rare codon tRNAs. These modified BL21 *E. coli* strains have been reported to improve the expression levels of proteins containing rare amino acid codons up to 100-fold (Kleber-Janke and Becker, 2000). Although it is possible to obtain up to 1 mg/litre of wild type bIGFBP-2 from

unmodified *E. coli* BL21 cells (Chapter 2), in other systems, single amino acid substitutions have been observed to affect protein expression levels. For example, Forsberg *et al.* (1997) found that the expression of light and heavy chain fragments of an antibody in *E. coli* (and the levels of proteins found in the growth medium) could be altered by changing only a few amino acids in the protein sequences.

Which residues in mutant 4.17B were responsible for the reduced IGF binding activity? To answer this question, it would be necessary to create single amino acid substitutions and to characterise each individual mutant. It may be possible that one, or all of the mutated residues in 4.17B contributed to the reduced IGF binding activity. Unfortunately, the difficulties experienced using the phage display approach (Chapter 3), and the inability to express and characterise more mutants in this study, failed to provide any further clues to answer this question.

Large changes to protein function are often generated by mutating several amino acids in a protein sequence (Wells, 1990). In this study, the four amino acids substituted in mutant 4.17B reduced IGF binding affinity only 3-fold. The marked effects observed for the bIGFBP-2 deletion mutant (80-fold reduction in IGF binding affinity, Forbes *et al.*, 1998) may be achieved if a greater number of residues in this region of the protein are mutated. For example, single amino acid substitutions of residues corresponding to Gly224 and Glu230 in bIGFBP-2 (not altered in 4.17B), reduced the IGF binding activity of IGFBP-5 between 4- to 6-fold (Song *et al.*, 2000). If these mutations were cooperative, in combination with the mutations in 4.17B, they would have greater effects on IGF binding activity. Furthermore, residues 231-236 of bIGFBP-2, which were also removed in the deletion mutant (Forbes *et al.*, 1998), were not investigated here. Although there is limited sequence homology in this region across the binding protein family (Figure 1.4), a role for residues 231-236 in IGF binding remains to be determined. Consequently, the investigation of the roles of these residues in IGF binding function forms the topic of Chapter 5.

4.5.2 Kinetic analysis using BIAcore™ - the importance of determining the IGF-IGFBP binding mechanism

In this study, BIAcore™ was chosen as a method to investigate the effects of amino acid substitutions on the ability of mutant 4.17B to bind to IGF. BIAcore™ was selected because it had previously been used in our laboratory to assess the binding of bIGFBP-2 mutants (containing N-terminal mutations) for IGF-I and IGF-II (Hobba *et al.*, 1998). Similar to the findings of Hobba *et al.* (1998), the binding curves observed for the interaction of wild type bIGFBP-2 with either IGF-I or IGF-II were found to deviate from pseudo-first-order kinetic behaviour. Such deviations have also been observed for studies performed on IGFBP-3 (Heding *et al.*, 1996) and on human IGFBP-6 (Marinaro *et al.*, 1999). Deviations of binding data from a simple 1:1 interaction model are common, and may often be attributed to experimental design (O'Shannessy and Winzor, 1996; Myszka, 1997; Schuck, 1997; Canziani *et al.*, 1999).

In this study care was taken to generate high quality kinetic data. Lower surface densities of binding protein were coupled to the sensor chip surfaces. The use of lower surface densities reduces steric hindrance and enables greater ligand accessibility within the dextran layer (Canziani *et al.*, 1999). Furthermore, moderate flow rates (50 µl/minute) of IGF analyte were used to reduce mass transport limitation effects. Deviations of the binding data as a result of mass transport effects, were rejected when attempts to fit the 1:1 binding model containing a mass transport coefficient (Appendix 1) did not improve the fits (Figures 4.9 to 4.12). Interestingly, different studies investigating the IGF-IGFBP interaction have reported variable effects of mass transport on data generated using the BIAcore™. For example, similar considerations (low surface densities and high flow rates of 100 µl/minute) were found to be important in a study analysing the IGF interaction with recombinant human IGFBP-5 (Kalus *et al.*, 1998). In contrast, two studies using BIAcore™ to analyse all 6 hIGFBPs (1-6) (Wong *et al.*, 1999) and human IGFBP-6 (Marinaro *et al.*, 1999) found that flow rate did not affect the association and dissociation rates of IGF with the binding protein. These differences in the effects of the rate of analyte delivery to the immobilised ligand may reflect the differences in the ways in which the different binding proteins interact with the IGFs (see Section 1.5.1). In support of this, Wong *et al.* (1999) showed that each of the 6 hIGFBPs (1-6) exhibited

different association and dissociation profiles when compared on sensor surfaces coupled to either IGF-I or IGF-II.

A further source of deviation from pseudo-first-order kinetics, can be effects due to amine coupling of bIGFBP-2 to a sensor chip surface. The use of this coupling procedure can lead to a mixed population of protein on the biosensor surface, with a range of different affinities for the analyte (O'Shannessy and Winzor, 1996). The amino acid sequence of bIGFBP-2 contains 14 lysine residues (Figure 1.5) and could potentially immobilise in many orientations. However, the immobilisation of wild type bIGFBP-2 (and mutant 4.17B) did not substantially affect the IGF binding activity of the protein (the observed Rmax was about 80% of the expected Rmax). This is consistent with the observations of Marinaro *et al.* (1999) who found that IGFBP-6, amine coupled to a carboxymethylated dextran surface, retained approximately 80% of the expected maximal binding capacity. Furthermore, evidence against surface heterogeneity was provided when attempts to fit the binding data, using the heterogeneous binding model, gave less than perfect fits. To confirm that the deviations from a simple 1:1 binding model were not a result of the amine coupling procedure, experiments could be conducted where either the binding protein or IGF were coupled to the sensor chip using more controlled immobilisation approaches. The use of a fusion tag (for example, a poly-histidine or a biotinylated sequence) at the C-terminal end of bIGFBP-2 (see Section 5.5) would create a sensor chip surface where all proteins were immobilised in the same orientation. This surface could be used to confirm that surface heterogeneity was not responsible for the deviations that resulted when attempts were made to fit a simple 1:1 binding model.

Although experimental design may explain the deviations from a simple 1:1 binding model, it is also possible that the interaction between IGF and bIGFBP-2 involves more complex binding mechanisms. Competitive solution binding assays of human IGFBP-1, -2 and -6 (Roghani *et al.*, 1991) and human IGFBP-5 (Sackett and McCusker, 1998) give evidence to suggest IGFBPs have both low and high affinity binding sites for the IGFs. One possible mechanism for the binding, which to date has not been explored for the interaction between IGF and IGFBP on the BIAcore™, is the two-state reaction model (with conformational change) (Appendix 1). It has previously been suggested that upon binding to the IGF, the IGFBPs undergo a conformational change. For example, a study by Arai *et al.*

(1996b) investigating the ability of bIGFBP-2 to bind to glycosaminoglycans, found that bIGFBP-2 could only interact when IGF was in complex with the binding protein. This was proposed to occur because a conformational change in the binding protein exposed amino acid sequences which enabled binding to glycosaminoglycans (Arai *et al.*, 1996b). Also, the enhanced proteolysis of IGFBP-4 in the presence of the IGFs (Section 1.4.3) may be explained by a conformational change. As can be seen in Figures 4.11 and 4.12, the two-state reaction model best fitted the binding curves obtained for the interaction between both IGF-I and IGF-II with the wild type bIGFBP-2. Furthermore, the apparent affinity constants determined using this model were similar to those described for bIGFBP-2 determined in solution binding assays (Bourner *et al.*, 1992). However, while the two-state reaction model could be fitted to the binding data obtained at each individual concentration of IGF analyte, the model was difficult to fit using a global approach (Figures 4.9 and 4.10). One possible reason for less than perfect global fits using this model (particularly at the higher concentrations of IGF) may be due to dimerisation of the IGF analyte. Self association of IGF however, has only been observed in NMR studies, which use high concentrations of IGF for structure determination (Cooke *et al.*, 1991; Terawasa *et al.*, 1994; Torres *et al.*, 1995). Although such high concentrations of IGF were not used in this study, the accumulation of IGF at the sensor chip surface may produce local concentration effects enabling the IGFs to dimerise. Interestingly, insulin (which has 45% identity with the IGFs, see Section 1.2) can self associate under certain concentrations and conditions (Jeffrey *et al.*, 1976; Helmerhorst and Stokes, 1987). By performing sedimentation equilibrium studies, such as those performed for insulin (for example, Jeffrey *et al.*, 1976) it would also be interesting to test if both IGF-I and IGF-II are able to self associate.

In summary, a knowledge of the binding mechanism between IGF and IGFBP would enable better interpretation of kinetic studies such as those performed in this thesis. The observations made in the current study show that further structural, biophysical and kinetic investigations are required to define completely the mechanism by which IGF and IGFBP interact.

Chapter Five

ALANINE SCANNING MUTAGENESIS OF RESIDUES

232-236 bIGFBP-2

5.1 Introduction

The C-terminal bIGFBP-2 deletion studies performed by Forbes *et al.* (1998) emphasized the importance of amino acids 222-236 for normal IGF binding activity. In Chapter 3, amino acids 221-230 were mutated, and a mutant library was screened by phage display. Characterisation of a mutant selected from this bIGFBP-2 library gave further evidence that amino acids in the region 221-230 were important for full IGF binding affinity (Section 4.5.1). However, the question still remained as to what role, if any, amino acids 231-236 would have in IGF binding function. To address this question, amino acid substitution studies were conducted and the mutant bIGFBP-2 molecules were characterised.

Due to the problems associated with the phage display system (Chapter 3), the roles of the amino acids were investigated using an alanine substitution approach. Because all cysteine residues in the C-terminal end of bIGFBP-2 have been shown to form disulphide bonds (Forbes *et al.*, 1998), to avoid any gross structural effects Cys231 was not mutated. Amino acids ^{232}KMSLN of bIGFBP-2 were sequentially mutated to alanine residues, and each mutant was expressed and purified for further characterisation.

Similar to the work described in Chapter 4, the IGF binding affinities of the mutated proteins were assessed using Western ligand blot and BIAcore™ analyses. The findings from these studies are discussed.

5.2 Materials

The restriction enzymes, *Cla* I and *Dpn* I were purchased from Amersham Pharmacia Biotech Pty Ltd (Castle Hill, NSW, Australia). *Stu* I and NEBuffer2 were obtained from New England Biolabs (Beverly, MA, USA). *Sma* I, *Xho* I, T4 DNA ligase, and the BresaSpin Gel Extraction kit (used to purify all DNA samples from agarose gel) were purchased from GeneWorks Ltd (Thebarton, SA, Australia). The Qiagen Plasmid Midi Kit (with Qiagen-tip 100) was purchased from Qiagen Pty Ltd (Clifton Hill, Vic., Australia). The plasmid pGF14 is described in Chapter 2 (Figure 2.4) and plasmid pGF8His is described in Figure 5.2. pBluescript® II KS+ was obtained from Stratagene, and pCH110 was purchased from Amersham Pharmacia Biotech Pty Ltd. The Stratagene® Quikchange™ site-directed

mutagenesis kit, polymerase *Pfu* and *Pfu* reaction buffer were obtained from Integrated Sciences (East Kew, Vic., Australia). All primers (crude purity) were synthesized by GeneWorks Ltd. Falcon tissue culture flasks (75 cm^2, 250 ml polystyrene flask, catalogue number 3111) and petri plates (100 x 20 mm polystyrene flask, catalogue number 3003) were sourced from Becton Dickson Labware (Franklin Lakes, NJ, USA). Dulbecco's Modified Eagle's Medium (DMEM), L-glutamine and trypsin were obtained from Gibco BRL (Glen Waverley, Vic., Australia). Insulin-transferrin-sodium selenite supplement (ITSS) was purchased from Roche Diagnostics (Sydney, NSW, Australia) and was prepared as described by the manufacturers. Gentamycin was from Pharmacia and Upjohn (Bentley, WA, Australia), trypan blue was obtained from Sigma Chemical Co. (St Louis, MO, USA), and foetal calf serum was purchased from Flow Laboratories (North Ryde, NSW, Australia). Filtration units (0.22 μm) for tissue culture medium were purchased from Millipore Corp. (Bedford, MA, USA). For transfection of mammalian cells, 0.4 cm gapped electroporation cuvettes and the Gene Pulser™ electroporation apparatus were purchased from Bio-Rad (Hercules, CA, USA). Potassium chloride was obtained from BDH Pty Ltd (Kilsyth, Vic., Australia). Salmon sperm DNA was obtained from Sigma Chemical Co. and was sheared both mechanically and by autoclave by Mr Mark Nezic (Department of Biochemistry, University of Adelaide). Mammalian expression medium was concentrated using an Amicon Bioseparations 8400 stirred ultrafiltration cell purchased from Adelab Scientific (Norwood, SA, Australia) containing a Pall Filtron disc membrane filter (type: Omega, 76 mm diameter with a 10 kDa nominal molecular weight cut-off; lot number 9172C), purchased from Crown Scientific Pty Ltd (Beverley, SA, Australia). Zymatrix Nickel-iminodiacetate (Ni-IDA) affinity resin was sourced from Bioserve (Heidleberg West, Vic., Australia), and an Econo-Pac column for Ni-IDA affinity resin was obtained from Bio-Rad. Nickel-nitrilotriacetate (Ni-NTA) conjugated to alkaline phosphatase was purchased from Qiagen Pty Ltd. The PE Brownlee™ Aquapore® C4 (100 x 10 mm) BU-300 column with 20 μm particles was sourced from Rainin LC and Supplies (Mulgrave, Vic., Australia). Imidazole and nickel sulphate were purchased from Sigma Chemical Co. KH_2PO_4 was obtained from May and Baker Australia Pty Ltd (West Footscray, Vic., Australia) and K_2HPO_4 was purchased from Ajax Chemicals (Sydney, NSW, Australia). The other chemicals, enzymes, and proteins used in this study are described in Sections 2.2, 3.2 and 4.2.

5.2.1 Buffers, solutions and media

The growth media (see below and Section 2.2.2) and antibiotic stocks were prepared by Mrs Jacquelyn Brinkman (Central Services Unit, Department of Biochemistry, University of Adelaide). Mammalian tissue culture medium DMEM and PBS (Section 2.2.2) were prepared by Mrs Jenny McLean (Department of Biochemistry, University of Adelaide). All solutions were made in redistilled water filtered using Milli-Q Ultra Pure Water System (Millipore Pty Ltd, North Ryde, NSW, Australia). Solutions marked (§) were sterilised by autoclaving.

Tissue culture media and buffers

Fantastic Terrific Broth (FTB) (§)
1.2% Bacto® tryptone, 2.4% Bacto® yeast extract, 0.4% glycerol
-after autoclaving, 17 ml 1 M KH_2PO_4 and 72 ml 1 M K_2HPO_4 was added to each litre of medium

1 litre Dulbecco's Modified Eagles Medium
DMEM (net weight, 13.4 g pack), 40 mM $NaHCO_3$, 20 mM HEPES, 0.012% (w/v) gentamycin
-adjusted to pH 7.5, and filter sterilised using 0.2 µm filter. Freshly supplemented with sterile 1 mM L-glutamine and 10% (v/v) FCS

1 litre Serum Free Medium
DMEM (net weight, 13.4 g pack), 40 mM $NaHCO_3$, 4.76 g HEPES, 0.12% gentamycin
-adjusted to pH 7.5, and filter sterilised using 0.2 µm filter. Freshly supplemented with sterile 1 mM L-glutamine, 0.01 mg/ml ITSS and 0.1 mM β-mercaptoethanol

Transfection buffer
20 mM HEPES, 137 µM NaCl, 5 mM KCl, 8 mM glucose
-adjusted to pH 7.0, filter sterilised using 0.2 µm filter and chilled to 4°C

Nickel chromatography solutions

8 x Binding buffer
40 mM imidazole, 4 M NaCl, 160 mM Tris
-adjusted to pH 7.9, and filtered using 0.45 µm filter

8 x Wash buffer
80 mM imidazole, 4 M NaCl, 160 mM Tris
-adjusted to pH 7.9, and filtered using 0.45 µm filter

4 x Elute buffer
2 M imidazole, 2 M NaCl, 80 mM Tris
-adjusted to pH 7.9, and filtered using 0.45 µm filter

4 x Strip buffer
400 mM EDTA, 2 M NaCl, 80 mM Tris
-adjusted to pH 7.9, and filtered using 0.45 µm filter

5.2.2 Bacterial strains

E. coli DH5α: *supE*44Δ*lac*U169(ϕ80*lacZ*ΔM15)*hsdR*17 *recA*1 *endA*1 *gyrA*96 *thi*-1 *relA*1

E. coli XL1-Blue cells are described in Section 3.2.2.

5.3 Methods

5.3.1 Quikchange™ site-directed mutagenesis to create amino acid substitutions at residues 232-236

For Quikchange™ site-directed mutagenesis, a fragment encoding the C-terminal end of bIGFBP-2 was cloned into the multiple cloning site of the plasmid pBluescript® II KS(+) (Stratagene® Integrated Sciences, Melbourne, Vic., Australia), to generate pBBP2. The fragment was obtained from phagemid pGF14 (Figure 2.4) by digestion with both *Stu* I and *Cla* I (using the conditions described by the enzyme suppliers). The plasmid pBluescript® II KS+ was cleaved with restriction enzymes *Cla* I and *Sma* I (using the conditions described by the enzyme suppliers). The 1.4 kilobase fragment encoding bIGFBP-2 and the 2.9 kilobase pBluescript® II KS+ fragment were resolved on agarose gel and purified. The fragments were ligated using the conditions described in Section 3.3.8, to generate the vector pBBP2.

The 3' end of the *bIGFBP-2* gene in plasmid pBBP2 was modified, to generate pBBP2mod (Figure 5.1). Using the BP2-SalI primer (Table 3.1) the *Sal* I restriction site was removed. This was performed to remove the additional valine and aspartate residues present at the C-terminal end of bIGFBP-2 (Figure 2.4). The PCR was performed in a 25 µl reaction containing 150 ng of primers BP2-SalI and SJHI (Table 3.1), 25 ng pBBP2 DNA, 0.25 mM dNTP, 1 x Pwo reaction buffer (with 2 mM $MgSO_4$) and 0.5 units Pwo polymerase. The reaction temperatures and cycling parameters, were those used for overlap extension PCR reaction in Section 3.3.4. The product of the PCR (327 base pairs) was resolved on agarose gel and purified. The PCR product and plasmid pBBP2 were digested using *BspE* I and *Pst* I (in 1 x NEBuffer3 in the presence of 0.1 mg/ml BSA, for 4.5 hours at 37°C). The cleaved PCR product (257 base pairs) and plasmid (4.1 kilobase) were resolved on agarose gel and purified. The purified fragments were ligated to form pBBP2mod in a final reaction volume of 18 µl, using the conditions described in Section 3.3.8. The ligation reaction was transformed

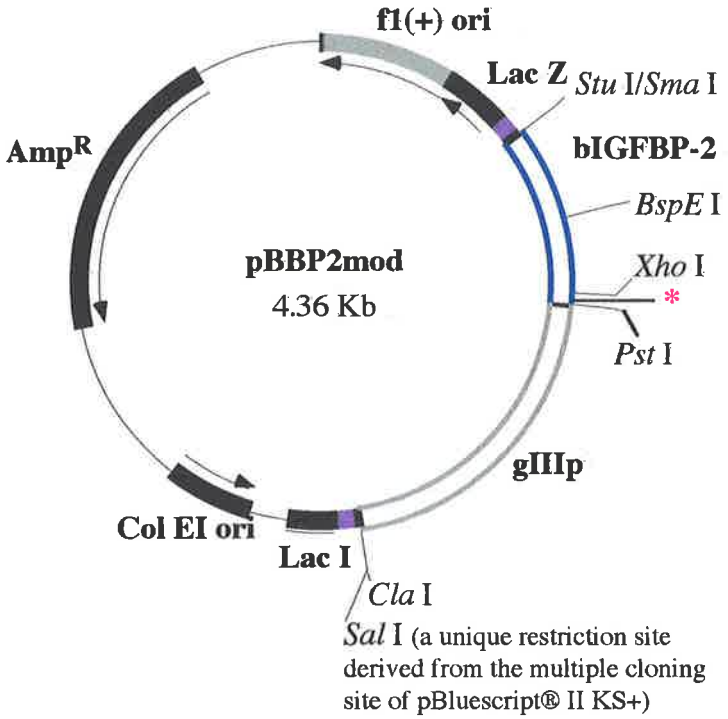

Figure 5.1 Plasmid pBBP2mod, used as a template for Quikchange™ mutagenesis to create the alanine substitution mutations in bIGFBP-2. The plasmid is a derivative of pBBP2 (Section 5.3.1). Plasmid pBBP2 was made by inserting a *Stu* I/*Cla* I fragment isolated from pGF14 (Figure 2.4) (3' end of bIGFBP-2 and the 5' end of gIIIp) into the multiple cloning site of pBluescript® II KS+ (coloured purple). The *Sal* I restriction site at the extreme 3' end of the bIGFBP-2 gene (*) was removed (Section 5.3.1) to generate pBBP2mod. Digestion with *BspE* I and *Xho* I enabled DNA encoding for the alanine mutations to be cloned into the mammalian expression vector, pGF8His (Figure 5.2).

into *E. coli* DH5α cells (Section 5.3.3). The sequence of the inserted DNA was confirmed using primers gIII and SJH1 (Table 3.1), and the method described in Section 3.3.12.

Quikchange™ mutagenesis was performed on vector pBBP2mod (Figure 5.1) using the procedure described in the Stratagene® instruction manual, with minor modifications. The primers for the mutagenesis reactions are described in Table 5.1. Each mutagenesis reaction contained 20 or 50 ng pBBP2mod plasmid, 125 ng of forward and reverse primer, 0.05 mM dNTPs, 1 x *Pfu* reaction buffer and 2.5 units *Pfu* polymerase in a final volume of 50 µl. The reactions were heated at 95°C for 30 seconds and were then cycled 18 times using the following parameters: 95°C for 30 seconds, 55°C for 1 minute and 68°C for 9 minutes. After cooling to 4°C, the pBBP2mod plasmid template was removed by digestion with 10 units of *Dpn* I overnight at 37°C. Each reaction (20 µl of the mutagenesis reaction) was transformed into 200 µl chemically competent *E. coli* XL1-Blue cells (Section 5.3.3). The DNA sequence of the clones was confirmed using primers SJH1 and gIII (Table 3.1, Section 3.3.12)

Primer	Sequence (5'-3')
forKA	CCTCAAACAGTGC**GCG**ATGTCTCTGAAC
revKA	GTTCAGAGACAT**CGC**GCACTGTTTGAGG
forMA	CAAACAGTGCAAG**GCG**TCTCTGAACGGG
revMA	CCCGTTCAGAGA**CGC**CTTGCACTGTTTG
forSA	CAGTGCAAGATG**GCG**CTGAACGGGCAG
revSA	CTGCCCGTTCAG**CGC**CATCTTGCACTG
forLA	GTGCAAGATGTCT**GCG**AACGGGCAGCGTG
revLA	CACGCTGCCCGTT**CGC**AGACATCTTGCAC
forNA	CAAGATGTCTCTG**GCG**GGGCAGCGTGGG
revNA	CCCACGCTGCCC**CGC**CAGAGACATCTTG
Vic2*	GCCTTCACACGCTAGGATT

Table 5.1 DNA primers used in sequencing, and in Quikchange™ mutagenesis to create amino acid substitutions at residues 232-236. For Quikchange™ mutagenesis, complementary primers were designed to create single alanine substitutions. The sense primers contain the prefix "for" and the antisense primers contain the prefix "rev". Primers containing the suffix KA, MA, SA, LA and NA were used to generate alanine substitutions at residues 232, 233, 234, 235 and 236 respectively. The nucleotides which were changed to alanines are marked in bold underlined text. * Primer Vic2 was designed by Dr Vicky Avery and is complementary to the DNA downstream of the 3' end of the *bIGFBP-2His* gene in the vector pGF8His.

5.3.2 Cloning the DNA encoding the alanine substitutions into pGF8His for mammalian expression

For protein expression, the alanine substitutions created in pBBP2mod were subcloned into the mammalian expression vector, pGF8His (Figure 5.2). The pBBP2mod and pGF8His constructs were each digested with *BspE* I and *Xho* I (using the conditions described by the manufacturer) to generate a 218 base pair and a 5.8 kilobase pair fragment respectively. The products were resolved on agarose gel and purified, and the fragments were ligated in final reaction volumes of 30 µl using the conditions described in Section 3.3.8. The ligations were transformed into chemically competent *E. coli* DH5α cells (Section 5.3.3). The identity of each clone was confirmed by DNA sequence analysis (Section 3.3.12), using the primers SJH1 (Table 3.1) and Vic2 (Table 5.1).

5.3.3 Chemically competent E. coli cells for transformation and maintenance of plasmid constructs

For maintenance and plasmid propagation, all plasmid constructs described in this chapter were transformed into chemically competent *E. coli* DH5α cells. For Quikchange™ mutagenesis, the reactions were transformed into chemically competent *E. coli* XL1-Blue cells. Chemically competent bacterial cells were prepared using the $CaCl_2$ method described in Sambrook *et al.* (1989). For transformation the procedures described in Sambrook *et al.* (1989) were followed. All batches of competent cells were transformed with known quantities of plasmid to determine the transformation efficiencies.

5.3.4 Medium scale preparation of DNA for transfection into COS-1 cells

Single colonies of *E. coli* DH5α cells containing the different plasmid constructs were used to inoculate 50 ml FTB (containing 100 µg/ml ampicillin). After overnight growth at 37°C, DNA was prepared from the cultures using the Qiagen Midi Plasmid kit (using the methods and solutions supplied by the manufacturer).

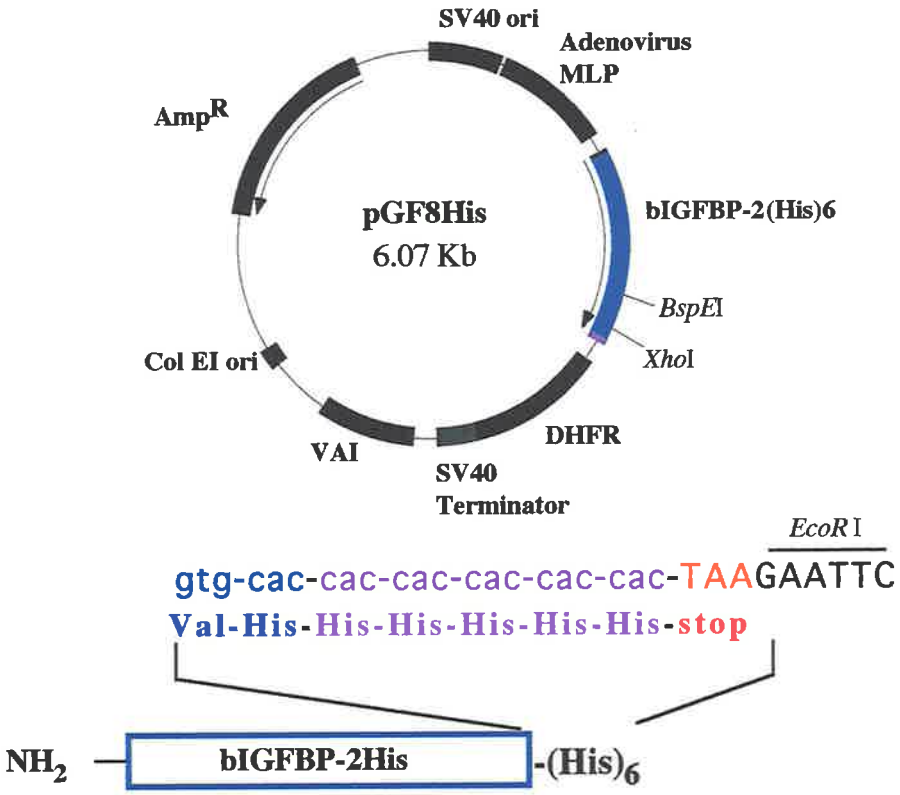

Figure 5.2 Plasmid pGF8His, used to express wild type bIGFBP-2His and bIGFBP-2His alanine mutants in COS-1 cells. The vector is a derivative of plasmid pGF8 (described in Forbes *et al.*, 1998), and was created by Ms Francine Carrick (Department of Biochemistry, University of Adelaide). To create pGF8His, the final 5 amino acids of bIGFBP-2 were mutated to histidine residues to generate a hexahistidine tag (the 6th to last amino acid is a histidine). The Colicin EI origin (Col EI ori) and β-lactamase ampicillin resitance gene (Amp^R) enabled pGF8His to be propagated in *E. coli*. Mammalian expression of bIGFBP-2His was under the regulation of the adenovirus major late promoter (MLP). The promoterless dihydrofolate reductase gene (DHFR) enhances mRNA stability and the SV40 origin of replication (SV40 ori) enables the plasmid to be replicated in mammalian cells. The adenoviral virus associated I RNA (VAI) suppresses the host cell's antiviral defence system, enabling translation and protein expression.

5.3.5 Mammalian cell transfection using electroporation

COS-1 cells were routinely maintained at 37°C in 5% CO_2 in DMEM culture medium. For protein expression, COS-1 cells were transiently transfected with either wild type or mutant pGF8His constructs using electroporation. To prepare electrocompetent cells, cells were grown in DMEM (Section 5.2.1) until they were approximately 80-90% confluent on the flask surface. Cells were washed 2 times in PBS and were then removed from the flasks by incubation in approximately 1 ml of 0.1% (w/v) trypsin for 5 minutes at room temperature (with gentle agitation to release the cells). Cells were resuspended in DMEM and were recovered by centrifuging at 1000 x g for 2 minutes at room temperature. The DMEM was removed and the cells were washed twice by resuspension in Transfection buffer (the cells were harvested between each wash as described above). Viable cell numbers were estimated by diluting a known volume of cells in trypan blue, and by counting the number of cells that remained unstained. After the second wash in Transfection buffer, cells were resuspended at a final concentration of 5 x 10^6 viable cells per 500 µl of Transfection buffer.

Transfections were performed using sterile pre-chilled electroporation cuvettes. Each cuvette contained 50 µl FCS, 50 µl sheared salmon sperm DNA (10 mg/ml) and 10-15 µg plasmid and 500 µl COS-1 cells. After mixing, the cuvettes were chilled at 4°C for 10 minutes, and were then subjected to a single electrical pulse (0.27 volts, 250 µF). After electroporation, the cuvettes were left at room temperature for 10 minutes, and the cells were then plated. In the small scale experiments, 5 x 10^6 cells were placed in 10 ml pre-warmed DMEM in a 10 cm petri dish. In larger scale experiments, 5 transfections were performed for each mutant construct, and the contents of each cuvette was placed in a 75 cm^2 culture flask containing 10 ml pre-warmed DMEM. After overnight growth, the growth medium was removed and cells were washed 2 times in PBS. Cells were then placed in pre-warmed serum-free medium (5 ml for petri plates, and 10 ml for 75 cm^2 flasks) for protein expression. In this medium, small scale transfections were grown overnight, after which medium was collected for analysis of protein expression. For larger scale experiments, the medium was collected (and 10 ml fresh serum-free medium was replaced daily) for a five day period before cells were discarded. Daily collections of medium were centrifuged to remove any contaminating cells and were stored frozen at -80°C in siliconised containers.

The efficiency of transfection was monitored by transfecting cells with a control vector, pCH110 which encodes β-galactosidase, and is described in the Amersham Pharmacia Biotech catalogue. After overnight incubation in serum-free medium, the cells were stained for β-galactosidase using the conditions described by Whyatt (1996). As a positive control for bIGFBP-2His expression, cells were transformed with the wild type pGF8His.

5.3.6 Purification and analysis of wild type and mutant bIGFBP-2His

bIGFBP-2His and mutant proteins were purified using nickel affinity chromatography and reverse phase HPLC. The guidelines described in the Novagen pET System Manual (6th Edition, 1995) were used to determine the optimal nickel affinity chromatography conditions. Optimisation of the conditions required for nickel affinity chromatography was performed using the wild type bIGFBP-2His protein. The optimal conditions are described below.

Frozen aliquots of conditioned medium (from each day of collection) were defrosted and pooled. The medium was adjusted to pH 7.9, and residual cell debris was removed by filtration through a 1 μm filter. The expression medium (250 ml) was concentrated 4- to 6-fold at 4°C by ultrafiltratration at 250 kPa using a nitrogen source.

In preparation for nickel affinity chromatography, Ni-IDA resin (the resin volume was approximately 1:15 of the volume of concentrated medium) was charged using 4 column volumes of 50 mM $NiSO_4$. The resin was equilibrated in 3 column volumes of Binding buffer, and then the concentrated medium was applied to the resin at room temperature by gravity flow. Non-specifically bound protein was washed away with 10 column volumes of Binding buffer, and then 6 column volumes of Wash buffer. Protein was eluted from the column using 6 column volumes of Elute buffer, and then the column was stripped by adding 5 column volumes of Strip buffer.

For HPLC purification, the Ni-IDA purified material was acidified by adding trifluoroacetic acid. The acidified sample was applied to a Brownlee Aquapore Butyl C4 (100 x 10 mm) column, previously pre-equilibrated with 25% HPLC buffer A and 75% HPLC buffer B (Section 2.2.1) at ambient temperature. Using both HPLC buffers A and B, the elution of bIGFBP-2His wild type and mutant samples was achieved using a linear gradient from 20-50% acetonitrile over 60 minutes at a flow rate of 1 ml/minute. The purified material

was lyophilised and stored at -20°C. The purity and quantity of each protein was determined using reverse phase HPLC as described in Section 2.3.5.

Both concentrated medium and purified protein were analysed on Coomassie stained 12.5% polyacrylamide gels (Section 2.3.4). For analysis of culture medium, 2 ml was concentrated using an Amicon Bioseparations Centricon® 10 centrifugal unit (using the methods described in the manual). The Western transfer, ligand and antibody blotting procedures used were those described in Sections 2.3.4 and 4.3.3. The blots probed with Ni-NTA (conjugated to alkaline phosphatase) were performed using the method described in the QIAexpress Ni-NTA conjugates manual (Qiagen).

Lyophilised samples of each bIGFBP-2His mutant (between 20-30 μg) were sent for analysis by electrospray mass spectrometry. The analysis was carried out on a Perkin Elmer SCI-EX API-300 triple quadrupole mass spectrometer at the Australian Research Council Electrospray Mass Spectrometry unit (Adelaide, Australia).

Samples of protein were sequenced as described in Section 2.3.5.

5.3.7 IGF binding analysis of the bIGFBP-2His mutants

Wild type bIGFBP-2, bIGFBP-2His and the alanine mutants were compared for IGF binding activity using Western ligand blot (Section 4.3.3) and BIAcore™ 2000 (Section 4.3.4) analysis.

5.4 Results

5.4.1 In vitro mutagenesis

To create the alanine substitutions in bIGFBP-2 using Quikchange™, the plasmid pBBP2 was constructed by ligating a *Stu* I/*Cla* I DNA fragment from pGF14 (including the region encoding amino acids 232-236 of bIGFBP-2) into the plasmid pBluescript® II KS+. The *bIGFBP-2* encoding fragment was then altered to remove the non-native extreme C-terminal valine and aspartate residues (created by a *Sal* I site) by PCR as described in the Section 5.3.1, to generate pBBP2mod (Figure 5.1). The identity of the clone was confirmed both by restriction digestion (Figure 5.3) and DNA sequence analysis.

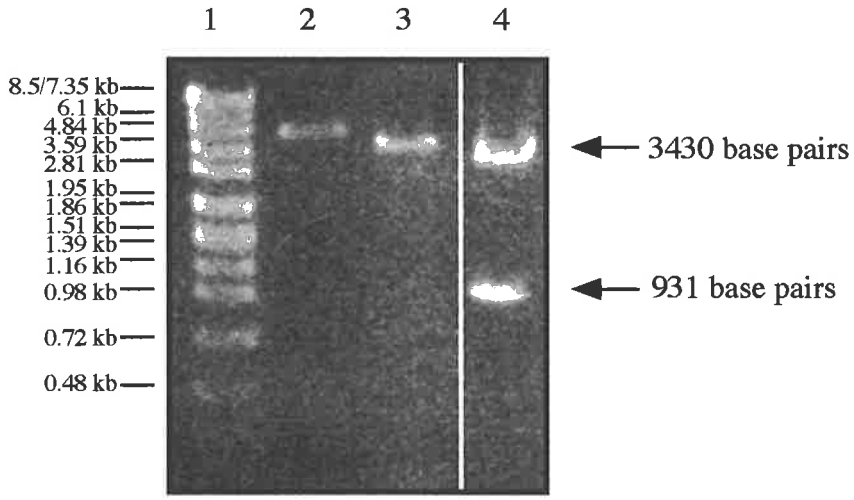

Figure 5.3 ***Sal*** **I restriction analysis of plasmid pBBP2mod used for Quikchange™ mutagenesis** . Lane 1 contains SPP1 molecular weight markers (the sizes are indicated to the left). Lane 2 contains undigested pBBP2mod. Lane 3 contains pBBP2mod linearised with*Sal* I restriction enzyme (4.36 kb), and lane 4 contains *Sal* I digested pBBP2 (the vector used to generate pBBP2mod). *Sal* I digestion of pBBP2 generated 2 fragments (marked with the arrows). The *Sal* I site at the 3' end of the *bIGFBP-2* gene was removed in the plasmid pBBP2mod (see Figure 5.1). pBBP2mod is linearised when digested with *Sal* I because it contains a single *Sal* I restriction site in the multiple cloning region derived from pBluescript® II KS+.

The primers designed to perform Quikchange™ mutagenesis are shown in Table 5.1. Forward and reverse primer pairs and pBBP2mod template were used in the DNA synthesis reactions. Parental pBBP2mod template was then removed by *Dpn* I digestion (restricts only the methylated DNA), and the remaining constructs were transformed into *E. coli* XL1-Blue cells. Each construct was confirmed by DNA sequence analysis and then a *BspE* I/*Xho* I segment of DNA (containing the alanine substitutions in bIGFBP-2) was subcloned into the mammalian expression vector, pGF8His. The plasmids pGF8His(KA), pGF8His(MA), pGF8His(SA), pGF8His(LA) and pGF8His(NA) were confirmed by DNA sequence analysis (Figure 5.4).

5.4.2 Expression and purification of mutant bIGFBP-2His proteins

Wild type bIGFBP-2His and the alanine mutants were expressed from the pGF8His vector by transient transfection into COS-1 cells. COS-1 cells were transformed with the plasmids by electroporation (Section 5.3.5). Using this procedure, the transformation efficiencies were estimated to be 1% (estimated by staining cells containing pCH110 for β-galactosidase). The expression of wild type and alanine mutant bIGFBP-2His proteins was first assessed in small scale expression experiments. The expression of each bIGFBP-2His analogue was confirmed both by SDS-PAGE and Western ligand blot analysis (Figure 5.5). The negative control lane in Figure 5.5, shows the low levels of endogenous monkey IGFBP-2 and IGFBP-3 which were expressed from these cells.

Larger scale transient transfections were performed (Section 5.3.5) to obtain sufficient quantities of the alanine mutant proteins for purification and characterisation. The media were harvested over 5 days and cells were then discarded. Cells expressing the different bIGFBP-2His alanine mutants over the 5 day period were morphologically indistinguishable from untransfected cells, or cells containing the pCH110 plasmid.

For protein purification, the conditioned medium was concentrated and applied to charged Ni-IDA affinity resin. Figure 5.6 shows both Ni-NTA and antibody blots of samples taken throughout the affinity purification of wild type bIGFBP-2His. As can be seen in Figure 5.6, bIGFBP-2 without the histidine tag does not bind to nickel (Ni-NTA blot, dot 17). Upon elution using 500 mM solution of imidazole, strong signals can be detected in both the Ni-NTA

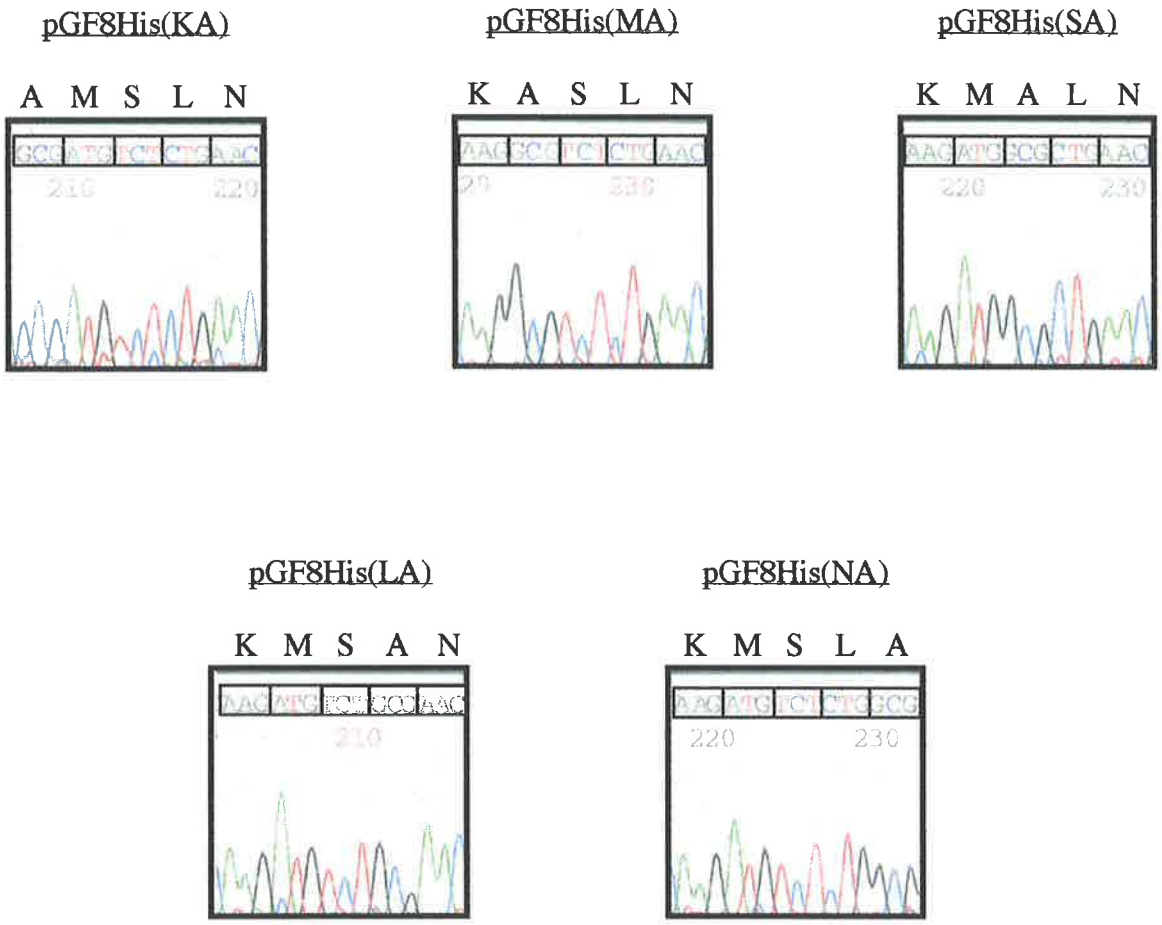

Figure 5.4 DNA sequence showing the presence of the alanine substitutions in the pGF8His mammalian expression plasmids. The DNA sequence was obtained using an internal bIGFBP-2 forward sequencing primer SJH1 (Table 2.1) and the method described in Section 3.3.12. The single letter amino acid codes above the DNA sequence data highlight the residues which were changed from the wild type sequence ^{232}KMSLN. Lys232Ala, Met233Ala, Ser234Ala, Leu235Ala and Asn236Ala are encoded for by pGF8His(KA), pGF8His(MA), pGF8His(SA), pGF8His(LA) and pGF8His(NA) repectively.

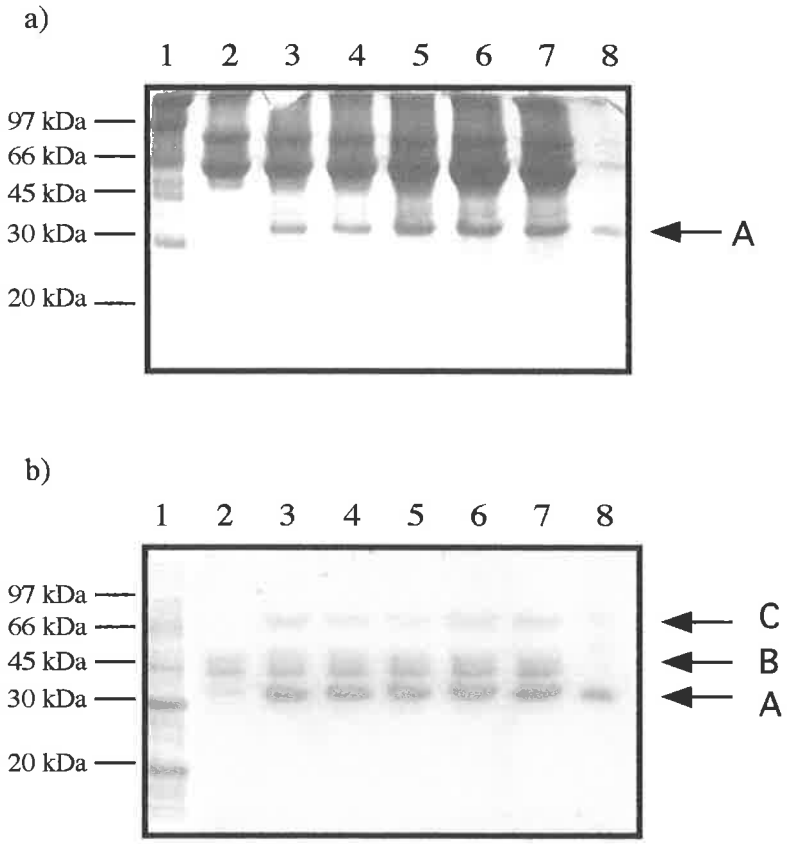

Figure 5.5 Small scale expression of wild type bIGFBP2His and the alanine mutants analysed by Coomassie stained 12.5% polyacrylamide gel, and ^{125}I IGF-II Western ligand blot.

a) Polyacrylamide gel containing concentrated conditioned medium from cells transfected with pCH110 (Lane 2), pGF8His(KA) (Lane 3), pGF8His(MA) (Lane 4), pGF8His(SA) (Lane 5), pGF8His(LA) (Lane 6) and pGF8His(NA) (Lane 7). Each lane contained the equivalent of 1 ml of conditioned medium. Lane 1 contains high-range [^{14}C] labelled Rainbow molecular weight markers (Amersham Pharmacia), and lane 8 contains 750 ng purified wild type bIGFBP-2His protein.

b) ^{125}I IGF-II ligand blot performed on a Western transfer of the gel described in (a). Band A represents full length bIGFBP-2His. The faint band observed in the negative control (lane 2) is endogenous monkey IGFBP-2. Band B represents endogenous monkey IGFBP-3, and band C corresponds with bIGFBP-2His dimer.

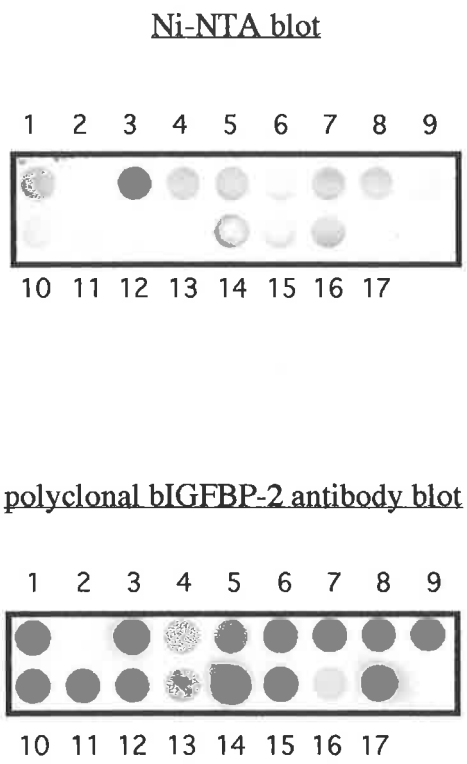

Figure 5.6 Analysis of the different fractions sampled during the nickel affinity purification of bIGFBP-2His. In this experiment, 70 ml of concentrated bIGFBP-2His containing medium was loaded onto 5 ml of Ni-IDA resin. The total load time for the medium was 40 minutes (by gravity flow). Each dot represents 500 μl of the fractions described below. Duplicate dot blots were prepared and probed with either Ni-NTA or polyclonal bIGFBP-2 antiserum. (1) Pooled COS-1 cell expression medium (total 250 ml unconcentrated); (2) concentrated medium- filtrate; (3) concentrated medium- retentate; (4) Ni-IDA column flow through at 15 minutes; (5) Ni-IDA column flow through at 25 minutes; (6) Bind buffer- wash 1; (7) Bind buffer- wash 2; (8) Bind buffer- wash 3; (9) Bind buffer- wash 4; (10) Bind buffer- wash 5; (11) Wash buffer- wash 1; (12) Wash buffer- wash 2; (13) Wash buffer- wash 3; (14) Eluted fractions 1-4 (pooled); (15) Eluted fractions 5 and 6 (pooled); (16) Strip buffer wash; (17) 500 ng bIGFBP-2 standard.

blot and the antibody blots (dots 14 and 15, Figure 5.6) corresponding to elution of bIGFBP-2His. After the elution, any protein still bound to the column was removed by performing the strip wash. Very little bIGFBP-2His protein was detected in this fraction (Figure 5.6, dot 16). The material eluted from the Ni-IDA columns was further purified using reverse phase HPLC. Figure 5.7 shows the HPLC profiles obtained for the different alanine mutants which had been purified using nickel affinity chromatography. Both wild type and mutant bIGFBP-2His proteins exhibited elution profiles from the HPLC column that were similar to those seen for bIGFBP-2. The retention times of the different mutant proteins were confirmed to be similar when samples were quantified using reverse phase HPLC (data not shown). The amounts of purified protein obtained for each of the pGF8His constructs is summarised in Table 5.2.

Protein	Quantity purified
pGF8His	280 µg
pGF8His(KA)	190 µg
pGF8His(MA)	160 µg
pGF8His(SA)	295 µg
pGF8His(LA)	168 µg
pGF8His(NA)	105 µg

Table 5.2 Summary of the quantities of purified bIGFBP-2His and alanine mutants obtained in this study. The proteins were purified using nickel affinity chromatography and reverse phase HPLC (Section 5.3.6), from 250 ml of conditioned medium. The quantities of protein were determined by HPLC (Section 2.3.5).

5.4.3 Characterisation of the alanine substituted bIGFBP-2His proteins

The purified proteins were analysed by Coomassie stained 12.5% non-reducing polyacrylamide gel (Figure 5.8). All proteins migrated as a single band, at the expected molecular weight. When the proteins were analysed by electrospray mass spectrometry, the mass observed for each mutant was within 0.03% of the predicted mass (Table 5.3). In the mass spectral analyses, each bIGFBP-2His sample was found to contain a protein that was approximately 355 mass units greater than the predicted mass for each bIGFBP-2His variant. N-terminal sequence analysis of purified mutants bIGFBP-2His(MA), bIGFBP-2His(SA) and bIGFBP-2His(LA) established that the contaminants were bIGFBP-2His variants containing the last 4 amino acids of the leader peptide sequence (the amino acids GARA). The quantities

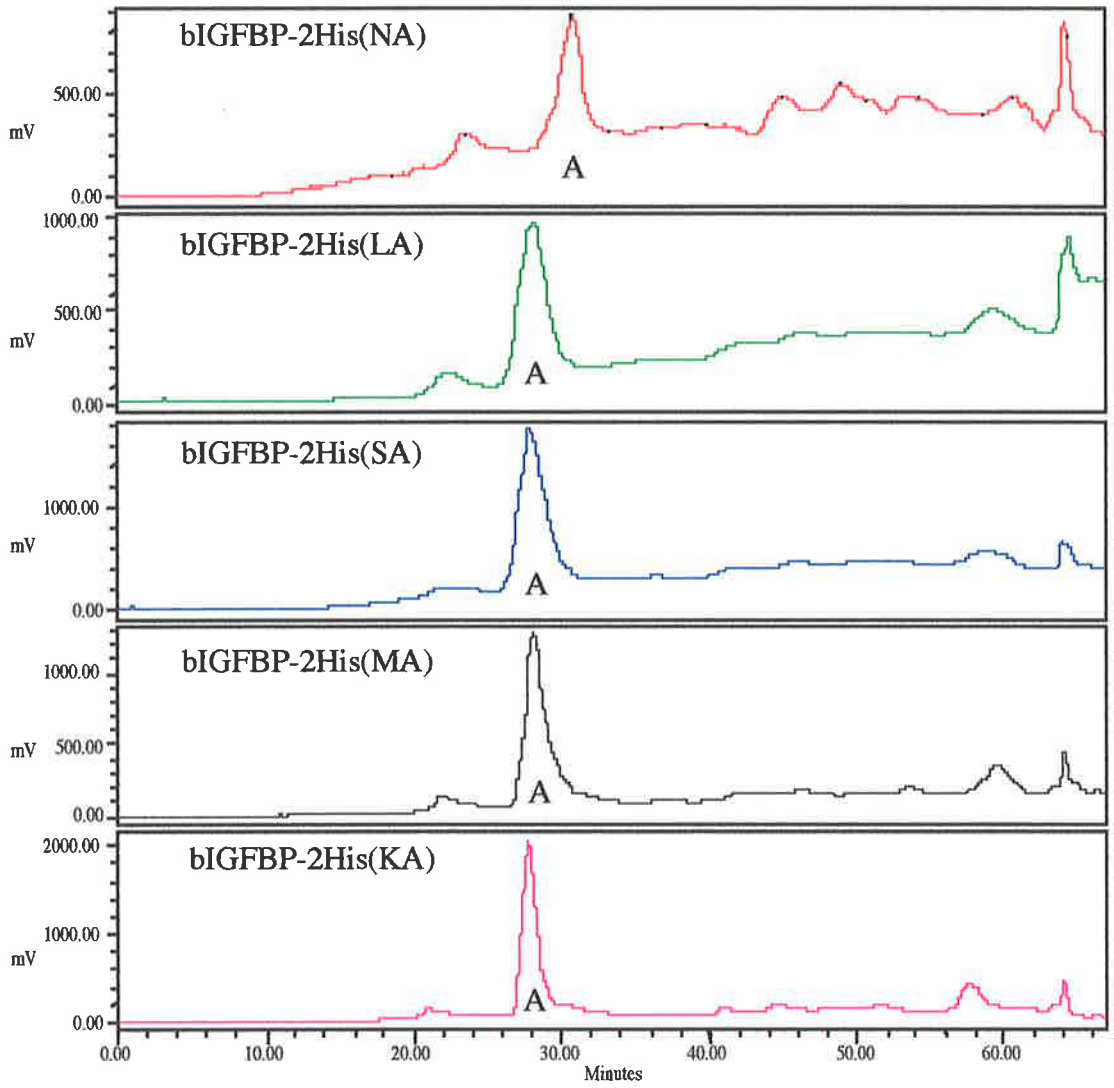

Figure 5.7 Reverse phase HPLC purification of the different bIGFBP-2His alanine mutants proteins. Fractions eluted from the nickel affinity columns were acidified and loaded onto the C4 HPLC column. Proteins were eluted using a 20-50% acetonitrile gradient over 60 minutes. The peaks marked A, correspond to the bIGFBP-2His alanine mutants.

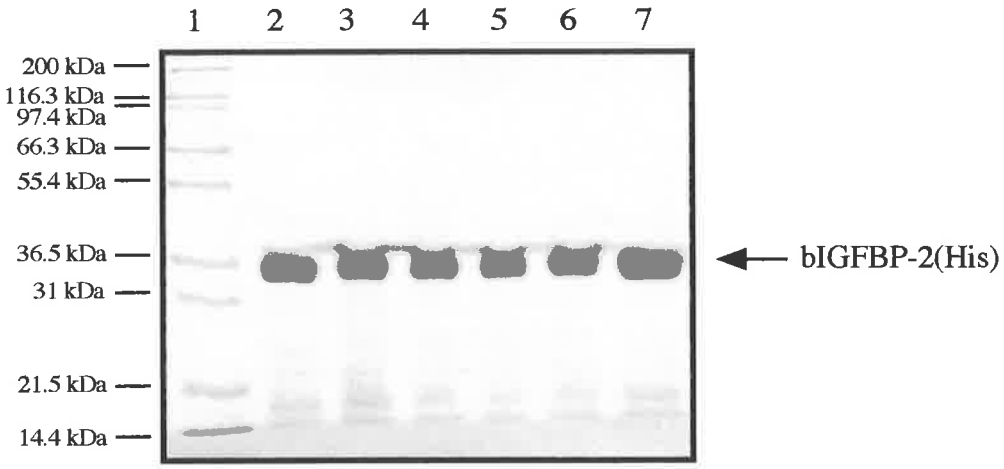

Figure 5.8 Analysis of the purified alanine bIGFBP-2His mutant proteins on a 12.5% Coomassie stained, non-reducing polyacrylamide gel. Lane 1 contains Novex™ Mark 12™ Wide range protein molecular weight markers. Lanes 2, 3, 4, 5, 6 and 7 contain 2 μg of purified bIGFBP-2His(KA), bIGFBP-2His(MA), bIGFBP-2His(SA), bIGFBP-2His(LA), bIGFBP-2His(NA) and wild type bIGFBP-2His protein.

of the contaminant were similar in each sample (observed in mass spectra and amino acid sequencing reactions), and were estimated to be approximately 30%.

Protein	Predicted Mass (Da)	Observed Mass (Da)
bIGFBP-2His	30815	30825
bIGFBP-2His(KA)	30760	30765
bIGFBP-2His(MA)	30757	30767
bIGFBP-2His(SA)	30801	30809
bIGFBP-2His(LA)	30775	30782
bIGFBP-2His(NA)	30774	30782

Table 5.3 Summary of the predicted and observed masses of the wild type and mutant bIGFBP-2 proteins. The observed masses were obtained by electrospray mass spectrometry (Section 5.3.6).

5.4.4 Western ligand blot analysis to examine the IGF binding activity of the alanine substituted bIGFBP-2His proteins

The IGF binding ability of the different alanine mutants was investigated by Western ligand blot (Figure 5.9). A comparison of the biotinylated IGF-I and mono-biotinylated IGF-II signal intensities observed for bIGFBP-2 and bIGFBP-2His showed that the proteins bound IGF with similar affinities. Furthermore, the alanine substitution mutants were unaffected in binding to either biotinylated IGF-I or mono-biotinylated IGF-II when compared to the bIGFBP-2His protein.

5.4.5 BIAcore™ analysis to examine the IGF binding activity of the alanine substituted bIGFBP-2His proteins

To further investigate the effects of the alanine substitutions on IGF binding activity, BIAcore™ experiments were performed as described in Section 4.3.4. A summary of the results are shown in Table 5.4. Analysis of the association and dissociation rates for bIGFBP-2 and bIGFBP-2His showed that there was no significant difference in their binding affinities for either IGF-I or IGF-II. Furthermore, the 30% bIGFBP-2His contaminant, containing the last four amino acids of the signal peptide (Section 5.4.3), did not affect the binding rates when compared to the rates observed from pure samples of bIGFBP-2 (the receptor grade standard purchased from Gropep). The alanine substitution mutants did not exhibit marked changes in their IGF binding affinities (Table 5.4). Analysis of the binding

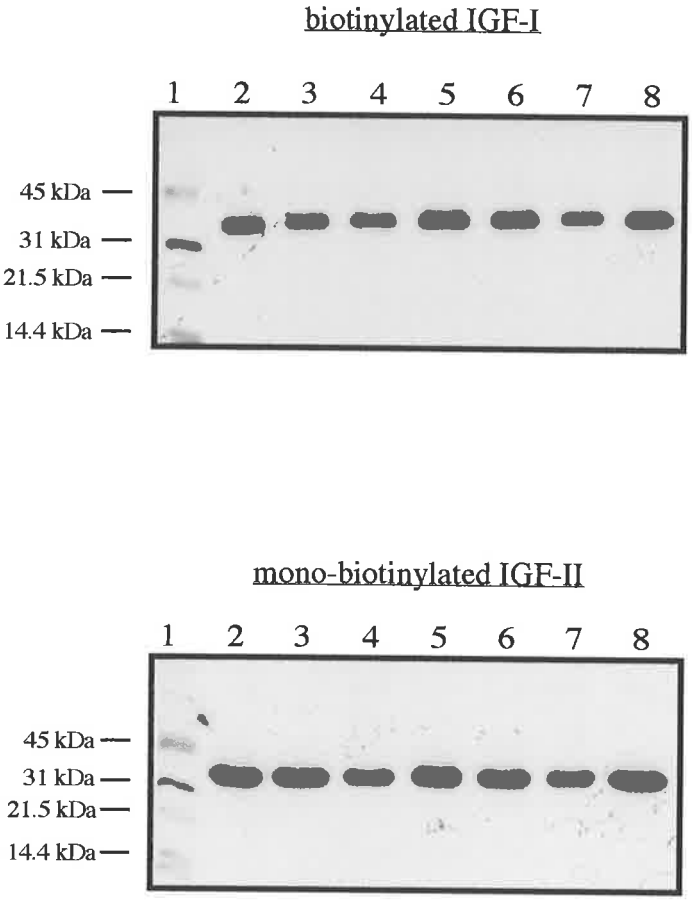

Figure 5.9 IGF binding analysis of the alanine bIGFBP2 mutant proteins using Western ligand blot. Duplicate blots were probed with either bIGF-I or bIGF-II. Lane 1 contains Bio-Rad Broad Range biotinylated protein molecular weight markers. Lanes 2 to 8 contain bIGFBP-2His(KA); bIGFBP-2His(MA); bIGFBP-2His(SA); bIGFBP-2His(LA); bIGFBP-2His(NA); bIGFBP-2His and wild type bIGFBP-2 protein. Following the ligand blot, the filters were probed with polyclonal bIGFBP-2 antibody. When the results of the immunoblots were used to standardise the amounts of binding protein present in each of the samples, there were no significant effects of the mutations on IGF binding activity (data not shown).

curves (Figure 5.10) and the ka1 association rates (Table 5.4) however did show subtle reductions in the association rates for the interaction of mutants bIGFBP-2His(SA) and bIGFBP-2His(LA) with both IGF-I and IGF-II. These reduced association rates were consistently observed for both mutants (Table 5.4). The same trends were also observed when the mutant proteins were injected over sensor chip surfaces coupled to either IGF-I or IGF-II.

IGF-I	ka1 x10^{5} (1/Ms)	ka2 x10^{-3} (1/s)	kd1 x10^{-2} (1/s)	kd2 x10^{-4} (1/s)	$K_{A(app)}$ x10^{9} [a] (1/M)	relative $K_{A(app)}$ [b]
bIGFBP-2	7.7±15%	6.3±11%	1.6±24%	3.8±4%	0.9	0.9
BP-2His	6.7±18%	7.3±6%	1.3±38%	3.9±8%	1.0	1.0
BP-2His(KA)	6.8±6%	7.7±8%	1.0±12%	2.8±8%	1.8	1.8
BP-2His(MA)	6.5±7%	6.6±7%	0.95±16%	3.2±7%	1.4	1.4
BP-2His(SA)	3.9±10%	10±9%	0.80±11%	3.3±8%	1.4	1.4
BP-2His(LA)	4.6±7%	9.3±10%	1.4±6%	3.2±28%	1.0	1.0
BP-2His(NA)	6.3±7%	6.8±5%	1.1±16%	2.7±29%	1.6	1.6

IGF-II	ka1 x10^{5} (1/Ms)	ka2 x10^{-3} (1/s)	kd1 x10^{-2} (1/s)	kd2 x10^{-4} (1/s)	$K_{A(app)}$ x10^{9} [a] (1/M)	relative $K_{A(app)}$ [b]
bIGFBP-2	11±18%	6.2±11%	1.8±46%	2.9±8%	1.3	0.6
BP-2His	9.5±13%	7.8±8%	1.5±29%	2.4±7%	2.1	1.0
BP-2His(KA)	8.8±10%	7.8±11%	1.0±22%	1.5±18%	4.2	2.0
BP-2His(MA)	9.4±8%	7.8±10%	1.2±22%	1.7±17%	3.7	1.7
BP-2His(SA)	5.2±21%	8.6±7%	0.78±36%	2.0±9%	3.0	1.4
BP-2His(LA)	7.1±16%	8.5±11%	1.6±13%	1.7±46%	2.8	1.3
BP-2His(NA)	10±12%	6.7±4%	1.42±20%	1.8±46%	2.8	1.3

Table 5.4 Summary of the kinetic rates derived from the interaction of IGF-I and IGF-II with immobilised bIGFBP-2, bIGFBP-2His and the alanine mutants. bIGFBP-2His is shown as BP-2His, and alanine mutants contain the prefix BP-2His and single letter codes showing the mutant protein identity. The kinetic rates were obtained using the two-state (conformational change) model (Section 4.3.4 and Appendix 1) and data analysis was performed on the 50 nM concentrations of IGF. The numbers are the means of the rates determined for 6 individual concentration curves, with the standard errors (at a 95% level of significance) for the association and dissociation rate values shown as a percentage of the mean.
a. The apparent affinity constant, $K_{A(app)}$, was obtained by calculating the following equation: $\frac{ka1}{kd1} x \frac{ka2}{kd2}$, where ka1 and ka2 represent the association rates, and kd1 and kd2 represent the dissociation rates (Appendix 1).
b. The relative $K_{A(app)}$ is the ratio:
$K_{A(app)}$(mutant bIGFBP-2His): $K_{A(app)}$(wild type bIGFBP-2His).

5.5 DISCUSSION

In this study, amino acids 232-236 of bIGFBP-2 were investigated by mutagenesis to determine their role in IGF binding activity. Single amino acid substitution mutants Lys232Ala, Met233Ala, Ser234Ala, Leu235Ala and Asn236Ala bIGFBP-2His were

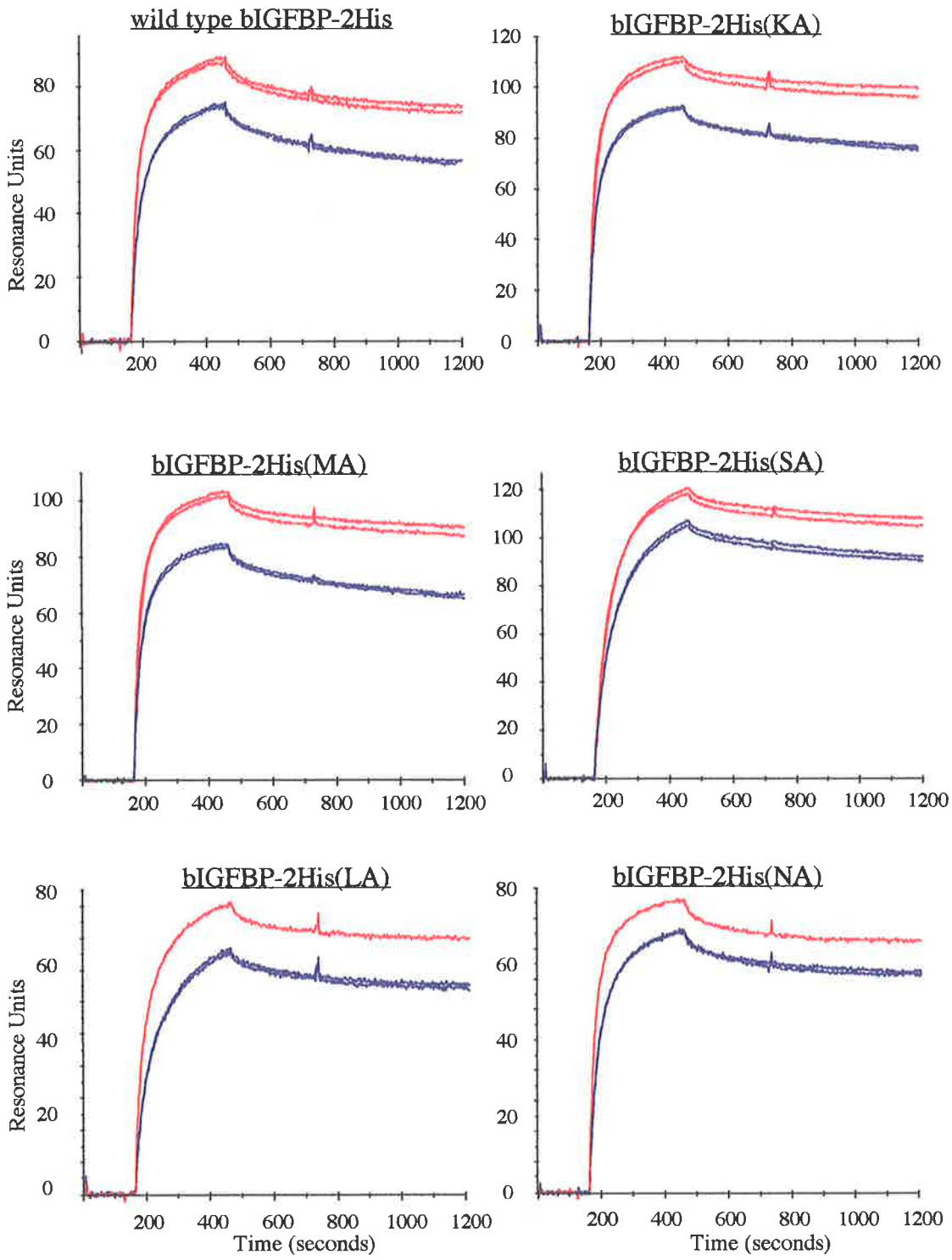

Figure 5.10 Sensorgrams of the binding of IGF-I and IGF-II to the different bIGFBP-2His wild type and alanine mutant coated sensor chips. In these examples, 50 nM IGF-I (___) and 50nM IGF-II (___) were injected over the binding protein surfaces at 50 µl/minute. Each sensor chip surface contains approximately 500 RU of coupled protein.

recombinantly expressed, purified and characterised for changes in affinities for IGF-I and IGF-II. Using both Western ligand blot and BIAcore™ analyses, there were no major effects on the affinity of the mutant molecules for both IGF-I and IGF-II. Analysis of the BIAcore™ data showed only subtle reductions in the IGF association rates for mutants bIGFBP-2His(SA) and bIGFBP-2His(LA). A reduced rate of association may suggest that the serine (which is conserved across all human binding proteins except for hIGFBP-4 which contains an alanine, Figure 1.4) and leucine residues may play minor roles in the interaction between bIGFBP-2 and the IGFs. Alternatively, changes to these residues may cause subtle structural changes to the protein which reduces the ability of IGF to associate with bIGFBP-2. As discussed in Section 4.5.1, in the absence of structural information it is difficult to predict the effects of these alanine substitutions. In future experiments, it would be interesting to combine the mutations Ser234Ala and Leu235Ala to see if the effects of the mutations are complementary.

Mutagenesis of human IGFBP-3 residues ^{228}KGRKR, to corresponding residues in human IGFBP-1, reduced IGF-II binding affinity 3-fold, with little effect on IGF-I (Firth *et al.*, 1998). As a result of this study it was suggested that this region made a minor contribution to the IGF binding site (Firth *et al.*, 1998). The corresponding amino acids in bIGFBP-2 are residues 235-239 (Figures 1.4 and 1.5), which partly overlap the region 232-236 that was investigated in this study. On their own, residues 235 and 236 of bIGFBP-2 were not found to have a major role in IGF binding activity. Also, the removal of positively charged residues in the same region in human IGFBP-5 (amino acids corresponding to bIGFBP-2 residues 232, 235, 237, 239) did not significantly affect the association constants for IGF-I determined by solution competition assays (Arai *et al.*, 1996a). The IGF-II binding effects of the human IGFBP-5 mutants were not examined by Arai *et al.* (1996a), but their results for IGF-I confirm the current findings.

In the past, purification of bIGFBP-2 from COS-1 cell conditioned medium involved a three step procedure, required to remove endogenous monkey IGFBP-2 and IGFBP-3 (Forbes *et al.*, 1998). In this study, a two step nickel affinity chromatography and reverse phase HPLC procedure generated pure preparations of binding protein that were free from contaminating monkey binding proteins. Nickel affinity chromatography was possible because the proteins studied here contained C-terminal hexahistidine tags. The hexahistidine tags were

created by the substitution of the final 5 amino acids of bIGFBP-2 for histidines (the 6th to last amino acid is a histidine, Figure 5.2). In addition to providing a useful handle for purifying bIGFBP-2 protein, in the wild type background the hexahistidine tag did not significantly affect the IGF binding activity of the protein. These results confirm the findings of the deletion studies by Forbes *et al.* (1998) which showed that the C-terminal 14 residues were not important for IGF binding activity. Furthermore, in this study the histidine tag did not noticeably reduce the levels of bIGFBP-2His protein expression from COS-1 cells, relative to the untagged bIGFBP-2 protein (Hobba, 1999).

As discussed in Section 4.5.1, protein tags may be useful in BIAcore™ studies to immobilise proteins in a single orientation. Proteins immobilised in a single orientation can reduce possible ligand heterogeneity, a phenomenon which can arise from amine coupling and can affect binding data interpretation. Although the histidine tag was useful for purification of bIGFBP-2His from culture medium, its use for immobilisation of bIGFBP-2 onto BIAcore™ sensor chip surfaces has been shown to be limited because the IGF analyte binds even more tightly to the bIGFBP-2His than does the latter to the Ni-NTA chip (personal communication with Dr Briony Forbes, Department of Biochemistry, University of Adelaide). The relatively low affinity of the hexahistidine tag for Ni-NTA sensor chip surfaces may possibly be improved by using longer histidine sequences. Nieba *et al.* (1997) showed that proteins which contained a single hexahistidine tag dissociated rapidly from Ni-NTA sensor chip surfaces ($K_D \approx 10^{-6}$ M). In their study, Nieba *et al.* (1997) demonstrated that it was necessary to have at least 12 histidine residues to efficiently immobilise proteins using this procedure. To use such a tag though, it would be necessary to ensure that the addition of further histidine residues would have no impact on the IGFBP to bind to IGF.

N-terminal sequence analysis and mass spectrometry revealed that all bIGFBP-2His and alanine mutant preparations possessed two forms of the binding protein. Approximately 70% of the protein in all the preparations consisted of bIGFBP-2His with the expected N-terminal sequence (Glu-Val-Leu-Phe-Arg). The remaining 30% of the protein contained N-terminal sequence corresponding to the last 4 residues of the bIGFBP-2 leader sequence (Bourner *et al.*, 1992), and the first residue of mature bIGFBP-2 (Gly-Ala-Arg-Ala-Glu). This alternative form of binding protein has been observed in preparations of bIGFBP-2 obtained by

COS-1 cell expression (Hobba, 1999). Prediction of the signal peptide cleavage points in bIGFBP-2 (Hobba, 1999) suggests that this longer form of bIGFBP-2 represents an alternatively processed form of the protein. The amount of this alternatively processed form of bIGFBP-2 has been shown to vary between 5% and 30% of the final protein preparation (Dr Briony Forbes, personal communication). In this study, the presence of approximately 30% of the GARA-bIGFBP-2His form was not found to change the kinetic rates observed for binding to either IGF-I or IGF-II, relative to a pure preparation of bIGFBP-2. Therefore this suggests that the GARA N-terminal extension on bIGFBP-2 does not affect IGF binding activity.

In this study, single alanine substitutions to residues 232-236 were not found to have a major effect on the IGF binding activity of bIGFBP-2. Therefore, in the 222-236 bIGFBP-2 deletion mutant of Forbes *et al.* (1998), it would appear that the loss of residues 232-236 was not responsible for the large drop in IGF binding activity. The results described in Chapter 4 and evidence in the literature (discussed in Section 4.5.1) would suggest that the effects of the deletion mutant were mostly a result of losing amino acids 221-230.

Chapter Six

FINAL DISCUSSION

6.1 General Summary

This thesis describes the use of amino acid substitution studies to assess the role of residues 221 to 236 in bIGFBP-2 for IGF binding activity. As discussed throughout this thesis, residues 221 to 236 were selected for analysis because C-terminal deletions studies performed on bIGFBP-2 had identified these residues as important IGF binding determinants (Forbes *et al.*, 1998). A phage display approach (Chapter 2) was used to screen a mutant bIGFBP-2 library containing amino acid substitutions at residues 221 to 230. As described in Chapter 3, after four rounds of panning on IGF-II ligand, there were no clear sequence preferences to suggest which residues were important for the ability of bIGFBP-2 to bind IGF. One interesting observation from the panning experiments was the selection against negatively charged amino acids in this region of the protein. This was particularly interesting when a mutant, 4.17B (characterised in Chapter 4) which had the following amino acid substitutions: Lys222Met, His223Gly, Leu228Gln and Lys229Glu, was found to have a reduced IGF binding activity. A reduced IGF binding activity, as a result of the amino acid substitutions, may explain the low numbers of negatively charged residues which remained after the phage panning procedures.

The finding that mutant 4.17B had a reduced ability to bind the IGFs, supports the results of the deletion studies performed by Forbes *et al.* (1998). Furthermore, alanine substitutions to amino acids 232 to 236 (Chapter 5) showed that these residues did not have a major role in IGF binding activity. In conclusion, these studies show that bIGFBP-2 amino acids in the region 221 to 230, and not 232 to 236, contain determinants which confer normal IGF binding activity.

6.2 A structural model for the C-terminal end of bIGFBP-2

NMR studies have only recently been used to define a structure for an N-terminal IGF binding fragment of IGFBP-5 (amino acids 40 to 92, Kalus *et al.*, 1998). However, information regarding the structure of the central and C-terminal regions of the binding proteins remains to be determined.

Interestingly, amino acid sequence alignments have shown that the C-terminal ends of the IGFBPs have homology to the thyroglobulin type-1 domain (Rechler, 1993; Guncar *et al.*, 1999). Based on this homology, it has been suggested that proteins containing this domain will share a common fold (Guncar *et al.*, 1999). During the course of this PhD, an X-ray crystal structure was published for the MHC class II-associated p41 Ii fragment, which had sequences typical of a thyroglobulin type-1 domain (Guncar *et al.*, 1999). In this paper, Guncar *et al.* published a sequence alignment which compared the p41 Ii fragment to other proteins, including human IGFBP-1 and IGFBP-3. This information was used to create a sequence alignment between the p41 Ii fragment and bIGFBP-2 (bIGFBP-2 amino acids Arg183 to Phe268; Figure 6.1). From this sequence alignment a structural model for the C-terminal end of bIGFBP-2 was constructed (Figure 6.2). The model was created using the HOMOLOGY module of the INSIGHT II software (version 98.0, MSI, San Diego), with the assistance of Dr Terry Mulhern (Department of Biochemistry and Molecular Biology, Unversity of Melbourne, Parkville, Vic., Australia). The regions of bIGFBP-2 which had no corresponding residues in the p41 fragment (denoted by the gaps in the p41 fragment sequence in Figure 6.1) are shown as extended loop structures (for example amino acids 196 to 211 of bIGFBP-2, Figure 6.2). In support for this model, the predicted disulphide bonding pattern is the same as that defined for the C-terminal cysteine residues in bIGFBP-2, and for the other binding proteins (Section 1.4.4).

In Figure 6.2, the region assessed by phage display is shown in green. The amino acids which were substituted in mutant 4.17B (amino acids 222, 223, 228 and 229) and were shown to be required for full IGF binding activity, are circled in red. On the structural model, these amino acids are located on a loop on one face of the protein segment (Figure 6.2). In contrast, the amino acids 232 to 236 which were not found to have a significant role in the IGF binding activity of bIGFBP-2, are located on a loop on the opposite face of the protein segment. The predicted C-terminal structure of bIGFBP-2 (Figure 6.2) therefore supports the findings from this study.

Furthermore, amino acid substitution studies in rat IGFBP-5, found that changes to the conserved Gly203 and Gln209 residues also affected IGF binding activity (Bramani *et al.*, 1999; Song *et al.*, 2000). When these residues were mapped onto the bIGFBP-2 C-terminal

Figure 6.1 Sequence alignment of p41 Ii and the equivalent C-terminal region in bIGFBP-2. The sequence alignment was based on the alignments created by Guncar *et al.* (1999). Residues in the bIGFBP-2 sequence which were modelled to the X-ray coordinates of p41 Ii (Guncar *et al.*, 1999) are marked *. The different secondary structural elements include: β-strands (*B*), α-helices (*H*), β-bridges (isolated interstrand H-bonds) (*b*), and turns (*T*). Gaps (-) were inserted into the p41 fragment sequence where there were no residues corresponding to bIGFBP-2 amino acids. These gap regions are shown as extended loop structures in Figure 6.2.

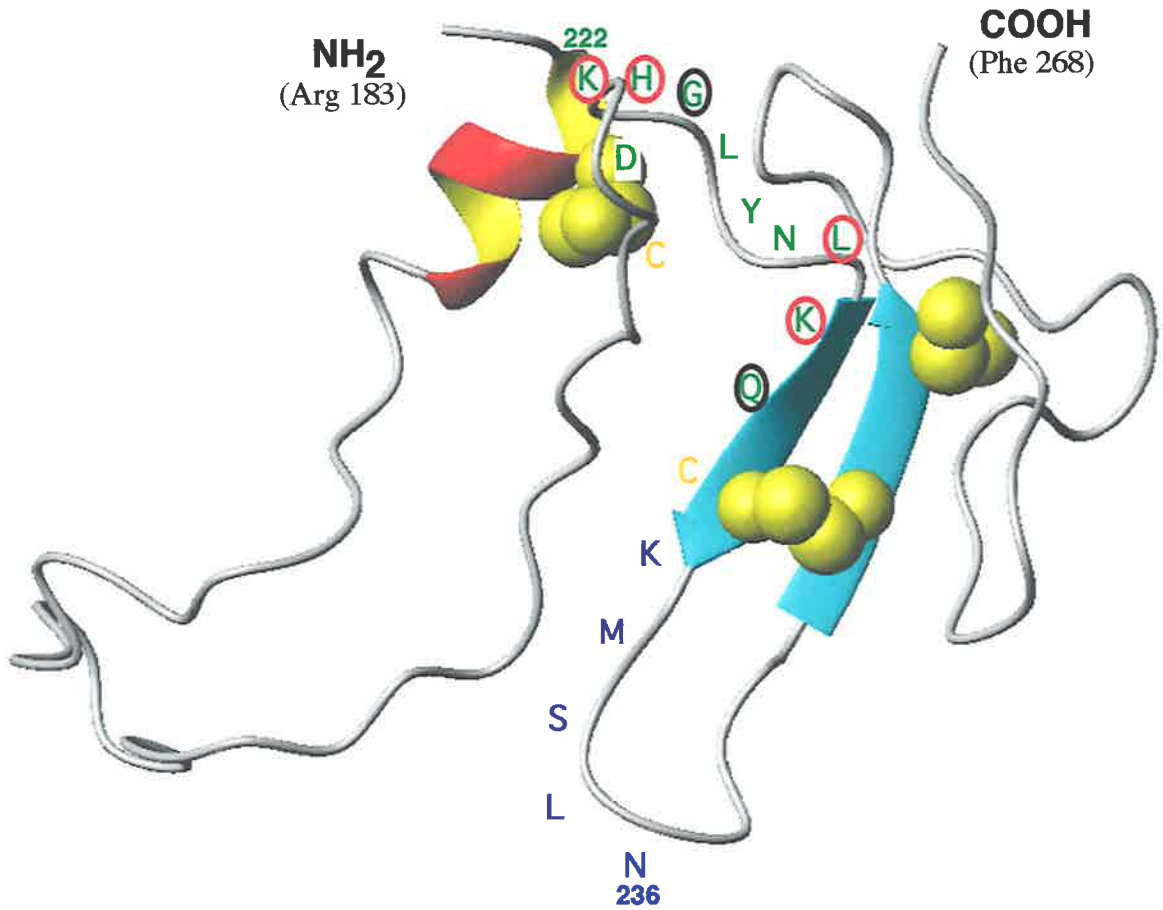

Figure 6.2 A structural model for the C-terminal end of bIGFBP-2. The model was generated from the sequence alignment of p41 Ii, a fragment of the MHC class II with homology to the thyroglobulin type-1 domain (Guncar *et al.*, 1999) (Figure 6.1). The location of the regions mutated in this study are shown in single letter amino acid letter code. The residues studied by phage display (Chapter 3) are shown in green. The residues changed in mutant 4.17B are circled in red. The amino acids mutated in human IGFBP-5 which affected IGF binding activity (Song *et al.*, 2000), are circled in black. The residues studied by alanine screen (Chapter 5) are marked in blue. The cysteine residues are marked in yellow, and disulphide bonded pairs are shown. This figure was created using MOLMOL (Koradi *et al.*, 1996).

model (Figure 6.2, circled in black), the amino acids were found to cluster to the region 221 to 230. These findings may suggest that the corresponding region in IGFBP-5, and possibly all 6 binding proteins, are similarly involved in IGF binding activity. This is supported by a high degree of sequence similarity in this amino acid stretch of the 6 human IGFBPs (Figure 1.4).

Limited amounts of purified mutant 4.17B (Chapter 4), made it difficult to determine whether structural changes to the protein were responsible for a reduction in IGF binding activity. Based on the model in Figure 6.2, it is possible that substitution of Lys229, could have disrupted the structure of the first β-strand and thus affected IGF binding function. To test this, it would be necessary to perform single amino acid substitution and structural studies such as those discussed in Section 4.5.1.

6.3 Considerations for future experiments

As discussed in Section 4.5.2 the use of BIAcore™ to analyse the interaction between bIGFBP-2 and the IGFs, highlighted the need to determine the mechanism by which binding proteins interact with both IGF-I and IGF-II. The results of this study suggest that the bIGFBP-2 and the IGFs may interact by a two-state reaction mechanism, whereby bIGFBP-2 undergoes conformational change. In the literature, bIGFBP-2 has been suggested to change its conformation when bound to IGF (see Section 4.5.2). However, further studies are required to confirm this. Conformational change of bIGFBP-2 may be assessed by using different biophysical techniques. For example, as discussed in Section 4.5.1 the lone Trp243 in bIGFBP-2 could be used to perform tryptophan fluorescence studies to detect changes in the structure of the binding protein in the presence of the IGF. Using this approach, Forbes *et al.* (2000) have preliminary results which suggest that tryptophan fluorescence studies may be useful to monitor changes to the structure of bIGFBP-2. Another way to assess changes to the conformation of the binding protein would be to conduct proteolytic studies, whereby the binding protein was proteolysed in the presence and absence of IGF. Such an approach has been used effectively to demonstrate the structural differences that exist between apo- and holo-myoglobin (Fontana *et al.*, 1997). A third approach could be to use NMR to detect changes to the structure of the binding protein when IGF is bound. However, an NMR approach is currently limited because it would rely on structural information for bIGFBP-2, which is

currently unavailable. A knowledge of the binding mechanism would enable the determination of more accurate kinetic rates for the IGF-IGFBP interaction. This would allow for better comparisons to be made between the kinetic rates determined in different laboratories, where currently different binding models are being used to estimate association and dissociation rates.

In addition to determining the mechanism by which the different binding proteins interact with the IGFs, the studies on the binding proteins would greatly benefit from more detailed structural knowledge. The knowledge of the IGFBP structure could be used to predict other amino acids which may be accessible for interacting with the IGFs. The structural knowledge could be also used to understand the effects of substitutions such as those created in this study. With recent NMR structural studies performed on N-terminal fragments of IGFBP-5 (Kalus *et al.*, 1998), and with the determination of the disulphide bonding pattern for the different IGFBPs (Section 1.4.4), the field is broadening in this direction. Knowing the structure of the C-terminal end of the binding protein family will also contribute to understanding the thyroglobulin type-1 domain folds, and whether an amino acid sequence can be a good predictor of protein structure.

We are still in the early stages of defining the residues on the binding proteins which are needed to enable IGF binding activity. Therefore studies are still required to isolate other regions of the binding proteins which confer IGF binding activity. In addition to using a deletion strategy like that used by Forbes *et al.* (1998), chemical modification approaches similar to the one used by Hobba *et al.* (1996) could be further pursued. A chemical modification strategy is ideal because such an approach does not depend on knowledge of a protein structure. Furthermore, it is possible to express sufficient amounts of wild type bIGFBP-2 to perform these studies. Hobba *et al.* (1996) iodinated tyrosine residues in bIGFBP-2 in the presence and absence of the IGFs. Using this approach they defined an N-terminal region of bIGFBP-2, which was confirmed by subsequent alanine substitution studies (Hobba *et al.*, 1998), to have a role in IGF binding activity. By targeting other amino acids, using different modifying reagents, it will be possible to generate more information about the IGF binding site. Alternative chemical modification approaches may include a non-specific modification strategy such as that used by Scaloni *et al.* (1999). Using methyl bromide, which was found to modify a range of amino acids and a mass spectrometry-Edman degradation

approach, Scaloni *et al.* (1999) could identify residues on deoxy-haemoglobin which interacted with 2,3-diphosphoglycerate. It would also be interesting to target positively charged residues in the binding proteins. For example, the negatively charged Glu3 of IGF-I (and Glu6 of IGF-II) is known to be important for the interaction of IGF with the binding proteins (Section 1.5.1). To assess the role of arginine residues in this interaction, the reagent phenylglyoxal could be used. A study by Wood *et al.* (1998) identified arginine residues in the active site of creatine kinase using a combination of phenylglyoxal modification and high resolution tandem mass spectrometry. Similarly, lysines could be assessed by using lysine modifying reagents such as 2,4,6-trinitrobenzene sulphonic acid (TNBS). There are currently many different types of chemical reagents which are commercially available which could be used to map the binding site of the IGF on the IGFBPs.

An alternative to chemical modification strategies is the deuterium exchange approach described by Ehring (1998). In that study, Ehring demonstrated the effectiveness of this approach by analysing residues on IGF-I which interact with IGFBP-1. In the first step, hydrogen/deuterium exchange was performed on both the IGF and IGFBP. The two proteins were allowed to form a complex, and then the deuterium was back exchanged with hydrogen. The backbone amide groups that participated in the interaction between the two proteins remained deuterated, and could be identified by proteolysis and mass spectrometry (Ehring, 1998).

Following chemical modification or hydrogen/deuterium exchange studies, it would be possible to define the critical IGF binding residues by substituting the amino acids for alanines (or by using conservative amino acid substitutions). The critical residues could then be targeted for further study using a phage display approach. In future studies, the problems associated with the bIGFBP-2 phage display system could be overcome by using the modifications described in Section 3.5. The problems associated with the phage display system may also be reduced if smaller numbers of amino acids are mutated and analysed.

In conclusion, recent studies show that binding proteins have functions other than binding to IGF (Section 1.4.1). A greater knowledge of the IGF binding site on the binding proteins will aid in further defining the IGF independent roles of the binding proteins. This could be investigated by removing the IGF binding site on IGFBPs, and looking at the function

of these proteins both *in vitro* and *in vivo*. Furthermore, a greater understanding of how IGFBPs bind to and control IGF action may aid in the development of IGF as a therapeutic agent. As discussed in Section 1.1, currently there is concern for the development of IGF to treat different physiological states because of the association of high levels of IGFs with cancers. This concern could be circumvented if we were better able to control IGF activity.

Chapter Seven

REFERENCES

Adams, S., Rosen, D. & Sommer, A. (1998). rhIGF-I/IGFBP-3 (somatokine) therapy for the treatment of osteoperosis. In *Molecular mechanisms to regulate the activities of insulin-like growth factors.* (Takano, K., Hizuka, N. & Takahashi, S. I., eds.), pp. 327-330. Elsevier, Amsterdam.

Arai, T., Parker, A., Busby, W. & Clemmons, D. R. (1994). Heparin, heparan sulfate, and dermatan sulfate regulate formation of the insulin-like growth factor-I and insulin-like growth factor-binding protein complexes. *J. Biol. Chem.* **269**(32), 20388-20393.

Arai, T., Clarke, J., Parker, A., Busby, W., Jr., Nam, T. & Clemmons, D. R. (1996a). Substitution of specific amino acids in insulin-like growth factor (IGF) binding protein-5 alters heparin binding and its change in affinity for IGF-I in response to heparin. *J. Biol. Chem.* **271**(11), 6090-6106.

Arai, T., Busby, W., Jr. & Clemmons, D. R. (1996b). Binding of insulin-like growth factor (IGF) I or II to IGF-binding protein-2 enables it to bind to heparin and extracellular matrix. *Endocrinology* **137**(11), 4571-4575.

Arany, E., Zabel, P., Freeman, D. & Hill, D. J. (1993). Elimination of radiolabelled recombinant human insulin-like growth factor binding protein-3 from the circulation, and its distribution amongst organs and tissues in adult male rats. *Regul. Pept.* **48**, 133-143.

Armstrong, J., Perham, R. N. & Walker, J. E. (1981). Domain structure of bacteriophage fd adsorption protein. *FEBS lett.* **135**(1), 167-172.

Bach, L. A., Thotakura, N. R. & Rechler, M. M. (1992). Human insulin-like growth factor binding protein-6 is O-glycosylated. *Biochem. Biophys. Res. Commun.* **186**(1), 301-307.

Bach, L. A., Hsieh, S., Sakano, K. I., Fujiwara, H., Perdue, J. F. & Rechler, M. M. (1993). Binding of mutants of human insulin-like growth factor-II to insulin-like growth factor binding proteins 1-6. *J. Biol. Chem.* **268**(13), 9246-9254.

Bach, L. A. (1999). The insulin-like growth factor system: basic and clinical aspects. *Aust. N.Z. J. Med.* **29**, 355-361.

Bagley, C. J., May, B. L., Szabo, L., McNamara, P. J., Ross, M., Francis, G. L., Ballard, F. J. & Wallace, J. C. (1989). A key functional role for the insulin-like growth factor-I amino-terminal pentapeptide. *Biochem. J.* **259**(3), 665-672.

Ballard, F. J., Wallace, J. C., Francis, G. L., Read, L. C. & Tomas, F. M. (1996). Des(1-3)IGF-I: a truncated form of insulin-like growth factor-I. *Int. J. Biochem. Cell. Biol.* **28**(10), 1085-1087.

Bar, R. S., Boes, M., Clemmons, D. R., Busby, W. H., Sandra, A., Dake, B. L. & Booth, B. A. (1990a). Insulin differentially alters transcapillary movement of intravascular IGFBP-1, IGFBP-2 and endothelial cell IGF-binding proteins in the rat heart. *Endocrinology* **127**(1), 497-499.

Bar, R. S., Clemmons, D. R., Boes, M., Busby, W. H., Booth, B. A., Dake, B. L. & Sandra, A. (1990b). Transcapillary permeability and subendothelial distribution of endothelial and amniotic fluid insulin-like growth factor binding proteins in the rat heart. *Endocrinology* **127**(3), 1078-1086.

Barbas, C. F. I., Kang, A. S., Lerner, R. A. & Benkovic, S. J. (1991). Assembly of combinatorial antibody libraries on phage surfaces: the gene III site. *Proc. Natl. Acad. Sci. U.S.A.* **88**, 7978-7982.

Barbas, C., Bain, J., Hoekstra, D. & Lerner, R. (1992). Semisynthetic combinatorial antibody libraries: a chemical solution to the diversity problem. *Proc. Natl. Acad. Sci. U.S.A.* **89**, 4452-4461.

Baserga, R., Resnicoff, M. & Dews, M. (1997). The IGF-I receptor and cancer. *Endocrine* **7**(1), 99-102.

Bass, S., Greene, R. & Wells, J. A. (1990). Hormone phage: an enrichment method for variant proteins with altered binding properties. *Proteins* **8**(4), 309-314.

Bastian, S. E. P., Walton, P. E. & Belford, D. A. (2000). Transport of circulating IGF-I and LR^3IGF-I from blood to extracellular wound fluid sites in rats. *J. Endocrinol.* **164**, 77-86.

Baxter, R. C. (1994). Insulin-like growth factor binding proteins in the human circulation: a review. *Horm. Res.* **42**, 140-144.

Bayne, M. L., Applebaum, J., Chicchi, G. G., Hayes, N. S., Green, B. G. & Cascieri, M. A. (1988). Structural analogs of human insulin-like growth factor-I with reduced affinity for serum binding proteins and the type-2 insulin-like growth factor receptor. *J. Biol. Chem.* **263**(13), 6233-6239.

Beekwilder, J., Rakonjac, J., Jongsma, M. & Bosch, D. (1999). A phagemid vector using the *E. coli* phage shock promoter facilitates phage display of toxic proteins. *Gene* **228**(1-2), 23-31.

Binkert, C., Lanwehr, J., Mary, J.-L., Schwander, J. & Heinrich, G. (1989). Cloning, sequence analysis and expression of a cDNA encoding a novel insulin-like growth factor binding protein-2 (IGFBP-2). *EMBO J.* **8**(9), 2497-2502.

Binoux, M. & Hossenlopp, P. (1988). Insulin-like growth factor (IGF) and IGF-binding proteins: comparison of human serum and lymph. *J. Clin. Endocrinol. Metab.* **67**(3), 509-514.

Binoux, M., Lalou, C., Mohseni-Zadeh, S., Angelloz-Nicoud, P., Daubas, C. & Babajko, S. (1998). Proteolytic fragments of IGF binding protein-3: physiological significance. In *Molecular mechanisms to regulate the activities of insulin-like growth factors.* (Takano, K., Hizuka, N. & Takahashi, S. I., eds.), pp. 99-106. Elsevier, Amsterdam.

Birnbacher, R., Amann, G., Breitschopf, H., Lassmann, H., Suchanek, G. & Heinz-Erian, P. (1998). Cellular localization of insulin-like growth factor-II mRNA in the human fetus and the placenta: detection with digoxigenin-labeled cRNA probe and immunocytochemistry. *Pediatr. Res.* **43**(5), 614-620.

Blundell, T. L., Bedarkar, S. & Humbel, R. E. (1983). Tertiary structures, receptor binding, and antigenicity of insulin-like growth factors. *Fed. Proc.* **42**(9), 2592-2597.

Boeke, J. D. & Model, P. (1982). A prokaryotic membrane anchor sequence: carboxyl terminus of bacteriophage f1 *gene III* protein retains it in the membrane. *Proc. Natl. Acad. Sci. U.S.A.* **79**, 5200-5204.

Boes, M., Booth, B. A., Sandra, A., Dake, B. L., Bergold, A. & Bar, R. S. (1992). Insulin-like growth factor binding protein (IGFBP) 4 accounts for the connective tissue distribution of endothelial cell IGFBPs perfused through the isolated heart. *Endocrinology* **131**(1), 327-330.

Bordo, D. & Argos, P. (1991). Suggestions for "safe" residue substitutions in site-directed mutagenesis. *J. Mol. Biol.* **217**, 721-729.

Boublik, Y., Di Bonito, P. & Jones, I. M. (1995). Eukaryotic virus display: engineering the major surface glycoprotein of the *Autographa californica* nuclear polyhedrosis virus (AcNPV) for the presentation of foreign proteins on the virus surface. *Biotechnology N.Y.* **13**(10), 1079-1084.

Bourner, M. J., Busby, W. H. J., Siegel, N. R., Krivi, G. G., McCusker, R. H. & Clemmons, D. R. (1992). Cloning and sequence determination of bovine insulin-like growth factor binding protein-2 (IGFBP-2): comparison of its structural and functional properties with IGFBP-1. *J. Cell. Biochem.* **48**(2), 215-226.

Bramani, S., Song, H., Beattie, J., Tonner, E., Flint, D. J. & Allan, G. J. (1999). Amino acids within the extracellular matrix (ECM) binding region (201-218) of rat insulin-like growth factor binding protein (IGFBP)-5 are important determinants in binding IGF-I. *J. Mol. Endocrinol.* **23**(1), 117-123.

Braulke, T. (1999). Type-2 IGF receptor: a multi-ligand binding protein. *Horm. Metab. Res.* **31**(2-3), 242-246.

Brinkman, A., Kortleve, D. J., Schuller, A. G. P., Zwarthoff, E. C. & Drop, S. L. S. (1991a). Site-directed mutagenesis of the N-terminal region of IGF binding protein-1: analysis of IGF binding capability. *FEBS lett.* **291**(2), 264-268.

Brinkman, A., Kortleve, D. J., Zwarthoff, E. C. & Drop, S. L. S. (1991b). Mutations in the carboxyl-terminal part of insulin-like growth factor (IGF)-binding protein-1 result in dimer formation and loss of IGF binding capacity. *Mol. Endocrinol.* **5**(7), 987-994.

Brown, A. L. & Rechler, M. M. (1990). Cloning of the rat insulin-like growth factor-binding protein-2 gene and identification of a functional promoter lacking a TATA box. *Mol. Endocrinol.* **4**(12), 2039-2051.

Brown, S. (1992). Engineered iron oxide-adhesion mutants of the *Escherichia coli* phage lambda receptor. *Proc. Natl. Acad. Sci. U.S.A.* **89**, 8651-8655.

Byun, D., Mohan, S., Kim, C., Suh, K., Yoo, M., Lee, H., Baylink, D. J. & Qin, X. (2000). Studies on human pregnancy-induced insulin-like growth factor (IGF)-binding protein-4 proteases in serum: determination of IGF-II dependency and localization of cleavage site. *J. Clin. Endo. Metab.* **85**(1), 373-381.

Camacho-Hubner, C., Woods, K. A., Miraki-Moud, F., Clark, A. J. & Savage, M. O. (1999). Insulin-like growth factor-I deficiency caused by a partial deletion of the IGF-I gene: effects of rhIGF-I therapy. *Growth Horm. IGF Res.* **9**(Supp B), 47-52.

Canziani, G., Zhang, W., Cines, D., Rux, A., Willis, S., Cohen, G., Eisenberg, R. & Chaiken, I. (1999). Exploring biomolecular recognition using optical biosensors. *Methods* **19**, 253-269.

Carter, P., Nilsson, B., Burnier, J. P., Burdick, D. & Wells, J. A. (1989). Engineering subtilisin BPN' for site specific proteolysis. *Proteins* **6**, 240-248.

Causin, C., Waheed, A., Braulke, T., Junghans, U., Maly, P., Humbel, R. E. & von Figura, K. (1988). Mannose 6-phophate/insulin-like growth factor II-binding proteins in human serum and urine. *Biochem. J.* **252**, 795-799.

Ceda, G. P., Fielder, P. J., Henzel, W. J., Louie, A., Donovan, S. M., Hoffman, A. R. & Rosenfeld, R. G. (1991). Differential effects of insulin-like growth factor (IGF)-I and IGF-II on the expression of IGF binding proteins (IGFBPs) in a rat neuroblastoma cell line: isolation and characterization of two forms of IGFBP-4. *Endocrinology* **128**(6), 2815-2824.

Charbit, A., Sobczak, E., Michel, M. L., Molla, A., Tiollais, P. & Hofnung, M. (1987). Presentation of two epitopes of the preS2 region of hepatitis B virus on live recombinant bacteria. *J. Immunol.* **139**(5), 1658-1664.

Chernausek, S. D., Smith, C. E., Duffin, K. L., Busby, W. H., Wright, G. & Clemmons, D. R. (1995). Proteolytic cleavage of insulin-like growth factor binding protein-4 (IGFBP-4): localization of cleavage site to non-homologous region of native IGFBP-4. *J. Biol. Chem.* **270**(19), 11377-11382.

Chuang, S. E., Chen, A. L. & Chao, C. C. (1995). Growth of *E. coli* at low temperature dramatically increases the transformation frequency by electroporation. *Nucleic Acids Res.* **23**(9), 1641.

Clackson, T. & Wells, J. A. (1994). *In vitro* selection from protein and peptide libraries. *Trends Biotechnol.* **12**(5), 173-184.

Clairmont, K. B. & Czech, M. P. (1989). Chicken and Xenopus mannose 6-phosphate receptors fail to bind insulin-like growth factor-II. *J. Biol. Chem.* **264**(28), 16390-16392.

Clemmons, D. R., Dehoff, M. L., Busby, W. H., Bayne, M. L. & Cascieri, M. A. (1992). Competition for binding to insulin-like growth factor (IGF) binding protein-2, -3, -4, and -5 by the IGFs and IGF analogs. *Endocrinology* **131**(2), 890-895.

Clemmons, D. R., Busby, W. H., Winter, S. & Moralez, A. (1999). Complement 1s is an IGFBP-5 protease that is synthesized and secreted by fibroblasts and smooth muscle cells and regulates IGFBP-5 actions. *Growth Horm. IGF Res.* **9**(5), 317.

Click, E. M. & Webster, R. E. (1997). Filamentous phage infection: required interactions with the TolA protein. *J. Bacteriol.* **179**(20), 6464-6471.

Cohen, P., Graves, H. C. B., Peehl, D. M., Kamarei, M., Giudice, L. C. & Rosenfeld, R. G. (1992). Prostate-specific antigen (PSA) is an insulin-like growth factor binding protein-3 protease found in seminal plasma. *J. Clin. Endocrinol.* **75**(4), 1046-1053.

Cohick, W. S. & Clemmons, D. R. (1993). The insulin-like growth factors. *Annu. Rev. Physiol.* **55**, 131-153.

Conover, C. A., Kiefer, M. C. & Zapf, J. (1993). Posttranslational regulation of insulin-like growth factor binding protein-4 in normal and transformed human fibroblasts: insulin-like growth factor dependence and biological studies. *J. Clin. Invest.* **91**(3), 1129-1137.

Conover, C. A. & Kiefer, M. C. (1993). Regulation and biological effect of endogenous insulin-like growth factor binding protein-5 in human osteoblastic cells. *J. Clin. Endocrinol. Metab.* **76**(5), 1153-1159.

Conover, C. A. & De Leon, D. D. (1994). Acid-activated insulin-like growth factor-binding protein-3 proteolysis in normal and transformed. *J. Biol. Chem.* **269**(10), 7076-7080.

Conover, C. A., Durham, S. K., Zapf, J., Masiarz, F. R. & Kiefer, M. C. (1995). Cleavage analysis of insulin-like growth factor (IGF)-dependent IGF-binding protein-4 proteolysis and expression of protease-resistant IGF-binding protein-4 mutants. *J. Biol. Chem.* **270**(9), 4395-4400.

Conover, C. A. (1998). IGFBP regulation by proteases. In *Molecular mechanisms to regulate the activities of insulin-like growth factors.* (Takano, K., Hizuka, N. & Takahashi, S. I., eds.), pp. 107-114. Elsevier, Amsterdam.

Cooke, R. M., Harvey, T. S. & Campbell, I. D. (1991). Solution structure of human insulin-like growth factor-I: a nuclear magnetic resonance and restrained molecular dynamics study. *Biochemistry* **30**(22), 5484-5491.

Cordes, C., Meima, R., Twiest, B., Kazemier, B., Venema, G., van Dijl, J. M. & Bron, S. (1996). The expression of a plasmid-specified exported protein causes structural plasmid instability in *Bacillus subtilis*. *J. Bacteriol.* **178**(17), 5235-5242.

Coverley, J. A. & Baxter, R. C. (1995). Regulation of insulin-like growth factor (IGF) binding protein-3 phosphorylation by IGF-I. *Endocrinology* **136**(12), 5778-5781.

Coverley, J. A. & Baxter, R. C. (1997). Phosphorylation of insulin-like growth factor binding proteins. *Mol. Cell. Endocrinol.* **128**(1-2), 1-5.

Crissman, J. W. & Smith, G. P. (1984). Gene-III protein of filamentous phages: evidence for a carboxyl-terminal domain with a role in morphogenesis. *Virology* **132**, 445-455.

Cull, M. G., Miller, J. F. & Schatz, P. J. (1992). Screening for receptor ligands using large libraries of peptide linked to the C-terminus of the lac repressor. *Proc. Natl. Acad. Sci. U.S.A.* **89**, 1865-1869.

Cunningham, B. C., Lowe, D. G., Li, B., Bennett, B. C. & Wells, J. A. (1994). Production of an atrial natriuretic peptide variant that is specific for type A receptor. *EMBO J.* **13**(11), 2508-2515.

Cwirla, S. E., Peters, E. A., Barrett, R. W. & Dower, W. J. (1990). Peptides on phage: a vast library of peptides for identifying ligands. *Proc. Natl. Acad. Sci. U.S.A.* **87**, 6378-6382.

D'Ercole, A. J., Stiles, A. D. & Underwood, L. E. (1984). Tissue concentrations of somatomedin C: further evidence for multiple sites of synthesis and paracrine or autocrine mechanisms of action. *Proc. Natl. Acad. Sci. U.S.A.* **81**, 935-939.

Dai, Z., Xing, Y., Boney, C. M., Clemmons, D. R. & D'Ercole, A. J. (1994). Human insulin-like growth factor-binding protein-1 (hIGFBP-1) in transgenic mice: characterization and insights into the regulation of hIGFBP-1 expression. *Endocrinology* **135**(4), 1316-1327.

Dall'Acqua, W. & Carter, P. (1998). Antibody engineering. *Curr. Opin. Struct. Biol.* **8**, 443-450.

De Vroede, M. A., Rechler, M. M., Nissley, S. P., Joshi, S., Burke, G. T. & Katsoyannis, P. G. (1985). Hybrid molecules containing the B-domain of insulin-like growth factor-I are recognized by carrier proteins of the growth factor. *Proc. Natl. Acad. Sci. U.S.A.* **82**, 3010-3014.

DeChiara, T. M., Efstratiadis, A. & Robertson, E. J. (1990). A growth-deficiency phenotype in heterozygous mice carrying an insulin-like growth factor-II gene disrupted by targeting. *Nature* **345**, 78-80.

Delhanty, P. J. & Han, V. K. (1992). The characterization and expression of ovine insulin-like growth factor-binding protein-2. *J. Mol. Endocrinol.* **9**(1), 31-38.

Delhanty, P. J. D. & Han, V. (1993). An RGD to RGE mutation in the putative membrane binding domain of IGFBP-2 inhibits its potentiation of IGF-II induced thymidine uptake by SCP cells. *Program of the 75th Annual Meeting of The Endocrine Society*, Abstract 22:56.

Devi, G. R., Byrd, J. C., Slentz, D. H. & MacDonald, R. G. (1998). An insulin-like growth factor-II (IGF-II) affinity-enhancing domain localized within extracytoplasmic repeat 13 of the IGF-II/mannose 6-phosphate receptor. *Mol. Endocrinol.* **12**(11), 1661-1672.

Dore, S., Kar, S. & Quirion, R. (1997). Rediscovering an old friend, IGF-I: potential use in the treatment of neurodegenerative diseases. *Trends Neurosci.* **20**(8), 326-331.

Dotto, G. P., Enea, B. & Zinder, N. D. (1981). Functional analysis of bacteriophage f1 intergenic region. *Virology* **114**(2), 463-473.

Dower, W. J., Miller, J. F. & Ragsdale, C. W. (1988). High efficiency transformation of *E. coli* by high voltage electroporation. *Nucleic Acids Res.* **16**(13), 6127-6145.

Duan, C., Ding, J., Li, Q., Tsai, W. & Pozios, K. (1999). Insulin-like growth factor binding protein-2 is a growth inhibitory protein conserved in zebrafish. *Proc. Natl. Acac. Sci. U.S.A.* **96**(26), 15274-15279.

Dubaquie, Y. & Lowman, H. B. (1999). Total alanine-scanning mutagenesis of insulin-like growth factor I (IGF-I) identifies differential binding epitopes for IGFBP-1 and IGFBP-3. *Biochemistry* **38**(20), 6386-6396.

Ehring, H. (1999). Hydrogen exchange/electrospray ionization mass spectrometry studies of structural features of proteins and protein/protein interactions. *Anal. Biochem.* **267**, 252-259.

Engstrom, W., Shokrai, A., Otte, K., Granerus, M., Gessbo, A., Bierke, P., Madej, A., Sjolund, M. & Ward, A. (1998). Transcriptional regulation and biological significance of the insulin like growth factor-II gene. *Cell. Prolif.* **31**(5-6), 173-189.

Feld, S. & Hirschberg, R. (1996). Growth hormone, the insulin-like growth factor system, and the kidney. *Endocr. Rev.* **17**(5), 423-480.

Firth, S. M., Ganeshprasad, U. & Baxter, R. C. (1998). Structural determinants of ligand and cell surface binding of insulin-like growth factor-binding protein-3. *J. Biol. Chem.* **273**(5), 2631-2638.

Firth, S. M. & Baxter, R. C. (1999). Characterisation of recombinant glycosylation variants of insulin-like growth factor binding protein-3. *J. Endocrinol.* **160**(3), 379-387.

Florini, J. R., Ewton, D. Z. & Coolican, S. A. (1996). Growth hormone and the insulin-like growth factor system in myogenesis. *Endocr. Rev.* **17**(5), 481-517.

Fontana, A., Zambonin, M., de Laureto, P. P., De Filippis, V., Clementi, A. & Scaramella, E. (1997). Probing the conformational state of apomyoglobin by limited proteolysis. *J. Mol. Biol.* **266**, 223-230.

Forbes, B., Szabo, L., Baxter, R. C., Ballard, F. J. & Wallace, J. C. (1988). Classification of the insulin-like growth factor binding proteins into three distinct categories according to their binding specificities. *Biochem. Biophys. Res. Commun.* **157**, 196-202.

Forbes, B. E., Turner, D., Hodge, S. J., McNeil, K. A., Forsberg, G. & Wallace, J. C. (1998). Localization of an insulin-like growth factor (IGF) binding site of bovine IGF binding protein-2 using disulfide mapping and deletion mutation analysis of the C-terminal domain. *J. Biol. Chem.* **273**(8), 4647-4652.

Forbes, B. E., Turner, D., Parkinson, E. J., Lucic, M. R. & Wallace, J. C. (2000). *To be presented at the IGFBP2000 4th International Workshop on IGF Binding Proteins, Terrigal, NSW, Australia.*

Forrer, P., Jung, S. & Pluckthun, A. (1999). Beyond binding: using phage display to select for structure, folding and enzymatic activity in proteins. *Curr. Opin. Struct. Biol.* **9**(4), 514-520.

Forsberg, G., Baastrup, B., Rondahl, H., Holmgren, E., Pohl, G., Hartmanis, M. & Lake, M. (1992). An evaluation of different enzymatic cleavage methods for recombinant fusion proteins, applied on des(1-3)insulin-like growth factor-I. *J. Protein Chem.* **11**(2), 201-211.

Forsberg, G., Forsgren, M., Jaki, M., Norin, M., Sterky, C., Enhorning, A., Larsson, K., Ericsson, M. & Bjork, P. (1997). Identification of framework residues in a secreted recombinant antibody fragment that control production level and localization in *Escherichia coli*. *J. Biol. Chem.* **272**(19), 12430-12436.

Fowlkes, J. & Freemark, M. (1992). Evidence for a novel insulin-like growth factor (IGF)-dependent protease regulating IGF-binding protein-4 in dermal fibroblasts. *Endocrinology* **131**(5), 2071-2076.

Fowlkes, J. L. & Serra, D. M. (1996). Characterization of glycosaminoglycan-binding domains present in insulin-like growth factor-binding protein-3. *J. Biol. Chem.* **271**(25), 14676-14679.

Francis, G. L., Read, L. C., Ballard, F. J., Bagley, C. J., Upton, F. M., Gravestock, P. M. & Wallace, J. C. (1986). Purification and partial sequence analysis of insulin-like growth factor-I from bovine colostrum. *Biochem. J.* **233**, 207-213.

Francis, G. L., Ross, M., Ballard, F. J., Milner, S. J., Senn, C., McNeil, K. A., Wallace, J. C., King, R. & Wells, J. R. E. (1992). Novel recombinant fusion protein analogues of insulin-like growth factor (IGF)-I indicate the relative importance of IGF-binding protein and receptor binding for enhanced biological potency. *J. Mol. Endocrinol.* **8**, 213-223.

Francis, G. L., Aplin, S. E., Milner, S. J., McNeil, K. A., Ballard, F. J. & Wallace, J. C. (1993). Insulin-like growth factor (IGF)-II binding to IGF-binding proteins and IGF receptors is modified by deletion of the N-terminal hexapeptide or substitution of arginine for glutamate-6 in IGF-II. *Biochem. J.* **293**(3), 713-719.

Francisco, J. A., Campbell, R., Iverson, B. L. & Georgiou, G. (1993). Production and fluorescence-activated cell sorting of *Escherichia coli* expressing a functional antibody fragment on the external surface. *Proc. Natl. Acad. Sci. U.S.A.* **90**, 10444-10448.

Froesch, E. R., Hussain, M. A., Donath, M. Y. & Zapf, J. L. (1998). Diabetes and the Heart: physiological and Therapeutiec Aspects of IGF-I. In *Molecular mechanisms to regulate the activities of insulin-like growth factors.* (Takano, K., Hizuka, N. & Takashi, S. I., eds.), pp. 11-22. Elsevier, Amsterdam.

Funk, B., Kessler, U., Eisenmenger, W., Hansmann, A., Kolb, H. J. & Kiess, W. (1992). The expression of insulin-like growth factor binding proteins is tissue specific during human fetal life and early infancy. *Acta. Endocrinol. Copenh.* **127**(2), 107-114.

Galiano, R. D., Zhao, L. L., Clemmons, D. R., Roth, S. I., Lin, X. & Mustoe, T. A. (1996). Interaction between the insulin-like growth factor family and the integrin receptor family in tissue repair processes. Evidence in a rabbit ear dermal ulcer model. *J. Clin. Invest.* **98**(11), 2462-2468.

Gansler, T., Furlanetto, R., Stokes Gramling, T., Robinson, K. A., Blocker, N., Buse, M. G., Sens, D. A. & Garvin, A. J. (1989). Antibody to type I insulin-like growth factor receptor inhibits growth of Wilms' tumor in culture and in athymic mice. *Am. J. Pathol.* **135**(6), 961-966.

Gay, E., Seurin, D., Babajko, S., Doublier, S., Cazillis, M. & Binoux, M. (1997). Liver-specific expression of human insulin-like growth factor binding protein-1 in transgenic mice: repercussions on reproduction, ante- and perinatal mortality and postnatal growth. *Endocrinology* **138**(7), 2937-2947.

Goldsmith, M. E. & Konigsberg, W. H. (1977). Adsorption protein of the bacteriophage fd: isolation, molecular properties, and location in the virus. *Biochemistry* **16**(12), 2686-2694.

Grant, R. A., Lin, T. C., Konigsberg, W. & Webster, R. E. (1981). Structure of the filamentous bacteriophage f1. *J. Biol. Chem.* **256**(1), 539-546.

Greenwood, J., Willis, A. E. & Perham, R. N. (1991). Multiple display of foreign peptides on a filamentous bacteriophage. *J. Mol. Biol.* **220**, 821-827.

Guex, N. & Peitsch, M. C. (1997). Swiss-model and the Swiss-PdbViewer: an environment for comparative protein modeling. *Electrophoresis* **18**, 2714-2723.

Guler, H. P., Zapf, J., Schmid, C. & Froesch, E. R. (1989). Insulin-like growth factors-I and -II in healthy man. Estimations of half-lives and production rates. *Acta Endocrinol. Copenh.* **121**(6), 753-758.

Guncar, G., Pungercic, G., Klemencic, I., Turk, V. & Turk, D. (1999). Crystal structure of MHC class II-associated p41 Ii fragment bound to cathespin L reveals the structural basis for differentiation between cathepsins L and S. *EMBO J.* **18**, 793-803.

Gustafson, T. A. & Rutter, W. J. (1990). The cysteine-rich domains of the insulin and insulin-like growth factor-I receptors are primary determinants of hormone binding specificity. *J. Biol. Chem.* **265**(30), 18663-18667.

Han, V. K., D'Ercole, A. J. & Lund, P. K. (1987). Cellular localization of somatomedin (insulin-like growth factor) messenger RNA in the human fetus. *Science* **236**, 193-197.

Hanes, J. & Pluckthun, A. (1997). *In vitro* selection and evolution of functional proteins by using ribosome display. *Proc. Natl. Acad. Sci. U.S.A.* **94**, 4937-4942.

Harrison, J. L., Williams, S. C., Winter, G. & Nissim, A. (1996). Screening of phage antibody libraries. *Methods Enymol.* **267**, 83-109.

Hashimoto, R., Ono, M., Fujiwara, H., Higashihashi, N., Yoshida, M., Enjoh Kimura, T. & Sakano, K. (1997). Binding sites and binding properties of binary and ternary complexes of insulin-like growth factor-II (IGF-II), IGF-binding protein-3, and acid-labile subunit. *J. Biol. Chem.* **272**(44), 27936-27942.

Heding, A., Gill, R., Ogawa, Y., De Meyts, P. & Shymko, R. M. (1996). Biosensor measurement of the binding of insulin-like growth factors-I and -II and their analogues to the insulin-like growth factor-binding protein-3. *J. Biol. Chem.* **271**(24), 13948-13952.

Helmerhorst, E. & Stokes, G. B. (1987). Self-association of insulin. Its pH dependence and effect of plasma. *Diabetes* **36**(3), 261-264.

Hernandez-Sanchez, C., Blakesley, V., Kalebic, T., Helman, L. & LeRoith, D. (1995). The role of the tyrosine kinase domain of the insulin-like growth factor-I receptor in intracellular signaling, cellular proliferation and tumorigenesis. *J. Biol. Chem.* **270**(49), 29176-29181.

Ho, P. J. & Baxter, R. C. (1997). Characterization of truncated insulin-like growth factor-binding protein-2 in human milk. *Endocrinology* **138**(9), 3811-3818.

Hobba, G. D., Forbes, B. E., Parkinson, E. J., Francis, G. L. & Wallace, J. C. (1996). The insulin-like growth factor (IGF) binding site of bovine insulin-like growth factor binding protein-2 (bIGFBP-2) probed by iodination. *J. Biol. Chem.* **271**(48), 30529-30536.

Hobba, G. D., Lothgren, A., Holmberg, E., Forbes, B. E., Francis, G. L. & Wallace, J. C. (1998). Alanine screening mutagenesis establishes tyrosine 60 of bovine insulin-like growth factor binding protein-2 as a determinant of insulin-like growth factor binding. *J. Biol. Chem.* **273**(31), 19691-19698.

Hobba, G. D. (1999). Studies to identify and characterise IGF-binding determinants of IGFBP-2. PhD thesis, University of Adelaide.

Hockney, R. C. (1994). Recent developments in heterologous protein production in *Escherichia coli*. *Trends Biotechnol.* **12**, 456-463.

Holly, J. M. P., Gunnell, D. J. & Davey Smith, G. (1999). Growth hormone, IGF-I and cancer. Less intervention to avoid cancer? More intervention to prevent cancer? *J. Endocrinol.* **162**, 321-330.

Honda, Y., Landale, E. C., Strong, D. D., Baylink, D. J. & Mohan, S. (1996). Recombinant synthesis of insulin-like growth factor-binding protein-4 (IGFBP-4): development, validation, and application of a radioimmunoassay for IGFBP-4 in human serum and other biological fluids. *J. Clin. Endocrinol. Metab.* **81**(4), 1389-1396.

Hoogenboom, H. R., Griffiths, A. D., Johnson, K. S., Chiswell, D. J., Hudson, P. J. & Winter, G. (1991). Multi-subunit proteins on the surface of filamentous phage: methodologies for displaying antibody (Fab) heavy and light chains. *Nucleic Acids Res.* **19**, 4133-4137.

Horton, R. M., Hunt, H. D., Ho, S. N., Pullen, J. K. & Pease, L. R. (1989). Engineering hybrid genes without the use of restriction enzymes: gene splicing by overlap extension. *Gene* **77**(1), 61-68.

Hossenlopp, P., Seurin, D., Segovia-Quinson, B., Hardoiun, S. & Binoux, M. (1986). Analysis of serum insulin-like growth factor binding proteins using Western blotting: use of the method for titration of the binding proteins and competitive binding sites. *Anal. Biochem.* **154**, 138-143.

Huhtala, M. L., Koistinen, R., Palomaki, P., Partanen, P., Bohn, H. & Seppala, M. (1986). Biologically active domain in somatomedin-binding protein. *Biochem. Biophys. Res. Comm.* **141**(1), 263-270.

Hwa, V., Oh, Y. & Rosenfeld, R. G. (1999). The insulin-like growth factor-binding protein (IGFBP) superfamily. *Endocr. Rev.* **20**(6), 761-787.

Iannolo, G., Minenkova, O., Petruzzelli, R. & Cesareni, G. (1995). Modifying filamentous phage capsid: limits in the size of the major capsid protein. *J. Mol. Biol.* **248**(4), 835-844.

Ilichev, A. A., Minenkova, O. O., Tat'kov, S. L., Karpyshev, N. N., Eroshkin, A. M., Petrenko, V. A. & Sandakhchiev, L. S. (1989). Production of a viable variant of the M13 phage with a foreign peptide inserted into the basic coat protein. *Dokl. Akad. Nauk. S.S.S.R.* **307**, 481-483.

Imai, Y., Busby, W. H., Jr., Smith, C. E., Clarke, J. B., Garmong, A. J., Horwitz, G. D., Rees, C. & Clemmons, D. R. (1997). Protease-resistant form of insulin-like growth factor-binding protein 5 is an inhibitor of insulin-like growth factor-I actions on porcine smooth muscle cells in culture. *J. Clin. Invest.* **100**(10), 2596-2605.

Jacobson, A. (1972). Role of F pili in penetration of bacteriophage f1. *J. Virol.* **10**(4), 835-843.

Jansson, M., Uhlen, M. & Nilsson, B. (1997). Structural changes in insulin-like growth factor (IGF) -I mutant proteins affecting binding kinetic rates to IGF binding protein-1 and IGF-I receptor. *Biochemistry* **36**(14), 4108-4117.

Jansson, M., Andersson, G., Uhlen, M., Nilsson, B. & Kordel, J. (1998). The insulin-like growth factor (IGF) binding protein-1 binding epitope on IGF-I probed by heteronuclear NMR spectroscopy and mutational analysis. *J. Biol. Chem.* **273**(38), 24701-24707.

Jeffrey, P. D., Milthorpe, B. K. & Nichol, L. W. (1976). Polymerization pattern of insulin at pH 7.0. *Biochemistry* **15**(21), 4660-4665.

Jones, J. I., D'Ercole, A. J., Camacho-Hubner, C. & Clemmons, D. R. (1991). Phosphorylation of insulin-like growth factor (IGF)-binding protein-1 in cell culture and *in vivo*: effects on affinity for IGF-I. *Proc. Natl. Acad. Sci. U.S.A.* **88**(17), 7481-7485.

Jones, J. I., Gockerman, A., Busby, W. H. Jr, Wright, G. & Clemmons, D. R. (1993a). Insulin-like growth factor binding protein 1 stimulates cell migration and binds to the alpha-5-beta-1 integrin by means of its Arg-Gly-Asp sequence. *Proc. Natl. Acad. Sci. U.S.A.* **90**(22), 10553-10557.

Jones, J. I., Gockerman, A., Busby, W. H. Jr, Camacho-Hubner, C. & Clemmons, D. R. (1993b). Extracellular matrix contains insulin-like growth factor binding protein-5: Potentiation of the effects of IGF-I. *J. Cell Biol.* **121**(3), 679-687.

Jones, J. I., Busby, W. H. J., Wright, G., Smith, C. E., Kimack, N. M. & Clemmons, D. R. (1993c). Identification of the sites of phosphorylation in insulin-like growth factor binding protein-1: regulation of its affinity by phosphorylation of serine-101. *J. Biol. Chem.* **268**(2), 1125-1131.

Jones, J. I. & Clemmons, D. R. (1995). Insulin-like growth factors and their binding proteins: biological actions. *Endocr. Rev.* **16**(1), 3-34.

Jyung, R. W., Mustoe, J. A., Busby, W. H. & Clemmons, D. R. (1994). Increased wound-breaking strength induced by insulin-like growth factor-I in combination with insulin-like growth factor binding protein-1. *Surgery* **115**(2), 233-239.

Kalebic, T., Tsokos, M. & Helman, L. J. (1994). *In vivo* treatment with antibody against IGF-I receptor suppresses growth of human rhabdomyosarcoma and down-regulates p34 cdc2. *Cancer Res.* **54**, 5531-5534.

Kalus, W., Zweckstetter, M., Renner, C., Sanchez, Y., Georgescu, J., Grol, M., Demuth, D., Schumacher, R., Dony, C., Lang, K. & Holak, T. A. (1998). Structure of the IGF-binding domain of the insulin-like growth factor-binding protein-5 (IGFBP-5): implications for IGF and IGF-I receptor interactions. *EMBO J.* **17**(22), 6558-6572.

Kane, J. F. (1995). Effects of rare codon clusters on high-level expression of heterologous proteins in *Escherichia coli*. *Curr. Opin. Biotechnol.* **6**, 494-500.

Kang, A. S., Barbas, C. F., Janda, K. D., Benkovic, S. J. & Lerner, R. A. (1991). Linkage of recognition and replication functions by assembling combinatorial antibody Fab libraries along phage surfaces. *Proc. Natl. Acad. Sci. U.S.A.* **88**, 4363-4366.

Karlsson, R., Michaelsson, A. & Mattsson, L. (1991). Kinetic analysis of monoclonal antibody-antigen interactions with a new biosensor based analytical system. *J. Immunol. Methods* **145**, 229-240.

Karlsson, R., Roos, H., Fagerstam, L. & Persson, B. (1994). Kinetic and concentration analysis using BIA technology. *Methods* **6**, 99-110.

Karlsson, R. & Falt, A. (1997). Experimental design for kinetic analysis of protein-protein interactions with surface plasmon resonance biosensors. *J. Immunol. Methods* **200**, 121-133.

Katz, B. A. (1997). Structural and mechanistic determinants of affinity and specificity of ligands discovered or engineered by phage display. *Annu. Rev. Biophys. Biomol. Struct.* **26**, 27-45.

Kay, B. K. & Hoess, R. H. (1996). Principles and applications of phage display. In *Phage display of peptides and proteins.* (Kay, B. K., Winter, J. & McCafferty, J., eds.), pp. 21-34. Academic Press, California.

Kay, B. K., Kurakin, A. V. & Hyde-DeRuyscher, R. (1998). From peptides to drugs via phage-display. *Drug Disc. Today* **3**(8), 370-378.

Kelly, S. M. & Price, N. C. (1997). The application of circular dichroism to studies of protein folding and unfolding. *Biochim. Biophys. Acta* **1338**(2), 161-185.

Khosla, S., Hassoun, A. A., Baker, B. K., Liu, F., Zein, N. N., Whyte, M. P., Reasner, C. A., Nippoldt, T. B., Tiegs, R. D., Hintz, R. L. & Conover, C. A. (1998). Insulin-like growth factor system abnormalities in hepatitis C-associated osteosclerosis. Potential insights into increasing bone mass in adults. *J. Clin. Invest.* **101**(10), 2165-2173.

Kiefer, L. L., Ittoop, O. R. R., Bunce, K., Truesdale, A. T., Willard, D. H., Nichols, J. S., Blanchard, S. G., Mountjoy, K., Chen, W. & Wilkison, W. O. (1997). Mutations in the carboxyl terminus of agouti protein decrease agouti inhibition of ligand binding to the melanocortin receptors. *Biochemistry* **36**(8), 2084-2090.

Kleber-Janke, T. & Becker, W. (2000). Use of modified BL21(DE3) *Escherichia coli* cells for high-level expression of recombinant peanut allergens affected by poor codon usage. *Prot. Exp. Purific.* **19**(3), 419-424.

Knappik, A. & Pluckthun, A. (1995). Engineered turns of a recombinant antibody improve its *in vivo* folding. *Protein Eng.* **8**(1), 81-89.

Koradi, R., Billeter, M. & Wuthrich, K. (1996). MOLMOL: a program for display and analysis of macromolecular structures. *J. Mol. Graph.* **14**(1), 51-55.

Krebber, A., Burmester, J. & Pluckthun, A. (1996). Inclusion of an upstream transcriptional terminator in phage display vectors abolishes background expression of toxic fusions with coat protein g3p. *Gene* **178**(1-2), 71-74.

Kubler, B., Schrameck, U., Draeger, C., Forssman, W. G., Braulke, T. & Standker, L. (1999). Identification of circulating human IGFBP-3 fragments. *Growth Horm. IGF Res.* **9**(5), 362.

Laajoki, L. G., Francis, G. L., Wallace, J. C., Carver, J. A. & Keniry, M. A. (2000). Solution structure and backbone dynamics of long-[Arg3]insulin-like growth factor-I. *J. Biol. Chem.* **275**, 10009-10015.

Lalou, C., Lassarre, C. & Binoux, M. (1995). A proteolytic fragment of insulin-like growth factor (IGF) binding protein-3 that fails to bind IGF is a cell growth inhibitor. *Prog. Growth Factor Res.* **6**(2-4), 311-316.

Landale, E. C., Strong, D. D., Mohan, S. & Baylink, D. J. (1995). Sequence comparison and predicted structure for the four exon-encoded regions of human insulin-like growth factor binding protein-4. *Growth Factors* **12**, 245-250.

Landwehr, J., Kaupmann, K., Heinrich, G. & Schwander, J. (1993). Cloning and characterization of the gene encoding murine insulin-like growth factor-binding protein-2, mIGFBP-2. *Gene* **124**(2), 281-286.

Laron, Z. (1999). Commentary. The essential role of IGF-I: Lessons from the long-term study and treatment of children and adults with Laron syndrome. *J. Clin. Endocrinol. Metab.* **84**(12), 4397-4404.

Lawrence, J. B., Oxvig, C., Overgaard, M. T., Sottrup-Jensen, L., Gleich, G. J., Hays, L. G., Yates III, J. R. & Conover, C. A. (1999). The insulin-like growth factor (IGF)-dependent IGF binding protein-4 protease is pregnancy-associated plasma protein-A. *Proc. Natl. Acad. Sci. U.S.A.* **96**, 3149-3153.

Leighton, P. A., Ingram, R. S., Eggenschwiler, A., Efstratiadis, A. & Tilghmam, S. M. (1995). Disruption of imprinting caused by deletion of the *H19* gene region in mice. *Nature* **375**, 34-39.

LeRoith, D. & Butler, A. A. (1999). Commentary. Insulin-like growth factors in pediatric health and disease. *J. Clin. Endocrinol. Metab.* **84**(12), 4355-4361.

Leung, D. W., Chen, E. & Goeddel, D. V. (1989). A method for random mutagenesis of a defined DNA segment using a modified polymerase chain reaction. *Technique* **1**, 11-15.

Lewitt, M. S., Denyer, G. S., Cooney, G. J. & Baxter, R. C. (1991). Insulin-like growth factor-binding protein-1 modulates blood glucose levels. *Endocrinol.* **129**(4), 2254-2256.

Lien, S., Francis, G. L. & Graham, L. D. (1999). Combinatorial strategies for the discovery of novel protease specificities. *Comb. Chem. High Throughput Screen.* **2**(2), 73-90.

Liu, J. P., Baker, J., Perkins, A. S., Robertson, E. J. & Efstratiadis, A. (1993). Mice carrying null mutations of the genes encoding insulin-like growth factor-I (*Igf-1*) and type 1 IGF receptor (*Igf1r*). *Cell* **75**(1), 59-72.

Logie, A., Boulle, N., Gaston, V., Perin, L., Boudou, P., Le-Bouc, Y. & Gicquel, C. (1999). Autocrine role of IGF-II in proliferation of human adrenocoritcal carcinoma NCI H295R cell line. *J. Mol. Endocrinol.* **23**(1), 23-32.

Lowman, H. B., Bass, S. H., Simpson, N. & Wells, J. A. (1991). Selecting high-affinity binding proteins by monovalent phage display. *Biochemistry* **30**(45), 10832-10838.

Lowman, H. B. & Wells, J. A. (1993). Affinity maturation of human growth hormone by monovalent phage display. *J. Mol. Biol.* **234**(3), 564-578.

Lubkowski, J., Hennecke, F., Pluckthun, A. & Wlodawer, A. (1999). Filamentous phage infection: crystal structure of g3p in complex with its coreceptor, the C-terminal domain of TolA. *Structure* **7**(6), 711-722.

Ludwig, T., Eggenschwiler, J., Fisher, P., D'Ercole, A. J., Davenport, M. L. & Efstratiadis, A. (1996). Mouse mutants lacking the type 2 IGF receptor (IGF2R) are rescued from perinatal lethality in *Igf2* and *Igf1r* null backgrounds. *Dev. Biol.* **177**(2), 517-535.

Macaulay, V. M. (1992). Insulin-like growth factors and cancer. *Br. J. Cancer* **65**, 311-320.

Magee, B. A., Shooter, G. K., Wallace, J. C. & Francis, G. L. (1999). Insulin-like growth factor-I and its binding proteins: a study of the binding interface using B-domain mutants. *Biochemistry* **38**(48), 15863-15870.

Maile, L. A. & Holly, J. M. P. (1999). Insulin-like growth factor binding protein (IGFBP) proteolysis: occurrence, identification, role and regulation. *Growth Horm. IGF Res.* **9**(2), 85-95.

Makowski, L. (1994). Phage display: structure, assembly and engineering of filamentous bacteriophage M13. *Curr. Opin. Struct. Biol.* **4**, 225-230.

Malyguine, E., Vannier, P. & Yot, P. (1980). Alternation of the specificity of restriction endonucleases in the presence of organic solvents. *Gene* **8**, 163-177.

Manes, S., Kremer, L., Albar, J. P., Mark, C., Llopis, R. & Martineza, C. (1997). Functional epitope mapping of insulin-like growth factor-I (IGF-I) by anti-IGF-I monoclonal antibodies. *Endocrinology* **138**(3), 905-915.

Manes, S., Llorente, M., Lacalle, R. A., Gomez-Mouton, C., Kremer, L., Mira, E. & Martinez-A., C. (1999). The matrix metalloproteinase-9 regulates the insulin-like growth factor-triggered autocrine response in DU-145 carcinoma cells. *J. Biol. Chem.* **274**(11), 6935-6945.

Marinaro, J. A., Jamieson, G. P., Hogarth, P. M. & Bach, L. A. (1999). Differential dissociation kinetics explain the binding preference of insulin-like growth factor binding protein-6 for insulin-like growth factor-II over insulin-like growth factor-I. *FEBS lett.* **450**, 240-244.

Marks, J. D., Hoogenboom, H. R., Griffiths, A. D. & Winter, G. (1992). Molecular evolution of proteins on filamentous phage. *J. Biol. Chem.* **267**(23), 16007-16010.

Martin, J. L., Ballesteros, M. & Baxter, R. C. (1992). Insulin-like growth factor-I (IGF-I) and transforming growth factor-beta 1 release IGF-binding protein-3 from human fibroblasts by different mechanisms. *Endocrinology* **131**(4), 1703-1710.

Maruyama, I. N., Maruyama, H. I. & Brenner, S. (1994). Lambda foo: a lambda phage vector for the expression of foreign proteins. *Proc. Natl. Acad. Sci. U.S.A.* **91**(17), 8273-8277.

Mathews, L. S., Norstedt, G. & Palmiter, R. D. (1986). Regulation of insulin-like growth factor-I gene expression by growth hormone. *Proc. Natl. Acad. Sci. U.S.A.* **83**, 9343-9347.

Mathews, L. S., Hammer, R. E., Behringer, R. R., D'Ercole, A. J., Bell, G. I., Brinster, R. L. & Palmiter, R. D. (1988). Growth enhancement of transgenic mice expressing human insulin-like growth factor-I. *Endocrinology* **123**(6), 2827-2833.

Mattheakis, L. C., Bhatt, R. R. & Dower, W. J. (1994). An *in vitro* polysome display system for identifying ligands from very large peptide libraries. *Proc. Natl. Acad. Sci. U.S.A.* **91**, 9022-9026.

Matthews, D. J. & Wells, J. A. (1993). Substrate phage: selection of protease substrates by monovalent phage display. *Science* **260**, 1113-1117.

McCafferty, J., Griffiths, A. D., Winter, G. & Chiswell, D. J. (1990). Phage antibodies: filamentous phage displaying antibody variable domains. *Nature* **348**(6301), 552-554.

Menouny, M., Binoux, M. & Babajko, S. (1997). Role of insulin-like growth factor binding protein-2 and its limited proteolysis in neuroblastoma cell proliferation: modulation by transforming growth factor-beta and retinoic acid. *Endocrinology* **138**(2), 683-690.

Mikawa, Y. G., Maruyama, I. N. & Brenner, S. (1996). Surface display of proteins on bacteriophage lambda heads. *J. Mol. Biol.* **262**, 21-30.

Mohan, S., Bautista, C. M., Wergedal, J. & Baylink, D. J. (1989). Isolation of an inhibitory insulin-like growth factor (IGF) binding protein from cell-conditioned medium: a potential local regulator of IGF action. *Proc. Natl. Acad. Sci. U.S.A.* **86**, 8338-8342.

Morgan, D. O., Edman, J. C., Standring, D. N., Fried, V. A., Smith, M. C., Roth, R. A. & Rutter, W. J. (1987). Insulin-like growth factor-II receptor as a multifunctional binding protein. *Nature* **329**(6137), 301-307.

Mulhern, T. D. & Booker, G. W. (1998). A third fibronectin-type-III domain in the insulin-family receptors. *Trends Biochem. Sci.* **23**(12), 465-466.

Myszka, D. G. (1997). Kinetic analysis of macromolecular interactions using surface plasmon resonance biosensors. *Curr. Opin. Biotechnol.* **8**, 50-57.

Nam, T. J., Busby, W. H., Jr. & Clemmons, D. R. (1994). Human fibroblasts secrete a serine protease that cleaves insulin-like growth factor-binding protein-5. *Endocrinology* **135**(4), 1385-1391.

Neumann, G. M., Marinaro, J. A. & Bach, L. A. (1998). Identification of O-glycosylation sites and partial characterization of carbohydrate structure and disulfide linkages of human insulin-like growth factor binding protein-6. *Biochemistry* **37**(18), 6572-6585.

Neumann, G. M. & Bach, L. A. (1999). The N-terminal disulfide linkages of human insulin-like growth factor-binding protein-6 (hIGFBP-6) and hIGFBP-1 are different as determined by mass spectrometry. *J. Biol. Chem.* **274**(21), 14587-14594.

Newman, J., Swinney, H. L. & Day, L. A. (1977). Hydrodynamic properties and structure of fd virus. *J. Mol. Biol.* **116**, 593-606.

Nice, E. C. & Catimel, B. (1999). Instrumental biosensors: new perspectives for the analysis of biomolecular interactions. *BioEssays* **21**, 339-352.

Nieba, L., Nieba-Axmann, S. E., Persson, A., Hamalainen, M., Edebratt, F., Hansson, A., Lidholm, J., Magnusson, K., Karlsson, A. F. & Pluckthun, A. (1997). BIACORE analysis of histidine-tagged proteins using a chelating NTA sensor chip. *Anal. Biochem.* **252**, 217-228.

O'Neil, K. T., Hoess, R. H., Raleigh, D. P. & DeGrado, W. F. (1995). Thermodynamic genetics of the folding of the B1 immunoglobulin-binding domain from streptococcal protein G. *Proteins* **21**(1), 11-21.

O'Shannessy, D. J. & Winzor, D. J. (1996). Interpretation of deviations from pseudo-first-order kinetic behavior in the characterization of ligand binding biosensor technology. *Anal. Biochemistry* **236**(2), 275-283.

Oh, Y., Mueller, H. L., Lee, D. Y., Fielder, P. J. & Rosenfeld, R. G. (1993). Characterization of the affinities of insulin-like growth factor (IGF)-binding protein -1 to -4 for IGF-I, IGF-II, IGF-I/insulin hybrid, and IGF-I analogs. *Endocrinology* **132**(3), 1337-1344.

Oh, Y., Yamanaka, Y., Kim, H. S., Vorwerk, P., Wilson, E., Hwa, V., Yang, D. H., Spagnoli, A., Wanek, D. & Rosenfelf, R. G. (1998). IGF-independent actions of IGFBPs. In *Molecular mechanisms to regulate the activities of insulin-like growth factors.* (Takano, K., Hizuka, N. & Takahashi, S. I., eds.), pp. 125-133. Elsevier, Amsterdam.

Okabe, E., Kajihara, J., Usami, Y. & Hirano, K. (1999). The cleavage site specificity of human prostate specific antigen for insulin-like growth factor binding protein-3. *FEBS lett.* **447**, 87-90.

Parker, A., Clarke, J. B., Busby, W. H. & Clemmons, D. R. (1996). Identification of the extracellular matrix binding sites for insulin-like growth factor-binding protein-5. *J. Biol. Chem.* **271**(23), 13523-13529.

Parmley, S. F. & Smith, G. P. (1988). Antibody-selectable filamentous fd phage vectors: affinity purification of target genes. *Gene* **73**(2), 305-318.

Perham, R. N., Terry, T. D., Willis, A. E., Greenwood, J., di Marzo Veronese, F. & Appella, E. (1995). Engineering a peptide epitope display system on filamentous bacteriophage. *FEMS Microbiol. Rev.* **17**(1-2), 25-31.

Petrik, J., Pell, J. M., Arany, E., McDonald, T. J., Dean, W. L., Reik, W. & Hill, D. J. (1999). Overexpression of insulin-like growth factor-II in transgenic mice is associated with pancreatic islet cell hyperplasia. *Endocrinology* **140**(5), 2353-2363.

Phillips, L. S., Pao, C. I. & Villafuerte, B. C. (1998). Molecular regulation of insulin-like growth factor-I and its principal binding protein, IGFBP-3. *Prog. Nucleic Acid Res. Mol. Biol.* **60**, 195-265.

Pintar, J. E., Cerro, J. A. & Wood, T. L. (1996). Genetic approaches to the function of insulin-like growth factor-binding proteins during rodent development. *Horm. Res.* **45**(3-5), 172-177.

Pintar, J., Schuller, A., Bradshaw, S., Cerro, C. & Grewal, A. (1998). Genetic disruption of IGF binding proteins. In *Molecular mechanisms to regulate the activities of insulin-like growth factors.* (Takano, K., Hizuka, N. & Takahashi, S. I., eds.), pp. 65-70. Elsevier, Amsterdam.

Pintar, J. E., Schuller, A. & Bradshaw, S. (1999). Combinatorial KOs of IGFBPs. *Growth Horm. IGF Res.* **9**(5), 308.

Polyak, S. W. (2000). Biotin protein ligase from *Saccharomyces cerevisiae*. PhD Thesis, University of Adelaide.

Qin, X., Strong, D. D., Baylink, D. J. & Mohan, S. (1998). Structure-function analysis of the human insulin-like growth factor binding protein-4. *J. Biol. Chem.* **273**(36), 23509-23516.

Rajaram, S., Baylink, D. J. & Mohan, S. (1997). Insulin-like growth factor-binding proteins in serum and other biological fluids: regulation and functions. *Endocr. Rev.* **18**(6), 801-831.

Rajkumar, K., Barron, D., Lewitt, M. S. & Murphy, L. J. (1995). Growth retardation and hyperglycemia in insulin-like growth factor binding protein-1 transgenic mice. *Endocrinology* **136**(9), 4029-4034.

Rasched, I. & Oberer, E. (1986). Ff coliphages: structural and functional relationships. *Microbiol. Rev.* **50**(4), 401-27.

Rauschnabel, U., Koscielniak, E., Ranke, M. B., Schuett, B. & Elmlinger, M. W. (1999). RGD-specific binding of IGFBP-2 to alpha5beta1-integrin of Ewing sarcoma cells. *Growth Horm. IGF Res.* **9**(5), 369.

Rechler, M. M. (1993). Insulin-like growth factor binding proteins. *Vitam. Horm.* **47**, 1-114.

Rechler, M. M. (1997). Growth inhibition by insulin-like growth factor (IGF) binding protein-3-what's IGF got to do with it? [editorial]. *Endocrinology* **138**(7), 2645-2647.

Rechler, M. M. & Clemmons, D. R. (1998). Regulatory actions of insulin-like growth factor-binding proteins. *Trends Endocrinol. Metab.* **9**(5), 176-183.

Rees, C., Clemmons, D. R., Horvitz, G. D., Clarke, J. B. & Busby, W. H. (1998). A protease-resistant form of insulin-like growth factor (IGF) binding protein-4 inhibits IGF-1 actions. *Endocrinology* **139**(10), 4182-4188.

Riechmann, L. & Holliger, P. (1997). The C-terminal domain of TolA is the coreceptor for filamentous phage infection. *Cell* **90**, 351-360.

Rinderknecht, E. & Humbel, R. E. (1978a). Primary structure of human insulin-like growth factor-II. *FEBS lett.* **89**(2), 283-286.

Rinderknecht, E. & Humbel, R. E. (1978b). The amino acid sequence of human insulin-like growth factor-I and its structural homology with proinsulin. *J. Biol. Chem.* **253**(8), 2769-2776.

Roden, L. D. & Myszka, D. G. (1996). Global analysis of macromolecular interaction measured on BIAcore. *Biochem. Biophys. Res. Comm.* **225**, 1073-1077.

Roghani, M., Lassarre, C., Zapf, J., Povoa, G. & Binoux, M. (1991). Two insulin-like growth factor (IGF)-binding proteins are responsible for the selective affinity for IGF-II of cerebrospinal fluid binding proteins. *J. Clin. Endo. Metab.* **73**(3), 658-666.

Rosenberg, A. H., Griffin, K., Washington, M. T., Patel, S. S. & Studier, F. W. (1996). Selection, identification, and genetic analysis of random mutants in the cloned primase/helicase gene of bacteriophage T7. *J. Biol. Chem.* **271**(43), 26819-26824.

Rosenfeld, R. G. (1998). IGF-I treatment of growth hormone deficiency. In *Molecular mechanisms to regulate the activities of insulin-like growth factors.* (Takano, K., Hizuka, N. & Takahashi, S. I., eds.), pp. 359-364. Elsevier, Amsterdam.

Russel, M. (1991). Filamentous phage assembly. *Mol. Microbiol.* **5**(7), 1607-1613.

Russo, V. C., Bach, L. A., Fosang, A. J., Baker, N. L. & Werther, G. A. (1997). Insulin-like growth factor binding protein-2 binds to cell surface proteoglycans in the rat brain olfactory bulb. *Endocrinology* **138**(11), 4858-4867.

Sackett, R. L. & McCusker, R. H. (1998). Multivalent cations depress ligand binding to cell-associated insulin-like growth factor binding protein-5 on human glioblastoma cells. *Endocrinology* **139**(4), 1943-1951.

Sakano, K., Enjoh, T., Numata, F., Fujiwara, H., Marumoto, Y., Higashihashi, N., Sato, Y., Perdue, J. F. & Fujita Yamaguchi, Y. (1991). The design, expression, and characterization of human insulin-like growth factor-II (IGF-II) mutants specific for either the IGF-II/cation-independent mannose 6-phosphate receptor or IGF-I receptor. *J. Biol. Chem.* **266**(31), 20626-20635.

Sambrook, J., Fritsch, E. F. & Maniatis, T. (1989). *Molecular cloning: a laboratory manual.* 2nd edit, Cold Spring Harbor Press, New York.

Sara, V. R., Carlsson-Skwirut, C., Andersson, C., Hall, E., Sjogren, B., Holmgren, A. & Jornvall, H. (1986). Characterization of somatomedins from human fetal brain: identification of a variant from of insulin-like growth factor-I. *Proc. Natl. Acad. Sci. U.S.A.* **83**, 4904-4907.

Sato, A., Nishimura, S., Ohkubo, T., Kyogoku, Y., Koyama, S., Kobayashi, M., Yasuda, T. & Kobayashi, Y. (1993). Three-dimensional structure of human insulin-like growth factor-I (IGF-I) determined by proton NMR and distance geometry. *Int. J. Pep. Prot. Res.* **41**(5), 433-440.

Scaloni, A., Ferranti, P., De Simone, G., Mamone, G., Sannolo, N. & Malorni, A. (1999). Probing the reactivity of nucleophile residues in human 2,3-diphosphoglycerate/deoxy-hemoglobin complex by aspecific chemical modifications. *FEBS lett.* **452**, 190-194.

Schechter, I. & Berger, A. (1967). On the size of the active site in proteases I. Papain. *Biochem. Biophys. Res Commun.* **27**, 157-162.

Schedlich, L. J., Young, T. F., Firth, S. M. & Baxter, R. C. (1998). Insulin-like growth factor-binding protein (IGFBP)-3 and IGFBP-5 share a common nuclear transport pathway in T47D human breast carcinoma cells. *J. Biol. Chem.* **273**(29), 18347-18352.

Schmid, C. (1995). Insulin-like growth factors. *Cell. Biol. Int.* **19**(5), 445-457.

Schmidt, B., Kiecke Siemsen, C., Waheed, A., Braulke, T. & von Figura, K. (1995). Localization of the insulin-like growth factor-II binding site to amino acids 1508-1566 in repeat 11 of the mannose 6-phosphate/insulin-like growth factor-II receptor. *J. Biol. Chem.* **270**(25), 14975-14982.

Schoen, T. J., Mazuruk, K., Waldbillig, R. J., Potts, J., Beebe, D. C., Chader, G. J. & Rodriguez, I. R. (1995). Cloning and characterization of a chick embryo cDNA and gene for IGF-binding protein-2. *J. Mol. Endocrinol.* **15**(1), 49-59.

Schuck, P. (1997). Use of surface plasmon resonance to probe the equilibrium and dynamic aspects of interactions between biological macromolecules. *Annu. Rev. Biophy. Biomol. Struct.* **26**, 541-566.

Schuller, A. G., Lindenbergh Kortleve, D. J., de Boer, W. I., Zwarthoff, E. C. & Drop, S. L. (1993). Localization of the epitope of a monoclonal antibody against human insulin-like growth factor binding protein-1, functionally interfering with insulin-like growth factor binding. *Growth Regul.* **3**(1), 32-34.

Sell, C., Rubini, M., Rubin, R., Liu, J. P., Efstratidadis, A. & Baserga, R. (1993). Simian virus 40 large tumor antigen is unable to transform mouse embryonic fibroblasts lacking type-I insulin-like growth factor receptor. *Proc. Natl. Acad. Sci. U.S.A.* **90**, 11217-11221.

Sepp-Lorenzino, L. (1998). Structure and function of the insulin-like growth factor-I receptor. *Breast. Cancer Res. Treat.* **47**(3), 235-253.

Simons, G. F., Konings, R. N. H. & Schonemakers, J. G. G. (1981). Genes *VI*, *VII*, and *IX* of phage M13 code for minor capsid proteins of the virion. *Proc. Natl. Acad. Sci. U.S.A.* **78**(7), 4194-4198.

Smith, G. P. (1985). Filamentous fusion phage: novel expression vectors that display cloned antigens on the virion surface. *Science* **228**, 1315-1317.

Smith, G. P. (1993). Preface: surface display and peptide libraries. *Gene* **128**, 1-2.

Smith, G. (1998). Patch engineering: a general approach for creating proteins that have new binding activities. *Trends Biochem. Sci.* **23**(12), 457-460.

Sommer, A., Maack, C. A., Spratt, S. K., Mascarenhas, D., Tressel, T. J., Rhodes, E. T., Lee, R., Roumas, M., Tatsuno, G. P., Flynn, J. A., Gerber, N., Taylor, J., Cudny, H., Nanney, L., Hunt, T. K. & Spencer, E. M. (1991). Molecular genetics and actions of recombinant insulin-like growth factor binding protein-3. In *Modern Concepts of Insulin-like Growth Factors.* (Spencer, E. M., ed.), pp. 715-728. Elsevier.

Song, H., Beattie, J., Campbell, I. W. & Allan, G. J. (2000). Overlap of IGF- and heparin-binding sites in rat IGF-binding protein-5. *J. Mol. Endocrinol.* **24**, 43-51.

Soos, M. A. & Siddle, K. (1989). Immunological relationships between receptors for insulin and insulin-like growth factor-I. Evidence for structural heterogeneity of insulin-like growth factor-I receptors involving hybrids with insulin receptors. *Biochem. J.* **263**(2), 553-563.

Spencer, E. M. & Chan, K. (1995). A 3-dimensional model for the insulin-like growth factor binding proteins (IGFBPs); supporting evidence using the structural determinants of the IGF binding site on IGFBP-3. *Prog. Growth Factor Res.* **6**(2-4), 209-214.

Standker, L., Wobst, P., Mark, S. & Forssmann, W. G. (1998). Isolation and characterization of circulating 13 kDa C-terminal fragments of human insulin-like growth factor binding protein-5. *FEBS lett.* **441**, 281-286.

Standker, L., Mark, S., Mostafavi, H., Honing, S., Braulke, T. & Forssmann, W. G. (1999). Characterization of circulating fragments of human IGFBP-4. *Growth Horm. IGF Res.* **9**(5), 362.

Standker, L., Braulke, T., Mark, S., Mostafavi, H., Meyer, M., Honing, S., Gimenez-Gallego, G. & Forssmann, W. (2000). Partial IGF affinity of circulating N- and C-terminal fragments of human insulin-like growth factor binding protein-4 (IGFBP-4) and the disulfide bonding pattern of the C-terminal IGFBP-4 domain. *Biochemistry* **39**, 5082-5088.

Steele-Perkins, G., Turner, J., Edman, J. C., Hari, J., Pierce, S. B., Stover, C., Rutter, W. J. & Roth, R. A. (1988). Expression and characterization of a functional human insulin-like growth factor-I receptor. *J. Biol, Chem.* **263**(23), 11486-11492.

Stemmer, W. P. C. (1994). Rapid evolution of a protein *in vitro* by DNA shuffling. *Nature* **370**, 389-391.

Stengele, I., Bross, P., Garces, X., Giray, J. & Rasched, I. (1990). Dissection of functional domains in phage fd adsorption protein. *J. Mol. Biol.* **212**, 143-149.

Szabo, L., Mottershead, D. G., Ballard, F. J. & Wallace, J. C. (1988). The bovine insulin-like growth factor (IGF) binding protein purified from conditioned medium requires the N-terminal tripeptide in IGF-1 for binding. *Biochem. Biophys. Res. Commun.* **151**(1), 207-214.

Tang, X. B., Dallaire, P., Hoyt, D. W., Sykes, B. D., O'Connor McCourt, M. & Malcolm, B. A. (1997). Construction of transforming growth factor alpha (TGF-alpha) phage library and identification of high binders of epidermal growth factor receptor (EGFR) by phage display. *J. Biochem. Tokyo* **122**(4), 686-690.

Terasawa, H., Kohda, D., Hatanaka, H., Nagata, K., Higashihashi, N., Fujiwara, H., Sakano, K. & Inagaki, F. (1994). Solution structure of human insulin-like growth factor-II: recognition sites for receptors and binding proteins. *EMBO J.* **13**(23), 5590-5597.

Thissen, J. P., Ketelslegers, J. M. & Underwood, L. E. (1994). Nutritional regulation of the insulin-like growth factors. *Endocr. Rev.* **15**(1), 80-101.

Thompson, J. D., Higgins, D. G. & Gibson, T. J. (1994). Clustal W: improving the sensitivity of progressive multiple sequence alignment through sequence weighting, position-specific gap penalties and weight matrix choice. *Nulceic Acids Res.* **22**(22), 4673-4680.

Torres, A. M., Forbes, B. E., Aplin, S. E., Wallace, J. C., Francis, G. L. & Norton, R. S. (1995). Solution structure of human insulin-like growth factor-II: Relationship to receptor and binding protein interactions. *J. Mol. Biol.* **248**(2), 385-401.

Tsuboi, R., Shi, C. M., Sato, C., Cox, G. N. & Ogawa, H. (1995). Co-administration of insulin-like growth factor (IGF)-I and IGF-binding protein-1 stimulates wound healing in animal models. *J. Invest. Dermatol.* **104**(2), 199-203.

Ullrich, A., Gray, A., Tam, A. W., Yang-Feng, T., Tsubokawa, M., Collins, C., Henzel, W., Le Bon, T., Kathuria, S., Chen, E., Jacobs, S., Francke, U., Ramachandran, J. & Fujita-Yamaguchi, Y. (1986). Insulin-like growth factor-I receptor primary structure: comparison with insulin receptor suggests structural determinants that define functional specificity. *EMBO J.* **5**(10), 2503-2512.

Upton, F. Z., Szabo, L., Wallace, J. C. & Ballard, F. J. (1990). Characterization and cloning of a bovine insulin-like growth factor-binding protein. *J. Mol. Endocrinol.* **5**(1), 77-84.

Upton, Z., Yandell, C. A., Degger, B. G., Chan, S. J., Moriyama, S., Francis, G. L. & Ballard, F. J. (1998). Evolution of insulin-like growth factor-I (IGF-I) action: *in vitro* characterization of vertebrate IGF-I proteins. *Comp. Biochem. Physiol. B. Biochem. Mol. Biol.* **121**(1), 35-41.

van Kleffens, M., Groffen, C. A. H., Dits, N. F. J., Lindenbergh-Kortleve, D. J., Schuller, A. G. P., Bradshaw, S. L., Pintar, J. E., Zwarthoff, E. C., Drop, S. L. S. & van Neck, J. W. (1999). Generation of antisera to mouse insulin-like growth factor binding proteins (IGFBP)-1 to -6: comparison of IGFBP protein and messenger ribonucleic acid localization in mouse embryo. *Endocrinology* **140**(12), 5944-5952.

Vieira, J. & Messing, J. (1987). Production of single-stranded plasmid DNA. *Methods Enzymol.* **153**, 3-11.

Vorwerk, P., Yamanaka, Y., Spagnoli, A., Oh, Y. & Rosenfeld, R. G. (1998). Insulin and IGF binding by IGFBP-3 fragments derived from proteolysis, baculovirus expression and normal human urine. *J. Clin. Endocrinol. Metab.* **83**(4), 1392-1395.

Wallace, J. C., Bagley, C. J., May, B. L., Ross, M., Francis, G. L. & Ballard, J. (1989). The use of IGF analogs to determine ligand specificity of different IGF binding proteins. In *Proceedings of International IGF-Binding Protein Workshop.* (Drop, S. L. S. & Hintz, R. L., eds.), pp. 225-229. Elsevier, Vancouver.

Wang, J. F., Hampton, B., Mehlman, T., Burgess, W. H. & Rechler, M. M. (1988). Isolation of a biologically active fragment from the carboxyl-terminus of the fetal rat binding protein for insulin-like growth factors. *Biochem. Biophys. Res. Comm.* **157**(2), 718-726.

Weber, M. M., Spottl, G., Gossl, C. & Engelhardt, D. (1999). Characterization of human insulin-like growth factor-binding proteins by two-dimensional polyacrylamide gel electrophoresis and Western ligand blot analysis. *J. Clin. Endo. Metab.* **84**(5), 1679-1684.

Wells, J. A., Vasser, M. & Powers, D. B. (1985). Cassette mutagenesis: an efficient method for generation of multiple mutations at defined sites. *Gene* **34**, 315-323.

Wells, J. A. (1990). Additivity of mutational effects in proteins. *Biochemistry* **29**(37), 8509-8517.

Whyatt, L. M. (1996). Systems for analysis of developmental control genes of the mouse. PhD thesis, University of Adelaide.

Won, W. & Powell-Braxton, L. (1998). Insulin-like growth factor gene targetting. In *Molecular mechanisms to regulate the activities of insulin-like growth factors.* (Takano, K., Hizuka, N. & Takahashi, S. I., eds.), pp. 57-63. Elsevier, Amsterdam.

Wong, M., Fong, C. & Yang, M. (1999). Biosensor measurement of the interaction kinetics between insulin-like growth factors and their binding proteins. *Biochim. Biophys. Acta* **1432**, 293-301.

Wood, T. L., Rogler, L., Streck, R. D., Cerro, J., Green, B., Grewal, A. & Pintar, J. E. (1993). Targeted disruption of IGFBP-2 gene. *Growth Regul.* **3**(1), 5-8.

Wood, T. D., Guan, Z., Borders, C. L., Chen, L. H., Kenyon, G. L. & McLafferty, F. W. (1998). Creatine kinase: essential arginine residues at the nucleotide binding site identified by chemical modification and high-resolution tandem mass spectrometry. *Proc. Natl. Acad. Sci. U.S.A.* **95**, 3362-3365.

Woolford, J. L. J., Steinman, H. M. & Webster, R. E. (1977). Adsorption protein of bacteriophage f1: solubilization in deoxycholate and localization in the f1 virion. *Biochemistry* **16**(12), 2694-2700.

Xu, Y., Papageorgiou, A. & Polychronakos, C. (1998). Developmental regulation of the soluble form of insulin-like growth factor-II/mannose 6-phosphate receptor in human serum and amniotic fluid. *J. Clin. Endocrinol. Metab.* **83**, 437-442.

Yakar, S., Liu, J. I., Stannard, B., Butler, A., Accili, D., Sauer, B. & Le Roith, D. (1999). Normal growth and development in the absence of hepatic insulin-like growth factor-I. *Proc. Natl. Acad. Sci. U.S.A.* **96**, 7324-7329.

Young, D. C., Zhan, H., Cheng, Q., Hou, J. & Matthews, D. J. (1997). Characterization of the receptor binding determinants of granulocyte colony stimulating factor. *Protein Sci.* **6**(6), 1228-1236.

Zabarovsky, E. R. & Winberg, G. (1990). High efficiency electroporation of ligated DNA into bacteria. *Nucleic Acids Res.* **18**(19), 5912.

Zadeh, S. M. & Binoux, M. (1997). The 16 kDa proteolytic fragment of insulin-like growth factor (IGF) binding protein-3 inhibits the mitogenic action of fibroblast growth factor on mouse fibroblasts with targeted disruption of the type-I IGF receptor gene. *Endocrinology* **138**(7), 3069-3072.

Zahn, K. (1996). Overexpression of an mRNA dependent on rare codons inhibits proteins synthesis and cell growth. *J. Bacteriol.* **178**(10), 2926-2933.

Zaina, S., Newton, R. V., Paul, M. R. & Graham, C. F. (1998). Local reduction of organ size in transgenic mice expressing a soluble insulin-like growth factor-II/mannose-6-phosphate receptor. *Endocrinology* **139**(9), 3886-3895.

Zaina, S. & Squire, S. (1998). The soluble type 2 insulin-like growth factor (IGF-II) receptor reduces organ size by IGF-II-mediated and IGF-II-independent mechanisms. *J. Biol. Chem.* **273**(44), 28610-28616.

Zapf, J., Born, W., Chang, J. Y., James, P., Froesch, E. R. & Fischer, J. A. (1988). Isolation and NH_2-terminal amino acid sequences of rat serum carrier proteins for insulin-like growth factors. *Biochem. Biophys. Res. Commun.* **156**(3), 1187-1194.

Zapf, J. (1995). Physiological role of the insulin-like growth factor binding proteins. *European J. Endocrinol.* **132**, 645-654.

Zhou, J., Liu, W. J., Peng, S. W., Sun, X. Y. & Frazer, I. (1999). Papillomavirus capsid protein expression level depends on the match between codon usage and tRNA availability. *J. Virol.* **73**(6), 4972-4982.

Appendix 1 The kinetic models used to evaluate the BIAcore™ 2000 data generated from the interaction between the IGFs and bIGFBP-2.

The models described below have been adapted from the BIAevaluation (version 3.0) manual. The bulk refractive index contribution has not been included in the models, because the data had been corrected for background responses. The bulk refractive index is a response change due to differences in the buffer composition.

LANGMUIR 1:1 BINDING MODEL

-Used to describe a simple 1:1 binding interaction between an analyte and a ligand. This is defined in Karlsson *et al.* (1991).

MODEL

$A + B \leftrightarrow AB$

Where total response = AB

DEFINITIONS

A	analyte (protein in solution)
[A]	concentration of analyte (M)
AB	complex formed between analyte and ligand
[AB]	concentration of the analyte-ligand complex (RU)
B	ligand (protein coupled to the sensor chip)
[B]	ligand concentration (RU), determined by Rmax - R
C	concentration of analyte (M)
ka	rate of analyte association with the ligand ($M^{-1}s^{-1}$)
kd	rate of analyte dissociation from the ligand (s^{-1})
R	response due to analyte binding (RU)
R_0	response (RU) at completion of analyte injection
Rmax	maximum analyte binding capacity (RU)

RATE EQUATION

This model is described by the following rate equation:

The net rate of complex formation = Complex formation - Complex decay

$$dAB/dt = (ka \,.\, [A] \,.\, [B] - kd \,.\, [AB])$$

$$dR/dt = ka \,.\, C \,.\, (Rmax - R) - kd \,.\, R$$

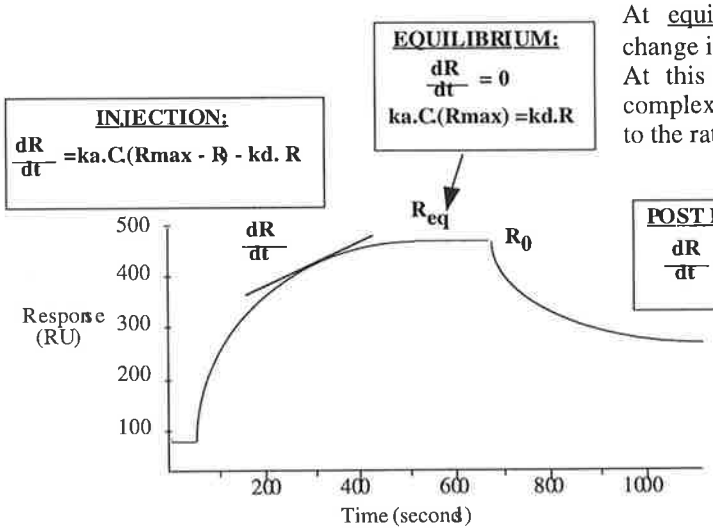

At equilibrium, there is no change in response with time. At this point, the rate of complex formation is equal to the rate of complex decay.

Post analyte injection, buffer is injected over the surface and dissociation occurs. The response over time is equal to the rate of complex decay.

LANGMUIR 1:1 BINDING WITH MASS TRANSPORT LIMITATIONS

-As for the Langmuir 1:1 binding model, but accounts for mass transport limitations. Mass transport limitations occur if the transfer of the analyte to the surface bound protein is slower than the kinetic binding rate. This model is described in Karlsson *et al.* (1994).

DEFINITIONS

A	analyte (protein in solution)
[A]	concentration of analyte (M)
AB	complex formed between analyte and ligand
[AB]	concentration of the analyte-ligand complex (RU)
B	ligand (protein coupled to the sensor chip)
[B]	ligand concentration (RU), determined by Rmax - R
ka	rate of analyte association with the ligand ($M^{-1}s^{-1}$)
kd	rate of analyte dissociation from the ligand (s^{-1})
R	response due to analyte binding (RU)
Rmax	maximum analyte binding capacity (RU)
Cs	concentration of analyte close to the sensor chip surface
k_t	rate constant for mass transport

RATE EQUATIONS

To account for mass transport limitations, the following expression is used:

$dCs/dt = kt.([A]-Cs) - (ka.Cs.[B] - kd.[AB])$

This expression describes the rate of transport of the analyte, A, to and from the surface. k_t is related to the generally accepted mass transport coefficient, k_m, by the expression:

$k_t \approx 10^9$ x molecular weight x k_m

Values for k_t are typically in the order of 10^8 for proteins with a molecular weight between 50-100 kDa.

As shown above, the model is described by the following rate equation:

$dAB/dt = (ka.[A].[B] - kd.[AB])$

In this case, the response takes into account the surface concentration of analyte.

Therefore, $dR/dt = ka.\ Cs.(Rmax-R)-kd.R$

HETEROGENEOUS LIGAND (PARALLEL REACTIONS)

-A model for ligand heterogeneity which describes an interaction between one analyte and two independent ligands bound to the sensor chip surface. Ligand heterogeneity can arise from contaminants in the ligand preparation, or from multiple point attachment of the ligand to the biosensor surface (for example, through amine coupling). Multiple point attachment may lead to the exposure of both high and low affinity analyte binding sites. This model is described in Karlsson *et al.* (1994).

MODEL

$A + B1 \leftrightarrow AB1$

$A + B2 \leftrightarrow AB2$

Where total response = AB1 + AB2

DEFINITIONS

A	analyte (protein in solution)
[A]	concentration of analyte (M)
AB1	complex formed between analyte and ligand 1
[AB1]	concentration of the analyte-ligand 1 complex (RU)
AB2	complex formed between analyte and ligand 2
[AB2]	concentration of the analyte-ligand 2 complex (RU)
B1	ligand 1 (protein 1 coupled to the sensor chip surface)
B2	ligand 2 (protein 2 coupled to the sensor chip surface)
ka1	rate of analyte association with the ligand B1 ($M^{-1}s^{-1}$)
ka2	rate of analyte association with the ligand B2 ($M^{-1}s^{-1}$)
kd1	rate of analyte dissociation from the ligand B1 (s^{-1})
kd2	rate of analyte dissociation from the ligand B2 (s^{-1})

RATE EQUATIONS

This model is described by two separate rate equations:

$dAB1/dt = (ka1.[A].[B1] - kd1.[AB1])$

$dAB2/dt = ([ka2].[A].[B2] - kd2.[AB2])$

The relative contributions of the 2 ligands can be determined using the BIAevaluation software.

TWO-STATE REACTION (CONFORMATIONAL CHANGE)

-A 1:1 binding of an analyte to an immobilised ligand, followed by a conformational change in the complex. The complex AB undergoes a conformational change to AB*. This model is described in Karlsson and Falt (1997).

MODEL

$A + B \leftrightarrow AB \leftrightarrow AB^*$

Where total response = AB + AB*

DEFINITIONS

A	analyte (protein in solution)
[A]	concentration of analyte (M)
B	ligand (protein coupled to the sensor chip)
[B]	ligand concentration (RU)
AB	complex formed between analyte and ligand
[AB]	concentration of the analyte-ligand complex (RU)
AB*	complex resulting from the conformational change of AB
[AB*]	concentration of the AB* complex (RU)
ka1	rate of analyte association with the ligand ($M^{-1}s^{-1}$)
ka2	rate of transition of AB to AB* (s^{-1})
kd1	rate of analyte dissociation from the ligand (s^{-1})
kd2	rate of transition of AB* to AB (s^{-1})

RATE EQUATIONS

This model is described by the following rate equations:

$dAB/dt = (ka1.[A].[B] - kd1.[AB]) - (ka2.[AB] - kd2.[AB^*])$

$dAB^*/dt = (ka2.[AB] - kd2.[AB^*])$

Addenda to Chapter One, Introduction, in response to examiner's comments:

Section 1.1 "IGF Protein Actions":

IGF activity can be potentiated by the presence of other hormones and growth factors (and *vice versa*). This synergistic effect has been observed when IGF-I has been combined with follicle-stimulating hormone, erythropoietin, colony factor, and with thyroid-stimulating hormone in different cell culture experiments (reviewed by Van Wyk, 1991; Jones and Clemmons, 1995).

Section 1.4.1 "IGFBP actions, tissue delivery and distribution", page 11, paragraph 1:

In addition to binding to ECM, there is evidence to show that IGFBP-5 associates with cell surfaces. Similar to IGFBP-3, heparin was found to reduce the binding of full-length IGFBP-5 to the surface of osteoblasts (Andress, 1995). Enzymatic treatment of cells to reduce glycosaminoglycan content on their surface however, did not affect cell surface interaction of IGFBP-5 (Andress, 1995). This gave evidence that the cell surface interaction of IGFBP-5 was not a result of binding to heparin. Cross-linking and affinity purification using IGFBP-5 as a bait protein resulted in the isolation of a 420 kDa cell surface receptor (Andress, 1995; Andress, 1998) which has yet to be fully characterised.

The demonstration that IGFBP-3 could associate with different glycosaminoglycans gave evidence that the binding protein could potentially interact with both cell surfaces and extracellular matrix (Fowlkes and Serra, 1996).

Section 1.5.2 "Residues on IGFBPs required for IGF interaction", page 27:

Using BIAcore, Kalus *et al.* (1998) demonstrated a nanomolar IGF binding affinity of an N-terminal fragment of IGFBP-5 (amino acids 40-92). Similar binding studies performed on a C-terminal fragment of IGFBP-5 failed to show IGF binding activity (Kalus *et al.*, 1998). Therefore, Kalus *et al.* (1998) proposed that IGFBP-5 contained only one high affinity binding site in the N-terminal region of the protein. Using molecular modeling, in this paper Kalus *et al.* hypothesised that Glu3 and Glu6 of IGF-I and IGF-II respectively interacted with N-terminal residues of IGFBP-5.

The inability of Kalus *et al.* (1998) to demonstrate IGF binding activity in the C-terminal domain of IGFBP-5 contradicts the observations of other researchers (Section 1.5.2). For example, Ho and Baxter (1997) presented evidence that the C-terminal region of IGFBP-2 interacted with the N-terminal end of IGF-II. The experimental approach used by Kalus *et al.* may explain their findings. In their study, biotinylated IGF was coupled to a streptavidin sensor chip surface. If IGF was biotinylated predominantly at the N-terminal residue (in contrast to lysine biotinylation), then the molecule would have been immobilised to the sensor chip through its N-terminal end. If the model proposed by Ho and Baxter (1997) is correct, the IGF residues important for interaction with the C-terminal fragment of IGFBP-5 were not readily accessible (giving the impression that the C-terminal fragment had no IGF binding activity). Unfortunately, neither the biotinylation nor the coupling of IGF to the sensor chip surface was characterised, and it is therefore difficult to comment on Kalus' findings. It would be possible to test the model proposed by Kalus *et al.* (1998) by assessing the interaction between the IGFBP-5 N-terminal fragment and N-terminal mutants of the IGFs (for example Des(1-3)IGF-I and Des(1-6)IGF-II). If Glu3 and Glu6 of IGF-I and IGF-II respectively interacted with the N-terminal amino acids in IGFBP-5, then binding to the N-terminal fragment would be dramatically reduced or abolished.

Additional references cited in the addenda:

Andress, D.L. (1995) Heparin modulates the binding of insulin-like growth factor (IGF) binding protein-5 to a membrane protein in osteoblastic cells. *J. Biol. Chem.* **270**(47):28289-28296.

Andress, D.L. (1998) Insulin-like growth factor-binding protein-5 (IGFBP-5) stimulates phosphorylation of the IGFBP-5 receptor. *Am. J. Physiol.* **274**:E744-E750.

Van Wyk, J. (1991) Frontiers of research on the somatomedins/insulin-like growth factors. In *Modern Concepts of Insulin-like Growth Factors*. (Spencer, E.M., ed.), pp691-703. Elsevier.